# ATTACHMENT 10

## WCAP-15163, REVISION 1, "TECHNICAL SUPPORT FOR IMPLEMENTING HIGH VOLTAGE ALTERNATE REPAIR CRITERIA AT HOT LEG LIMITED DISPLACEMENT TSP INTERSECTIONS FOR SOUTH TEXAS PLANT UNIT 2, MODEL E STEAM GENERATOR," MARCH 1999, (NON-PROPRIETARY)

Westinghouse Non-Proprietary Class 3

WCAP-15164
Revision 1

# TECHNICAL SUPPORT FOR IMPLEMENTING HIGH VOLTAGE ALTERNATE REPAIR CRITERIA AT HOT LEG LIMITED DISPLACEMENT TSP INTERSECTIONS FOR SOUTH TEXAS PLANT UNIT 2, MODEL E STEAM GENERATOR

Westinghouse Energy Systems

WCAP- 15164
Revision 1

SG 99-01-001

# Technical Support for Implementing High Voltage Alternate Repair Criteria at Hot Leg Limited Displacement TSP Intersections for South Texas Plant Unit 2, Model E2 Steam Generators

March 1999

Westinghouse Electric Company
Nuclear Services Division
Pittsburgh, PA 15230

# Technical Support for Implementing High Voltage Alternate Repair Criteria at Hot Leg TSP Intersections for South Texas Plant Unit 2, Model E Steam Generators

## Table of Contents

## List of Tables

## List of Tables (continued)

## List of Tables (continued)

## List of Figures

## List of Figures (continued)

## List of Figures (continued)

## List of Figures (continued)

## List of Figures (continued)

# 1.0 INTRODUCTION

For ODSCC occurring within the span of tube support plate (TSP) intersections in Westinghouse designed steam generators, voltage-based alternate repair criteria can be implemented according to the guidelines of NRC GL 95-05. For steam generators with ¾" diameter tubing, the voltage-based repair limit is very conservatively established at 1 volt to meet the probability of burst criterion of $10^{-2}$ and the criterion that the total leakage be less than the allowable leakage to maintain offsite dose limits during the limiting accident. The calculation basis for the ARC according to GL 95-05 assumes that the indications are free-span indications, despite the additional requirement that the entire indication must be contained within the span of the TSP, since it is assumed that the TSPs will displace during the limiting accident to expose the tube flaw.

This report provides technical support for implementing higher voltage ARC at TSP intersections for the Westinghouse Model E2 steam generators (S/Gs) at South Texas Unit-2. A 3 volt repair limit is conservatively recommended. The analyses included in this report demonstrate that the TSP displacements for the majority of the TSPs in the steam generators during postulated limiting accident conditions are small, and less than a value conservatively established to permit use of leak test data that provides a bounding leak rate for Indications Restricted from Burst (IRBs). The proposed higher voltage ARC apply only to the TSPs that have maximum displacement less than the conservative limit established.

When TSP displacements in a steam line break (SLB) event are limited to negligible levels, the axial tube burst probability is also reduced to negligible levels. For very large bobbin voltage indications with cellular corrosion morphology, it could be possible for the axial pressure loads on the tube to cause axial tensile tearing of the indications. This condition establishes the structural limit for voltage repair limits. This limit is developed in this report and shown to be much higher than any indications reasonably expected at South Texas Unit 2 for the 3-volt repair limits recommended in this report. Thus, repair limits with limited TSP displacement are primarily dictated by the requirement to limit accident condition leakage to acceptable levels.

The analyses presented in this report include hydraulic analyses for postulated SLB conditions to obtain the time dependent pressure drop hydraulic loads on the TSPs (Sections 4 and 5). Analyses of a postulated SLB transient initiating from full power and from Hot Standby conditions were performed to determine the most conservative loads. Comparisons of the analysis results with a prior RELAP5 analysis of Model D4 steam generators are presented, along with studies to define the sensitivity of the loads to various modeling and computational options. For conservatism, a factor of 1.5 increase in the RELAP5 predicted loads is applied to envelop the results of load sensitivity evaluations.

Structural analyses that apply the hydraulic loads to determine the TSP displacements are presented in Sections 6 and 7. The structural model presented in Section 6 is specific to the South Texas Unit 2 steam generators, and it accounts for the design features that provide support to the TSPs. The TSP displacement results are presented in Section 7. Based on the results of the displacement analyses presented in Section 7, the hot leg intersections of TSPs C through M are selected for which the higher voltage ARC are recommended. Implementation of higher voltage ARC for TSPs, N through Q, requires a physical modification to limit TSP displacement and is addressed in a separate report. Although it meets the displacement criteria, TSP R is excluded for convenience since it is above plate Q.

Section 8 summarizes the results of tests to determine the bounding leak rate for indications restricted from burst (IRB), that is, tube flaws that are constrained within the span of the TSPs and, therefore, cannot burst. The limit of applicability for the IRB bounding leak rate, with respect to TSP displacement during a postulated SLB, is also presented based on the test data.

The analysis methods for SLB leak rate and tube burst probability assessments given in Section 9 are consistent with the requirements of the NRC GL 95-05. An extension of the leak rate methodology is included for potentially overpressurized indications within the confines of the TSP (an IRB) and the methodology for this analysis is also given in Section 9. This section also includes development of the voltage-based structural limit for axial tensile tearing as the applicable structural limit with tube expansion.

Because the predicted tube displacements depend on structural features such as stayrods and wedges to support the TSPs, an inspection plan to verify the integrity of these features is presented in Section 10.

The requirements on limiting TSP displacements to obtain negligible tube burst probabilities are developed in Section 11. Section 11 integrates the analyses and results of applicable tests performed, as presented in the prior report sections, to develop the alternate repair criteria with tube expansion for South Texas Unit 2. Inspection and SLB analysis requirements are also given in Section 11.

## 2.0 SUMMARY AND CONCLUSIONS

This report documents the technical support for high voltage Alternate Repair Criteria (ARC) at TSP intersections for the Model E2 S/Gs of South Texas. A 3.0 volt repair limit is proposed for the hot leg TSP intersections at plates C through M, and a 1.0 volt repair limit, according to the guidelines of GL 95 -05, is proposed for the FDB, all cold leg TSP intersections and the hot leg TSP intersection at TSPs N through R [1]. The technical assessments of this report support a full APC repair limit of 17 volts or higher for hot leg intersections in TSPs C through M without physical modification in the steam generators. Physical modifications are available to justify application of the 3 volt repair limit to all of the hot leg tubes except as noted above; however, these physical modifications are described in a separate report.

The overall conclusions and recommendations for the ARC, and a summary of the technical basis for the ARC as presented in this report are provided in this section.

### 2.1 Overall Conclusions

Although TSP displacements up to [ ]$^{a,c}$ inch are adequate to restrict the total axial tube burst probabilities to a negligible $10^{-5}$ during a postulated SLB event, limiting the acceptable maximum TSP displacements to $\leq$ 0.15 inch leads to an associated tube burst probability of $<10^{-10}$ for a single tube. These bounding tube burst probabilities have been obtained by the extremely conservative assumption that all hot leg TSP intersections have through-wall cracks exposed by the TSP displacements. Negligible TSP displacements were shown to occur in plates C through M when subjected to postulated SLB transient loading using a conservative multiplier of 1.5 on the predicted loads.

Since axial tube burst probabilities are negligibly small for the limited TSP displacements, repair limits to preclude burst are effectively not required and tube repair requirements may be primarily based on limiting accident condition leakage to acceptable levels. At very high voltage levels for crack morphologies that include cellular corrosion, it is possible that the axial pressure loads on the tube could cause tensile tearing of an indication. This limit represents the structural limit applicable for TSP displacements limited to $\leq$0.15" and, based on available data, is estimated to exceed [ ]$^{a,c}$ volts at the lower 95% confidence level on the data, for the $3\Delta P_{NO}$ structural margin guideline of draft Regulatory Guide 1.121.

Although voltage repair limits at least as high as [ ]$^{a,c}$ volts are justifiable for TSP displacements that are limited to $\leq$0.15" , a 3.0 volt repair limit is proposed for the hot leg TSP intersections for the tube support plates shown to displace $\leq$0.15" at South Texas Unit 2. For the TSPs for which the displacement during a postulated SLB event is >0.15", for the hot leg intersections at plate R, for the entire FDB and for all cold leg TSP

[1] South Texas Unit 2 includes 15 tubes in steam generator D that are made of thermally treated Alloy 600 instead of the mill annealed Alloy 600 utilized for the remainder of the tubes. These tubes have been excluded from the application of the ODSCC ARC, Reference 1, based on the absence of pulled tube data to confirm the ODSCC morphology. Thermally treated Alloy 600 is less susceptible than mill annealed Alloy 600 to stress corrosion attack. Consequently, it is unlikely that ODSCC at the TSPs will be observed in these tubes in any case. If ODSCC should be observed in one, or more, of these tubes, the economic impact of repairing these tubes will be less than pulling a tube to verify the ODSCC morphology.

intersections, a voltage repair limit of 1.0 volt, consistent with the requirements of GL 95-05, has been justified in Reference 1.

The inspection requirements for the higher voltage ARC are essentially the same as required for the ARC according to GL 95-05, although supplemental inspections are required as described in Section 2.2 below to verify that the structural model is consistent with the as-built structure of the steam generators.

## 2.2 Summary

### 2.2.1 Overall Approach to Alternate Repair Criteria for South Texas Unit 2

The approach applied to develop the ARC basis is to:

- Define acceptable TSP displacements to achieve a negligible tube burst probability (a value of $10^{-5}$ is considered negligibly small compared to the NRC GL 95-05 reporting guideline of $10^{-2}$).
- Utilize conservative SLB hydraulic loads on the TSPs (a 1.5 margin on the expected loads obtained from the RELAP5 code is used to envelope uncertainties).
- Show by analysis that TSP displacements during postulated accident loading are less than the displacements tested in the Indications Restricted from Burst (IRB) tests to utilize the bounding leak rate test results from these tests.
- Demonstrate by structural analyses that the maximum TSP displacement is significantly smaller than the acceptable displacements established to meet tube burst probability goals.

### 2.2.2 TSP Displacement for Negligible Probability of Burst

To obtain a negligible probability of burst, an acceptable TSP displacement of [ ]$^{a,c}$ inch was very conservatively developed by

a) assuming that all TSPs are uniformly displaced and
b) by making the bounding assumption that these displacements exposed throughwall cracks at all hot leg TSP intersections (43,659 throughwall indications).

At a uniform TSP displacement of [ ]$^{a,c}$ inch, the total probability of burst for a steam generator at a $\Delta p$ of 2560 psi is less than $10^{-5}$. This value is negligibly small compared to the conservative limit on probability of burst of $10^{-2}$ given in NRC GL 95-05 for ODSCC at the TSPs. With a factor of 1.5 is applied on the transient loads calculated using RELAP5 to envelop modeling and calculation uncertainties, the maximum displacement for TSPs C through M is <0.15" , and for plates N through Q is [ ]$^{a,c}$. (The maximum displacement for plate R is [ ]$^{a,c}$; however this plate is excluded from the high voltage ARC for inspection convenience). At the goal TSP displacement of 0.15 inch, the probability of burst is less than $4x10^{-19}$ for a single tube and less than $2x10^{-15}$ total for the steam generator.

The above total probabilities of burst consider all of the hot leg intersections displaced by the same maximum distance (see Section 9). Only TSPs C through M are recommended for application of the 3 volt repair criterion, thus, the total probability of burst for these plates is less than the values noted above. Consequently, the incremental probability of burst from the tube intersections at these plates is negligible, and only the leakage must be calculated. Indications at plates N though R, hot leg, at the FDB, and at all cold leg intersection will be treated as freespan indications for calculation of the probability of burst consistent with the guidelines of NRC GL 95-05.

2.2.3 TSP Displacement to Utilize IRB Leak Rate Test Results

High-energy leak rate tests were performed to determine the leak rates for indications restricted from burst (IRB). Section 8 summarizes these tests. The bounding leak rate for South Texas Unit 2 SLB pressure differential of 2405 psi, based on the PORVs for pressure relief, is 5.0 gpm. The bounding leak rate is based on tests with offsets (TSP displacements) up to 0.21 inch. The design value of TSP displacement for the South Texas Unit 2 tube limited displacement ARC was set at 0.15 inches to provide additional conservatism compared to the acceptable displacement of 0.21 inch for utilization of the IRB leak rate.

The 0.15 inch TSP displacement goal was established to permit an option for in situ leak testing. The difference between the SLB leak rate for the small goal displacement of 0.15 inch and the in-situ test leak rate would be expected to be negligible, even for the unlikely, high-voltage indications for which the through-wall crack length may be aligned with the edge of the TSP. Thus, the in-situ leak rates can be expected to be representative of the leak rates with lower TSP displacement, and can be applied to improve the accuracy of leak rate calculations for condition monitoring assessments if a few large indications are found in an inspection.

2.2.4 Hydraulic Load Analyses

Section 4 discusses the hydraulic modeling of the steam generators, and Section 5 presents the results of the RELAP5 analysis.

Hydraulic loads on the TSPs for application to the TSP displacement analyses were obtained using the RELAP5 code. The analyses show that the TSP loads are higher for a SLB event at hot standby operating conditions than for full power conditions. The hot standby loads are used for the displacement analyses even though only a small fraction of the operating cycle is spent at hot standby conditions. The reference hot standby (and full power) loads are based on use of test-based TSP loss coefficients. The test-based loss coefficients generally compare well with, and are more conservative than, the calculated loss coefficients. The RELAP5 modeling and analysis of the steam generators are discussed in Section 5.

Sensitivity analyses were performed to assess the dependence of the TSP loads on modeling and calculation uncertainties. Table 2-1 summarizes the sensitivity analyses performed. When the potential modeling uncertainties or analysis options that could increase the TSP

hydraulic loads over the reference or expected base case results are combined, the TSP loads can be bounded by a factor of 1.5 increase over the reference loads. This factor of 1.5 increase on the reference hot standby loads was applied to ensure conservative loading for the TSP displacement analyses.

2.2.5 Tube Repair Limits

Since the negligible displacement of TSPs C through M under postulated SLB loading practically eliminates tube burst as a credible event at all TSP locations, draft Regulatory Guide 1.121 guidelines for structural margins are inherently satisfied at both normal operating and accident conditions, including a postulated SLB event. Consequently, tube repair limits are not required to satisfy tube burst margins, and tube repair would be required only as necessary to satisfy allowable leakage limits. At very high bobbin voltages corresponding to relatively large ODSCC indications compared to the GL-95-05 1 volt repair limit for 3/4 inch tubing, a structural limit based on axial tensile tearing of indications with cellular or IGA (not significant at TSP intersections) corrosion becomes applicable for the axial pressure differentials across the tube. Available pulled tube and laboratory specimen data on axial tensile tests and measured, undegraded tube cross sectional area were used to estimate the tensile tearing structural limit. Based on a regression analysis of the residual tube cross sectional area to bobbin voltage, the tensile structural limit at the lower 95% confidence bound on the data, as adjusted for lower tolerance limit material properties at operating temperatures, is greater than [ ]$^{a,c}$ volts. With a conservative factor of two allowance for crack growth and NDE uncertainties (a factor of [ ]$^{a,c}$ is typical based on the ARC experience), the full ARC repair limit would be about [ ]$^{a,c}$ volts.

For South Texas Unit 2, a tube repair limit of > 3.0 volts is conservatively applied for the hot legs of TSPs C through M. Bobbin voltage indications $\leq$ 3.0 volts can be left in service independent of RPC (or equivalent probe) confirmation as a flaw indication. Bobbin indications > 3.0 volts are repaired independent of RPC confirmation.

For indications at the FDB (Plate A), plates N through R, and at all cold leg TSP intersections, the NRC GL 95-05 repair limits are to be applied. Reference 1 requested approval of a 1.0 volt tube repair limit for 3/4 inch diameter tubing in the South Texas Unit 2 steam generators, consistent with NRC GL 95-05 For the locations where the 1 volt repair criteria apply, South Texas Unit 2 bobbin indications > 1.0 volt and less than or equal to the upper voltage limit calculated according to the guidelines of GL 95-05 are to be repaired if confirmed as flaw indications by RPC inspection. Bobbin indications greater than the upper voltage repair limit are to be repaired independent of RPC confirmation. The upper voltage repair limit is based on the structural limit reduced by allowances for growth and NDE uncertainties. The structural limit is dependent on the latest database applied to develop the burst pressure versus bobbin voltage correlation and is to be updated on a periodic basis. The upper voltage repair limit is updated to the latest database and plant specific growth rate data at each inspection outage at which the alternate plugging criteria of this report are applied. For FDB intersections, which have large tube to plate clearances, the structural limit is based on a $3\Delta P_{NO}$ structural margin. At cold leg TSP

intersections and the applicable hot leg intersections at plates N through R, for which the small clearances provide constraint against tube burst, the structural limit is based on a $1.43\Delta P_{SLB}$ structural margin. Based on the latest 3/4 inch diameter database and on growth rates evaluated for South Texas Unit 2 (Reference 1), the upper voltage repair limits developed are 2.48 volts for indications at the FDB and 3.03 volts for indications at cold leg TSPs.

The tube repair limits applicable to South Texas Unit 2 support plate intersections are summarized in Table 2-2, together with the supporting inspection requirements.

2.2.6 Inspection Requirements

The steam generator tube inspection requirements for applying the tube repair limits of this report are the same as those required by the NRC GL 95-05 with adjustment of the RPC inspection requirements for hot leg TSP C through M intersections to reflect the higher tube repair limits. All hot leg TSP intersections with bobbin voltages >3 volts will be inspected with an RPC (or equivalent) probe. In addition, a minimum sample inspection of 100 intersections with bobbin indications <3 Volts will be applied at hot leg TSP C through M intersections. The GL95-05 1-volt RPC threshold is applied for the 1 volt repair limit for FDB, plates N through R and all cold leg TSP intersections.

The stainless steel TSPs in the South Texas Unit 2 steam generators eliminate corrosion denting as a consideration. Therefore, no special inspection requirements related to corrosion induced dents are required, and no exclusion zones[2] due to denting are required.

2.2.7 SLB Analyses

SLB leak rates must be calculated for both the hot leg and cold leg TSP indications, including the FDB. Tube burst probability analyses are required for all cold leg TSP indications, for all FDB indications and for the hot leg indications in TSPs N through R for the actual voltage distribution found by inspection at each outage for condition monitoring and operational assessment.

The leakage calculations are consistent with the methods given in NRC GL 95-05, except that the hot leg TSP indications for plates C through M require an additional component for the potentially overpressurized indications. The freespan leakage calculations are based on the EPRI methodology for correlating probability of leakage and SLB leak rates with bobbin voltage as described in Reference 2. The modifications to the freespan leak rate calculations to account for potentially overpressurized hot leg indications are given in Section 11.6.

The probability of an overpressurized condition is defined as the probability of a free span burst. With overpressurization, the flanks of the crack face can open until contact is made with the inside surface of the tube hole in the TSP. For this condition, bounding analyses can be made for the leak rates associated with the overpressurized indications. The SLB

[2] Fifteen tubes in steam generator D that are thermally treated Alloy 600 tubes are excluded (see Section 2.0).

leak rate for the overpressurized indications is then obtained as the probability of free span burst (probability of leakage with an overpressurized indication) times the bounding leak rate for an overpressurized indication

Tube burst probability analyses are required only for cold leg TSP indications, all FDB indications and hot leg indications in plates N through R. Burst probability calculations for hot leg indications in plates C through M are not required since the limited displacement of these plates under postulated SLB loading results in negligible burst probabilities. The resulting burst probabilities are to be compared to the NRC GL 95-05 reporting guideline of $10^{-2}$. The calculation methods are contained in Reference 2.

### 2.2.8 Steam Generator Internals Inspection

In addition to inspection of the tubes, it is also necessary to verify the integrity of the SG internals components and structure to ensure that the actual TSP displacements are not greater than the results of the TSP displacement analysis. Section 10 provides the inspection plan for the SG structural components. Sampling visual inspections of the TSPs, stayrods, wedges and vertical backing bars that support the TSPs will be performed to the extent that access to these components is available and radiation exposure and risk of foreign objects in the SG permit. The TSPs will be 100% inspected by EC to verify absence from unacceptable TSP cracking. The top TSP wedges, vertical backing bars and preheater stayrods, spacers and nuts will be inspected in one of the SGs. These inspection, along with the results of prior inspections in both Units 1 and 2 will be used to verify the structural integrity of the Unit 2 SG internals to support the higher voltage ARC.

## 2.3 References

1. SG-98-01-004; South Texas Project Unit 2 Technical Justification for License Amendment to Implement NRC Generic Letter GL 95-05 Voltage Based Repair Criteria for Steam Generator Tube ODSCC; January 1998
2. WCAP-14277; SLB Leak Rate and Tube Burst Probability Analysis Methods for ODSCC at TSP Intersections; (Rev 1), December 1996.

**Table 2-1**
**Thermal Hydraulic Base and Sensitivity Analyses**

| Case | Initial Condition | Model Option | Loss oefficient | reak Flow | Water Level (inch) | Time Step (sec.) |
|---|---|---|---|---|---|---|
| **Base Cases** | | | | | | |
| Base Case -1 | Full Power | E | Calc. | Nom. | 530 | 0.001 |
| Base Case -2 | Hot Standby | E | Calc. | Nom. | 530 | 0.001 |
| **Sensitivity Study** | | | | | | |
| D4 S/G Model Options | Hot Standby | D4 | Calc. | Nom. | 530 | 0.001 |
| Westinghouse Loss Coeff. | Hot Standby | E | Westing-house | Nom. | 530 | 0.001 |
| ncreased Break Flow | Hot Standby | E | Calc. | +10% | 530 | 0.001 |
| ncreased Break Flow | Hot Standby | E | Calc. | +20% | 530 | 0.001 |
| Reduced Water Level | Hot Standby | E | Calc. | Nom. | 503 | 0.001 |
| Reduced Time Step | Hot Standby | E | Calc. | Nom. | 530 | 0.0001 |
| Radial Discretization | Hot Standby | E | Calc. | Nom. | 530 | 0.001 |
| Revised Separator Model | Hot Standby | E | Calc. | Nom. | 530 | 0.001 |

**Table 2-2**
**Summary of ARC Requirements**
**for South Texas Unit 2**

| Parameter/Action | Requirement |
|---|---|
| • Hot Leg Voltage Limit for Plates C through M | • Repair bobbin indications > 3 volts; not dependent on RPC confirmation |
| • Cold Leg , FDB and Plates N through R, Hot Leg, Voltage Limit | • Repair bobbin indication > 1 volt if confirmed by RPC and if voltage < upper repair limit<br>• Repair bobbin indications > upper repair limit |
| • Upper Repair Limit (does not apply for hot leg intesections, Plates C through M) | • Update each inspection |
| • Indication Voltage Growth Rate | • Use larger of 2 prior cycles growth rate( see GL 95-05, 2.a.2) |
| • Indications outside the TSP | • Repair and notify NRC prior to restart |
| • Circumferential Indications | • Repair and notify NRC prior to restart |
| • Exclusion Zones | • None for South Texas Unit 2 (15 thermally treated Alloy 600 tubes in SG D are excluded because of material differences) |
| • Bobbin Inspections | • 100% Hot Leg TSPs<br>• 100% FBD<br>• 100% Cold Leg TSP to the lowest TSP with ODSCC. The lowest CL TSP with ODSCC to be determined by a 20% sample of CL TSP intersections |
| • Hot Leg TSP (C through M) Bobbin Indications > 3 volts<br>• Cold Leg TSP, Hot Leg TSP (N through R) and FDB indications > 1 volt | • Inspect with RPC (or equivalent probe) |

**Table 2-2 (continued)**
**Summary of ARC Requirements**
**for South Texas Unit 2**

| Parameter/Action | Requirement |
|---|---|
| • Hot Leg TSP (C through M) indications ≤ 3 volts | • RPC sample of 100 |
| • Mechanically induced dent signals > 5 volts<br>• Bobbin mixed residuals signals that could potentially mask flaw responses near, or above, the voltage repair limits | • Inspect with RPC (or equivalent probe) |
| • SLB Leak Rates and Burst Probability | • Evaluate for actual voltage distribution and for projected EOC voltage distribution<br>- GL 95-05 methods for all CL TSP, HL TSP (plates N through Q) and FDB<br>- GL 95-05 methods modified for potential overpressurized tubes in HL TSP<br>• Notify NRC if licensed limits are exceeded<br>• Include in 90-day report |

# 3.0 MODEL E2 S/G DESIGN DESCRIPTION

## 3.1 Overall Design

The South Texas Unit 2 steam generators are of the Westinghouse Model E2 preheat steam generator design. Each steam generator (S/G) contains [ [1] ]$^{a,c}$ sq. ft. of heat transfer area per S/G. Figure 3-1 shows the steam generator layout; a detailed layout of the preheater region is shown in Figure 3-2. Primary coolant enters the hot leg channelhead and passes through the U-tubes, which transfer heat from the primary side to water on the secondary side, where the water is converted to steam. The feedwater enters the S/G through the preheater inlet nozzle into the preheater region (see Figure 3-2). The feedwater flow entering the preheater nozzle is directed to the bottom of the preheater by a water box at the nozzle, from where it flows upward through a series of preheater baffle plates which discharge the flow upward into the tube bundle. As the secondary fluid passes through the tube bundle, it is converted to a water/steam mixture that passes upward through the transition cone region of the S/G shell, into the primary and secondary moisture separators in the upper shell region. Water is separated from the steam before the dry steam exits the S/G via the steam outlet nozzle. Water removed by the moisture separators flows down the downcomer, which is the annulus between the shell and the wrapper surrounding the tube bundle region. Upon reaching the tubesheet, the water is once again directed upward through the flow distribution baffle into the tube bundle. A partition plate between plates B and L (see Figure 3-2) separates the preheater and hot leg sides of the S/G. Below plate B and above plate L, secondary flow can cross between the hot and cold leg sides of the S/G.

The S/G tubes pass through tube support plates (TSPs) which provide lateral support to the tubes and contain circulation holes through which the water/steam passes upward through the tube bundle. On the cold leg side in the preheater region, these support plates contain no circulation holes, and act to direct the flow across the tubes; therefore, these plates are also referred to as baffle plates. The flow distribution baffle, at an elevation of [ ]$^{a,c}$ inches above the top of the tubesheet, distributes flow across the tubesheet and upward through a cutout in the plate on the hot leg side.

During normal operation, a slight pressure drop exists across each TSP or baffle plate. This pressure drop causes small displacement of the TSPs relative to the tubes during normal operating conditions. At hot standby conditions, there is no secondary flow or pressure drop across the TSPs. However, during postulated accident conditions such as steam line break (SLB), pressure differentials across individual TSPs can act to displace

[1] South Texas Unit 2 includes 15 tubes in steam generator D that are made of thermally treated Alloy 600 instead of the mill annealed Alloy 600 utilized for the remainder of the tubes. These tubes have been excluded from the application of the ODSCC ARC based on the absence of pulled tube data to confirm the ODSCC morphology. Thermally treated Alloy 600 is less susceptible than mill annealed Alloy 600 to stress corrosion attack. Consequently, it is unlikely that ODSCC at the TSPs will be observed in these tubes in any case. If ODSCC should be observed in one, or more, of these tubes, the economic impact of repairing these tubes will be less than pulling a tube to verify the ODSCC morphology.

unsupported regions of the TSPs in such a manner as to potentially uncover degradation within the TSP crevice. The following sections provide specific design information concerning the Model E2 baffle and support plates.

## 3.2 Tube Support Plate Design

The Model E2 steam generators at South Texas Unit 2 utilize Type 405 stainless steel support plates with drilled (round) tube holes set on a square pitch of [ ]$^{a,c}$ inches. The TSPs are [ ]$^{a,c}$ inch thick, except for the uppermost TSP (Plate R) which is [ ]$^{a,c}$ inches thick. With the exception of the flow distribution baffle and preheater baffle plates (described below), the tube support plates also include flow circulation holes measuring [ ]$^{a,c}$ inch in diameter, set on a square pitch of [ ]$^{a,c}$ inches within the tube hole array.

The tube support plates of the South Texas Unit 2 S/Gs may be classified as one of three types: the flow distribution baffle, preheater baffle plates, and tube support plates. The flow distribution baffle (FDB), located [ ]$^{a,c}$ inches above the top of the tubesheet, is comprised of two halves, with the cold leg side containing no circulation holes or cutouts; a crescent-shaped cutout on the hot leg side permits the secondary fluid to pass upward through the tube bundle. In the FDB, the drilled tube holes measure [ ]$^{a,c}$ in diameter (nominal), compared to the [ ]$^{a,c}$ OD of the tube. The enlarged FDB holes allow some secondary fluid to pass upward through the tube/FDB crevices.

The preheater baffle plates, shown in Figure 3-3, contain [ ]$^{a,c}$ (nominal) diameter drilled tube holes and no circulation holes. Their function is to provide lateral support to the tubes and direct the flow back and forth across the tubes as the feedwater passes upward through the preheater. Westinghouse uses letter designations for the baffle plates at various elevations, with "A" representing the FDB and "B", "D", "E", "G", and "H" representing preheater baffle plates with no circulation holes.

On the hot leg side, two semi-circular plates ("C" and "F") with [ ]$^{a,c}$ diameter (nominal) tube holes as well as [ ]$^{a,c}$ diameter (nominal) circulation holes are located at the elevations of the "D" and "G" preheater baffle plates (see Figure 3.2). These plates permit flow upward through the tube bundle and provide lateral support for the tubes. Plates "J" and "K", on the hot and cold leg side of the S/G at the top of the preheater, similarly contain [ ]$^{a,c}$ diameter tube holes and [ ]$^{a,c}$ diameter circulation holes. The remainder of the tube support plates, "L", "M", "N", "P" and "Q" are full size circular plates with similar tube and circulation holes. In addition, the "L" through "Q" plates contain central flow slots along the tube lane (located on the centerline of the plate) to enhance flow upward through the bundle.

## 3.3 Tube Support Plate Supports

The FDB, TSPs and preheater baffle plates are supported vertically using several support mechanisms, including seven tierods/spacers in each half of the tube bundle. Preheater baffle plates A, B, D, E, G and H are supported by eighteen additional stayrods. In addition, the plates are supported by vertical bars, located above and below the plates, which are welded to either the ID of the wrapper, the impingement plate or the partition plate. Wedges located around the circumference of each plate provide in-plane support. The wedges, too, are welded to either the wrapper ID, the impingement plate or the partition plate. The tapered design of the wedges provides additional resistance to upward movement of the plates in addition to providing in-plane support.

Section 6.2 provides a detailed description of the Model E2 S/G TSP support system. Figure 6-1 shows a schematic of the tube bundle region. The support locations for each of the plates are shown in Figures 6-2 to 6-12. Detailed descriptions of the support components, including the tierods, spacer bars, and wedge groups, are provided in Section 6.2.

## 3.4 Secondary System Considerations

The steam generator secondary side consists of a natural circulation loop with feedwater inlets and a steam outlet. The steam generator water level at South Texas Unit 2 is maintained at 530" above the top of the tubesheet. The current T/H analysis considers a normal water level of 530" for the reference analysis applicable to South Texas Unit 2.

The preheater section (Figure 3.2) is on the cold leg of the steam generator, and is bounded by plate B at the lower end, and plate L at the upper end. The preheater is separated from the hot leg by a divider plate, located on the centerline of the steam generator, that extends from the elevation of plate B to plate L. Above plate L, there is no physical separation of the cold leg from the hot leg.

The feedwater enters the preheater of the generator through the main feedwater nozzle, and the bulk of the flow is directed downward by the water box. The feedwater then flows upward through five crossflow passes defined by the cutouts in the preheater baffle plates D,E,G and H. The preheater flow continues upward and leaves the preheater to join the flow from the hot leg side, after passing upward through the tube support plate L. A small fraction of the feedwater flow exits the bottom of the preheater through the tube/baffle hole clearance in the bottom baffle (plate B), where it mixes with the small amount of upward flow passing through the tube hole clearance in the cold leg of the FDB. This combined volume flows across the top of the FDB toward the hot leg, where it mixes with the upward flow coming through the cutout in the hot leg of the FDB. The upward flow through the FDB cutout is the flow from the downcomer, e.g., the recirculating water flowing from the moisture separators. As the fluid approaches the

first tube support plate in the hot leg side, axial flow becomes dominant. Boiling takes place and the flow moves upward along the hot leg side.

The hot and cold leg tube bundle flows meet above TSP L. The combined flow moves upward while boiling continues, leaving the tube bundle and entering the primary separators. A large portion of the water is separated by the primary separators and returned to the water reservoir. The steam with the remaining entrained moisture then enters the secondary separators. This entrained moisture is trapped by a system of hook and pocket vanes and returned to the water reservoir. The steam then leaves the steam generator through the steam outlet nozzle, while the water removed from the steam is re-circulated via the downcomer.

The Model E2 S/Gs utilize a venturi type flow limiter in the steam outlet nozzle. The venturi flow area at the throat is about [ ]$^{a,c}$ ft$^2$, while the steam line flow area is about [ ]$^{a,c}$ ft$^2$; therefore, the critical discharge flow is controlled by the flow limiter throat area of [ ]$^{a,c}$ ft$^2$ when a guillotine steam line break is postulated.

## Figure 3.1

## Model E2 Steam Generator Layout

a,c

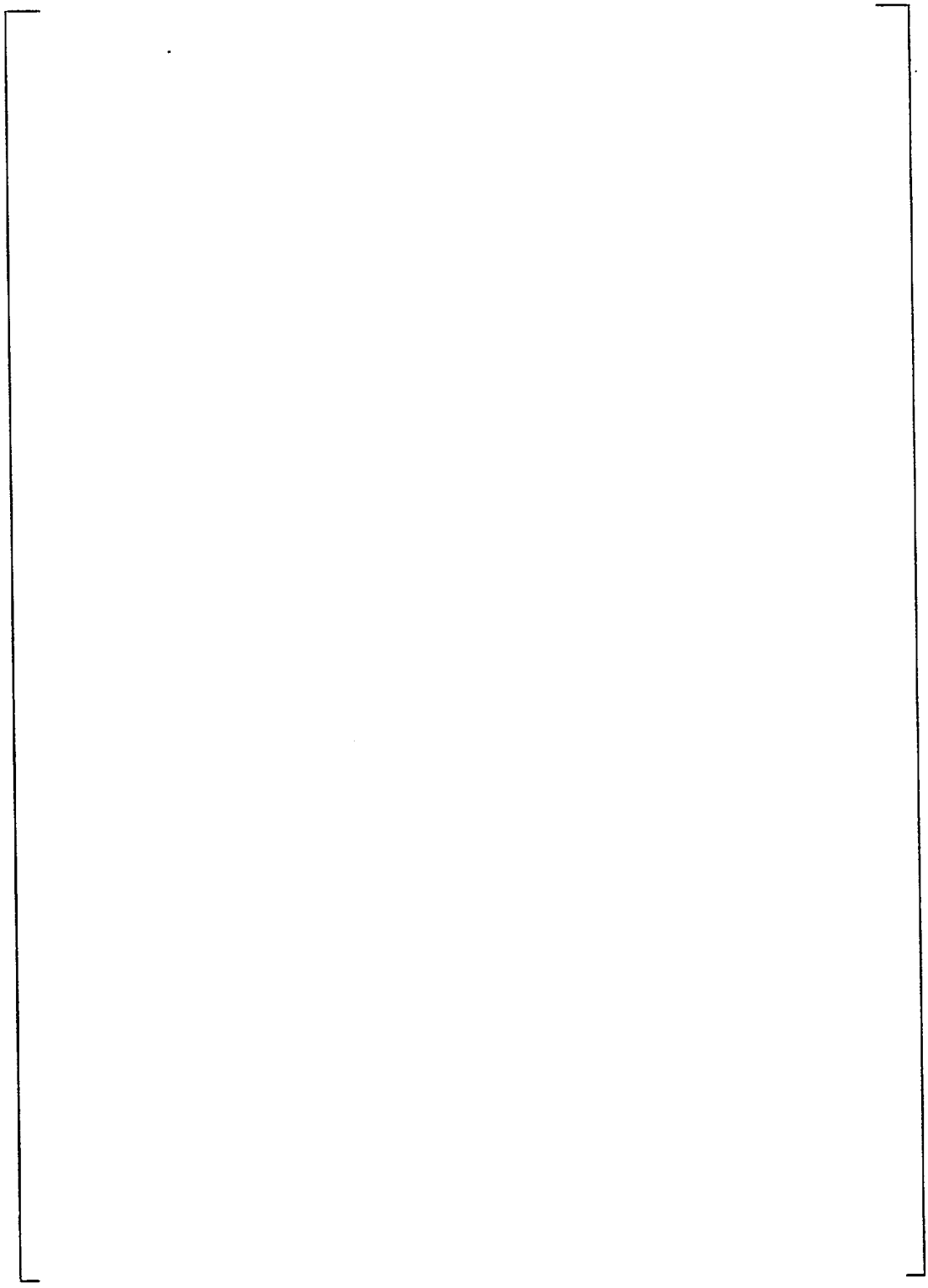

## Figure 3.2

## Model E2 Steam Generator Preheater Region

a , c

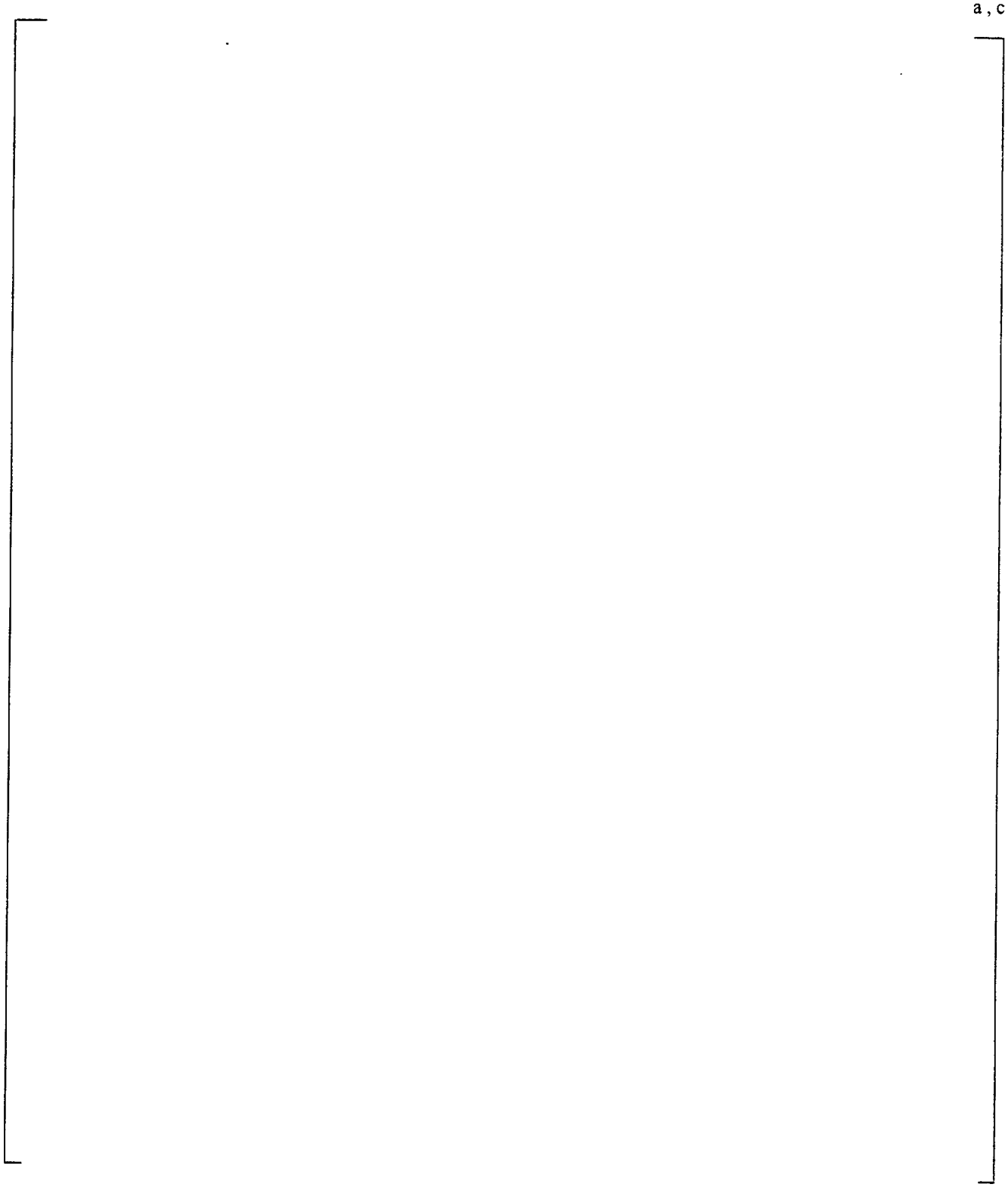

**Figure 3.3**

**Flow Distribution and Preheater Baffle Plates** a, c

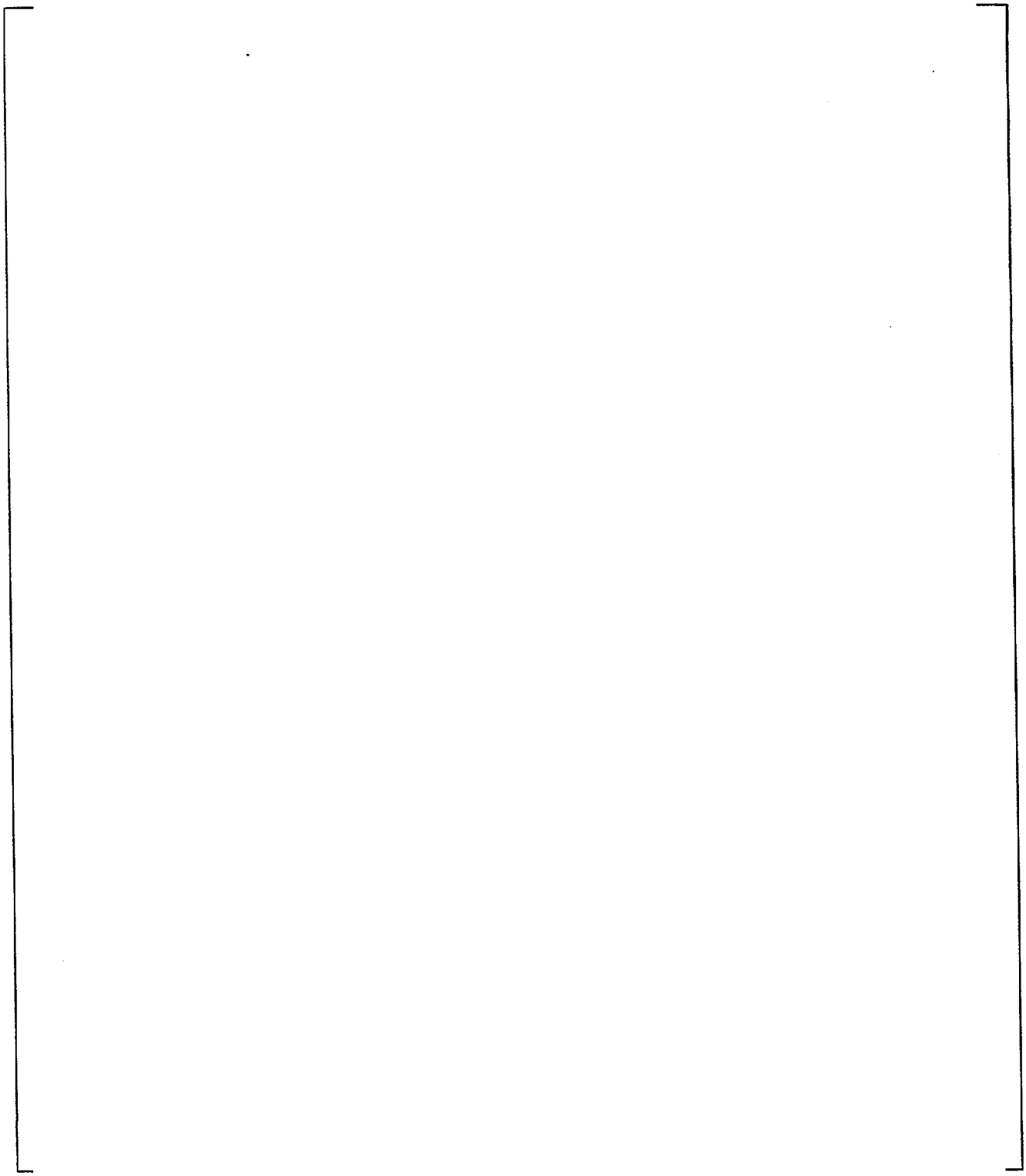

# 4.0 THERMAL HYDRAULIC MODELING

A postulated steam line break (SLB) event results in blowdown of steam and water. The fluid blowdown leads to rapid depressurization of the secondary side. Pressure drops develop and exert hydraulic loads on the tube support plates (TSPs) or baffle plates. These hydraulic loads were determined for the Model E2 steam generator using the RELAP5/MOD3 computer code.

Westinghouse contracted with MPR Associates, Inc. to perform the thermal-hydraulic analysis, which is reported in detailed MPR reports, References 4-1 and 4-2. The following sections summarize the basic modeling approach developed in these reports.

## 4.1 Applicable Analysis Codes

The RELAP5/MOD3 Code is an advanced thermal-hydraulic code, which has been used as a tool to analyze transients for light water reactor systems including steam generators. MOD3 is the third major variant of the code. Relap5 has been applied to analysis of SLB transients for the Model 51 (Reference 4-3) and for the Model D4 (Reference 4-4).

The RELAP5/MOD3 Code equation set provides a two-fluid, non-equilibrium system simulation. The six-equation set - continuity, momentum and energy equations for each phase - is used to solve for the dependent variables. These variables include local pressure and for each phase, specific internal energy, void fraction and velocity. Constitutive models represent the interphase drag and mass transfer, flow regimes in vertical and horizontal flow, and wall friction.

## 4.2 Model E2 RELAP5 Models

The RELAP5 computer model for Model E2 steam generator is composed of a network of nodes and connectors that represent the secondary side fluid, steam tube metal heat transfer and the primary coolant. Figures 4-1 and 4-3 show the nodal layout of the secondary side of the Model E2 steam generator. Figure 4-2 presents the nodal network of the secondary fluid, primary fluid and tube metal. The computational model consists of the following elements:

- 27 fluid nodes representing the primary side water volumes.
- 26 fluid junctions between primary side nodes.
- 41 fluid nodes representing secondary side steam and water volumes.
- 49 fluid junctions between secondary side nodes.
- 25 heat structures representing the primary coolant tube metal; each structure is capable of transferring heat between designated primary and secondary nodes.

In addition to the nodalization of the RELAP5 model, a number of thermal and hydraulic options (or switches) for each node and junction must be selected. Table 4-1 gives an overview of the options selected for the baseline case and for a case which is part of the sensitivity study discussed in Sections 4.5 and 5.3.

## 4.3 Model E2 S/G Operating Conditions

A postulated steam line break event could be initiated from any operating condition. Two bounding conditions for normal operation were assumed for this analysis, full power and hot standby. The following Model E2 full power and hot standby operating conditions were established by the RELAP5 Code prior to initiation of the SLB event:

| Full Power Operating Conditions | | |
|---|---|---|
| Primary Flow | = | 3.49x106 lbm/hr |
| Primary Thot/Tcold | = | 626/560°F |
| Primary Operating Pressure | = | 2250 psia |
| Feedwater Flow | = | 4.24x106 lbm/hr |
| Feedwater Temperature | = | 440°F |
| Steam Pressure | = | 1100 psia |
| Water Level | = | 530 inches |
| Circulation Ratio | = | 2.35 |

| Hot Standby Conditions | | |
|---|---|---|
| Primary Flow | = | 3.49x106 lbm/hr |
| Primary Thot/Tcold | = | 567/567 □F |
| Primary Operating Pressure | = | 2250 psia |
| Feedwater Flow | = | 0 lbm/hr |
| Feedwater Temperature | = | Not Applicable |
| Steam Pressure | = | 1200 psia |
| Water Level | = | 530 inches |

Except for water level, which was varied as part of the sensitivity study described below, these conditions were maintained for all cases evaluated.

## 4.4 Calculation of TSP Loading from Dynamic Analysis

The primary purpose of this thermal-hydraulic evaluation was to develop the TSP loading that occurs during a postulated SLB event. It can be shown that the force on an orifice plate (e.g., a TSP) resulting from the transient, blowdown-type flow of a compressible fluid in a pipe can be calculated from a form loss coefficient and the time dependent local fluid conditions. The orifice pressure drop is equal to a loss coefficient times the fluid dynamic head. The RELAP5 code has been used for dynamic analysis of two-phase blowdown flow resulting from a postulated SLB event and is used to generate the relevant hydraulic

conditions. The TSP form loss coefficients for the support plates were calculated using conventional formulations, and input into the RELAP5 model for the base case analysis. The form loss coefficients and the hydraulic conditions calculated using the RELAP model were input to a post processor to calculate the individual TSP pressure drop vs time histories, which are the basis for TSP loads. The final TSP loads were determined by adjusting the base case results for the final form loss factors and the results of the sensitivity studies (Sections 4.5 and 5.3) to provide a conservative load basis for the TSP deflection analysis.

Loss coefficients, based on Westinghouse laboratory test data that correlate the loss coefficient to the flow area ratio for different tube support plates were utilized to determine the final, conservative pressure drop for each TSP. Figure 4-4 shows the test data and the correlation of the loss coefficient for determining the pressure drop through a TSP. The correlation constant ranges from [ ]$^{a,c}$, and its best estimate is [ ]$^{a,c}$.

The support plate loss coefficient correlation for the Westinghouse data, Figure 4-4, is incorporated into the Westinghouse steam generator performance analysis codes. The calculation of circulation ratio by these performance codes supports the validity of this correlation. The circulation ratio depends on the total pressure drop through the circulation loop, which consists of the downcomer, tube bundle and the primary moisture separators. The downcomer has a small pressure drop; thus, the major pressure drops come from various TSPs and swirl vanes of the primary moisture separator. Figure 4-5 shows the excellent prediction of the circulation ratio by the GENF Code using the correlation for the TSP loss coefficients compared to the test data, indicating that the use of the test-based form loss coefficients for the TSPs is appropriate.

Table 4-2 compares the loss coefficients calculated using the correlation of Westinghouse test data with those calculated by MPR and input to RELAP5. The letter designations of the support plates appearing in the left hand column are identified in Figure 4-1. HL and CL refer to the section of the TSP on the hot leg and cold leg side of the tube lane, respectively. The loss coefficients are displayed for flow in both the forward (up/positive) and reverse (down/negative) direction. For some plates, the two loss coefficients are different based on the MPR calculation since different approach areas were assumed, depending on the direction of flow. The loss coefficients based on the test data are not significantly different than those calculated by conventional formulations; however, the test based loss coefficients are somewhat more conservative for calculation of the TSP loads.

## 4.5 RELAP5 Model Sensitivity Studies

The RELAP5 model and operating conditions described in the previous sections form the base case for TSP loads. In order to determine the effects of some of the key modeling and operating condition assumptions inherent in the base case, a sensitivity study was performed. The results of this study were used to develop a multiplier for the base case

TSP loads which would assure that conservative TSP loads were used for the structural analysis.

The sensitivity analyses were performed for the main steam line break analysis from hot standby conditions because these conditions resulted in the highest loads on the support plates (see Reference 4-1). The study included the specific analysis cases described below. The detailed results from these cases are discussed in Section 5.3.

Model D4 RELAP5 Model Options

The RELAP5 code has been previously utilized to calculate the TSP loads for the model D4 SGs in support of implementation of high voltage ARC implementation at Plants AA and AB. During that effort, the analysis options, which determine details regarding the solution technique to be used by RELAP5, were set differently than those used for the current base case analysis of the Model E2 SG. This analysis case repeats the Model E2 analysis using the same options that were used for the Model D4 SG analysis. The differences in the analysis options selected for the two models of steam generators are summarized in Table 4-1.

Westinghouse TSP Loss Coefficients

The baseline analyses utilized calculated loss coefficients for the tube support plates. Subsequent to these analyses, Westinghouse provided design loss coefficients for all tube support plates to MPR Associates,Inc. This analysis case uses the Westinghouse loss coefficient correlation of Figure 4-4 to determine the effect of this parameter on the TSP loads.

Increase in Break Flow

In order to determine the sensitivity of the TSP pressure drop results to the magnitude of the break flow rate, the break flow rate was arbitrarily increased by both ten and twenty percent.

Thin Support Plate Control Volumes

The loads on the tube support plates are a result of the pressure difference across the tube support plate. For a transient analysis, the pressure difference between two control volumes calculated by RELAP5 includes terms in the momentum equation that are not directly applied to the support plates. Therefore, the direct use of the pressure difference between the adjacent control volumes may result in a significant over-estimate of the load on the tube support plate. The Model E2 base case analysis utilized the density and the velocity of the fluid mixture passing through a support plate to determine the load on the support plate, given the loss coefficient. The prior Model D4 analysis used thin control volumes adjacent to the support plates so that the pressure difference could be calculated

directly. This analysis case uses the Model D4 approach to calculate the loads on the support plates for comparison to the Model E2 base case analysis results.

Low Water Level

The steam line break from the baseline, hot standby conditions assumed the water level was at the normal level of 530 inches above the tube sheet. Since support plate loads tend to increase with reduced water level, this analysis case assumed the initial water level is at 503 inches above the tubesheet. This water level is a lower bound of the expected range, based on measurement uncertainties.

Model Radial Discretization

The baseline cases assume one-dimensional flow in the tube bundle by specifying a single flow path in the upper tube bundle (see Figure 4-1, control volumes 39-34). To determine the effect of radial variations of the fluid conditions in the tube bundle, three control volumes near the top of the tube bundle were subdivided radially for this analysis case. The nodes added to the upper bundle model are shown in Figure 4-6. This analysis case permits examination of the effects of radial pressure variation on TSP pressure drop.

Reduced Time Step

The time step was reduced by a factor of ten for this analysis to confirm that the time step selected for the baseline analysis was small enough to provide accurate results.

Revised Separator Model

A simple separator model was used for the baseline analyses. The separator model specifies the outlet quality at the junctions leaving the separator as a function of the void fraction in the separator volume. In particular, the outlet quality varies linearly between zero and one as a function of the void fraction. The end points of the linear variation are specified as input parameters to the separator model. This analysis case selects a different set of endpoints for the linear variation to determine the sensitivity of the results to the separator model used.

## 4.6 References

1. MPR-1884 Rev. 0, Hydraulic Analysis of Postulated Steam Line Break for the Model E2 Steam Generator, November 1997.

2. MPR-1918 Rev. 0, Sensitivity Analysis for the Hydraulic Analysis of Postulated Steam Line Break for the Model E2 Steam Generator, February 1998.

3. WCAP-14707, Model 51 S/G Limited Tube Support Plate Displacement Analysis for Dented or Packed Crevices, August, 1996.

4. WCAP-14273, Technical Support for Alternate Plugging Criteria with Tube Expansion at Tube Support Plate Intersections for Braidwood-1 and Byron-1 Model D4 Steam Generators, February 1995. (Addendum 1 used RELAP5 TSP loads)

## Table 4-1

## RELAP5/MOD3 Option Selection

| | Model E2 Simulation (Baseline Model in Reference 1) | Model E2 Simulation (Using D4 Options for Sensitivity Study in Reference 2) |
|---|---|---|
| **Parameters for Volumes** | | |
| Thermal front tracking | off | off |
| Mixture level tracking | off | off |
| Water packing scheme | on | on |
| Vertical stratification model | on | on (except nodes 30 & 31) |
| Interphase friction | rod bundle correlation in tubed region, pipe correlation elsewhere | rod bundle correlation in tubed region, pipe correlation elsewhere |
| Wall friction | on | on (except nodes 32 & 33) |
| Non-equilibrium - Tube bundle | off (i.e., Equilibrium) | off (i.e., Equilibrium) |
| Non-equilibrium - Downcomer | on | off (i.e., Equilibrium) |
| Non-equilibrium - Rest of model | on | on |
| **Parameters for Junctions** | | |
| Modified energy equation PV term | off | off |
| Counter current flow limit (CCFL) | off | off |
| Horizontal stratification | off | off |
| Choking | on | on (except primary side nodes & one of preheater baffle) |
| Abrupt area change | off | off |
| Non-homogeneous | on (except at break, junction 27)) | on (except at break, junction 27) |
| Momentum flux | on | on |
| Separator junction | default | default |

## Table 4-2
## Comparison of Westinghouse and Calculated TSP Loss Coefficients

a,c

| | | | | |
|---|---|---|---|---|
| | | | | |
| | | | | |
| | | | | |
| | | | | |
| | | | | |
| | | | | |
| | | | | |
| | | | | |
| | | | | |
| | | | | |
| | | | | |
| | | | | |
| | | | | |
| | | | | |
| | | | | |
| | | | | |
| | | | | |
| | | | | |
| | | | | |
| | | | | |

**Figure 4-1. Schematic of Model E2 Steam Generator**
(Secondary Side Fluid Nodes Shown)

a,c

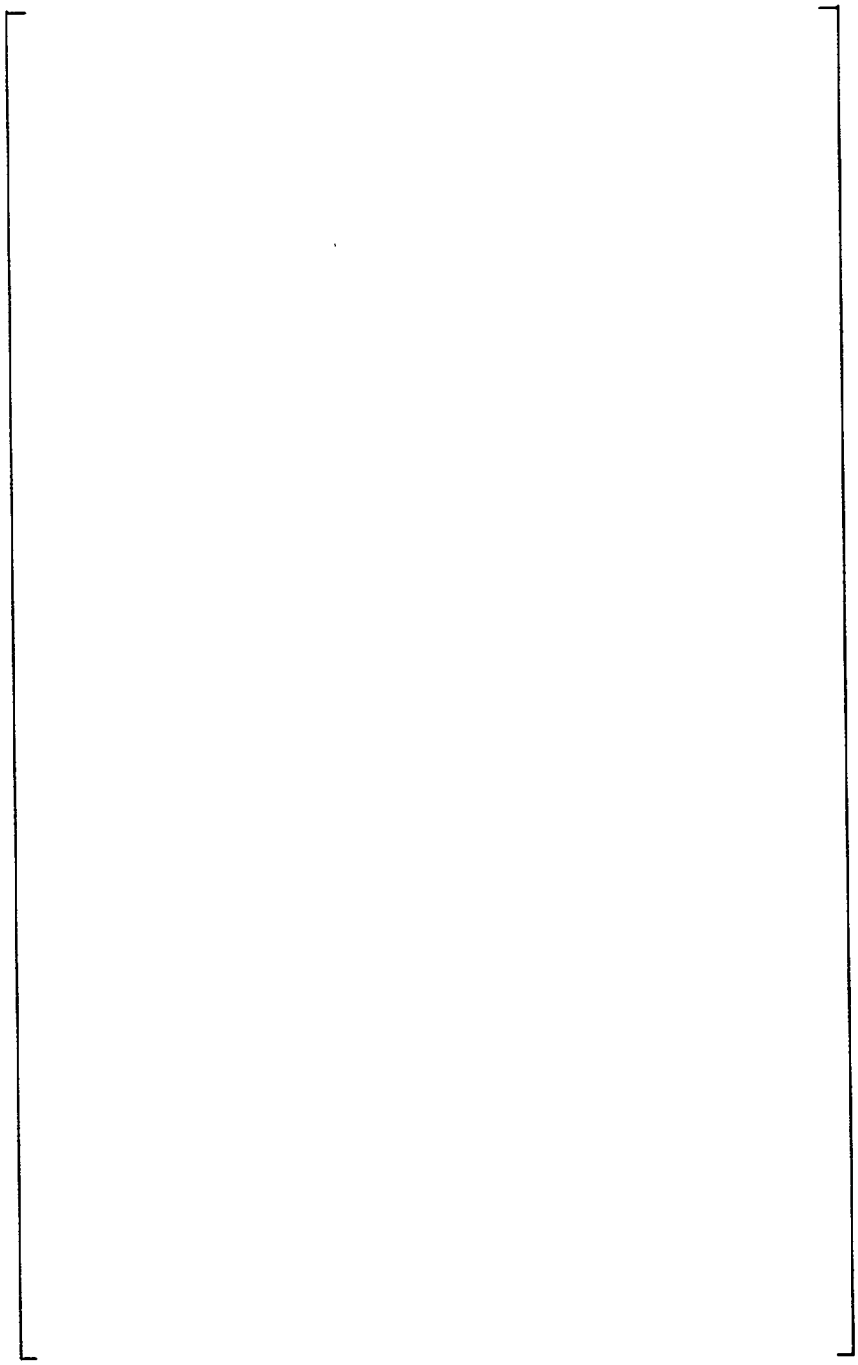

a,c

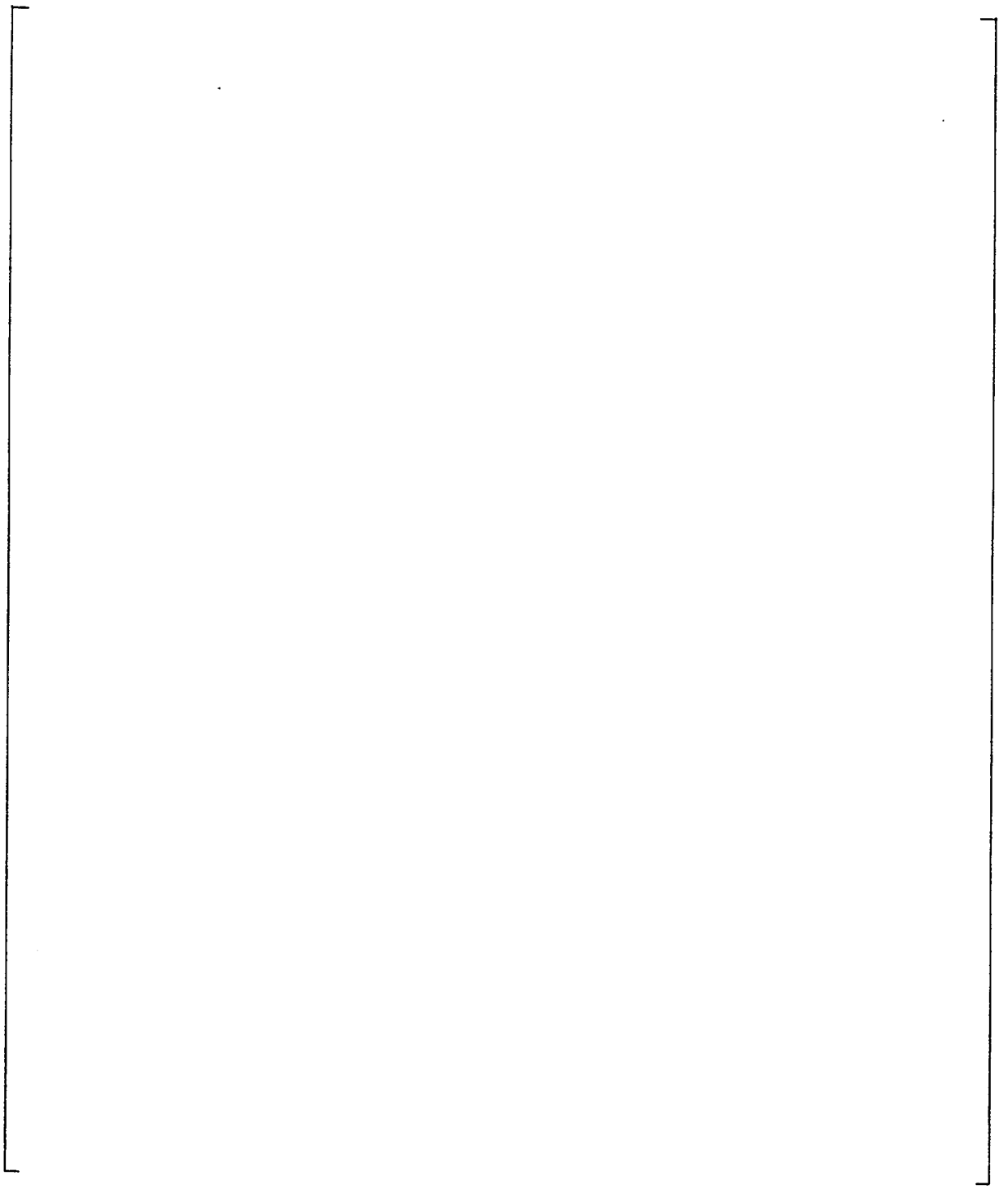

**Figure 4-2. Model E2 S/G Computer Model; Tubes and Primary Side**

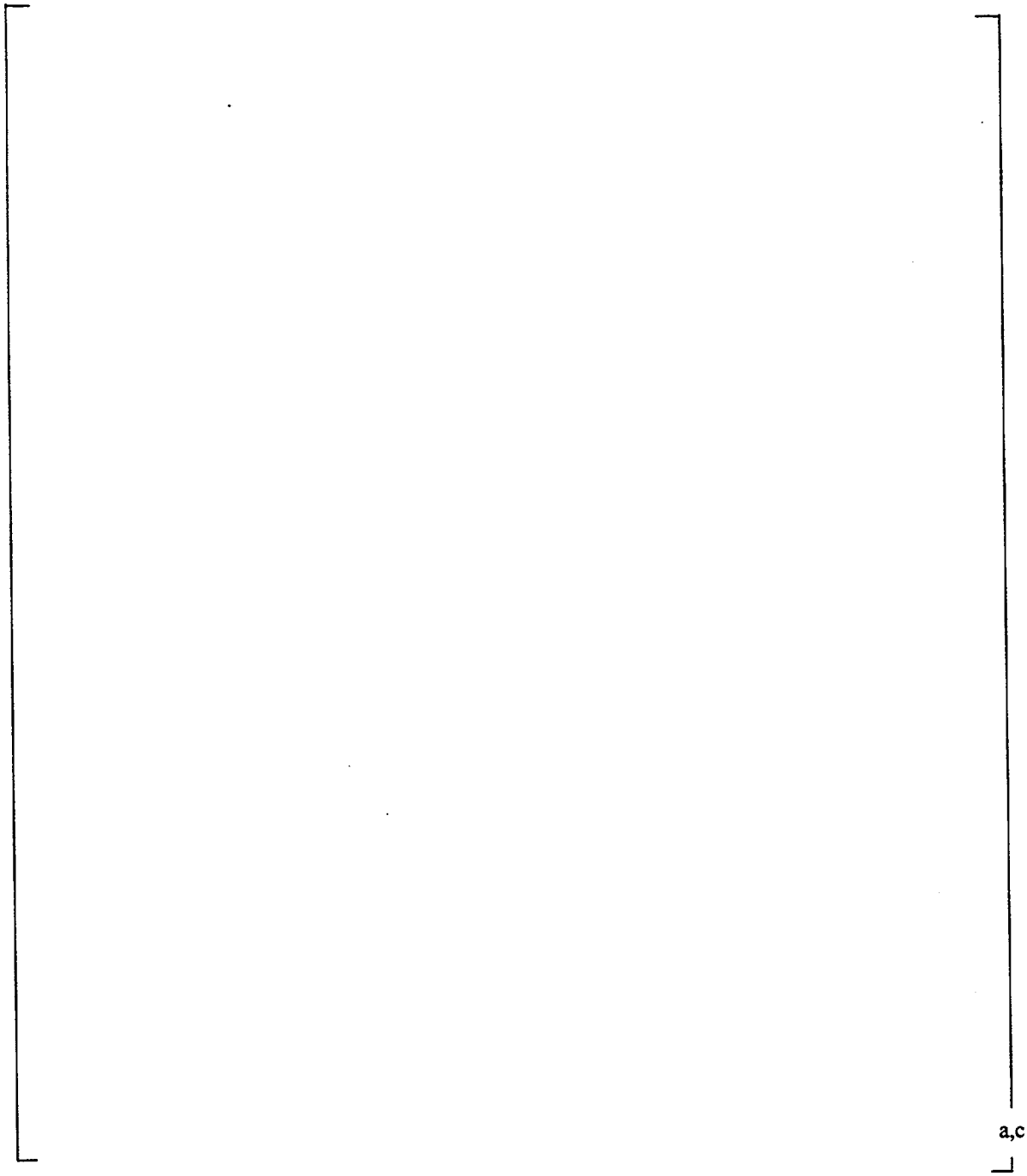

a,c

**Figure 4-3. Model E2 S/G - Secondary Side**

a,c

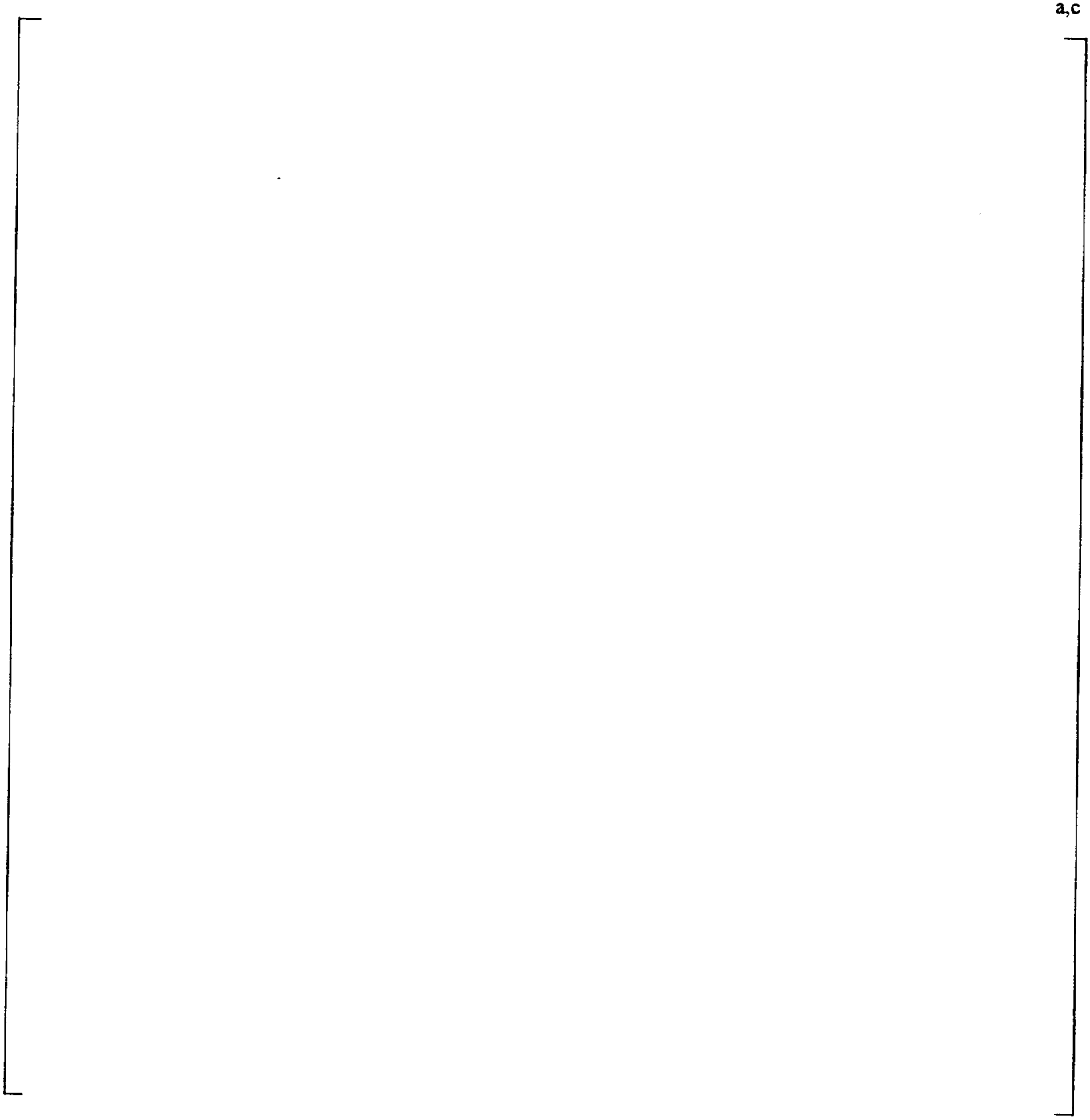

**Figure 4-4. Test Data Correlation for TSP Loss Coefficients**

a,c

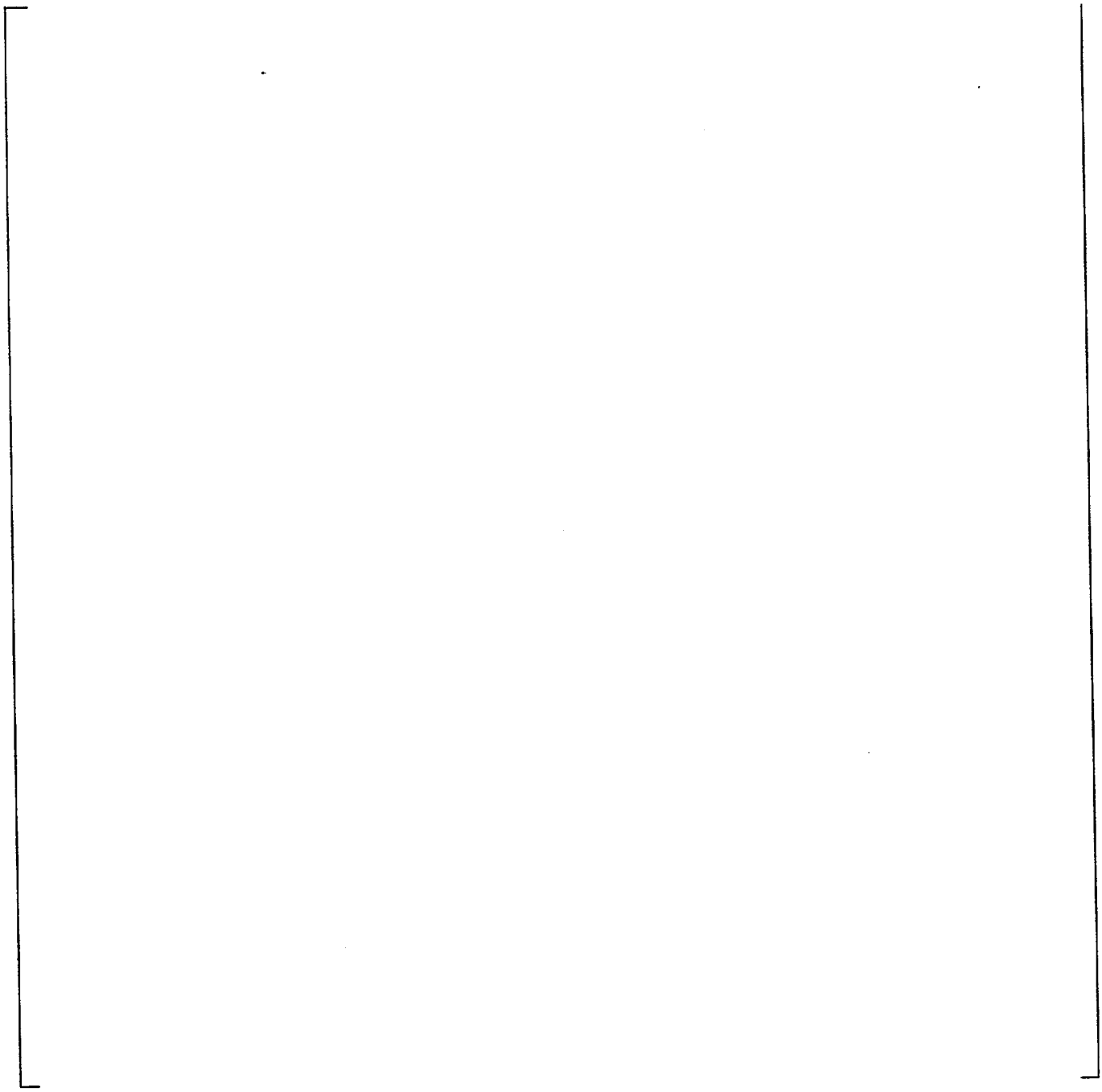

**Figure 4-5. GENF Verification, Circulation Ratio vs. Load**

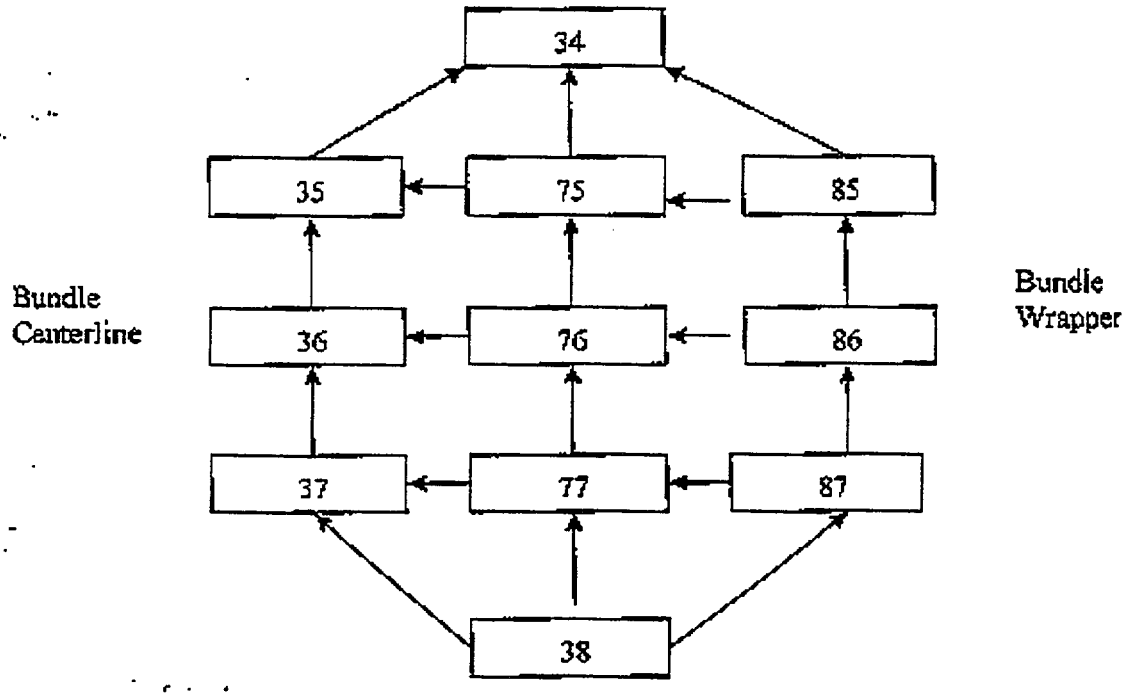


**Figure 4-6. RELAP5 Model E2 S/G Radial Discretization**

# 5.0 STEAM LINE BREAK HYDRAULIC LOADS ON TUBE SUPPORT PLATES

## 5.1 Analysis Plan

The load on a tube support plate is proportional to the hydraulic pressure drop across the TSP. The pressure drop across each plate during a SLB event is calculated using the RELAP5/MOD3 computer code as described in Section 4. Extensive RELAP5 analyses were performed to determine the TSP hydraulic loading and to assess its sensitivity to various analysis and modeling options. The results of these analyses are reported in this section.

The RELAP5 analyses included two base case analyses for a SLB, (a) initiated from both hot standby and (b) initiated from full power conditions. A sensitivity study was performed to determine the effects of some of the key modeling and operating condition assumptions inherent in the base case. The sensitivity study was performed using only the hot standby initial conditions as the base case since this case leads to higher TSP loads. The results of the sensitivity study were used to develop an adjustment factor for the base case TSP pressure drop to assure that conservative TSP loads were input to the structural analysis.

The adjustment factor was applied to the TSP pressure differentials generated for the case with the Westinghouse TSP loss coefficients as described in Section 4. The Westinghouse loss coefficients are based on test data, and are more conservative (see Table 4-1), resulting in higher, more conservative TSP loads. The TSP bounding reference loads are used to develop the bounding TSP displacements discussed in Section 7.

A summary list of the RELAP5 analyses performed, including base cases and sensitivity studies, is given in Table 5-1. A detailed description of each of these evaluations is provided in Section 4.

## 5.2 Base Case Analyses

Prior to initiating the SLB transient, a steady state condition was established for a period of time. For the full power case, two key design operating parameters, circulation ratio and primary temperature difference, were shown to be established to define the steady state condition. The steady state RELAP5 conditions, using the calculated loss coefficients, are compared to the steady state design values for these parameters.

| | **Design** | **RELAP5 Model** | **Difference** |
|---|---|---|---|
| Circulation Ratio | [ ]$^{a,c}$ | [ ]$^{a,c}$ | 0.0% |
| Primary Coolant ($T_{hot}$ - $T_{cold}$) (°F) | [ ]$^{a,c}$ | [ ]$^{a,c}$ | 3.9% |

For the case using the Westinghouse, test-based loss coefficients, the calculated circulation

ratio was [ ]$^{a,c}$.

The comparison for both the circulation ratio and the primary coolant temperature drop is good and shows that the modeling accurately represents the actual steam generator. Good agreement for the circulation ratio for both the calculated loss coefficients and the Westinghouse test-based loss coefficients indicates that the secondary side flow paths include the proper distribution of flow resistance. The exact agreement for the circulation ratio using the calculated loss coefficients is considered fortuitous based on the models for the remainder of the recirculation loop. Good agreement for the primary coolant temperature drop indicates that the total heat transfer load is calculated properly.

The steam line break was simulated by a 10-millisecond ramp reduction in the boundary pressure downstream of the steam nozzle, after a good steady state solution had been established. The following sections summarize the results of the base case analyses using the calculated loss coefficients, including the pressure drop across each of the tube support plates. Figure 5-1 shows the location and identification of each of the TSPs.

### 5.2.1 Results for a Break from Full Power

Figure 5.2 shows the steam generator secondary side pressure (See Figure 4.3 for node definition) for a break from full power, and Figure 5.3 shows the corresponding break flow from the steam generator for the same transient. Figures 5.4 through 5.7 present the pressure differentials across the tube support plates for groups of tube support plates identified by letter. A suffix indicating hot leg (HL) or cold leg (CL) is added for plates with separate results for the two plate halves.

Positive pressure differentials represent the condition of upward flow; negative pressure differentials represent the condition of downward flow. Small oscillations in the pressure drop are related to numerical calculation variations resulting from the time step used for the analysis. A subsequent sensitivity evaluation (Section 5.3.7), which utilized a time step 1/10 the value used in this base case, showed that the small oscillations were generally not present with the smaller time step.

### 5.2.2 Results for a Break from Hot Standby

Figures 5.8 through 5.13 show the results for the base case of a SLB event initiated from hot standby conditions, also based on the use of the calculated loss coefficients. As in the case from full power, they include transient results for secondary side steam pressure, break flow and pressure differentials across the tube support plates and preheater baffles.

### 5.2.3 Comparison of Full Power and Hot Standby Initial Conditions

Table 5-2 summarizes the peak TSP pressure differential across each TSP from the analysis of transients discussed above. The peak pressure differences are listed for both of the base case transients. For most plates, the peak pressure difference is larger for the SLB event

initiating from the hot standby condition than that for the event initiating from the full power condition. This provides the basis for selecting the transient initiating from hot standby conditions as more limiting. Another observation from this comparison is that the flow split (between upflow and downflow in the bundle) occurs much lower in the bundle for the break from full power than for the break from hot standby. The plates in the preheater (plates B, D, E, G, H and K) experience widely different peak pressure differentials between the two base cases because of their significantly different flow resistances compared to the other plates, and because the flow split occurs within the preheater on the cold leg side of the bundle.

In general, the calculated tube support plate pressure differentials for the Model E steam generator are small when compared to previous analyses (Reference 1) which have been done for the Model D4 steam generators. The factors that contribute to this are

a) the larger flow areas through the tube support plates for the Model E SGs and
b) the ratio of the area of the break to the volume of the steam generator is considerably smaller for the Model E than for the Model D-4,.

The larger flow area through the TSPs results in lower flow resistance for the Model E. The smaller ratio of break area to volume for the Model E results in a somewhat slower depressurization and correspondingly lower velocities in the steam generator during the blowdown.

### 5.2.4 Characteristics of the Base Case Transients

Some of the characteristics of the SLB blowdown and tubes support pressure differences for the two base cases are noteworthy. The secondary pressure blowdown from full power, Figure 5.2, decreases in a steady fashion with few small oscillations. The break flow, Figure 5.3, also decreases steadily throughout the transient as the pressure difference across the flow limiter decreases. In contrast, the secondary pressure blowdown from hot standby, Figure 5.8, shows a break point at 2 seconds after the start of the transient, which is followed by small pressure oscillations about the mean decreasing pressure level. The break point at 2 seconds is the result of the two-phase mixture interface reaching the steam nozzle. The break flow rate, Figure 5.8, increases sharply at this 2 second mark, indicating a much higher density of the break flow through the flow limiter. The pressure oscillations after 2 seconds for the SLB initiated from hot standby conditions are interpreted to be the result of the sudden change in flow rate at the nozzle feeding back and forth through the bundle.

For the plates in the upper bundle, the pressure differential transients for the two base cases (full power and hot standby) are quite similar in character. The pressure differences for the upper bundle plates, plates M,N, P, Q and R (Figures 5-4 and 5-10), reach their peak before 0.5 seconds following the break and then decline to much lower values for the remainder of the transient. Small variations in pressure difference near the peak of the transient are negligible compared to the absolute peak value.

Early in time, the pressure difference transients for the lowest plates on the hot leg side,

plates A & C ( Figures 5.5 & 5.11), are free of large pressure spikes in the first half second following the initiation of an SLB event. This differs from the Reference 1 analyses for the Model D4 SG, which showed significant spikes for these plates in this time interval. These spikes are shown on Figure 5.14 and are repeated with an expanded time scale on Figure 5.15. The absence of spikes in the Model E analysis results is attributed to a well established steady state condition prior to the initiation of the transient.

## 5.3 Input Assumptions for Sensitivity Analyses

Table 5-1 summarizes the input assumptions for the sensitivity analyses and how these assumptions compare to the basis for the base cases. The objective of the sensitivity analyses was to determine a bounding factor that would conservatively envelop the calculational sensitivities. This factor would be applied to the more conservative of the base cases considered to assure that the load input for the TSP displacement analysis (Section 7) would be a conservative bounding basis.

For all of the sensitivity analyses, the SLB events were initiated from the hot standby condition since this case produces the highest and more conservative TSP loading. Table 5-3 summarizes the sensitivity studies by presenting the peak TSP pressure difference for each plate. All of the sensitivity study analyses listed in Table 5-1 are included, along with the base case initiated from hot standby using the calculated loss coefficients.

In the bottom portion of Table 5-3, the peak TSP pressure differences are normalized to the case run with Westinghouse TSP loss coefficients. As noted in section 5.1, this case was chosen as the reference base case to which the bounding multiplier was to be applied, since this case resulted in the most conservative TSP loads. In Table 5-3, all the normalized values remain below 1.5 with two exceptions:

1) The cold leg side of plate A for the thin control volume case (factor of [ ]$^{a,c}$),
2) Plate E for the low water level case (factor of [ ]$^{a,c}$).

Plate A typically has a small pressure differential, about 11% of the highest plate pressure differential in this analysis. As shown in Figure 5.16, the high peak value for the A-plate occurred during a pressure spike, which was not present in the base case analysis. The Plate E loads are about 13% of the highest loaded plate. Because both plates A-CL and E are low loaded plates, and because the factor for Plate A is based on a spike in the pressure drop curve, neither of these plates was considered in establishing the bounding sensitivity factor. It is noted that neither plate A nor plate E would be included in the application of the high voltage ARC. Plate A is the flow distribution baffle, and plate E is one of the baffle plates in the preheater in the cold leg of the steam generator.

A value of 1.5 was selected as the bounding multiplier, which would be applied to all TSP loads to account for potential calculational sensitivities. For all of the TSP location for which the high voltage ARC would be recommended, this multiplier bounds all of the peak pressure differences from the sensitivity study, in most cases by a significant ratio. For the

hot leg of plates C through M, the maximum observed factor is 1.34 for plate L for the low water level case. Therefore, the 1.5 multiplier for TSP loads, applied to the base case with Westinghouse loss coefficients, provides a conservative calculation load input basis for the TSP displacement analysis (Section7).

In addition to showing the effect of the input assumptions on the TSP peak pressure differences, it is of important to note that the character of blowdown and pressure difference transients were not significantly altered for any of the sensitivity study cases. The results of these sensitivity studies are presented in the following sections, using the results for plates P and Q. The results for plates P and Q, and the corresponding discussion of the sensitivity cases are typical for all of the plates. The results for all of the plates are contained in Reference 1. The results of each study listed in Table 5-1, are discussed in turn. A detailed description of the modeling changes and assumptions for each case are discussed in Section 4.5.

### 5.3.1 Model D4 RELAP Model Assumptions

Figure 5.17 compares the blowdown secondary pressure and leak rate for the baseline case with the case that incorporated the Model D4 modeling assumptions. The transients are seen to be essentially identical. Similarly, the pressure difference plots for the Q & R plates, Figure 5.18, differ only in minor details.

### 5.3.2 Westinghouse TSP Loss Coefficients

The TSP loss coefficient changes from the base line calculated values to Westinghouse test result values are small and the TSP pressure losses represent a small change in the blowdown process. As could be expected, the blowdown secondary pressure and leak rate are not materially affected, Figure 5.19. The pressure difference plots, Figure 5.20, confirm the peak pressure differences in Table 5-3, showing almost no effect of the Westinghouse loss coefficient for Plate R and a small increase in the Q plate pressure difference. Otherwise, the transients show the same characteristics.

### 5.3.3 Increase in Break Flow by 20%

Figure 5.21 shows the imposed 20% increase in break flow rate along with the expected increase in secondary pressure blowdown rate which results from it. The pressure difference transients, Figure 5.22, show the increased pressure differences across both the R & Q plates and the shorter transient time, which result from the increased break flow.

### 5.3.4 Thin DP Elements

The use of thin control volumes to determine the TSP pressure drop can lead to stability issues during the analysis. The results of this case demonstrate the appropriateness of using large control volumes, which include the support plate, and then extracting the TSP pressure difference using a post processor.

The blowdown parameters, Figure 5.23, do not change from the baseline. The pressure differences for this case were taken directly from the RELAP output, without post-processing. Figure 5.24 show that the pressure difference transients compare quite favorably with the base line case.

5.3.5 Reduced Water Level

Water level represents probably the most significant parameter affecting steam generator blowdown and TSP pressure difference. Figure 5.25 shows how a water level reduction from 530 inches to [ ]$^{a,c}$ inches affects the blowdown. (A water level of [ ]$^{a,c}$ inches is a lower bound of the expected range, based on measurement uncertainties.) The increase in break flow when the two-phase interface reaches the flow limiter is delayed. At this point the secondary steam pressure is lower, but only by about 30 psi. The lower mass and inertia in the bundle results in a higher fluid acceleration, causing a increase in the TSP pressure difference peak in the initial 0.5 seconds of the transient (Figure 5.26).

5.3.6 Radial Discretization

The addition of two radial nodes to three control volumes in the upper part of the bundle (see section 4-5 for model change description) had no material effect on the SLB transient and the radial variation of pressure difference across the plate was not significant. Figure 5.27 shows no discernible difference in the blowdown characteristics from the baseline. Figure 5.28 shows that the pressure difference transients for the P & Q plates are also unchanged. In addition, Figures 5.29 &30 show that the radial variation of pressure difference across these plates is not significant. This evaluation confirms that the one-dimensional treatment of blowdown in the tube bundle is appropriate for calculating TSP loads.

5.3.7 Time Step Reduction

Figure 5.31 shows that a factor of 10 reduction in time step has a minor impact on the blowdown leak rate, resulting in an insignificant change in the blowdown secondary pressure. The R & Q plate pressure differences, Figure 5.32, are not significantly impacted. This observation is typical for all of the plates as demonstrated by Figure 5.33, which shows similar results for plates L and M. The analysis using the smaller time step did not exhibit the small oscillations on the pressure drop curves; thus, these oscillations are interpreted to be an artifact of the numerical calculation with the larger time step. This conclusion applies for all of the plates; the results for the other plates are contained in Reference 1 and are similar to those shown in Figures 5.32 and 5.33.

5.3.8 Revised Separator Model

As could be expected, the separator model affects the break flow transient, Figure 5.34, since the separator model determines, in part, the quality and therefore density of the steam-water mixture reaching the steam nozzle. This small change in break flow has a minimal effect on secondary pressure blowdown rate and the R & Q plates pressure differences are virtually unaffected.

## 5.4 Conclusions

The evaluation of a postulated steam line break at the nozzle of a Model E steam generator, using the RELAP5 Code, has explored a wide range of input modeling and initial condition assumptions. The calculated TSP pressure difference transients, which are used to calculate the structural loads, are self consistent and show minor impacts from the various assumptions made. The TSP pressure difference transients for an SLB initiated from hot standby, are conservatively represented by the RELAP5 case using Westinghouse TSP loss coefficients. The use of these pressure differences with a 1.5 multiplier to calculate plate loadings is judged to conservatively bound the plate loadings which might occur during a postulated SLB event.

## 5.5 References

1. MPR-1918 Rev. 0, Sensitivity Analysis for the Hydraulic Analysis of Postulated Steam Line Break for the Model E Steam Generator, February 1998.

**Table 5-1**
**Matrix of RELAP Cases**

| Case | Initial Condition | Model Option | Loss Coeffi-cient | Break Flow | Water Level (inch) | Time Step (sec.) |
|---|---|---|---|---|---|---|
| **Base Cases** | | | | | | |
| Base Case -1 | Full Power | E | Calc. | Nom. | 530 | 0.001 |
| Base Case -2 | Hot Standby | E | Calc. | Nom. | 530 | 0.001 |
| **Sensitivity Study** | | | | | | |
| D4 S/G Model Options | Hot Standby | D4 | Calc. | Nom. | 530 | 0.001 |
| estinghouse Loss Coeff. | Hot Standby | E | Westing-house. | Nom. | 530 | 0.001 |
| Increased Break Flow | Hot Standby | E | Calc. | +10% | 530 | 0.001 |
| Increased Break Flow | Hot Standby | E | Calc. | +20% | 530 | 0.001 |
| Reduced Water Level | Hot Standby | E | Calc. | Nom. | 503 | 0.001 |
| educed Time Step | Hot Standby | E | Calc. | Nom. | 530 | 0.0001 |
| Radial Discretization | Hot Standby | E | Calc. | Nom. | 530 | 0.001 |
| Revised Separator Model | Hot Standby | E | Calc. | Nom. | 530 | 0.001 |

**Table 5-2**
**Comparison of Peak TSP Pressure Differences for Base Cases**

a,c

[

]

a,c

**Table 5.3 Maximum Pressure Differentials**

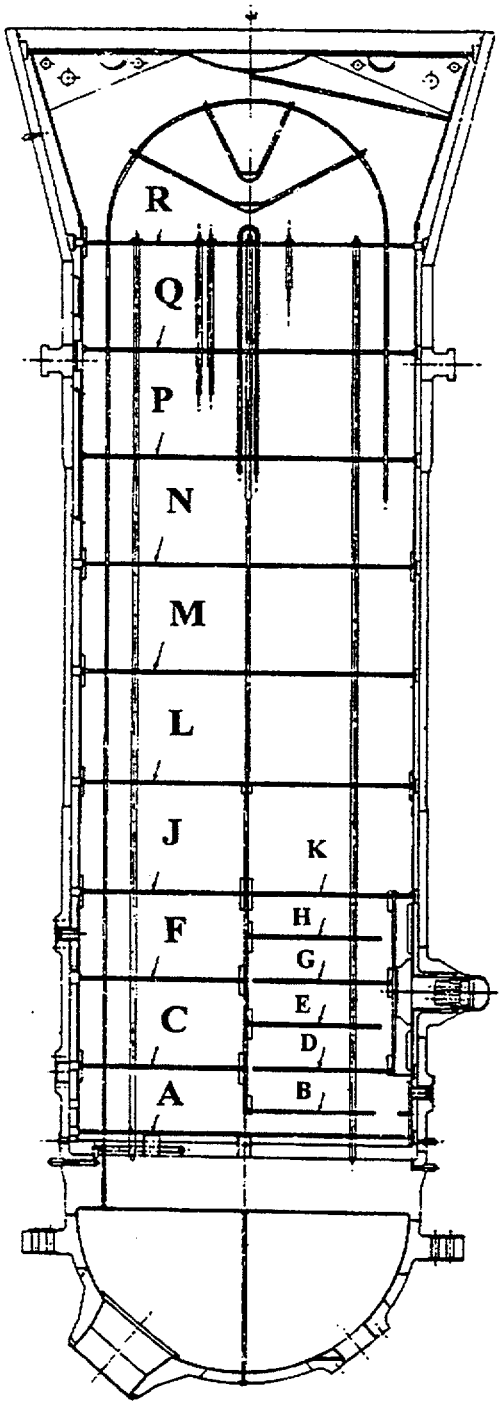


**Figure 5.1 TSP Letter Designations**

a

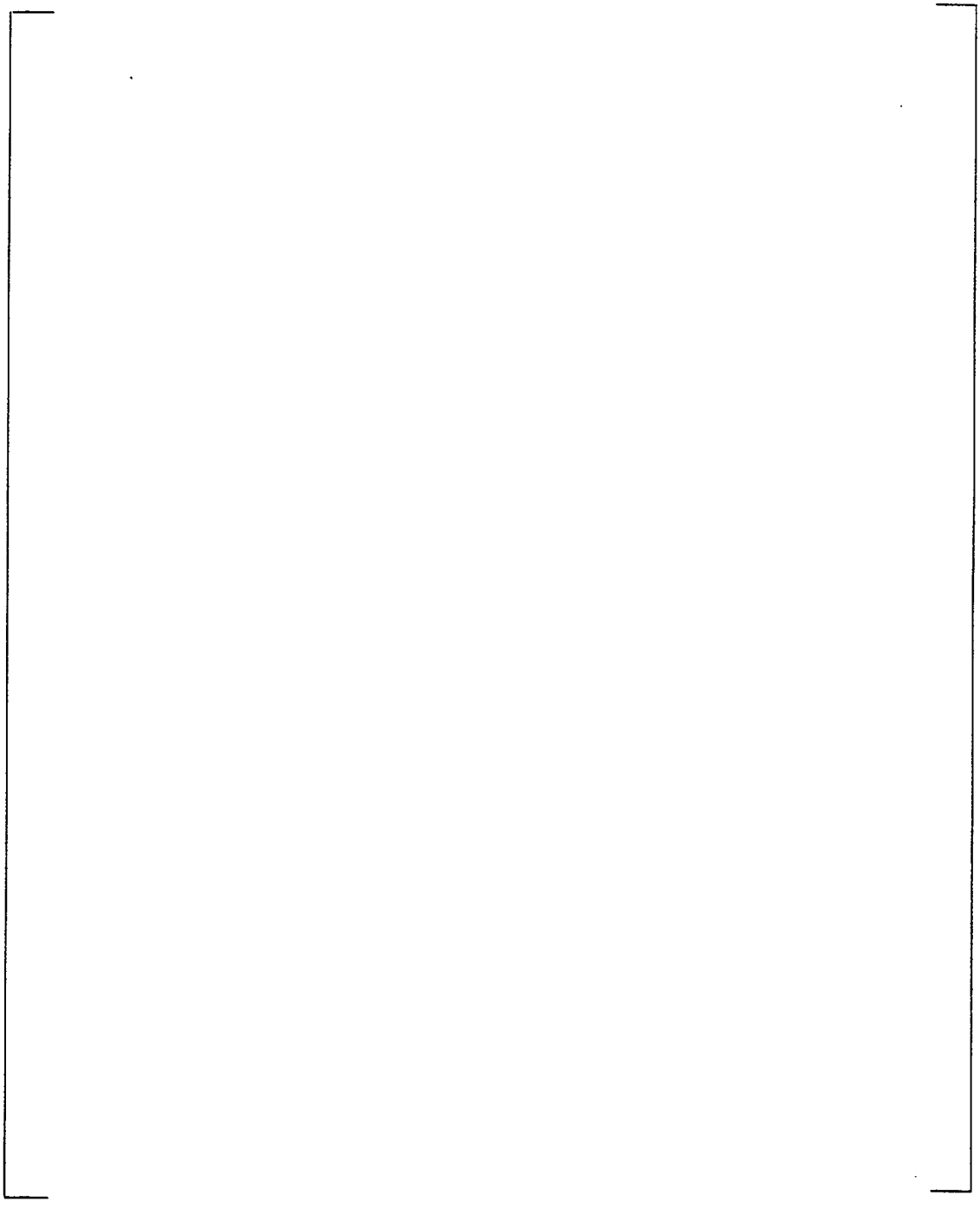

**Figure 5.2**
**Secondary Side Pressure at Top of S/G, Base Case SLB from Full Power**

a

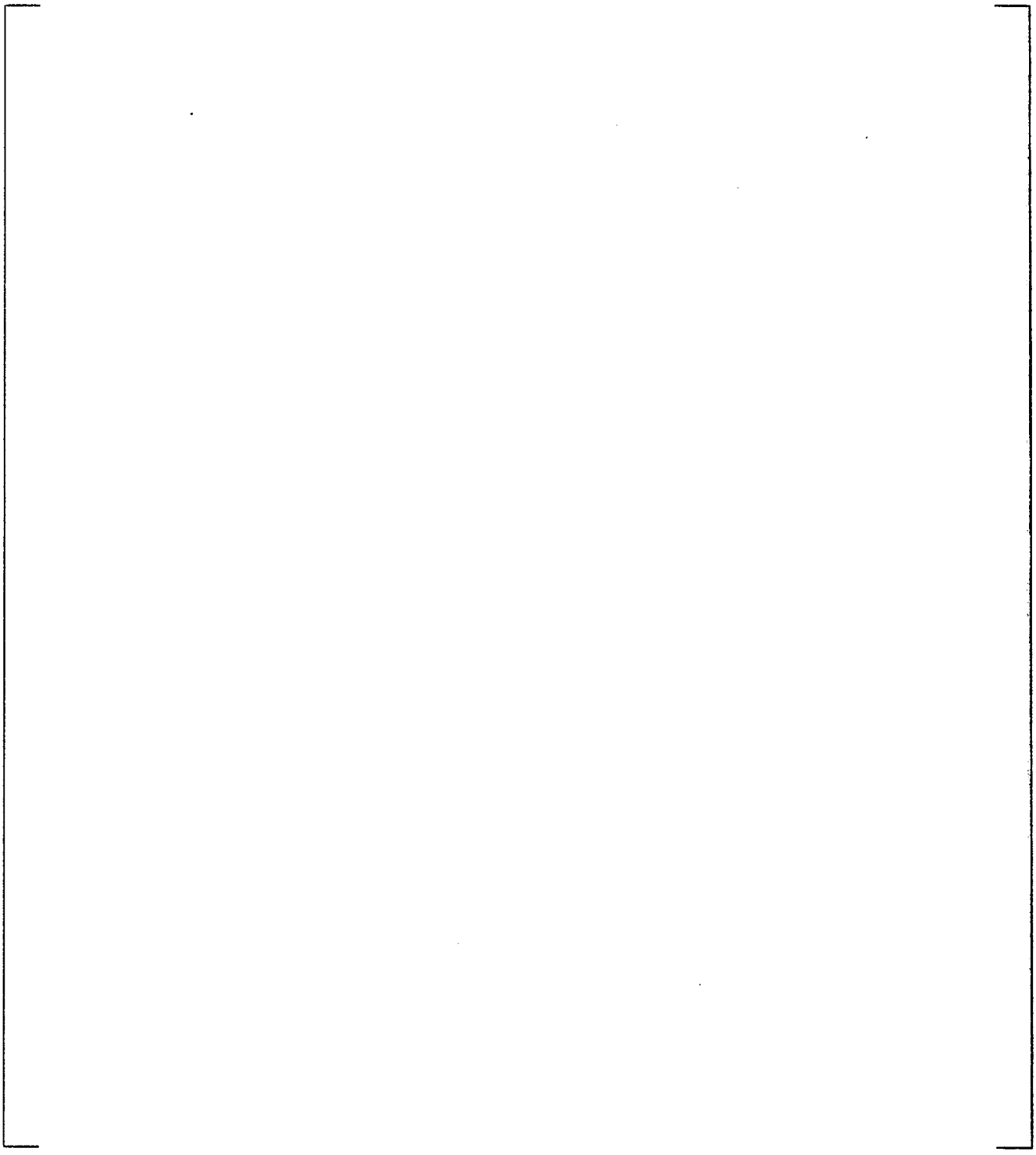

**Figure 5.3 Break Flow, Base Case SLB from Full Power**

a

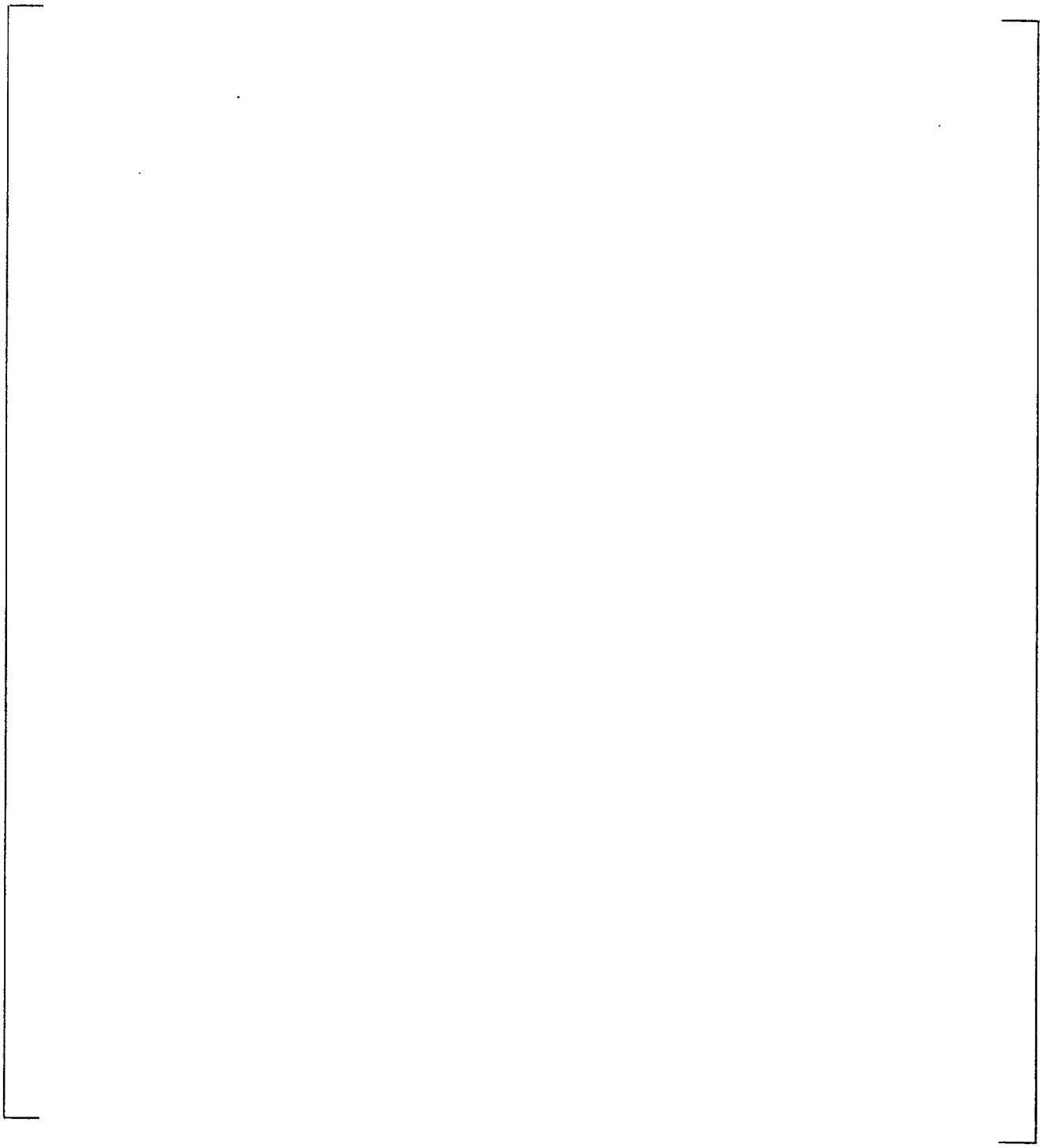

**Figure 5.4 TSP Pressure Drop SLB from Full Power, Plates M, N, P, Q, R**

a

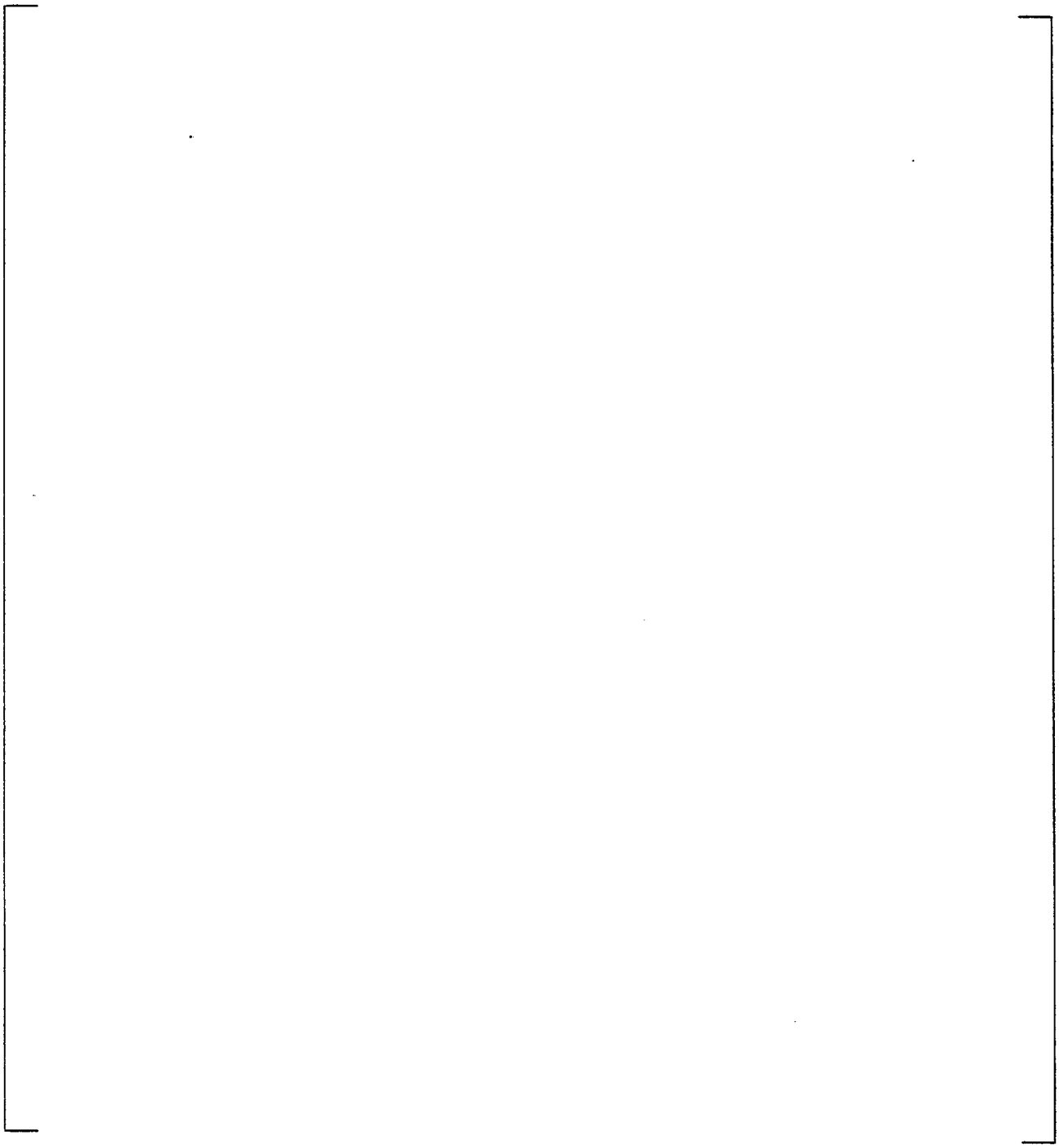

**Figure 5.5 TSP Pressure Drop SLB from Full Power, Plates A(HL), C, F, J, L(HL)**

a

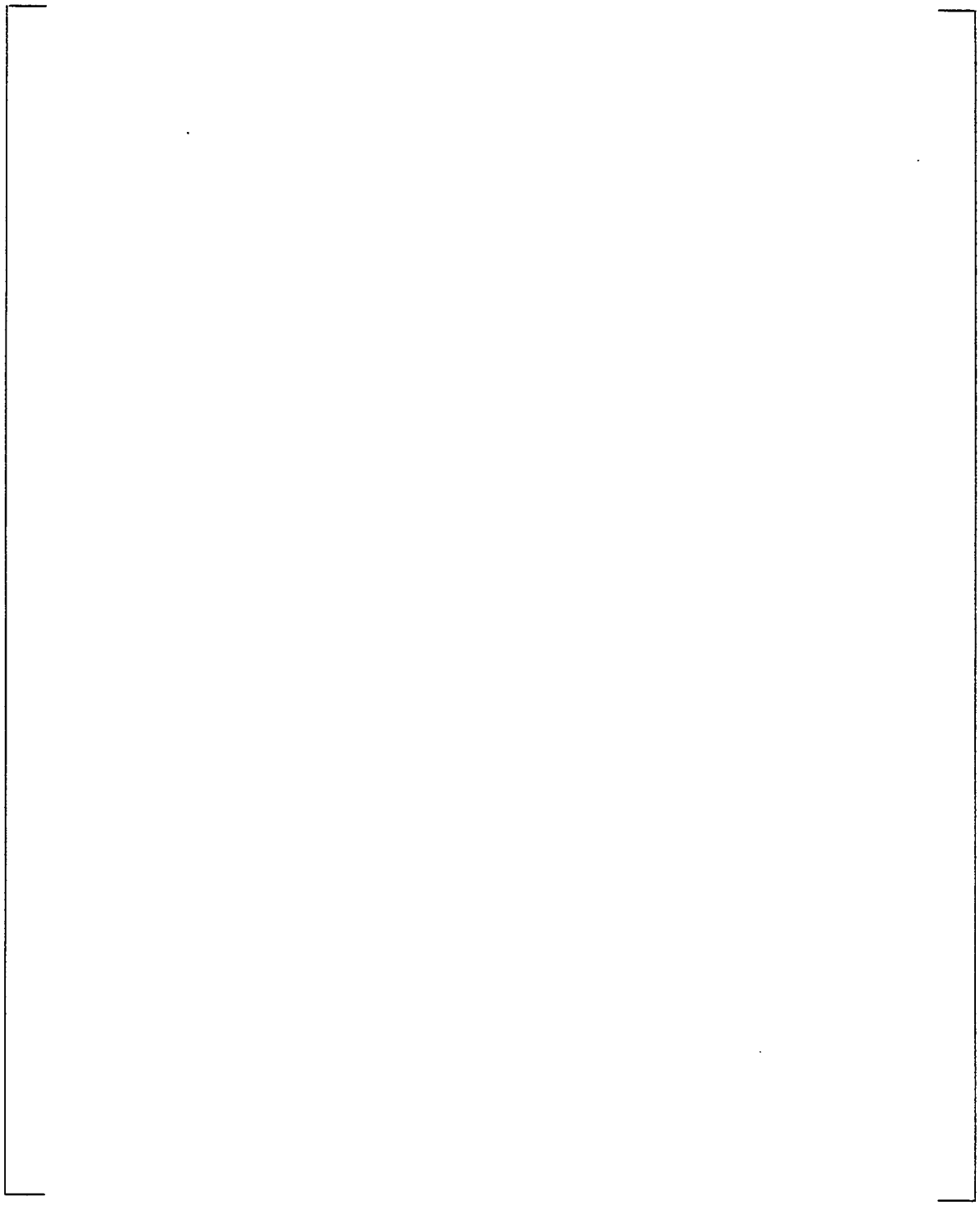

**Figure 5.6 TSP Pressure Drop SLB from Full Power, Plates G, H, K, L(CL)**

a

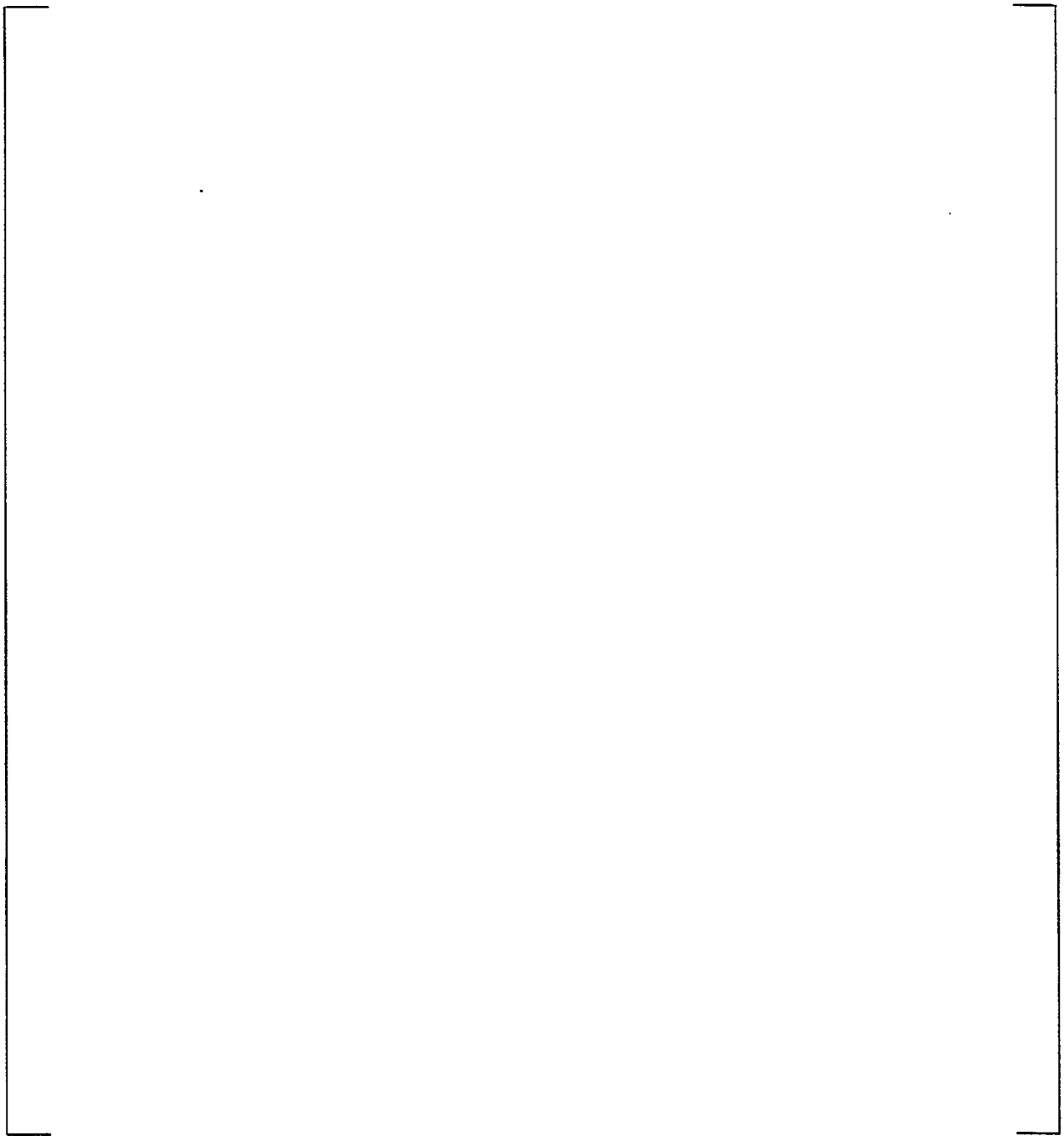

**Figure 5.7 TSP Pressure Drop; SLB from Full Power; Plates A(CL), B,D E**

a

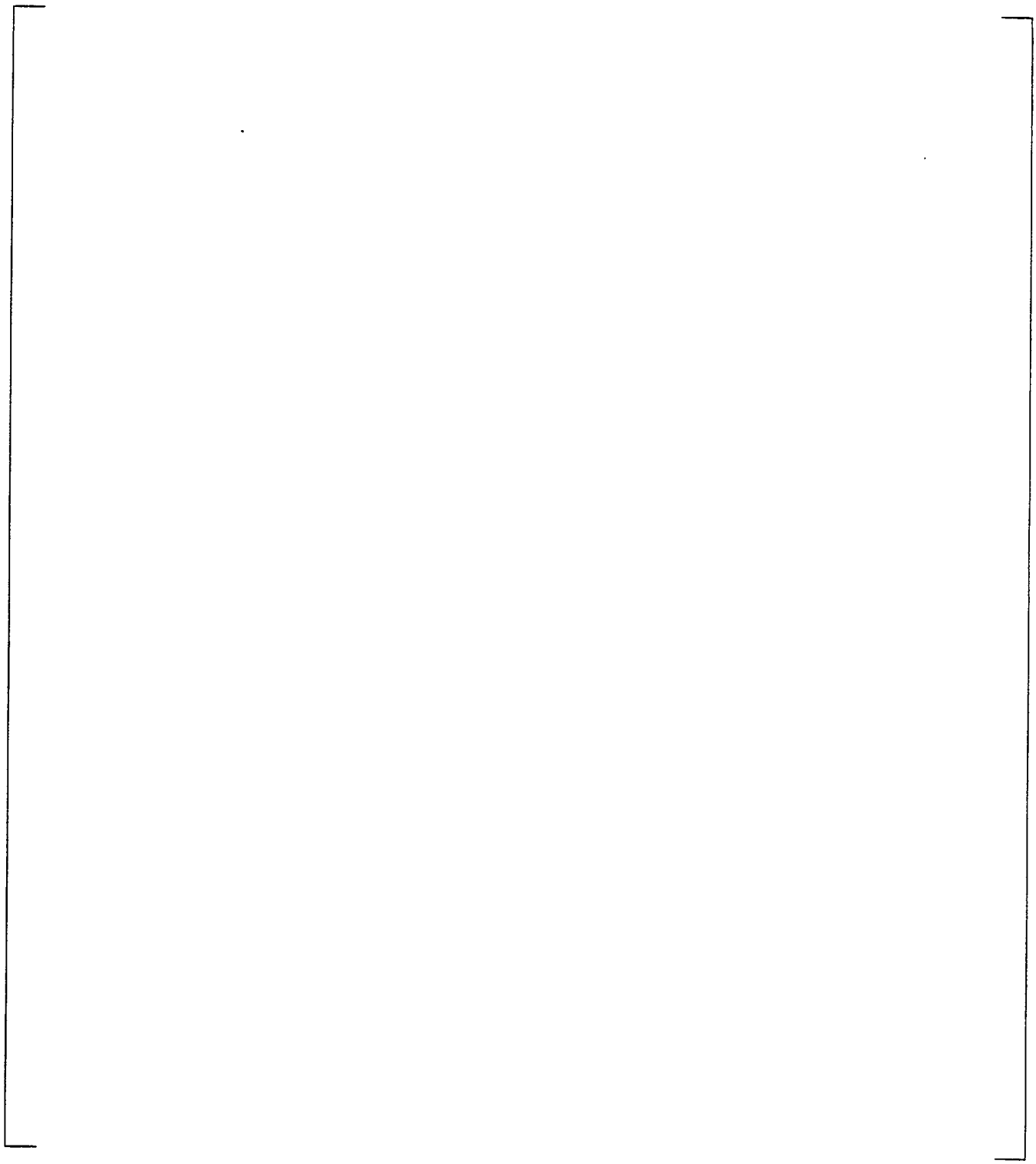

**Figure 5.8 Secondary Side Pressure at Top of S/G, Base Case SLB from Hot Standby**

a

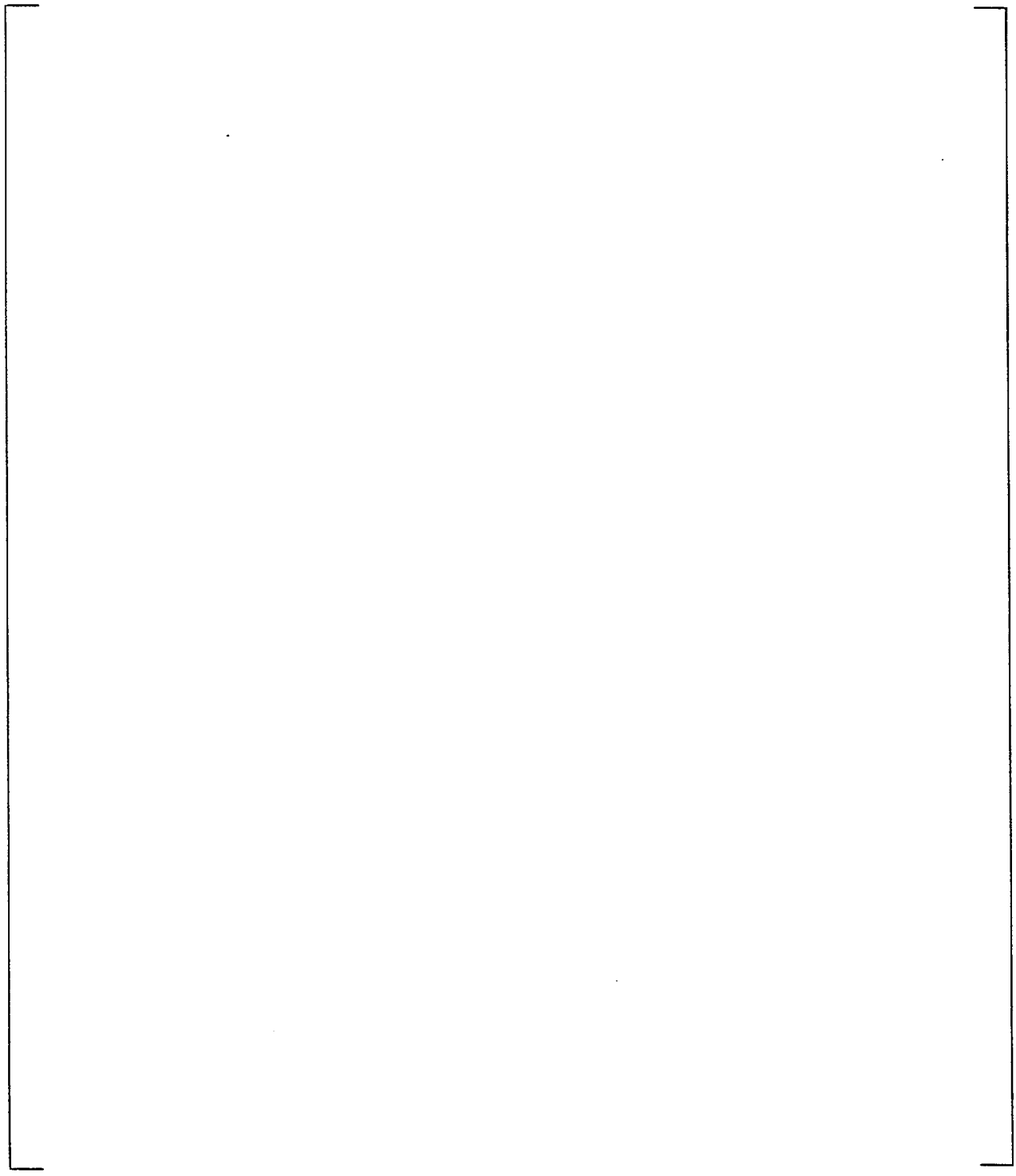

**Figure 5.9 Break Flow, Base Case SLB from Hot Standby**

a

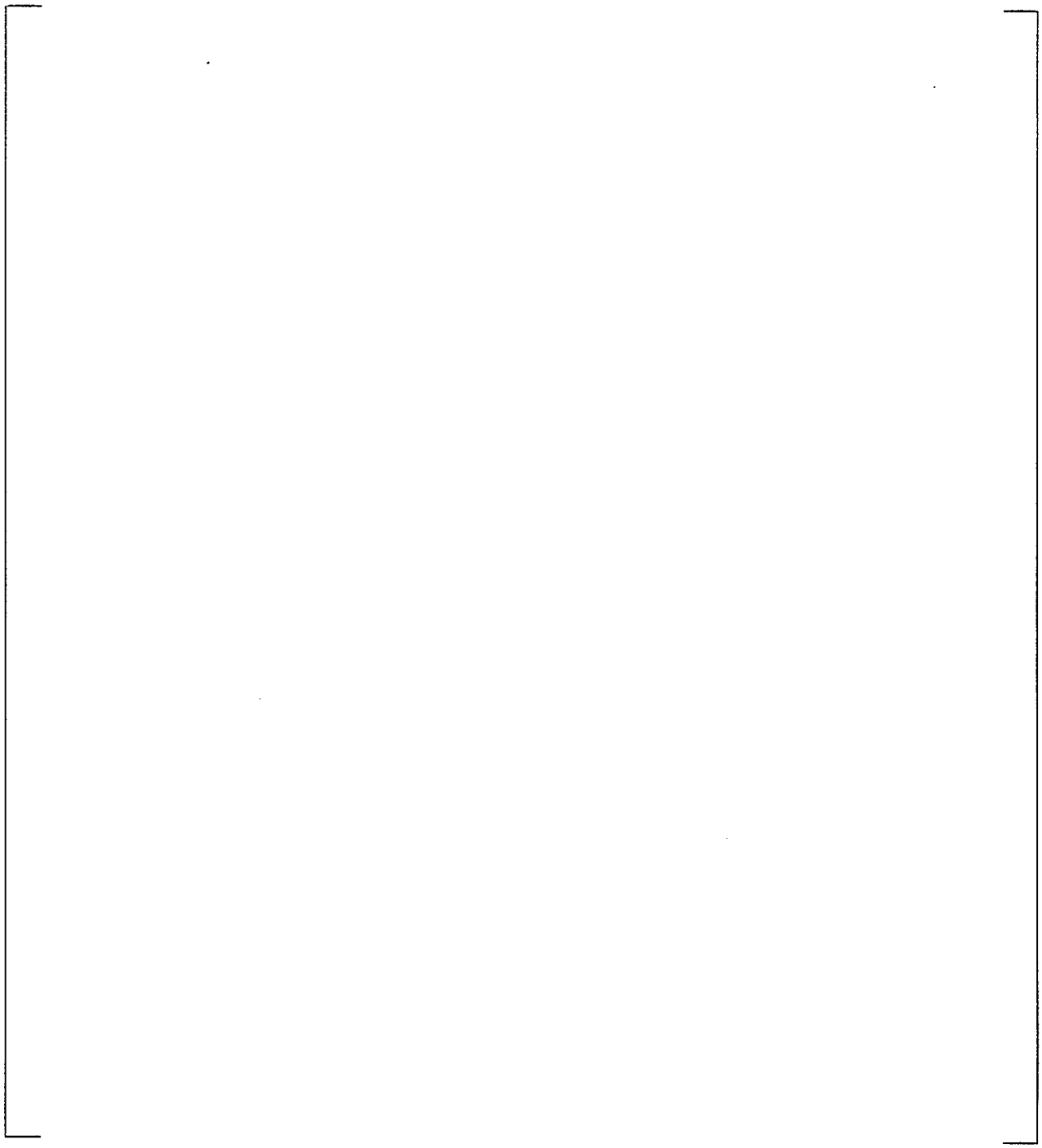

**Figure 5.10 TSP Pressure Drop SLB from Hot Standby, Plates M, N, P, Q, R**

a

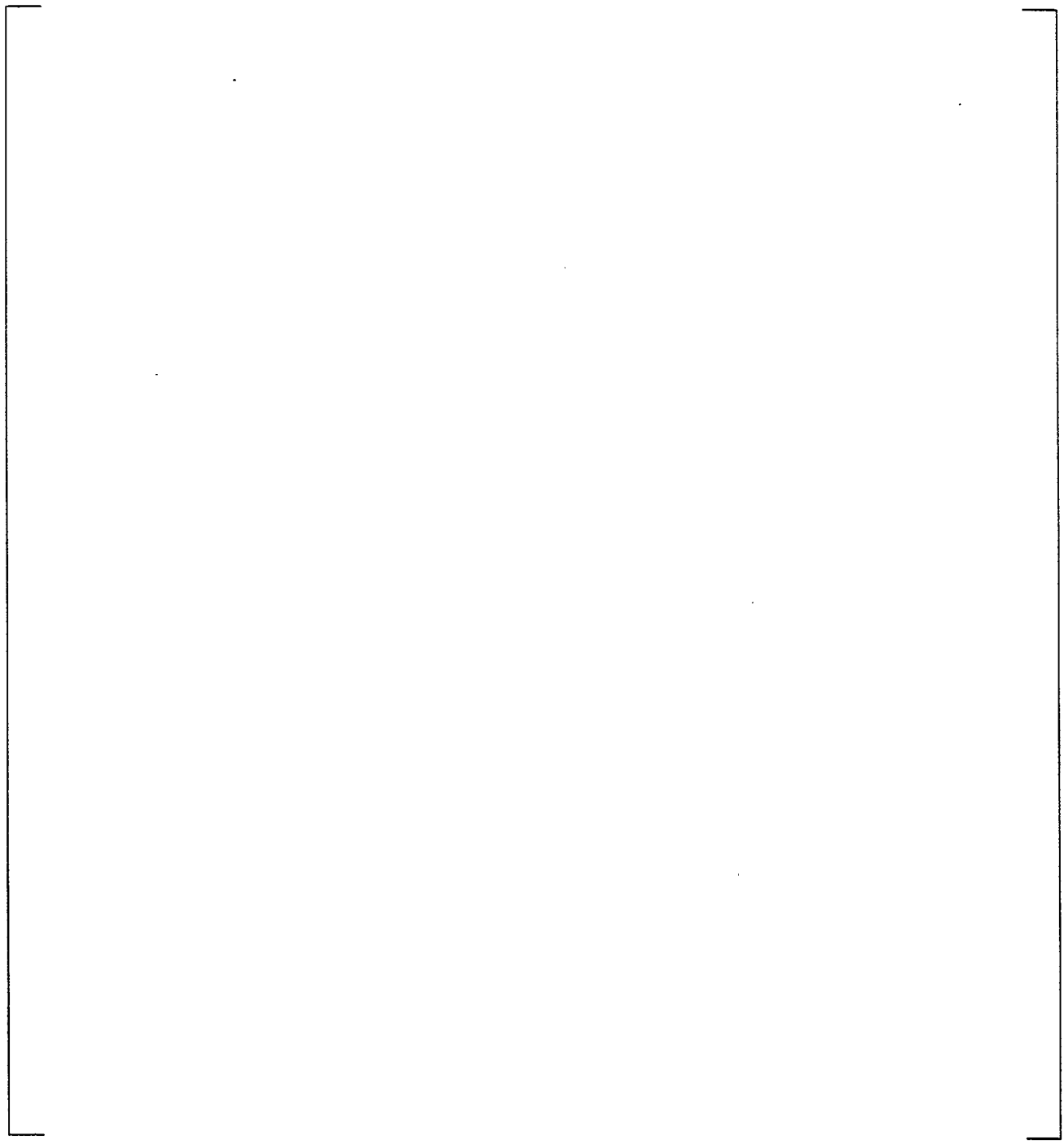

**Figure 5.11 TSP Pressure Drop SLB from Hot Standby, Plates A(HL), C, F, J, L(HL)**

a

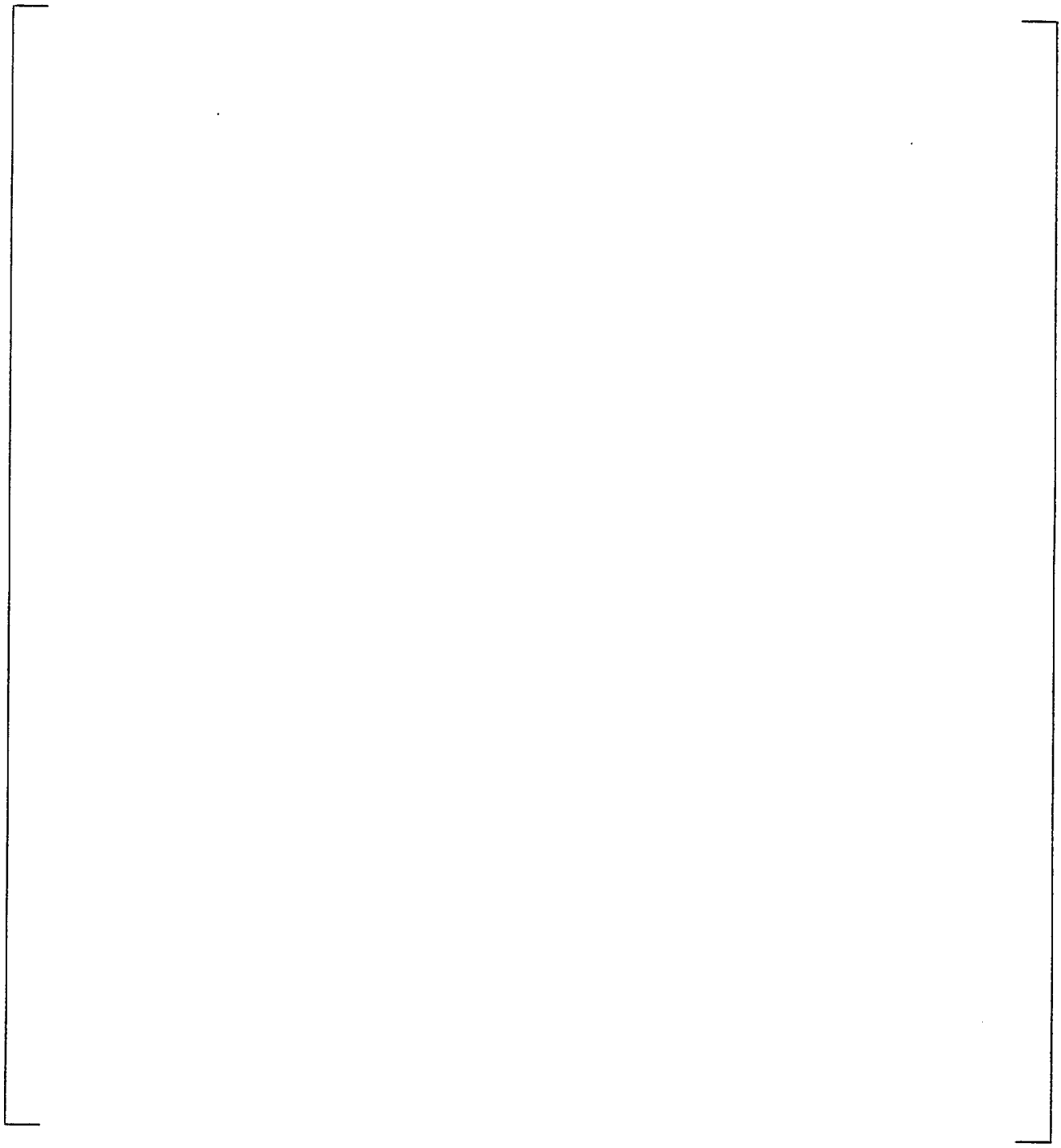

**Figure 5.12 TSP Pressure Drop SLB from Hot Standby, Plates G, H, K, L(CL)**

a

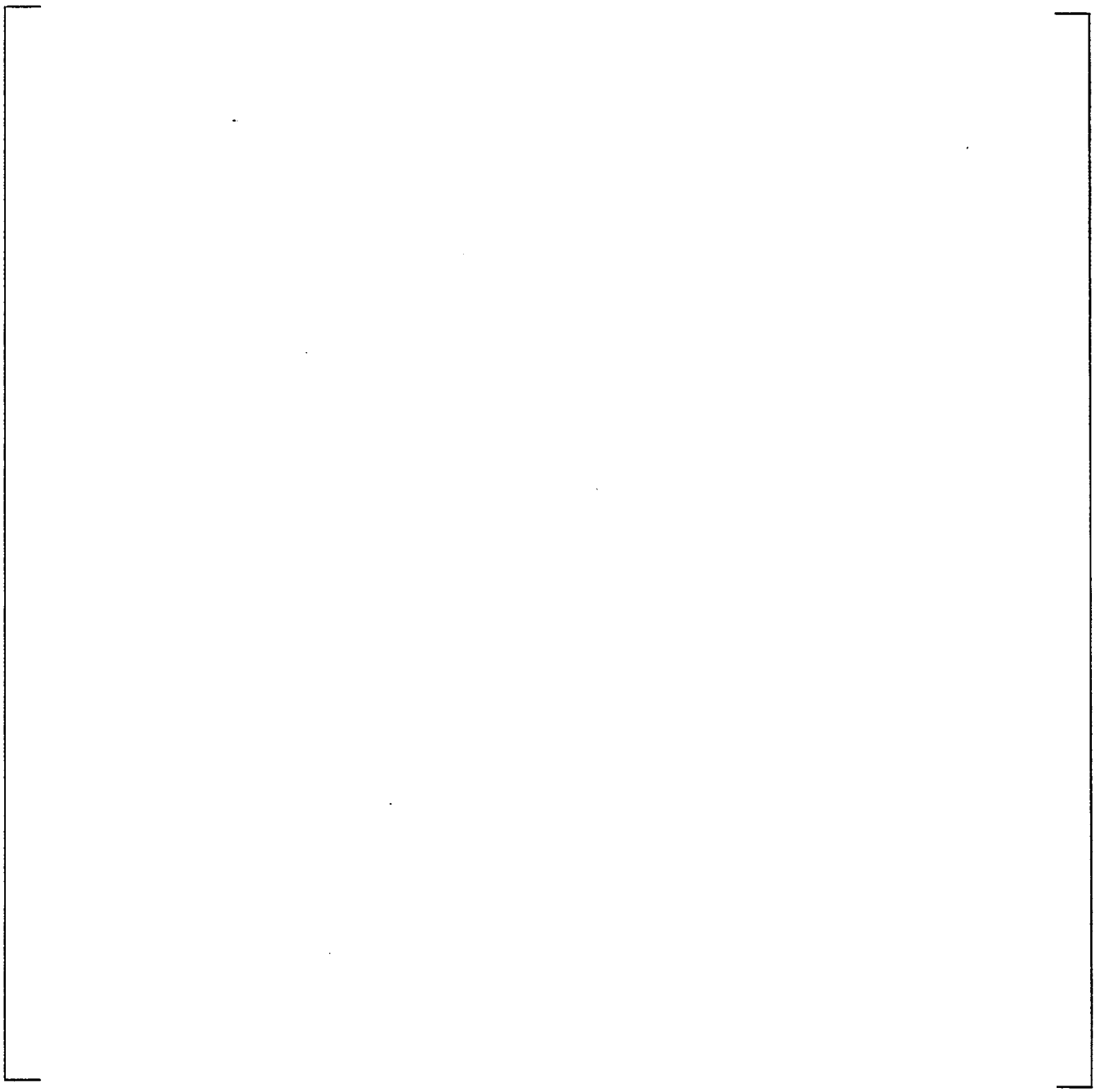

**Figure 5.13 TSP Pressure Drop SLB from Hot Standby, Plates A(CL), B, D, E**

a

**Figure 5.14**
**Model D4, TSP Pressure Drop SLB from Hot Standby, Plates A(HL), C**

a

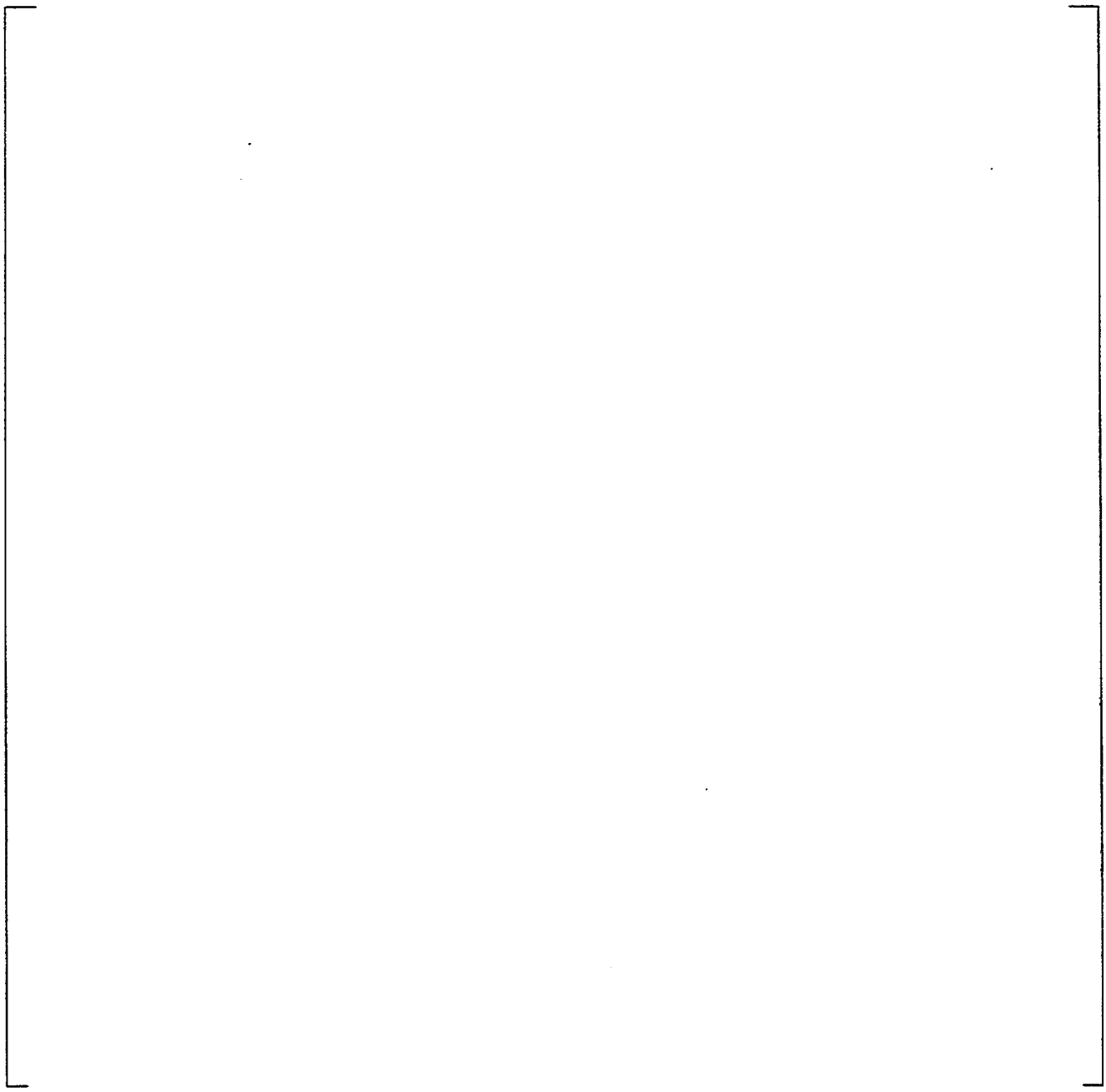

**Figure 5.15 Model D4, TSP Pressure Drop SLB from Hot Standby, Plates A(HL), C; Expanded Time Scale**

a

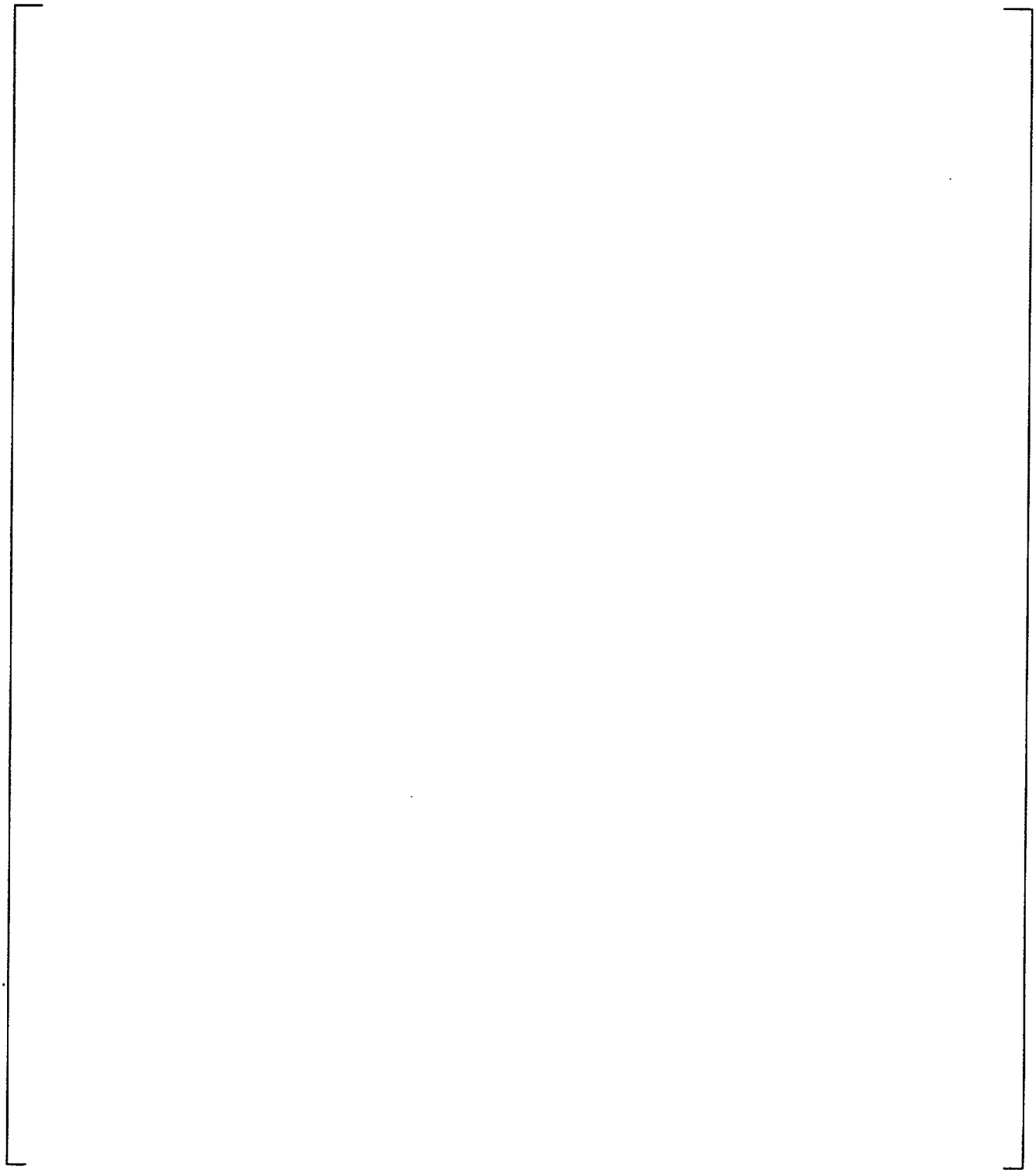

**Figure 5.16 Plate A Pressure Differential for SLB from Hot Standby for Evaluating Thin Control Volume Case**

a

**Figure 5.17 Secondary Side Pressure and Break Flow, Model D4 Parameters**

a

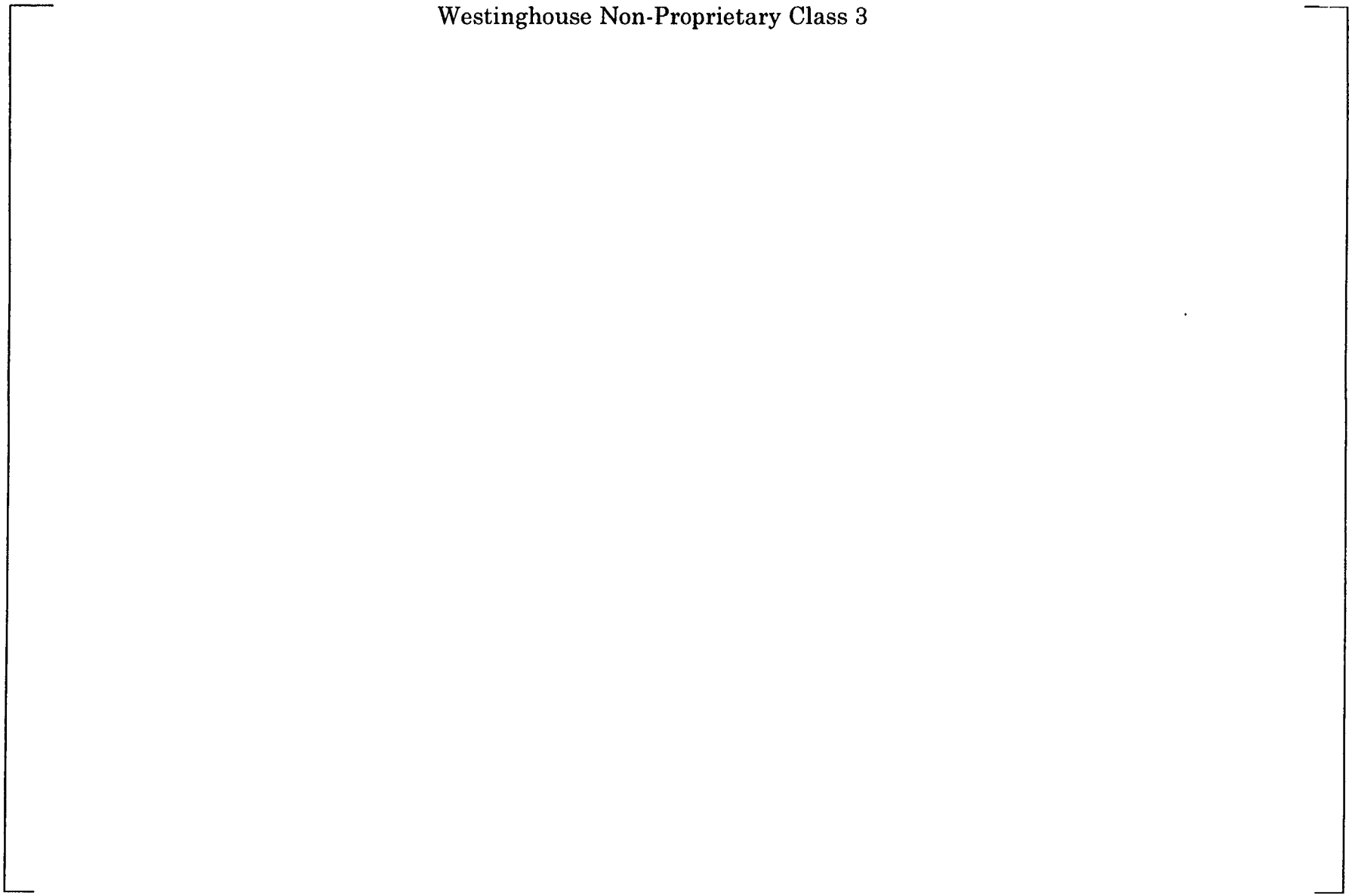

**Figure 5.18 Pressure Difference for Plates Q & R, Model D4 Parameters**

a

**Figure 5.19 Secondary Side Pressure and Break Flow, Westinghouse TSP Loss Coefficients**

**Figure 5.20 Pressure Difference for Plates Q & R, Westinghouse TSP Loss Coefficients**

a

**Figure 5.21 Secondary Side Pressure and Break Flow, 20% Increase in Break Flow**

a

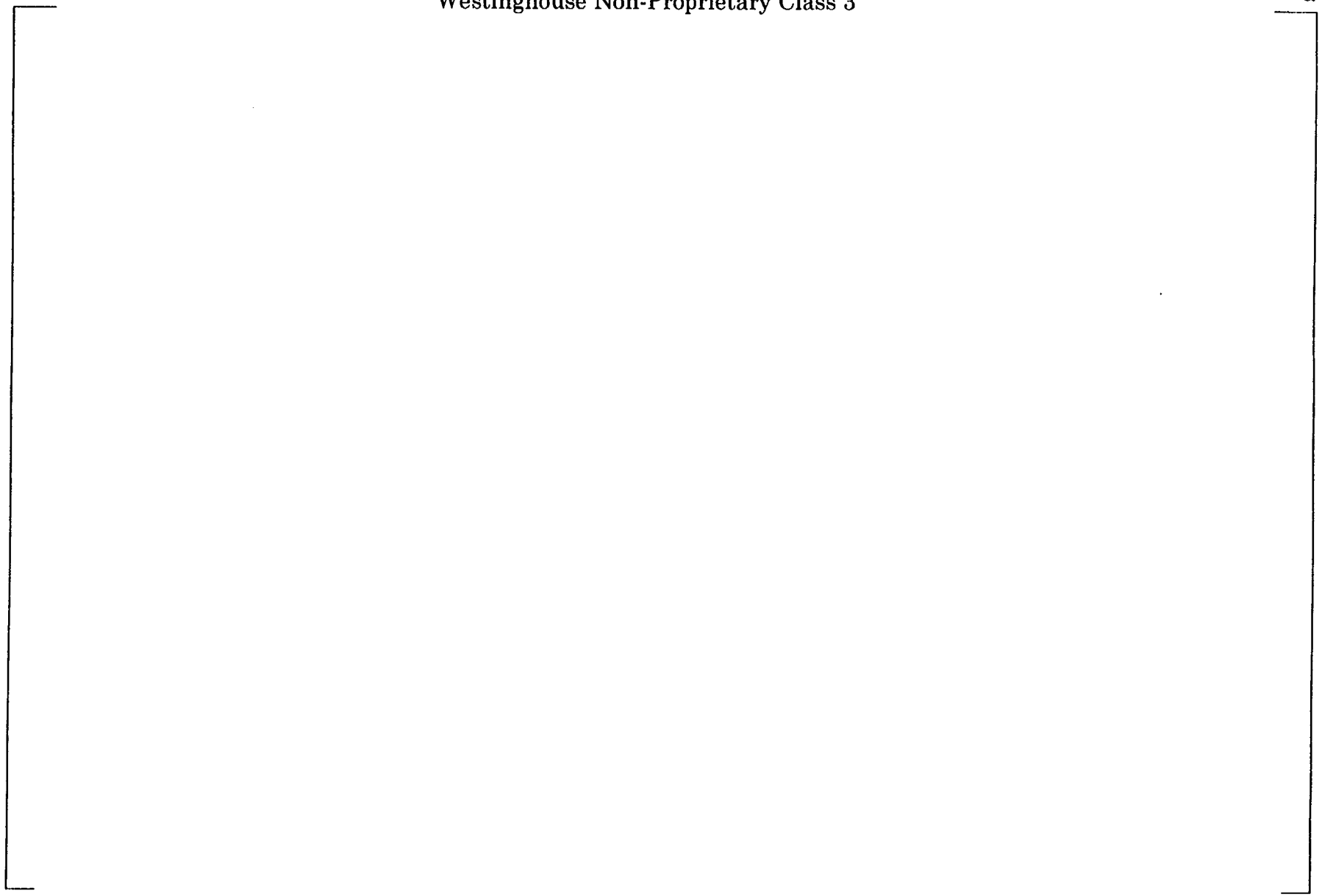

**Figure 5.22 Pressure Difference for Plates Q & R, 20% Increase in Break Flow**


**Figure 5.23 Secondary Side Pressure and Break Flow, Thin Support Plate Volumes**

**Figure 5.24 Pressure Difference for Plates Q & R, Thin Support Plate Volumes**

a

**Figure 5.25 Secondary Side Pressure and Break Flow, Low Water Level**

a

**Figure 5.26 Pressure Difference for Plates Q & R, Low Water Level**

a

**Figure 5.27 Secondary Side Pressure and Break Flow, Radial Discretization**

a

**Figure 5.28 Pressure Difference for Plates Q & R, Radial Discretization**

a

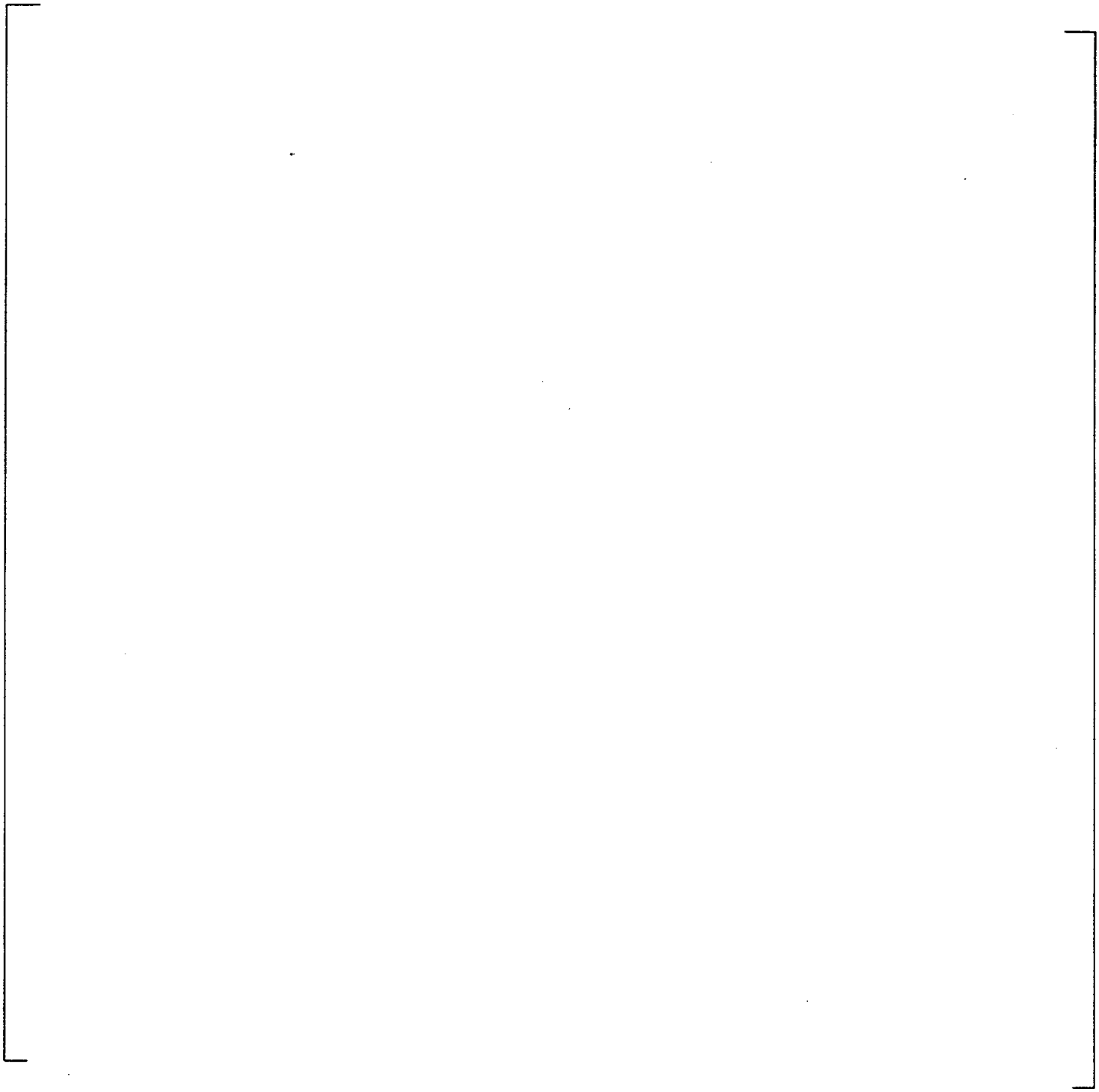

**Figure 5.29 Q Plate Pressure Difference, Radial Variation**

a

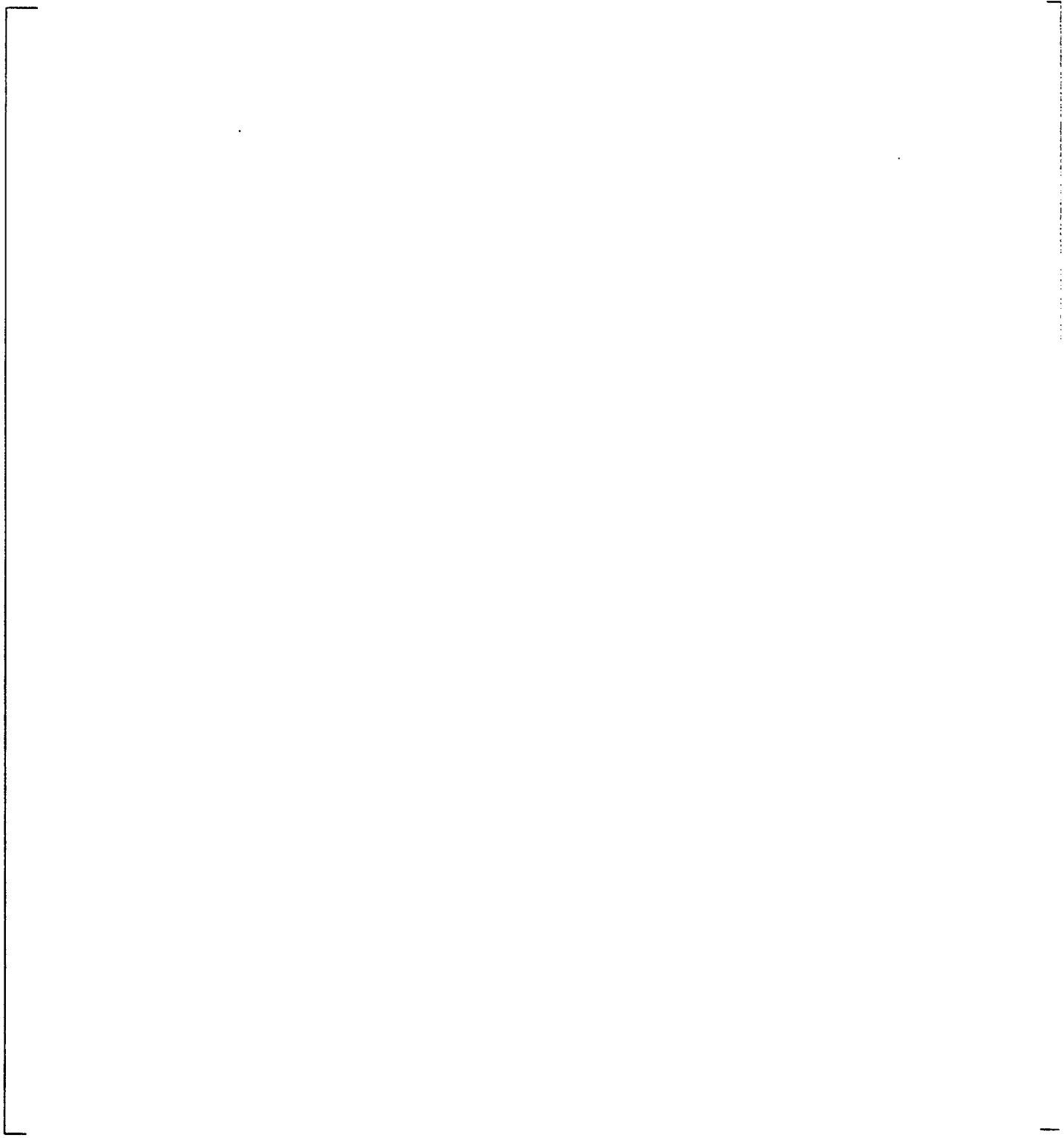

**Figure 5.30 P Plate Pressure Difference, Radial Variation**

a

**Figure 5.31 Secondary Side Pressure and Break Flow, Reduced Time Step**

**Figure 5.32 Pressure Difference for Plates Q & R, Reduced Time Step**

a

**Figure 5.33 Pressure Difference for Plates L & M, Reduced Time Step**


**Figure 5.34 Secondary Side Pressure and Break Flow, Revised Separator Model**

a

**Figure 5.35 Pressure Difference for Plates Q & R, Revised Separator Model**

# 6.0 STRUCTURAL MODELING FOR TSP DISPLACEMENTS

## 6.1 Introduction

Section 6.0 summarizes the structural modeling of the Model E tube bundle to determine relative tube / plate motions under steam line break loads. The analysis involves the preparation of a finite element model that simulates the structural response of the tube bundle. The model will include 180° of the tube bundle, due to hot-to-cold leg asymmetry resulting from the presence of the preheater. The model includes the channel head, shell, wrapper, partition plate, impingement plate in the preheater waterbox, all of the flow baffles and tube support plates, and the stayrods and spacers. The WECAN computer code, a general-purpose finite element code, is used to develop the model. The model is composed mainly of shell elements, with beam elements used to model the stayrods, spacers, and tubes. Calculations are performed to define applicable dynamic degrees of freedom (DOF) for each plate. Once the DOF are determined, a global substructure is generated for the overall tube bundle. The dynamic response of the plates is then calculated using the special purpose computer program ***"pltdym"***. Both the WECAN and ***"pltdym"*** computer codes have been verified and placed under configuration control.

Once the dynamic response of the tube support plates has been determined, calculations are performed to assure the applicability of the elastic analysis approach in determining the resulting displacements. These calculations consist of showing that the stayrods / spacers remain elastic throughout the transient, that significant yielding of the tube support plates does not occur, and that the welds joining the vertical bars and wedges (which provide vertical restraint for the plates) to the partition plate and wrapper remain in tact.

Additional details for all aspects of the structural modeling are provided in the following sections.

## 6.2 TSP Support System

The various tube support plates (TSPs) are supported vertically using several support mechanisms. A schematic of the tube bundle region is shown in Figure 6-1, with each of the plates identified. All of the plates are supported by fourteen stayrods / spacers. For the plates in the preheater region, Plates A, B, D, E, G, and H, there are an additional eighteen stayrods that provide support to vertical motion. In addition, the plates are supported by vertical bars above and below the plates that are welded to the inside of the wrapper, and to the impingement plate and the partition plate. The in-plane support for the TSPs is provided by wedges located

around the circumference of each plate. Wedges are welded to the inside of the wrapper, and also to the impingement and partition plates. The wedges are intended to provide in-plane support for the plates. However, the wedges also provide resistance to upward vertical motion of the plates due to the sloped face of the wedge face that interfaces with the plates.

Regarding the stayrods and spacers, the (non-preheater) stayrods are bars that are threaded into the tubesheet and run the full height of the tube bundle with a nut on the upper side of the top TSP, Plate R. (For the central stayrod, the lower end is threaded into a special coupling welded to the top of the partition plate.) Around the outside of the stayrods are spacers that are located between each of the support plates. For the non-preheater stayrods and spacers, there is no rigid link between the spacer and the support plates. The lack of a rigid link between the spacers and TSPs results in a non-linear dynamic system.

In the preheater region, the stayrods are segmented rods that are tack welded to Plate A and then run between the various baffle plates. Each segment is threaded into the bottom end of the stayrod immediately above it. The stayrods are of smaller diameter than the other stayrods, and pass through tube holes. Unlike, the full bundle stayrods that pass through the tube support plates without any interaction, the preheater stayrods interface with each of the plates due to their different geometries. However, there are no spacers surrounding the preheater stayrods as with the full bundle stayrods.

The various support locations for the plates are shown in Figures 6-2 through 6-12. Figure 6-2 shows the locations of the full bundle stayrods / spacers, and Figure 6-3 shows the locations of the preheater stayrods. Plate / wrapper support locations are shown in Figures 6-4 through 6-12. Schematics of the wedge and vertical bar interfaces with the wrapper are shown in Figures 6-13 and 6-14, respectively.

## 6.3 Finite Element Model

The overall finite element model is shown in Figure 6-15. With the exception of the stayrods, all of the structural components are modeled using three dimensional shell elements. The stayrods are modeled using three-dimensional beam elements. The spacers are incorporated in the dynamics code through stiffnesses that are coupled to the various plates as appropriate.

In modeling the plates, the cutouts along the tubelane, the cutout for Plate A in the center of the hot leg, and the cutouts at the outer edge of several of the plates are accounted for. In terms of material properties, equivalent properties are specified only in the tubed regions of the plate. Solid (non-perforated) plate properties are

used along the tubelane and at the periphery of the plates. The solid outer rim of each of the plates is conservatively assumed to extend from the outer edge of the outermost hole to the edge of the plate. The width of the plate rim varies from 1.26 inches to 2.11 inches. The median rim width is 1.62 inches, and is the value used for this analysis.

## 6.4 Material Properties

A specification of component materials is contained in Table 6-1. Summaries of the applicable material properties are provided in Tables 6-2 through 6-10. The properties in these tables are taken from the 1974 edition (through summer 1976 addenda) of the ASME Code, the applicable code edition for the Unit 2 steam generators. Based on prior SLB analyses, the limiting initial conditions for the transient is hot standby, and the peak pressure loads occur during the initial 1.5 seconds of the transient. At hot standby, the steam generator is at a uniform temperature of 567°F. Since temperature dependent properties cannot be used in substructures, properties for the finite element model are based on the initial conditions for the transient, or 567°F.

The material properties for the tubesheet and tube support plates are modified to account for the tube penetrations and flow holes. The density is also modified to account for the added mass of the secondary side fluid. Additional details of the material property modifications are provided below.

## 6.5 Revised Material Properties

The material properties for the tubesheet and tube support plates are modified to account for the tube penetrations, flow holes, and various cutouts. The properties that are modified are Young's modulus, Poisson's ratio, and the material density. In the case of the TSPs, the density is additionally modified to account for the added mass of the secondary side fluid.

### 6.5.1 Young's Modulus / Poisson's Ratio

Due to the presence of flow holes in the TSPs, but not in the tubesheet, Plate A, or the preheater plates, two different formulations are used to modify the material properties. Although different formulations are used for the two geometries, the calculations use the same methodology in each case. Due to square penetration patterns, different properties exist in the pitch and diagonal directions. The first step is to establish equivalent parameters for Young's modulus and Poisson's ratio in the pitch and diagonal directions ($E_p^*/E$, $E_d^*/E$, $\nu_d^*$, $\nu_p^*$), respectively. The equivalent Young's modulus for the overall plate is taken as the average of the pitch

and diagonal directions. The next step is to determine an equivalent value for the shear modulus, G*/G, for the plate. This is done in a similar manner as for Young's modulus, starting with values in the pitch and diagonal directions, and then taking an average of the two values. The equivalent value for Poisson's ratio is then determined from the relationship between Young's modulus and the shear modulus. A summary of the resulting effective plate properties for Young's Modulus and Poisson's ratio is provided in Table 6-11.

6.5.2 Material Density

There are two aspects to revising the plate density. The first is based on a ratio of solid plate area to the modeled area. The second aspect corresponds to the plate moving through and displacing the secondary side fluid, creating an "added mass" effect. In calculating the added mass, the formulation shown below is used.

$$m_a = \rho_f \left( \frac{A_e^2}{A_h} \right) I_{eff}$$

$$I_{eff} = l + \left( \frac{8d}{3\pi} \right) \left( 1 - \frac{d}{2b} \right)$$

where,

$\rho_f$ = fluid density
$A_e$ = solid area of plate
$A_h$ = flow area
$l$ = hole length (plate thickness)
d = hole diameter
b = hole pitch

The first step in the process of calculating revised densities for the plates is to determine the applicable areas for the metal and the fluid. Summaries of the actual and modeled plate areas are summarized in Table 6-12.

The resulting added mass is a direct function of the fluid density. Because the dynamic analysis cannot account for the change in fluid density with time, the analysis uses an average density value for the transient. A review of the pressure time history loads (presented in Section 5) shows that the maximum plate loads occur during the initial 1.5 seconds of the transient. Thus, the densities are averaged over the initial 1.5 seconds. In addition, the individual plate densities are averaged to arrive at an overall average density for the bundle. For the SLB from full power, two densities are calculated, one for the hot leg and plates above the

preheater, and one for the plates in the preheater, where the water density is higher due to the colder temperature of the incoming feedwater.

Summaries of the resulting fluid and structural masses, together with the resulting effective densities are summarized in Tables 6-13 and 6-14 for SLB from hot standby and SLB from full power, respectively.

## 6.6 Dynamic Degrees of Freedom

In setting up the global substructure, it is necessary to define the dynamic degrees of freedom (DOF) for the system. In order to define dynamic degrees of freedom for the TSPs, two sets of modal calculations are performed for each plate. The first set of calculations determines plate mode shapes and frequencies using a large number of degrees of freedom. The second set of calculations involves repeating the modal analysis, using a significantly reduced set of degrees of freedom. The reduced DOF are selected to predict all frequencies for a given plate up to approximately 75 hertz to within 10% of the frequencies for the large set of DOF. A frequency of 75 hertz was selected as a cutoff, as it is judged that higher frequencies have a small energy content compared to the lower frequencies, and will not have a significant contribution to the plate response.

In performing the modal analyses, the plates are, in general, treated on an individual basis. That is, only the plate under consideration remains active. The remainder of the plate structures are inactive. In addition to the plate being evaluated, the stayrods and spacers are also active depending on the direction of the dominant SLB load, which occurs during the first 1.5 seconds of the transient. For plates experiencing dominant downward loads, the plate is coupled to the spacers, which are then constrained against vertical motion at the top of the tubesheet. For plates experiencing dominant upward loads, the plates are coupled to the spacers, which are then coupled to the stayrod at the top plate, with the stayrods constrained at the tubesheet surface.

The plates are also constrained against vertical motion at the vertical bar locations. At the wedge locations, a method similar to that for the spacers is used. For plates experiencing a predominant upward load, the plates are also constrained against vertical motion at the wedge locations (along the wrapper only). The wedges can only support an upward load since they are welded to the wrapper.

For plates in the preheater area, a modified approach is used. The SLB loads on the preheater plates is such that the lower plates are loaded in the down direction, and the upper plates in the up direction, with the B plate receiving the highest load of any plate in the tube bundle. The preheater stayrods will tend to hold the plates

together, and limit vertical motion. Thus, in performing the modal calculations for the preheater plates, each of the plates B, D, E, G, and H are active, along with the preheater stayrods. However, in order to isolate the response of any given plate, the mass of the other plates is set to zero. Thus, the stiffness of the overall system is accounted for, but only the mass of the affected plate is included.

A comparison of the natural frequencies for the full and reduced sets of DOF for the plates is provided in Table 6-15. Based on the tabular summary, the reduced set of DOF is concluded to provide a good approximation of the plate response. Mode shape plots for Plate R for the full and reduced set of DOF for the first five modes are shown in Figures 6-16 to 6-20, and 6-21 to 6-25, respectively. Due to variations in plate geometries and support conditions, the number and location of the reduced set of DOF varies from plate to plate. The final set of DOF for the hot leg of upper three plates, P, Q, and R, which are typical of the non-preheater plates, are shown in Figures 6-26, 6-27, and 6-28, respectively. (Note that for the plates above the preheater, Plates L - R, the DOF are symmetric for the hot and cold legs.) For the preheater plates, the additional support provided by the preheater stayrods, causes the fundamental frequencies to be higher than for the non-preheater plates. This results in the preheater plates generally having more DOF than the non-preheater plates. Figures 6-29 and 6-30 show the locations of the DOF for plates D and E, which are typical of most of the cold leg preheater plates.

## 6.7 Displacement Boundary Conditions

The displacement boundary conditions for the substructure generation consist primarily of prescribing symmetry conditions along the "Y" axis for each of the components. Vertical constraint is provided on the channel head ring at the 0°, 90°, and 180° locations, where the vertical column supports interface with the ring.

## 6.8 Application of Pressure Loading

The SLB pressure loads act on each of the TSPs. Thus, in generating the substructures, load vectors are prescribed for each of the plates using a reference load of 1 psi. The reference loads are scaled during the dynamic analysis to the actual time-history (transient) loading conditions.

The transient pressure drops summarized in Section 5 are relative to the control volume for each of the plates. The area over which the hydraulic pressure acts corresponds to the area inside the wrapper minus the tube area. Thus, the pressure drops through the plates must be scaled based on a ratio of the plate area in the structural model to the control volume area in the hydraulic model. Before applying the pressure time histories to the structural model they are scaled based on a ratio

of the plate area in the structural model to the control volume area in the hydraulic model.

The loads applied to the finite element model also include the 1.5 uncertainty factor resulting from the sensitivity analysis discussed in Section 5.4. For the steam line break event initiating from full power, the 1.5 factor is applied to the change in transient pressure from time equal zero, rather than the absolute pressure.

## 6.9 Integration Time Step

The iteration time step used to solve the time history response to the TSP is 0.0002 second. This time step was selected based on similar analyses for other model steam generators. The frequencies of response of the structures in the prior analysis and the period of the applied loading are consistent with the present analysis. The period of the applied loading is on the order of 1.50 second, resulting in a significant number of solution steps.

## Table 6-1

## Summary of Component Materials
## South Texas Unit 2

a,c

[

]

## Table 6-2

## Summary of Material Properties
## SA 533 Grade A, Class 2

| | | Temperature - °F | | | | | | |
|---|---|---|---|---|---|---|---|---|
| Property | Code Ed. | 70 | 200 | 300 | 400 | 500 | 600 | 700 |
| Young's Modulus | 74 (S76) | 29.90 | 29.50 | 29.00 | 28.60 | 28.00 | 27.40 | 26.60 |
| | | | | | | | | |
| Coefficient of Thermal | 74 (S76) | 6.07 | 6.38 | 6.60 | 6.82 | 7.02 | 7.23 | 7.44 |
| Expansion | | | | | | | | |
| | | | | | | | | |
| Density | --- | 0.284 | 0.283 | 0.283 | 0.282 | 0.281 | 0.281 | 0.280 |
| | | 7.35 | 7.33 | 7.315 | 7.299 | 7.282 | 7.264 | 7.246 |
| | | | | | | | | |

| Property | Units |
|---|---|
| Young's Modulus | psi x 1.0E06 |
| | |
| Coefficient of Thermal | in/in/ °F x 1.0E-06 |
| Expansion | |
| | |
| Density | $lb/in^3$ |
| | $lb\text{-}sec^2/in^4$ x 1.0E-4 |
| | |

## Table 6-3

## Summary of Material Properties
## SA 508 Class 2a

| | | Temperature - °F | | | | | | |
|---|---|---|---|---|---|---|---|---|
| Property | Code Ed. | 70 | 200 | 300 | 400 | 500 | 600 | 700 |
| Young's Modulus | 74 (S76) | 29.90 | 29.50 | 29.00 | 28.60 | 28.00 | 27.40 | 26.60 |
| | | | | | | | | |
| Coefficient of Thermal | 74 (S76) | 6.07 | 6.38 | 6.60 | 6.82 | 7.02 | 7.23 | 7.44 |
| Expansion | | | | | | | | |
| | | | | | | | | |
| Density | --- | 0.284 | 0.283 | 0.283 | 0.282 | 0.281 | 0.281 | 0.280 |
| | | 7.35 | 7.33 | 7.315 | 7.299 | 7.282 | 7.264 | 7.246 |
| | | | | | | | | |

| Property | Units |
|---|---|
| Young's Modulus | psi x 1.0E06 |
| | |
| Coefficient of Thermal | in/in/ °F x 1.0E-06 |
| Expansion | |
| | |
| Density | $lb/in^3$ |
| | $lb\text{-}sec^2/in^4$ x 1.0E-4 |
| | |

## Table 6-4

## Summary of Material Properties
## SA 516 Grade 70

| | | Temperature - °F | | | | | | |
|---|---|---|---|---|---|---|---|---|
| Property | Code Ed. | 70 | 200 | 300 | 400 | 500 | 600 | 700 |
| Young's Modulus | 74 (S76) | 27.90 | 27.70 | 27.40 | 27.00 | 26.40 | 25.70 | 24.80 |
| | | | | | | | | |
| Coefficient of Thermal | 74 (S76) | 6.07 | 6.38 | 6.60 | 6.82 | 7.02 | 7.23 | 7.44 |
| Expansion | | | | | | | | |
| | | | | | | | | |
| Density | --- | 0.284 | 0.283 | 0.283 | 0.282 | 0.281 | 0.281 | 0.280 |
| | | 7.35 | 7.33 | 7.315 | 7.299 | 7.282 | 7.264 | 7.246 |
| | | | | | | | | |

| Property | Units |
|---|---|
| Young's Modulus | psi x 1.0E06 |
| | |
| Coefficient of Thermal | in/in/ °F x 1.0E-06 |
| Expansion | |
| | |
| Density | $lb/in^3$ |
| | $lb\text{-}sec^2/in^4$ x 1.0E-4 |
| | |

## Table 6-5

## Summary of Material Properties
## SA 533 Grade B, Class 2

| | | Temperature - °F | | | | | | |
|---|---|---|---|---|---|---|---|---|
| Property | Code Ed. | 70 | 200 | 300 | 400 | 500 | 600 | 700 |
| Young's Modulus | 74 (S76) | 29.90 | 29.50 | 29.00 | 28.60 | 28.00 | 27.40 | 26.60 |
| | | | | | | | | |
| Coefficient of Thermal | 74 (S76) | 6.07 | 6.38 | 6.60 | 6.82 | 7.02 | 7.23 | 7.44 |
| Expansion | | | | | | | | |
| | | | | | | | | |
| Density | --- | 0.284 | 0.283 | 0.283 | 0.282 | 0.281 | 0.281 | 0.280 |
| | | 7.35 | 7.33 | 7.315 | 7.299 | 7.282 | 7.264 | 7.246 |
| | | | | | | | | |

| Property | Units |
|---|---|
| Young's Modulus | psi x 1.0E06 |
| | |
| Coefficient of Thermal | in/in/ °F x 1.0E-06 |
| Expansion | |
| | |
| Density | $lb/in^3$ |
| | $lb\text{-}sec^2/in^4$ x 1.0E-4 |
| | |

## Table 6-6

## Summary of Material Properties
## SA 285 Grade C

| | | Temperature - °F | | | | | | |
|---|---|---|---|---|---|---|---|---|
| Property | Code Ed. | 70 | 200 | 300 | 400 | 500 | 600 | 700 |
| Young's Modulus | 74 (S76) | 27.90 | 27.70 | 27.40 | 27.00 | 26.40 | 25.70 | 24.80 |
| | | | | | | | | |
| Coefficient of Thermal | 74 (S76) | 6.07 | 6.38 | 6.60 | 6.82 | 7.02 | 7.23 | 7.44 |
| Expansion | | | | | | | | |
| | | | | | | | | |
| Density | --- | 0.284 | 0.283 | 0.283 | 0.282 | 0.281 | 0.281 | 0.280 |
| | | 7.35 | 7.33 | 7.315 | 7.299 | 7.282 | 7.264 | 7.246 |
| | | | | | | | | |

| PROPERTY | UNITS |
|---|---|
| Young's Modulus | psi x 1.0E06 |
| | |
| Coefficient of Thermal | in/in/ °F x 1.0E-06 |
| Expansion | |
| | |
| Density | $lb/in^3$ |
| | $lb\text{-}sec^2/in^4$ x 1.0E-4 |
| | |

## Table 6-7

## Summary of Material Properties
## SA 240 Type 405

| | | Temperature - °F | | | | | | |
|---|---|---|---|---|---|---|---|---|
| Property | Code Ed. | 70 | 200 | 300 | 400 | 500 | 600 | 700 |
| Young's Modulus | 74 (S76) | 29.20 | 28.70 | 28.30 | 27.70 | 27.00 | 26.00 | 24.80 |
| | | | | | | | | |
| Coefficient of Thermal | 74 (S76) | 5.24 | 5.50 | 5.66 | 5.81 | 5.96 | 6.13 | 6.26 |
| Expansion | | | | | | | | |
| | | | | | | | | |
| Density | --- | 0.284 | 0.283 | 0.283 | 0.282 | 0.281 | 0.281 | 0.280 |
| | | 7.35 | 7.33 | 7.315 | 7.299 | 7.282 | 7.264 | 7.246 |
| | | | | | | | | |

| Property | Units |
|---|---|
| Young's Modulus | psi x 1.0E06 |
| | |
| Coefficient of Thermal | in/in/ °F x 1.0E-06 |
| Expansion | |
| | |
| Density | $lb/in^3$ |
| | $lb\text{-}sec^2/in^4$ x 1.0E-4 |
| | |

## Table 6-8

## Summary of Material Properties
## SA 696 Grade C

| | | Temperature - °F | | | | | | |
|---|---|---|---|---|---|---|---|---|
| Property | Code Ed. | 70 | 200 | 300 | 400 | 500 | 600 | 700 |
| Young's Modulus | 74 (S76) | 29.90 | 29.50 | 29.00 | 28.30 | 27.40 | 26.70 | 25.40 |
| | | | | | | | | |
| Coefficient of Thermal | 74 (S76) | 6.07 | 6.38 | 6.60 | 6.82 | 7.02 | 7.23 | 7.44 |
| Expansion | | | | | | | | |
| | | | | | | | | |
| Density | --- | 0.284 | 0.283 | 0.283 | 0.282 | 0.281 | 0.281 | 0.280 |
| | | 7.35 | 7.33 | 7.315 | 7.299 | 7.282 | 7.264 | 7.246 |
| | | | | | | | | |

| Property | Units |
|---|---|
| Young's Modulus | psi x 1.0E06 |
| | |
| Coefficient of Thermal | in/in/ °F x 1.0E-06 |
| Expansion | |
| | |
| Density | $lb/in^3$ |
| | $lb\text{-}sec^2/in^4$ x 1.0E-4 |
| | |

## Table 6-9

## Summary of Material Properties
## SA 106 Grade B

| | | Temperature - °F | | | | | | |
|---|---|---|---|---|---|---|---|---|
| Property | Code Ed. | 70 | 200 | 300 | 400 | 500 | 600 | 700 |
| Young's Modulus | 74 (S76) | 27.90 | 27.70 | 27.40 | 27.00 | 26.40 | 25.70 | 24.80 |
| | | | | | | | | |
| Coefficient of Thermal | 74 (S76) | 6.07 | 6.38 | 6.60 | 6.82 | 7.02 | 7.23 | 7.44 |
| Expansion | | | | | | | | |
| | | | | | | | | |
| Density | --- | 0.284 | 0.283 | 0.283 | 0.282 | 0.281 | 0.281 | 0.280 |
| | | 7.35 | 7.33 | 7.315 | 7.299 | 7.282 | 7.264 | 7.246 |
| | | | | | | | | |

| Property | Units |
|---|---|
| Young's Modulus | psi x 1.0E06 |
| | |
| Coefficient of Thermal | in/in/ °F x 1.0E-06 |
| Expansion | |
| | |
| Density | $lb/in^3$ |
| | $lb\text{-}sec^2/in^4$ x 1.0E-4 |
| | |

## Table 6-10

## Summary of Material Properties
## SB 166

| | | Temperature - °F | | | | | | |
|---|---|---|---|---|---|---|---|---|
| Property | Code Ed. | 70 | 200 | 300 | 400 | 500 | 600 | 700 |
| Young's Modulus | 74 (S76) | 31.70 | 30.90 | 30.50 | 30.00 | 29.60 | 29.20 | 28.60 |
| | | | | | | | | |
| Coefficient of Thermal | 74 (S76) | 7.13 | 7.40 | 7.56 | 7.70 | 7.80 | 7.90 | 8.00 |
| Expansion | | | | | | | | |
| | | | | | | | | |
| Density | --- | --- | 0.306 | 0.305 | 0.305 | 0.304 | 0.303 | 0.302 |
| | | --- | 7.923 | 7.905 | 7.886 | 7.867 | 7.847 | 7.828 |
| | | | | | | | | |

| Property | Units |
|---|---|
| Young's Modulus | psi x 1.0E06 |
| | |
| Coefficient of Thermal | in/in/ °F x 1.0E-06 |
| Expansion | |
| | |
| Density | $lb/in^3$ |
| | $lb\text{-}sec^2/in^4$ x 1.0E-4 |
| | |

## Table 6-11

## Summary of Equivalent Plate Properties

a,c

[ ]

## Table 6-12

## Summary of Plate Areas

a,c

[

]

## Table 6-13

## Summary of Effective Plate Densities

### *Steam Line Break From Hot Standby*

a,c

**Table 6-14**

**Summary of Effective Plate Densities**

***Steam Line Break From Full Power***

a,c

[ ]

a,c

## Table 6-15

## Comparison of Natural Frequencies Full Versus Reduced DOF

a,c

**Table 6-15 (Continued)**

**Comparison of Natural Frequencies**
**Full Versus Reduced DOF**

a,c.

[

]

**Table 6-15 (Continued)**

**Comparison of Natural Frequencies**
**Full Versus Reduced DOF**

a,c

[

]

**Figure 6.1 Tube Bundle Geometry**
**South Texas Unit 2 Steam Generator**

a,c

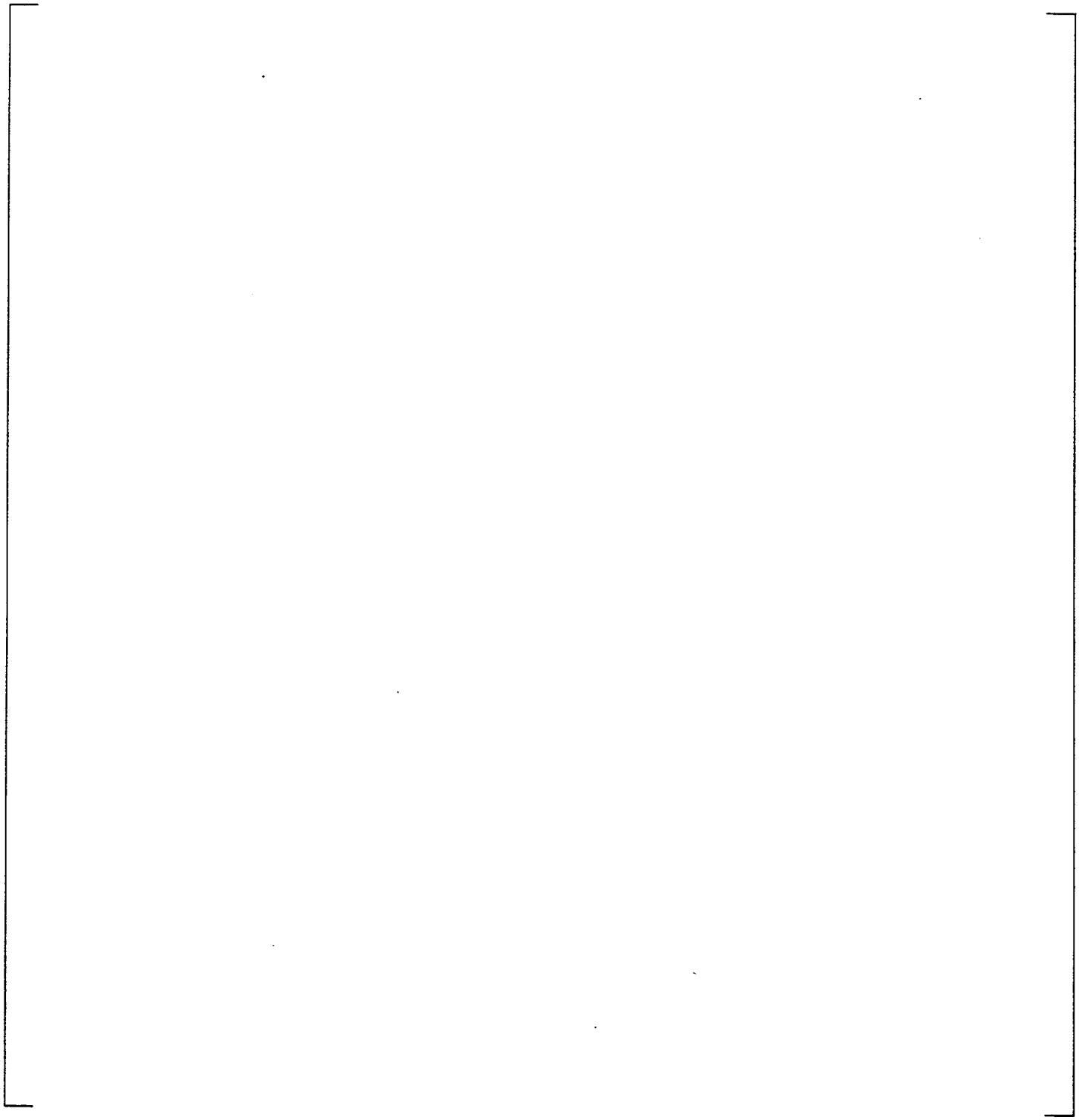

**Figure 6.2 Full Bundle Stayrod Locations**

a,c

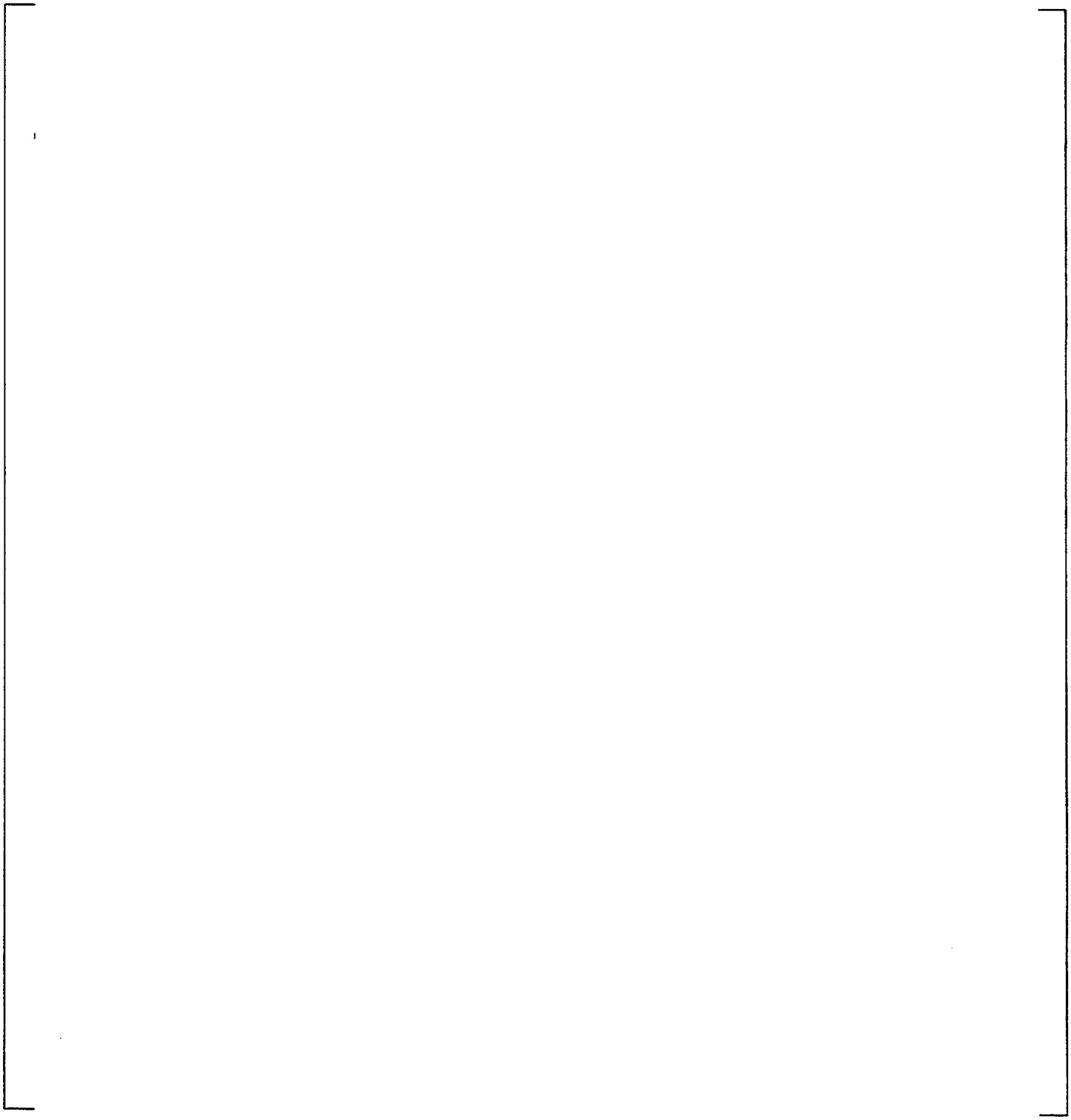

## Figure 6.3 Preheater Stayrod Locations

a,c

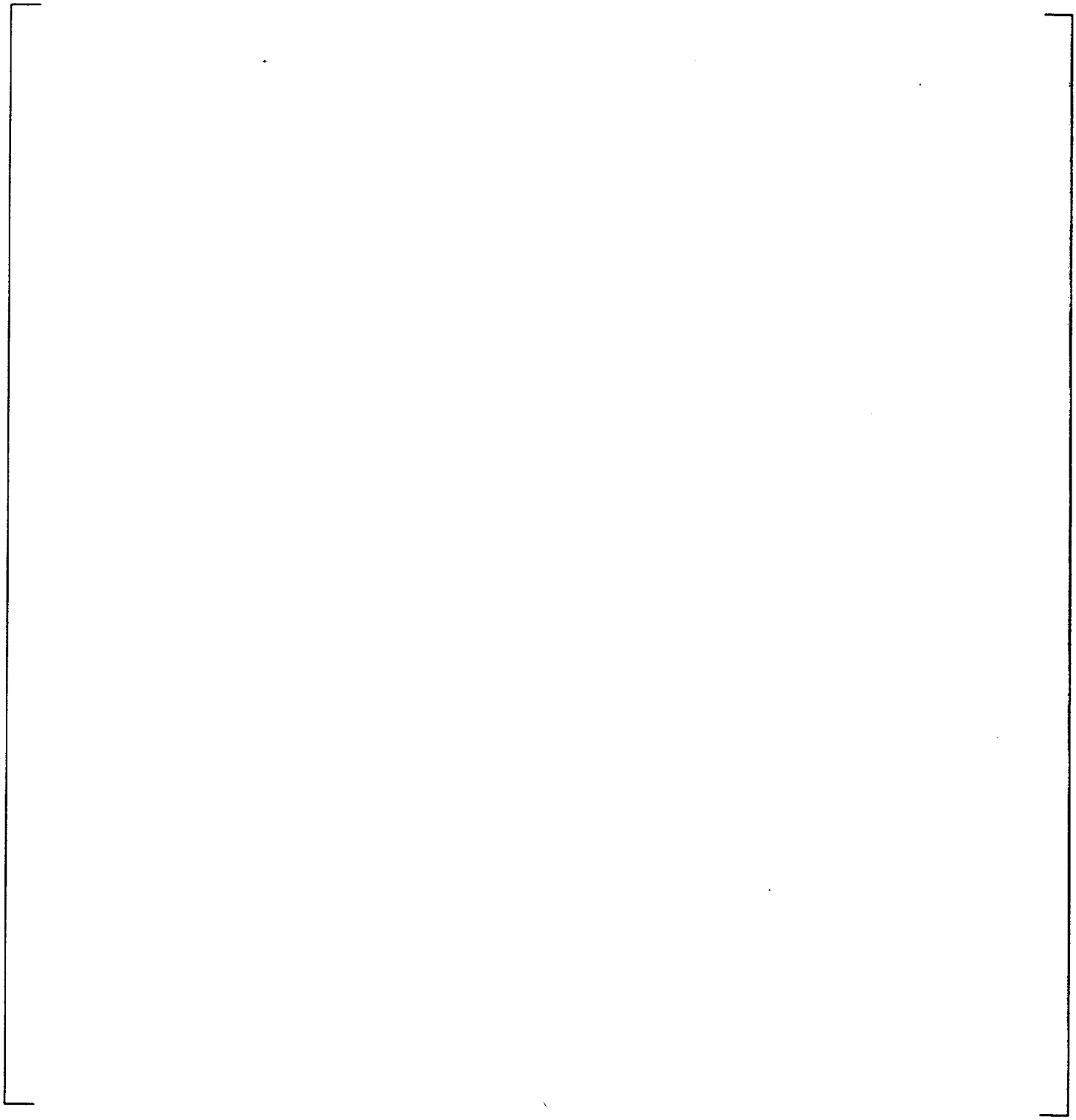

**Figure 6.4 Plate A Support Locations**

a,c

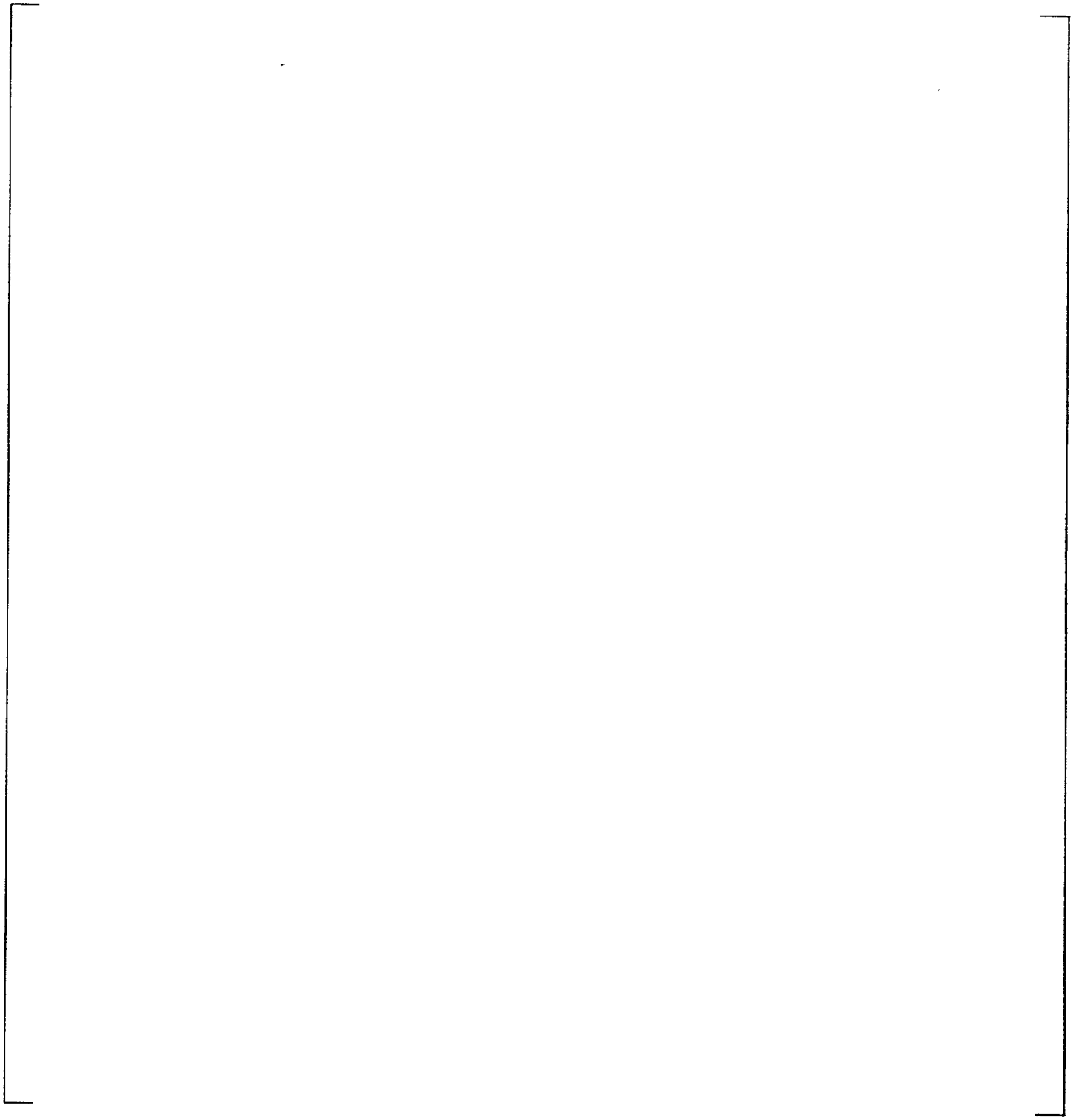

## Figure 6-5 Plate B Support Locations

a,c

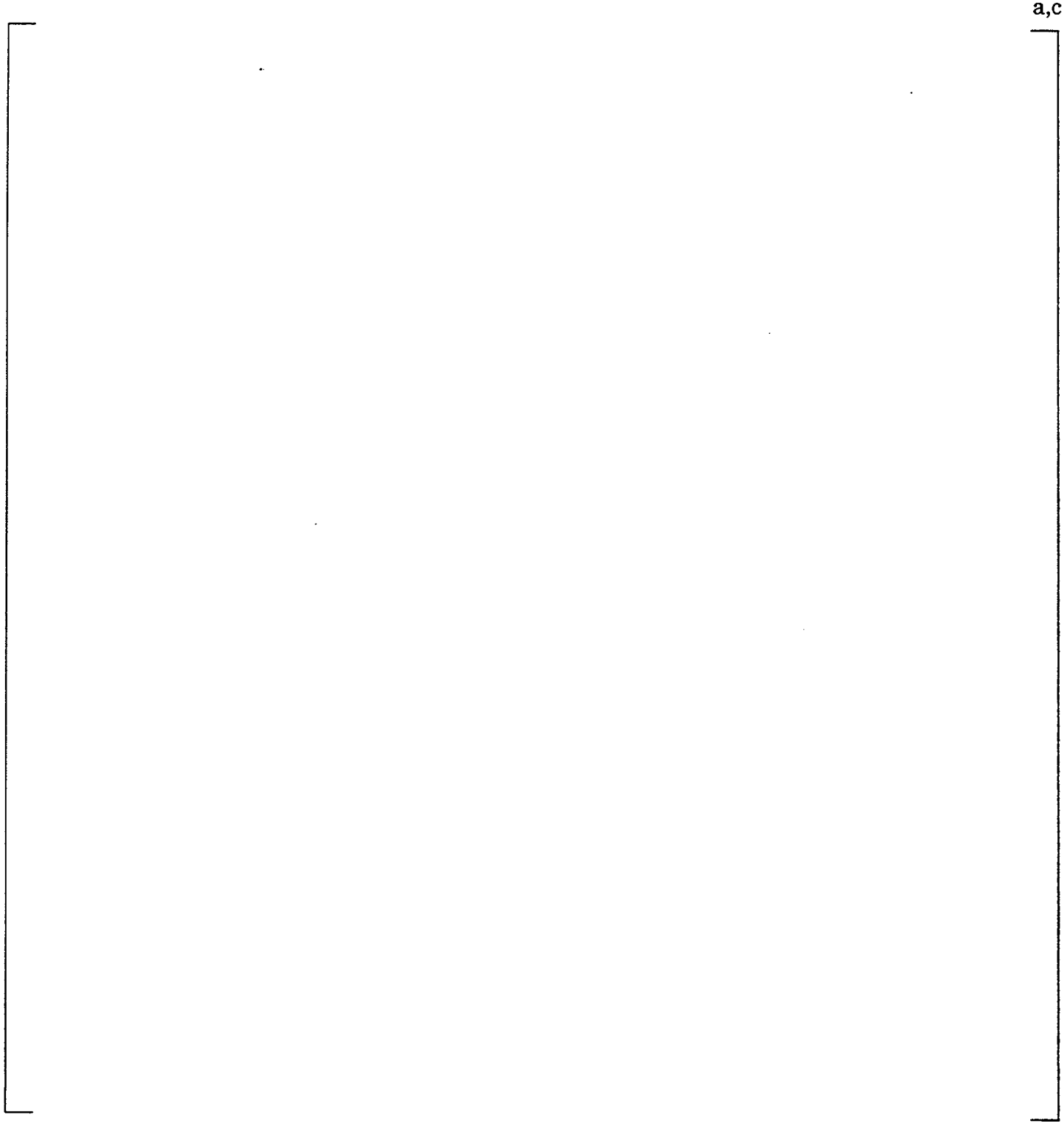

**Figure 6.6 Plates C/D Support Locations**

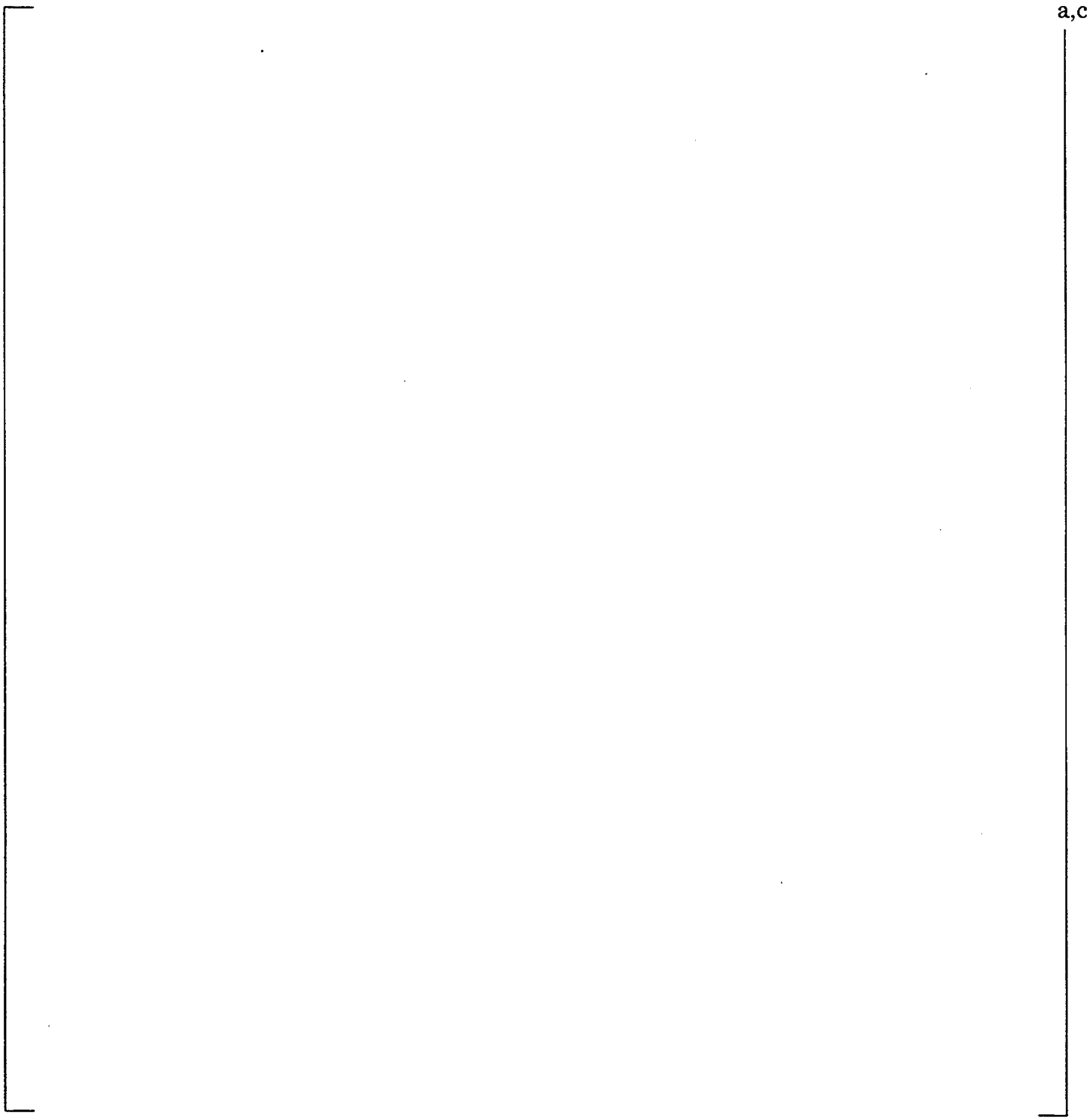

## Figure 6.7 Plates E, H Support Locations

a,c

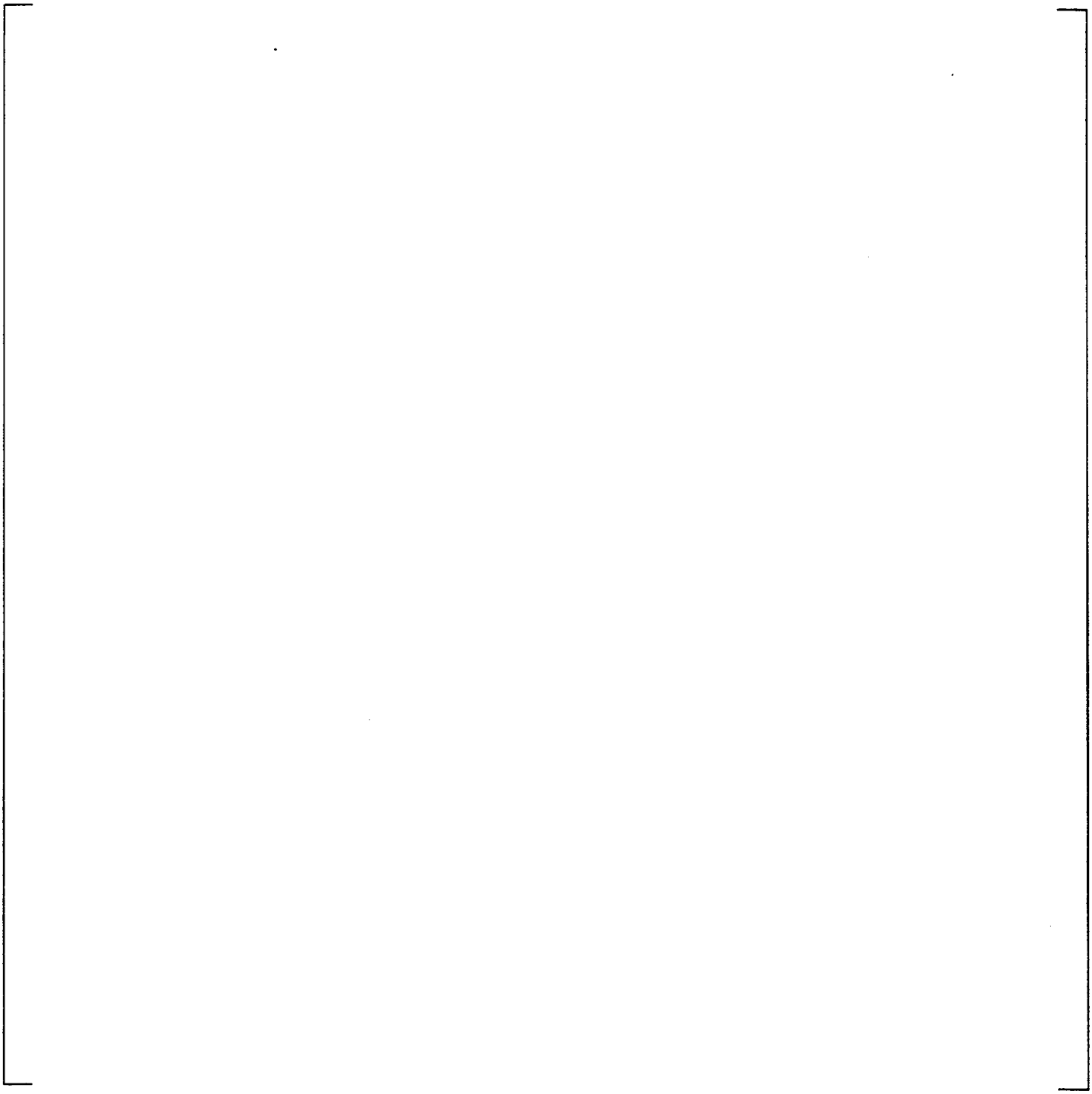

**Figure 6.8 Plates F/G Support Locations**

a,c

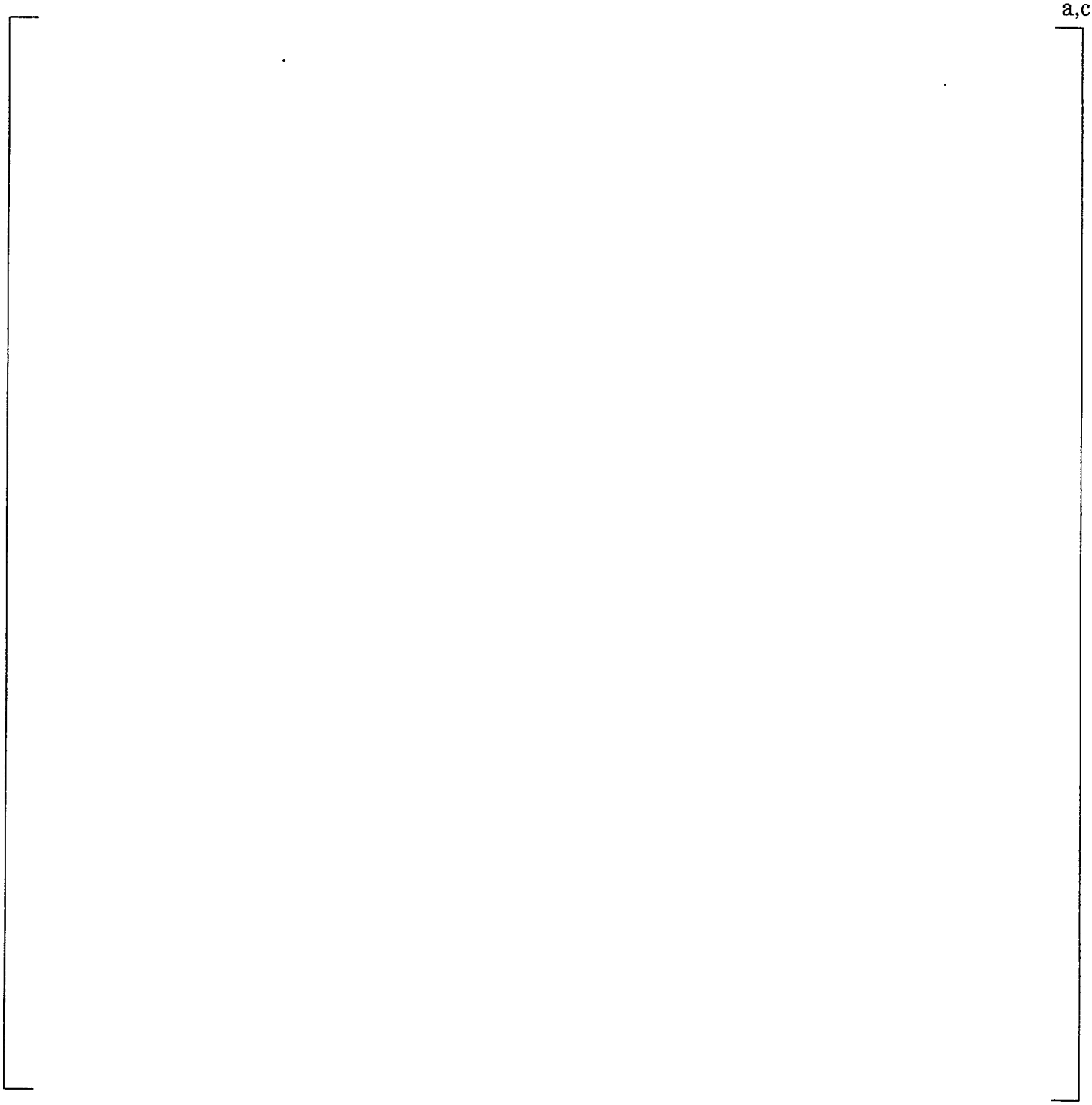

**Figure 6.9 Plates J/K Support Locations**

a,c

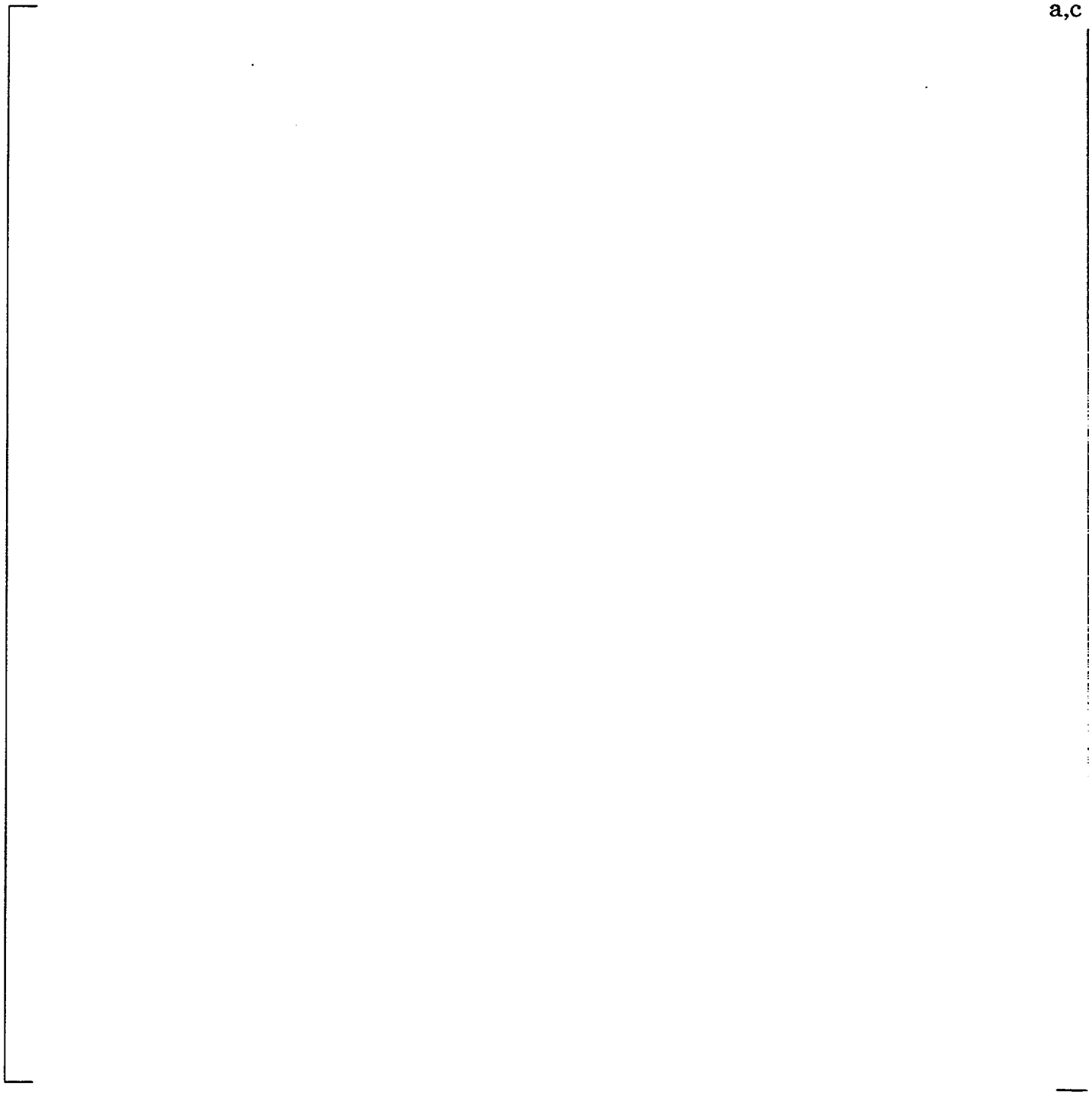

**Figure 6.10 Plates L, M, P Support Locations**

a,c

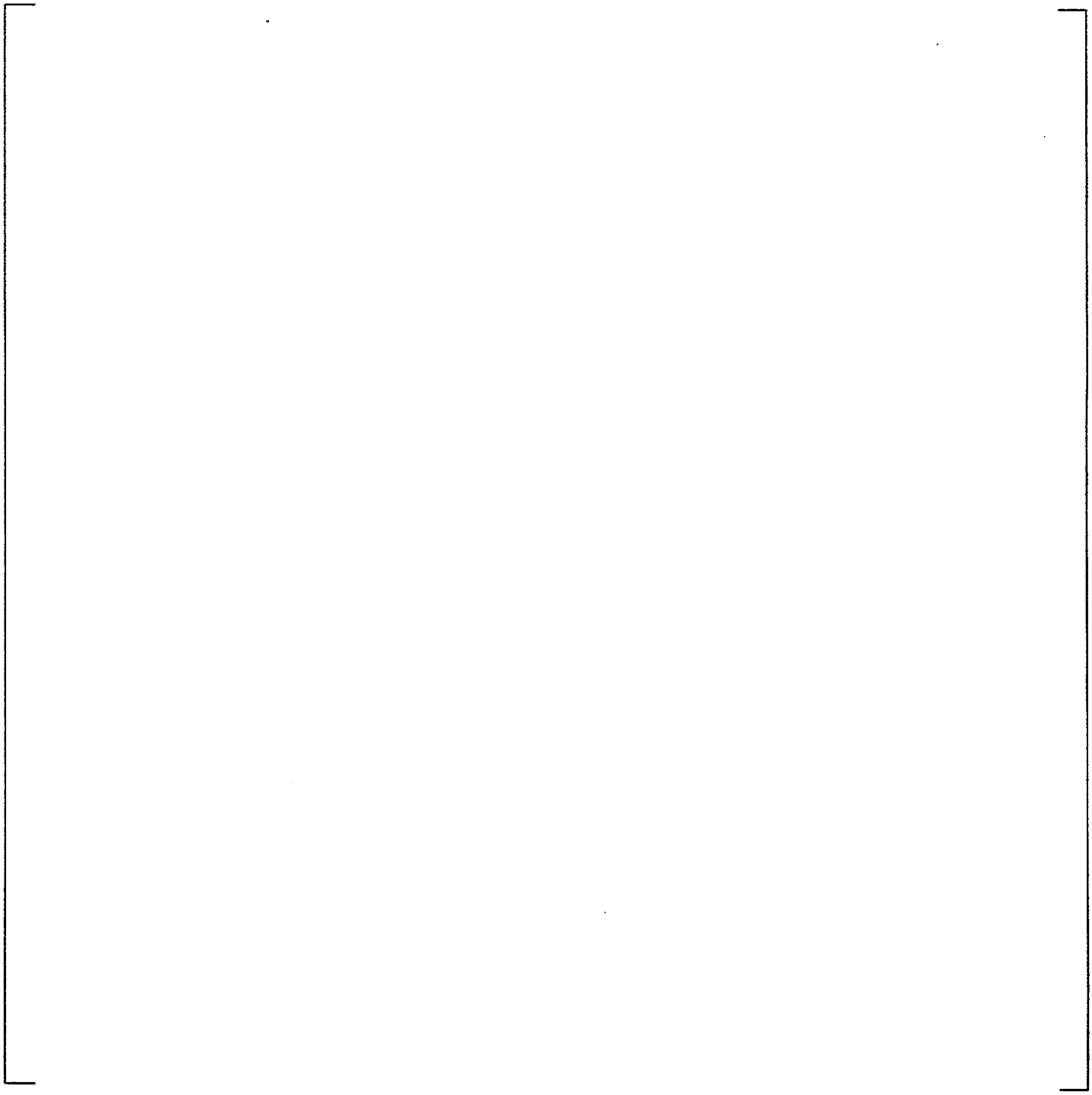

**Figure 6.11 Plates N, Q Support Locations**

a,c

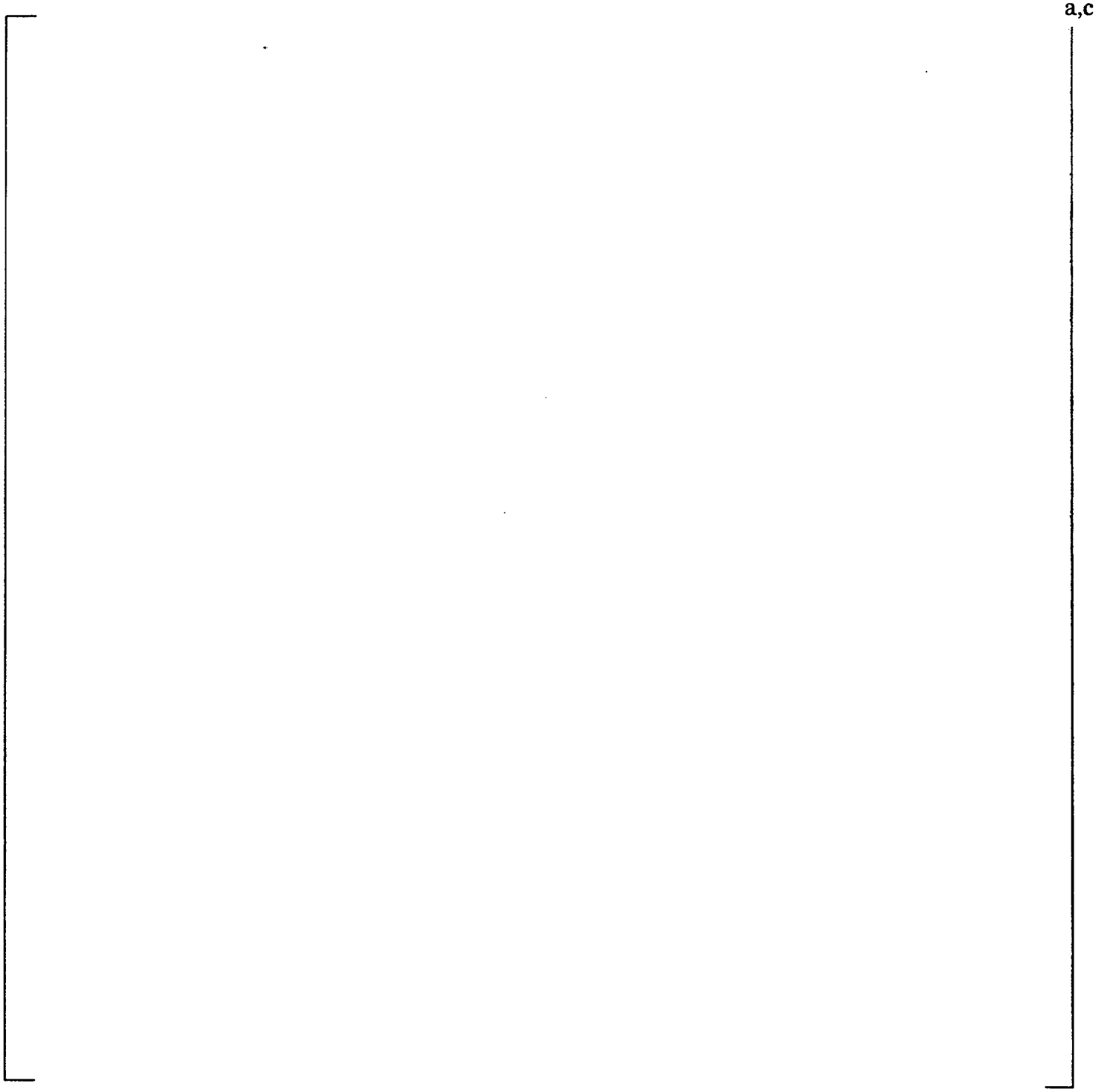

**Figure 6.12 Plate R Support Locations**

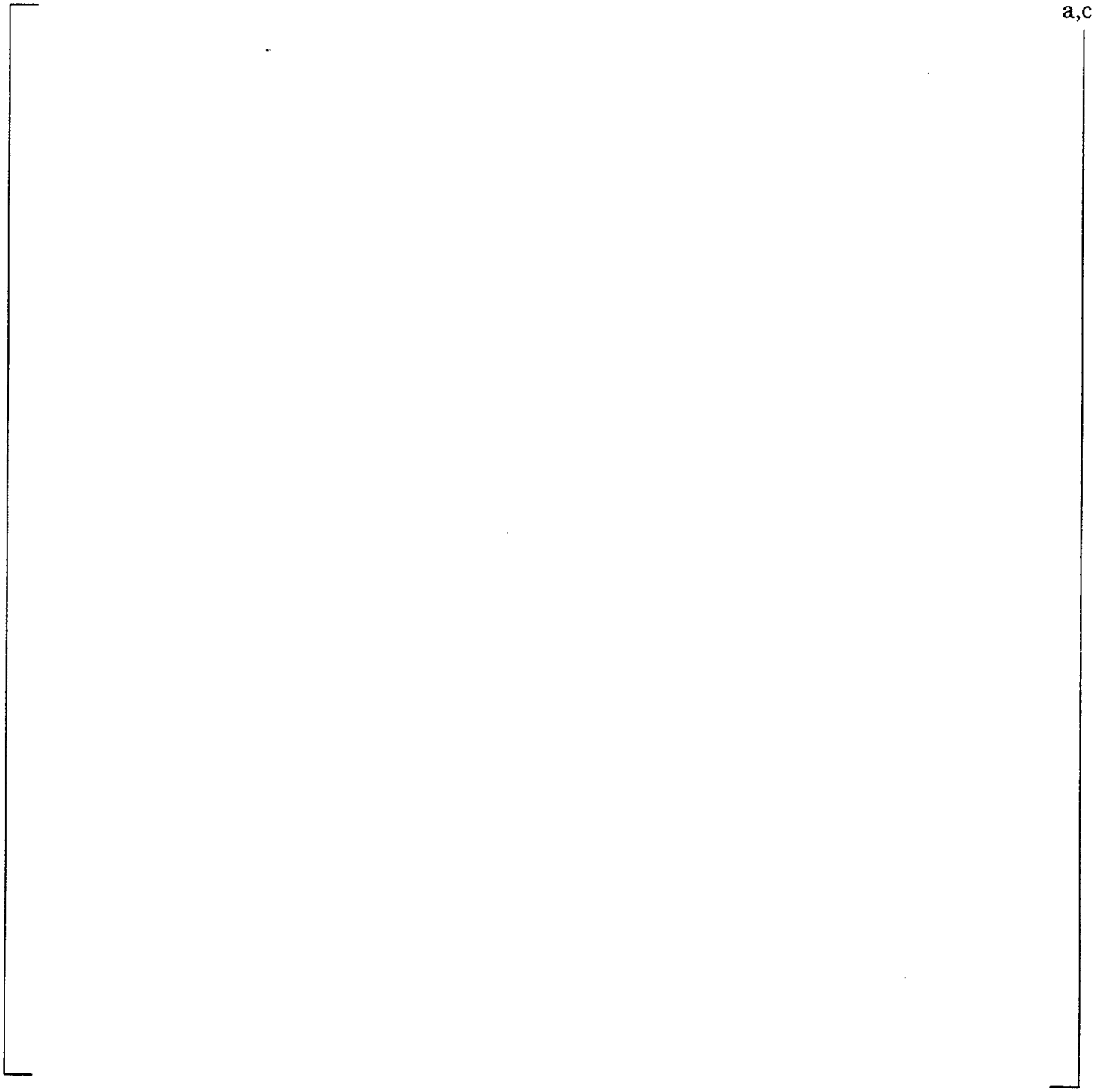

**Figure 6.13 Schematic of Wedge / Wrapper Interface**

a,c

**Figure 6.14 Schematic of Vertical Bar / Wrapper Interface**

a,c

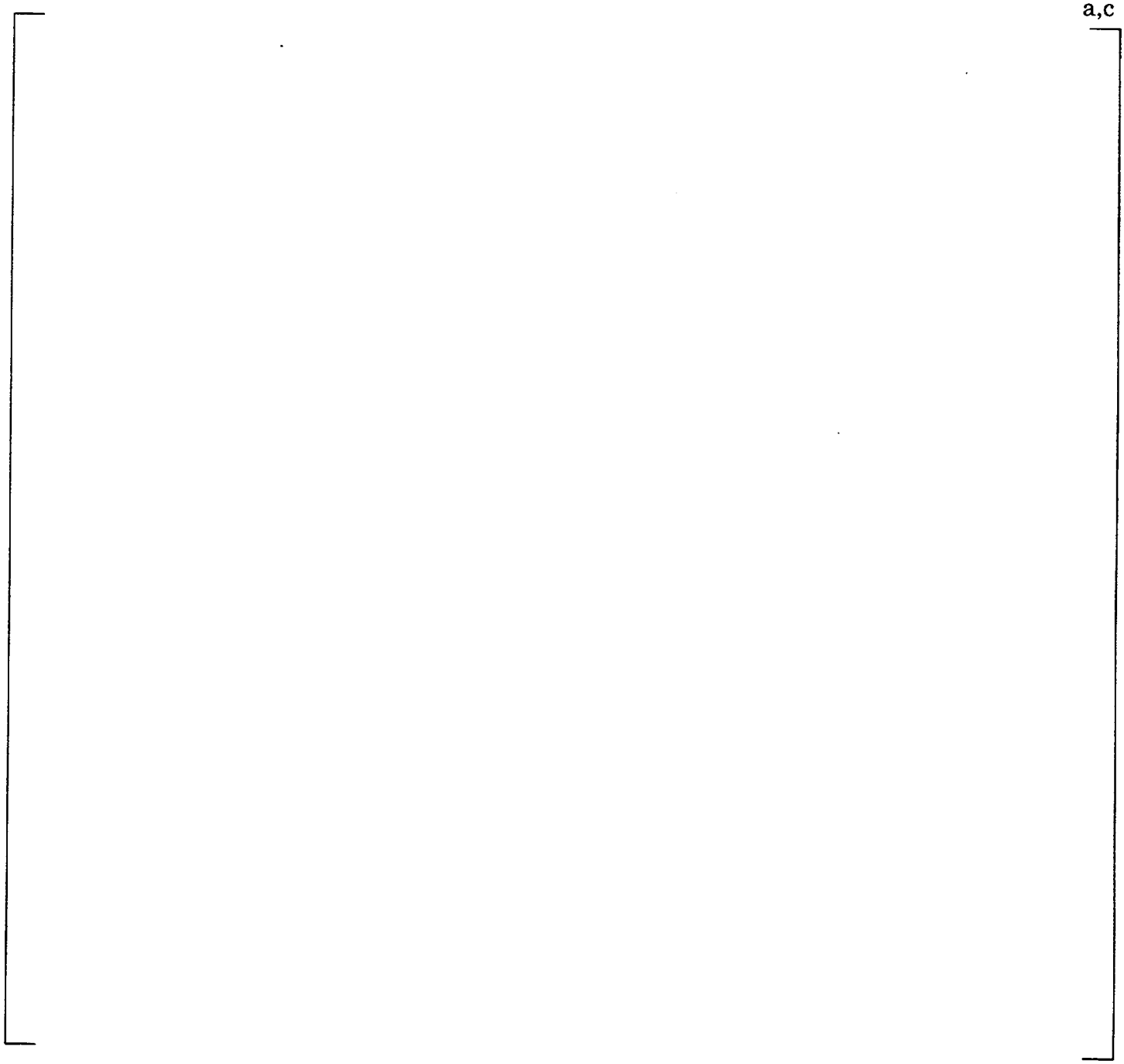

**Figure 6.15 Overall Finite Element Model**

a,c

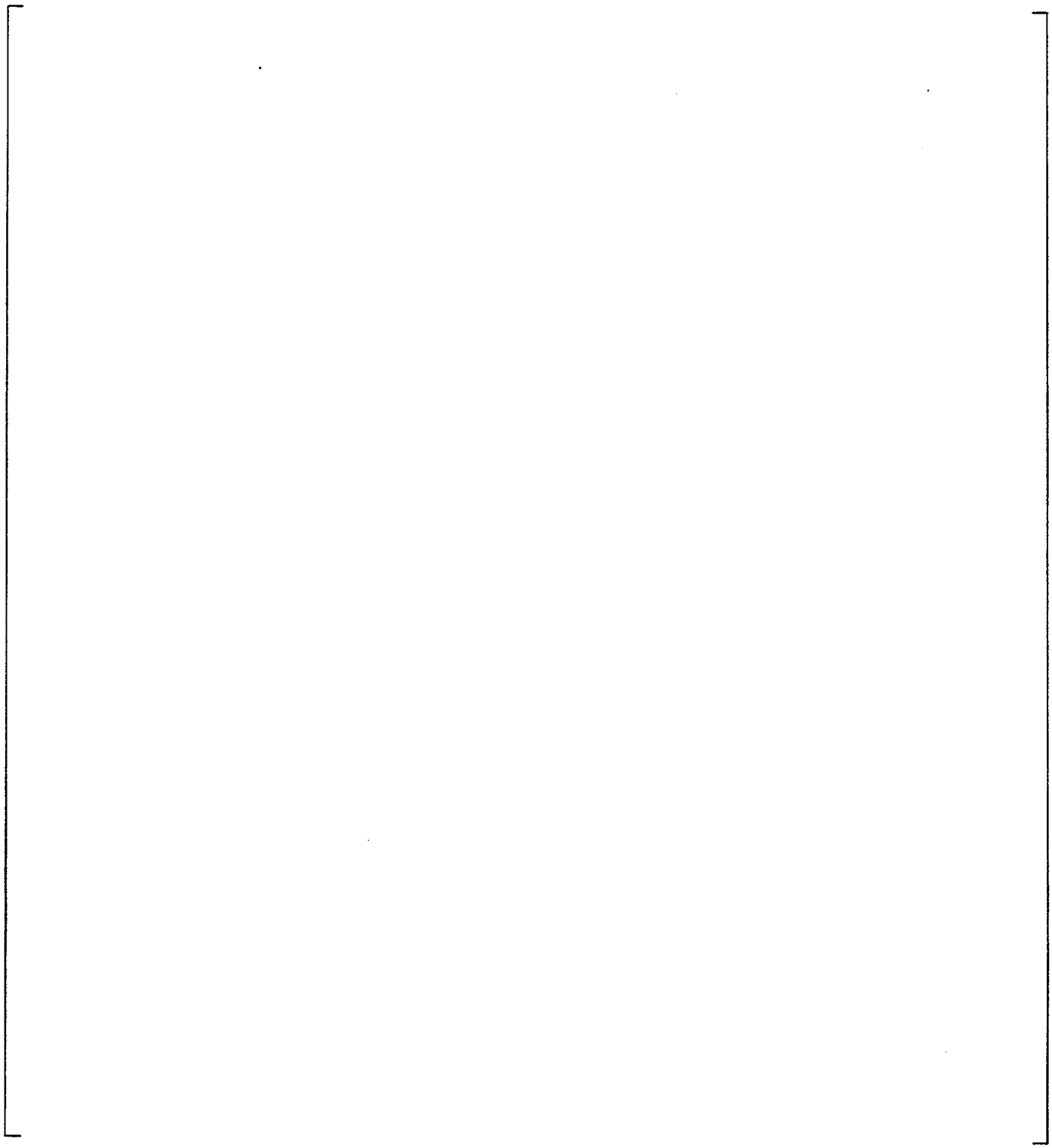

**Figure 6.16 Mode Shape Plot - Plate R**
**Full Set of DOF**
**Mode 1**

a,c

**Figure 6.17 Mode Shape Plot - Plate R**
**Full Set of DOF**
**Mode 2**

a,c

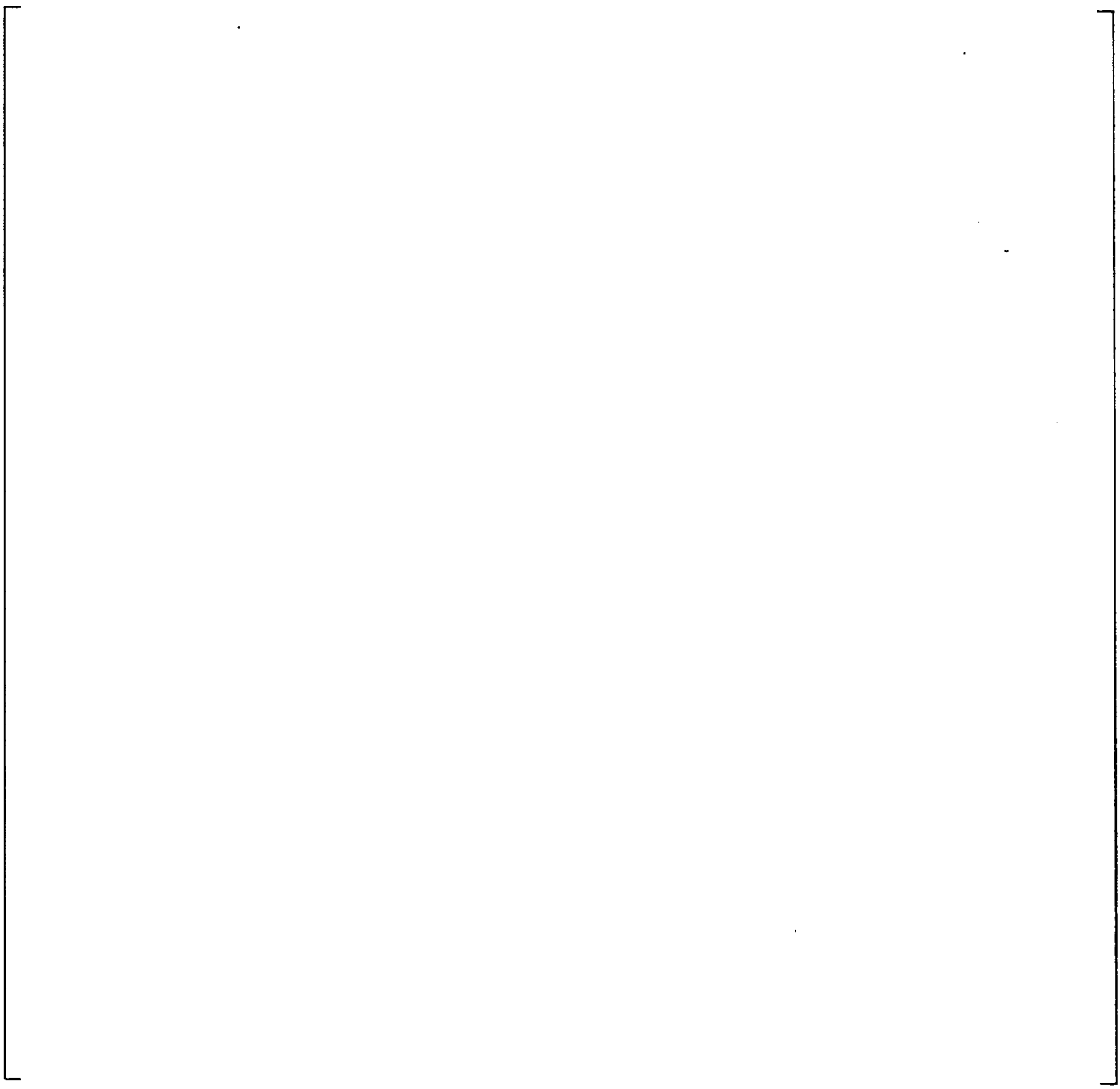

**Figure 6.18 Mode Shape Plot - Plate R**
**Full Set of DOF**
**Mode 3**

a,c

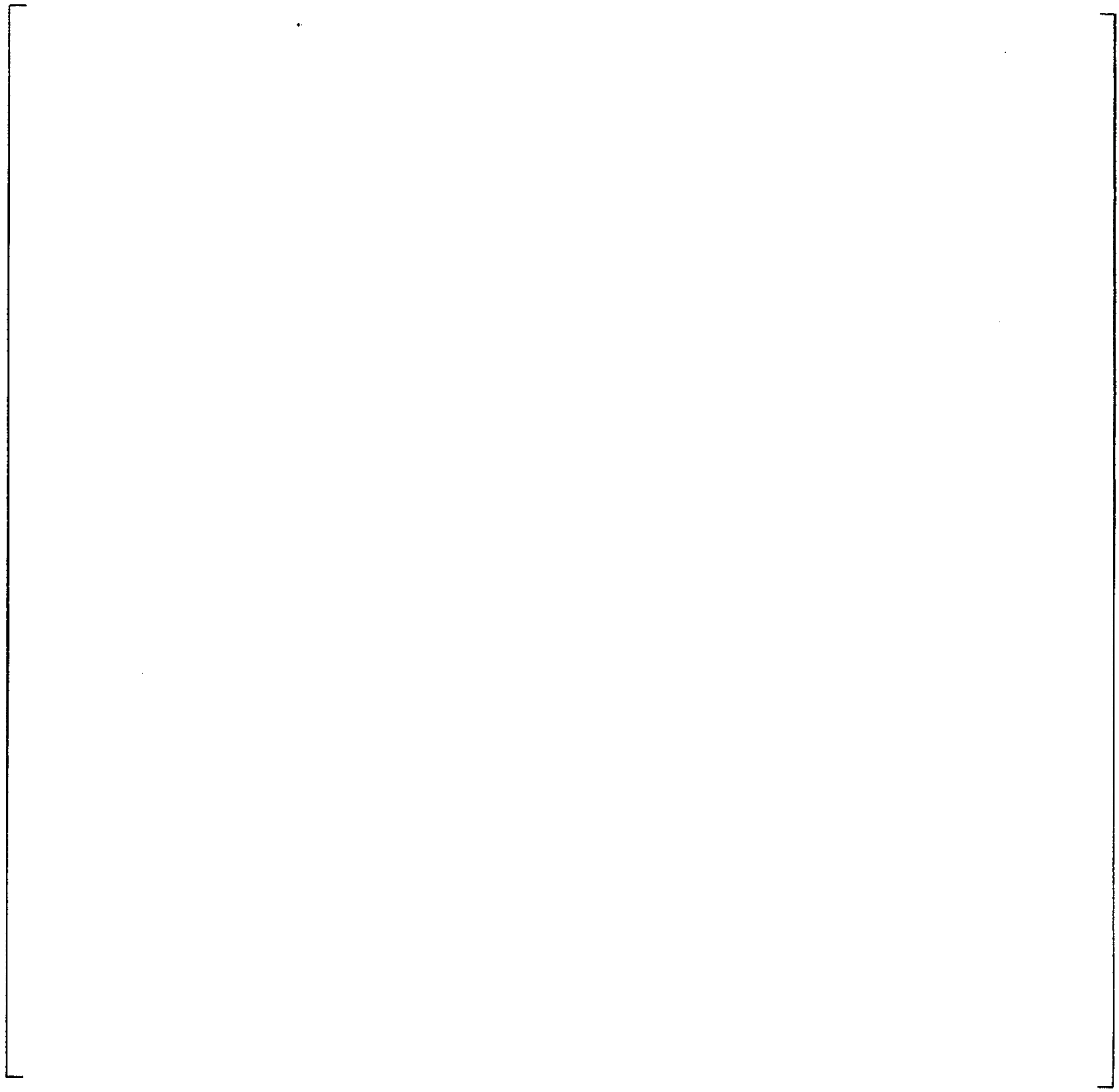

**Figure 6.19 Mode Shape Plot - Plate R**
**Full Set of DOF**
**Mode 4**

a,c

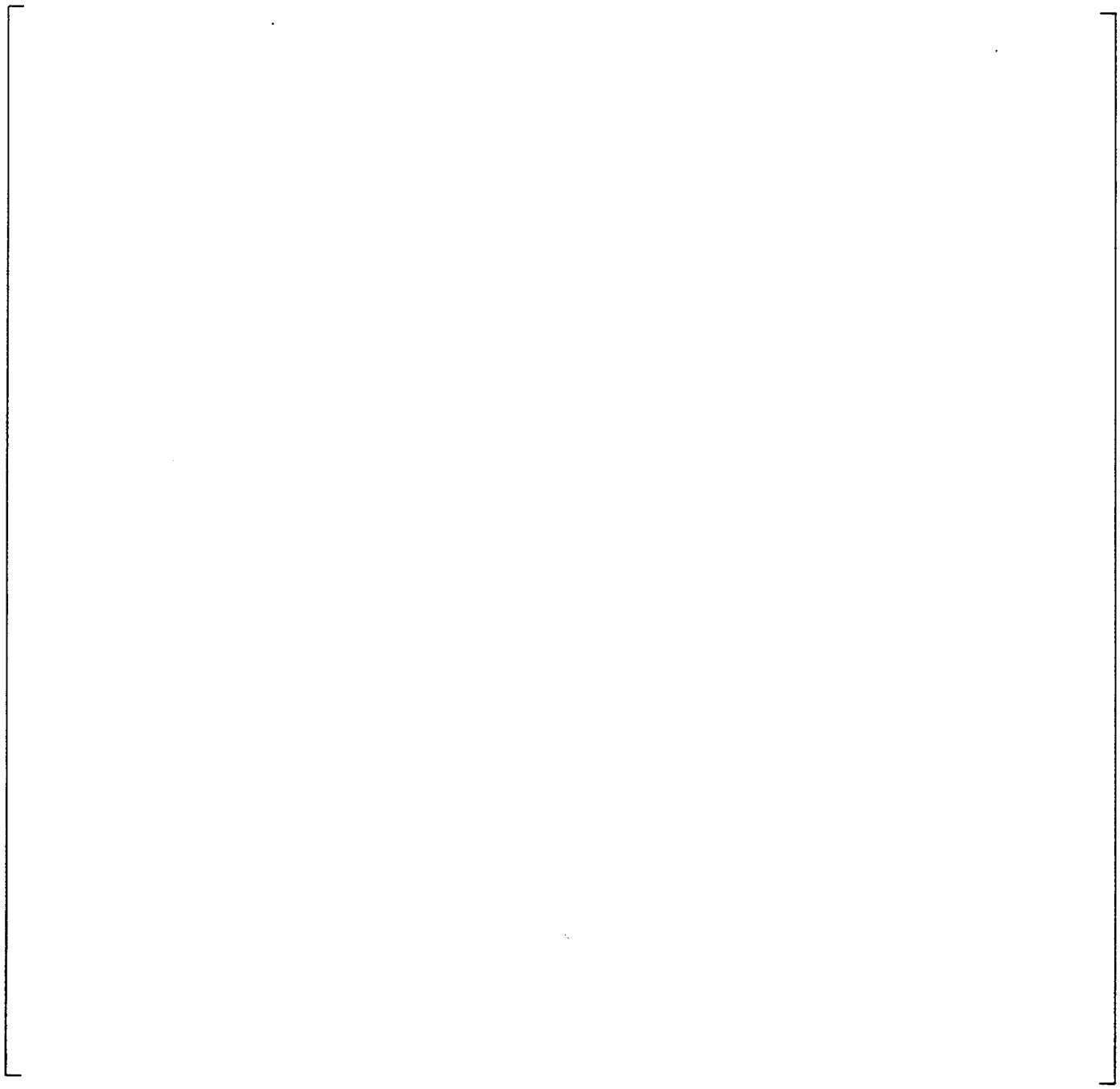

**Figure 6.20 Mode Shape Plot - Plate R**
**Full Set of DOF**
**Mode 5**

a,c

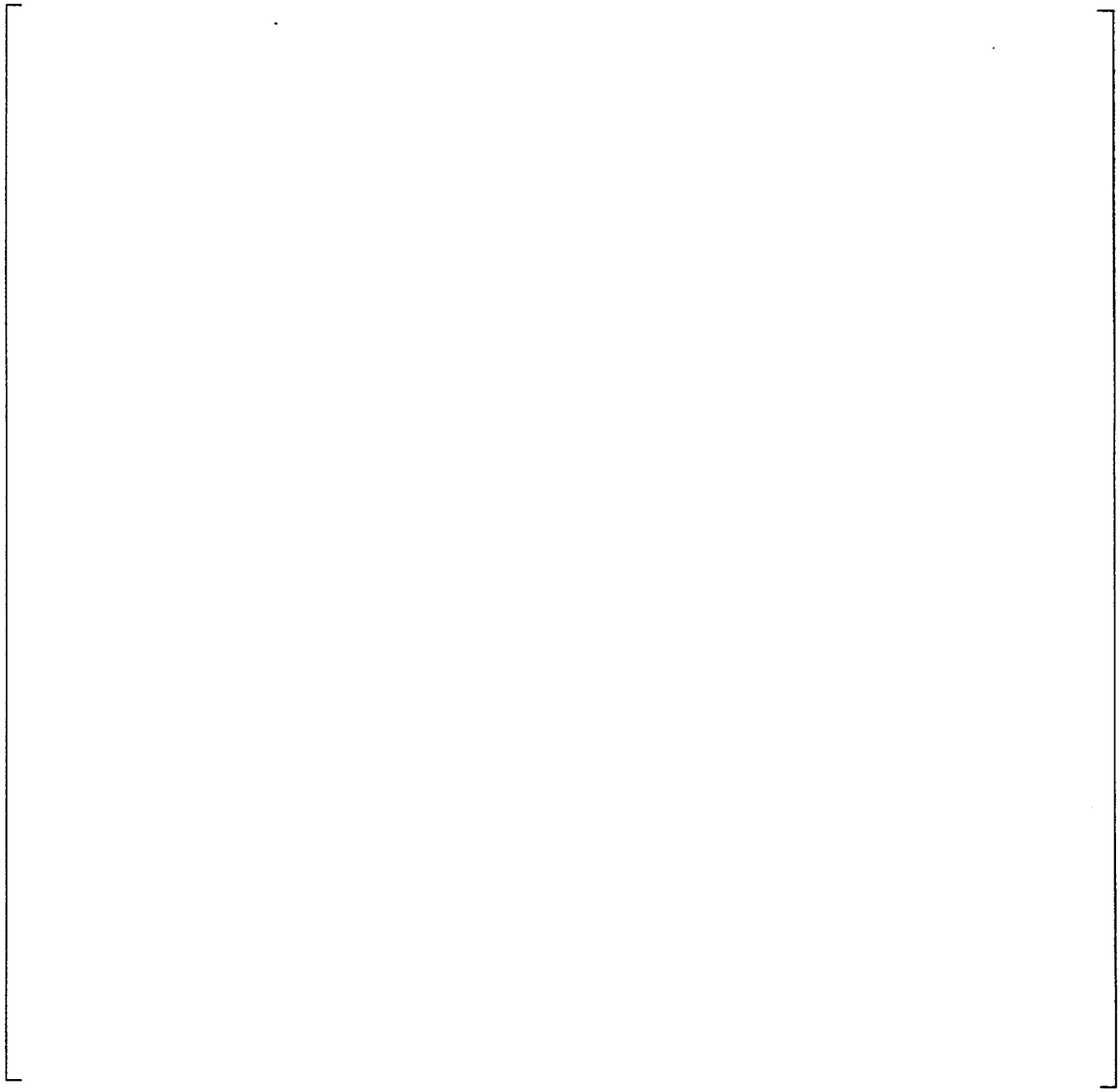

**Figure 6.21 Mode Shape Plot - Plate R**
**Reduced Set of DOF**
**Mode 1**

a,c

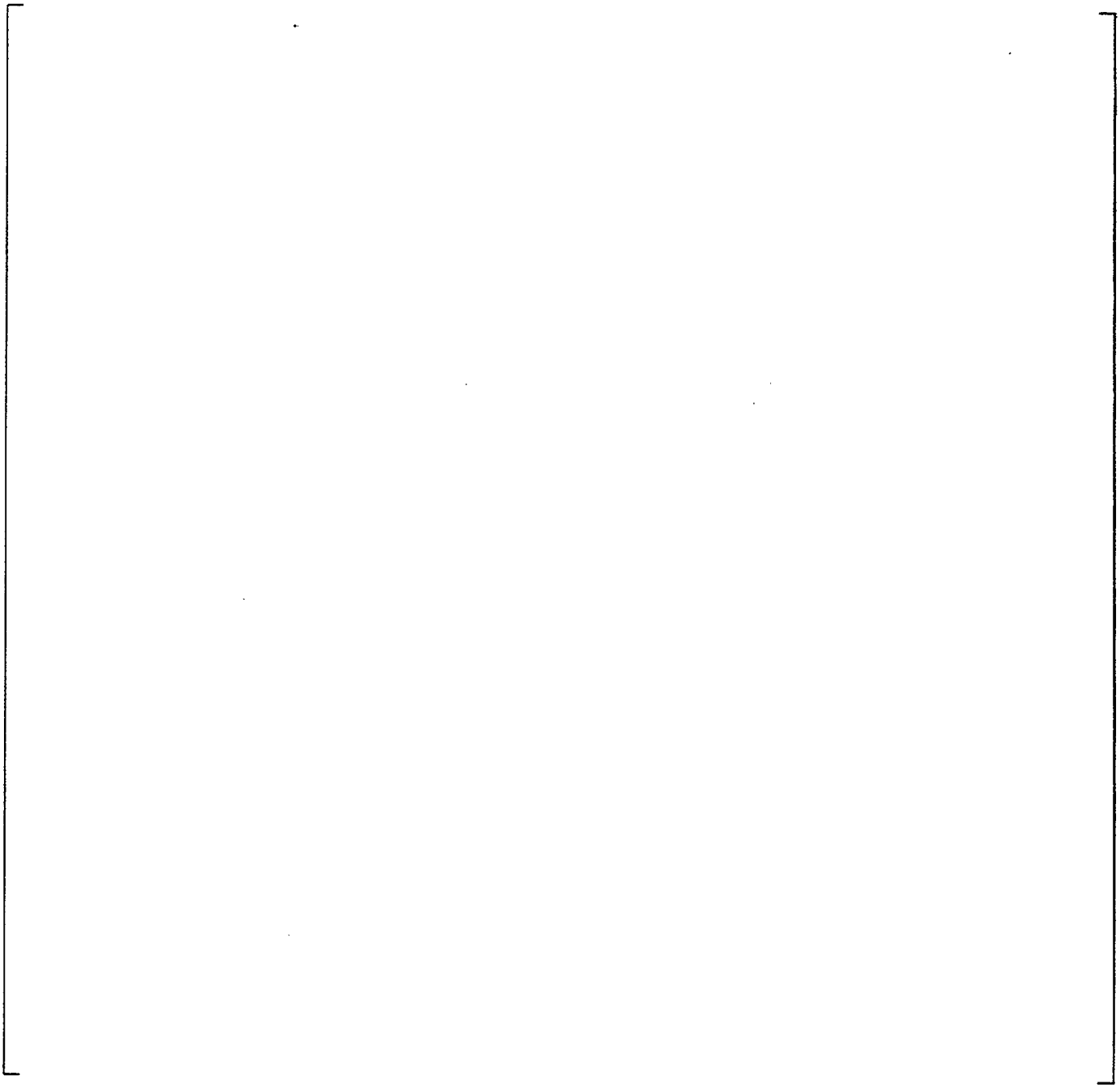

**Figure 6.22 Mode Shape Plot - Plate R**
**Reduced Set of DOF**
**Mode 2**

a,c

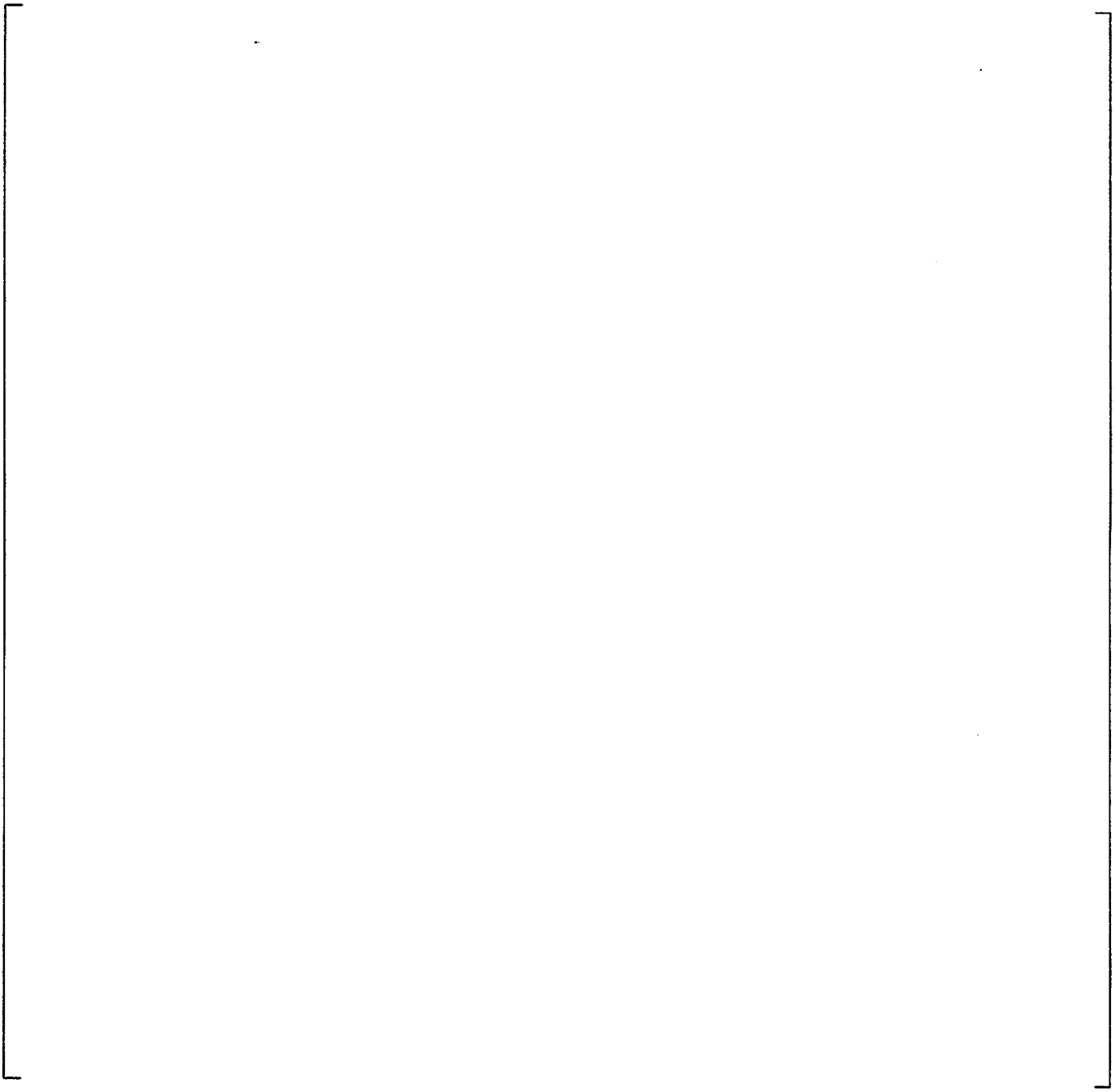

**Figure 6.23 Mode Shape Plot - Plate R**
**Reduced Set of DOF**
**Mode 3**

a,c

**Figure 6.24 Mode Shape Plot - Plate R**
**Reduced Set of DOF**
**Mode 4**

a,c

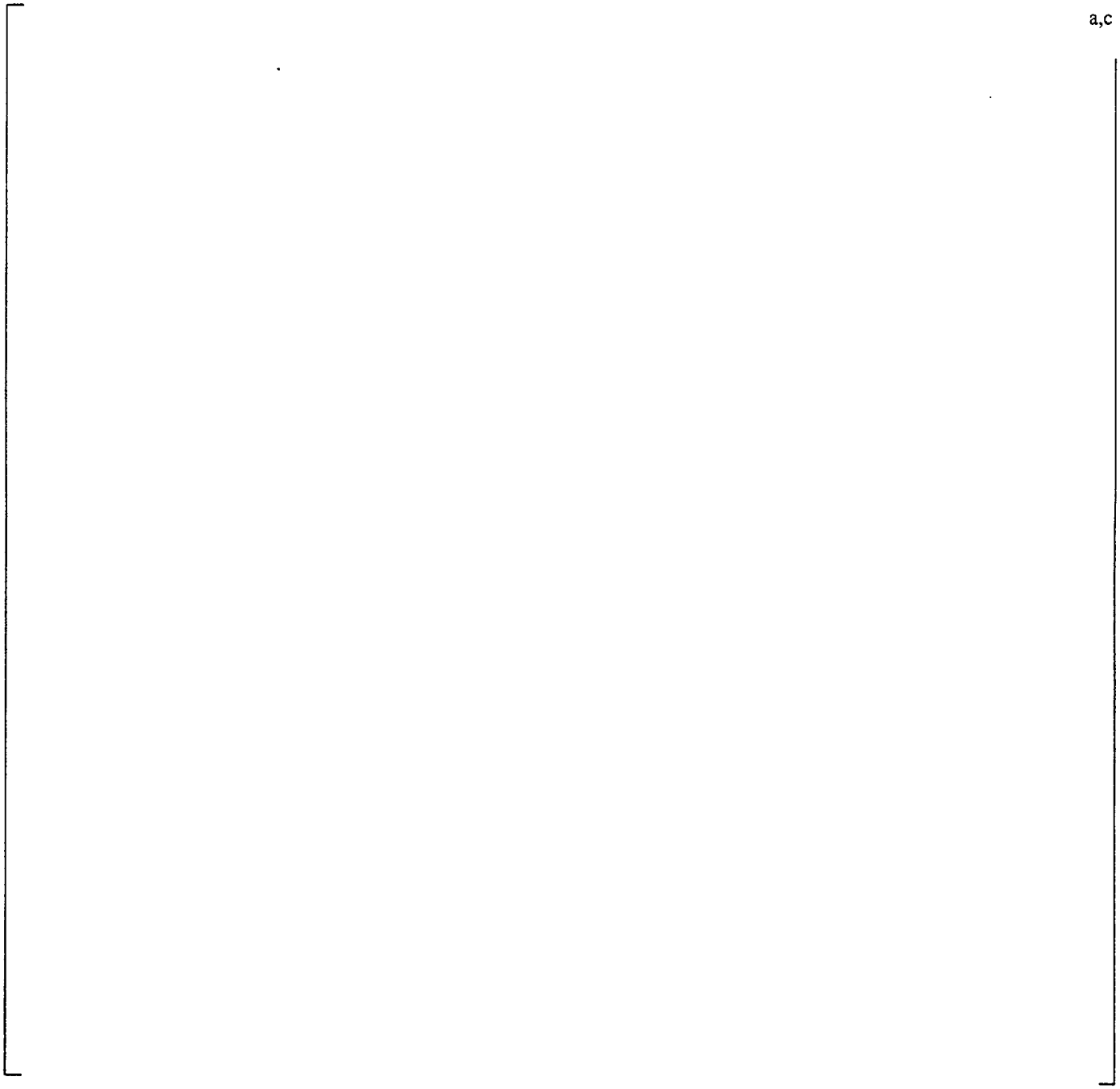

**Figure 6.25 Mode Shape Plot - Plate R**
**Reduced Set of DOF**
**Mode 5** a,c

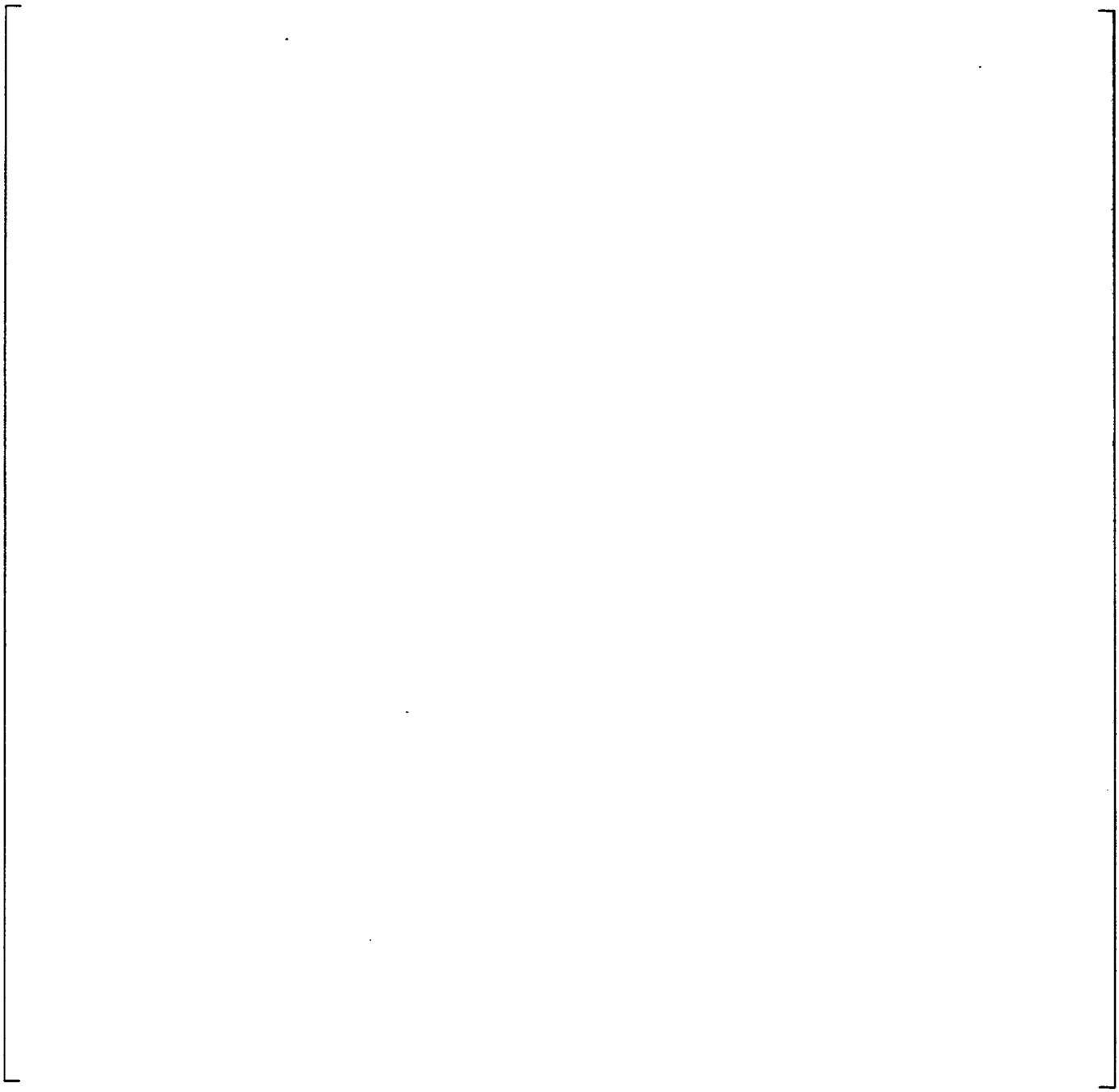

**Figure 6.26 Dynamic Degrees of Freedom**
**Plate P - Hot Leg**

a,c

**Figure 6.27 Dynamic Degrees of Freedom**
**Plate Q - Hot Leg**

a,c

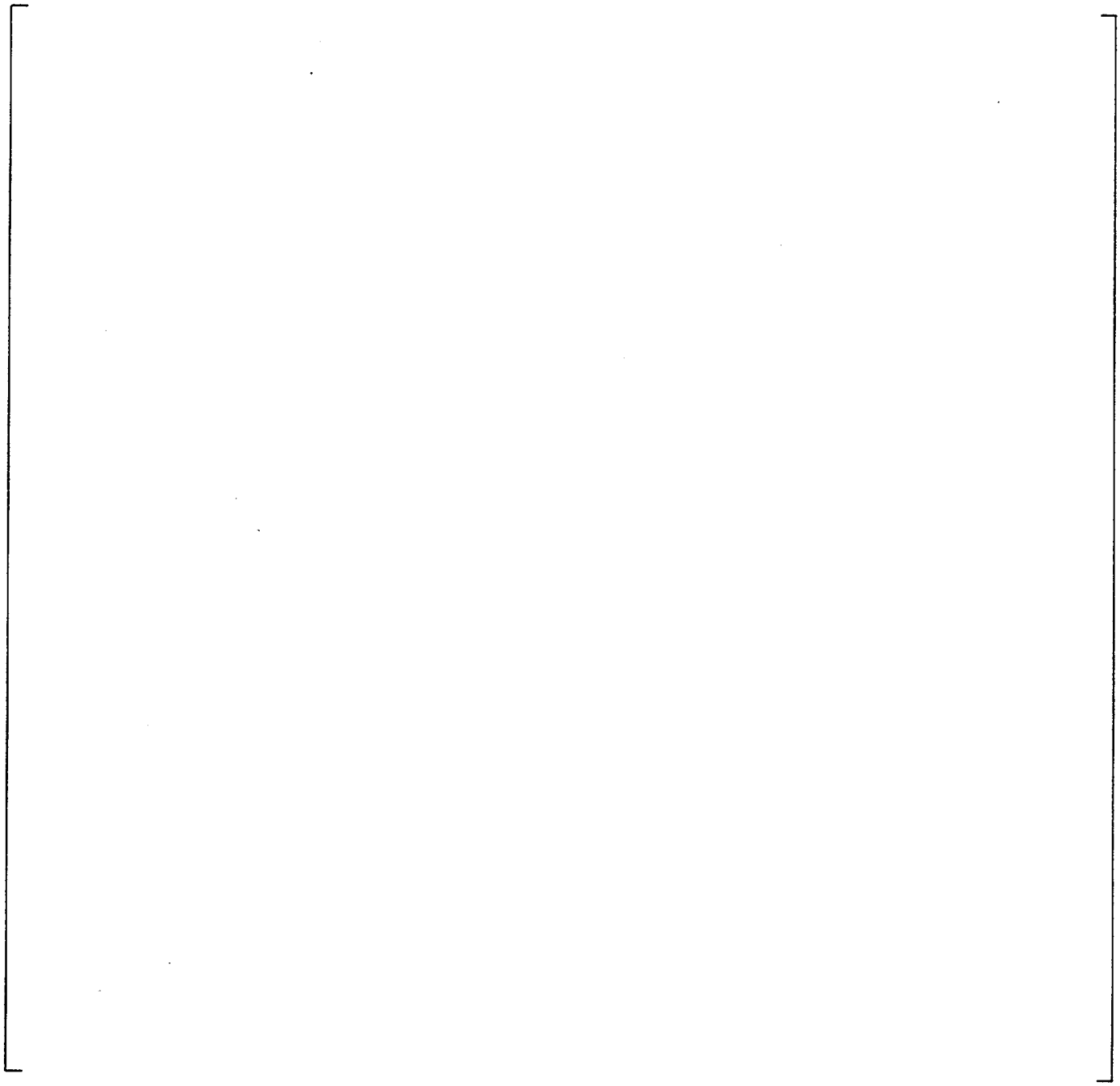

**Figure 6.28 Dynamic Degrees of Freedom**
**Plate R - Hot Leg**

a,c

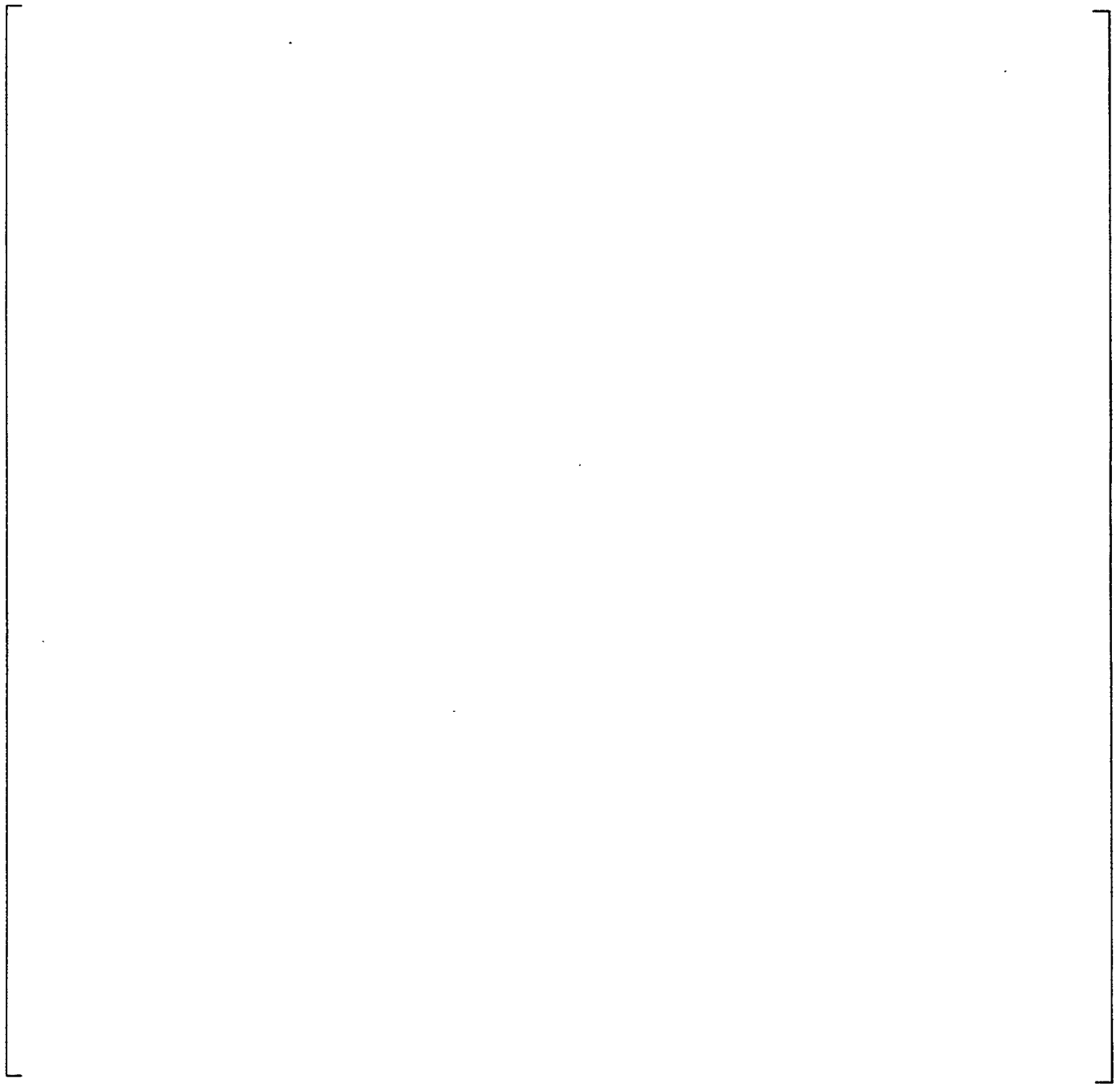

**Figure 6.29 Dynamic Degrees of Freedom**
**Plate D - Cold Leg**

a,c

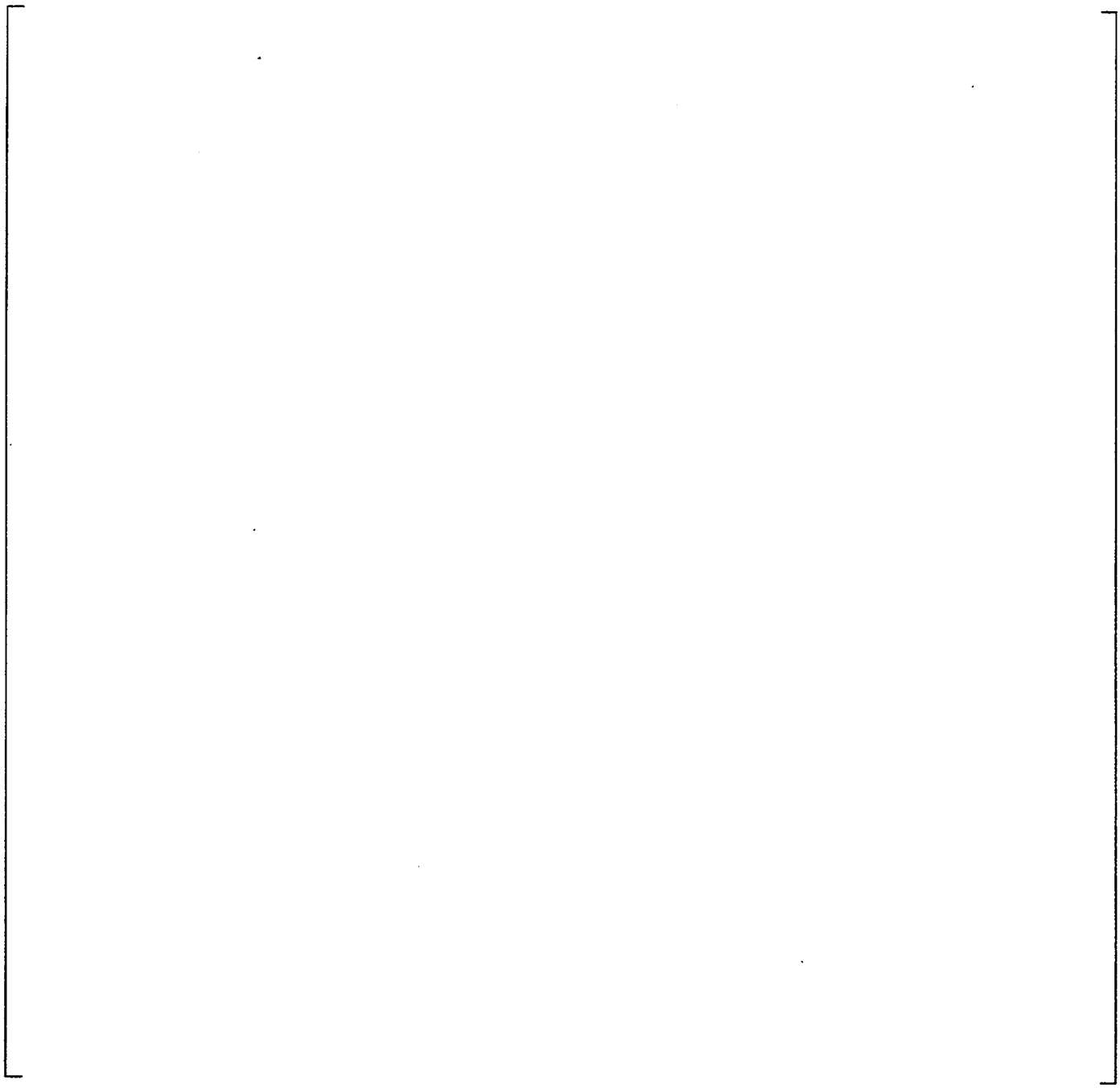

**Figure 6.30 Dynamic Degrees of Freedom**
**Plate E - Cold Leg**

a,c

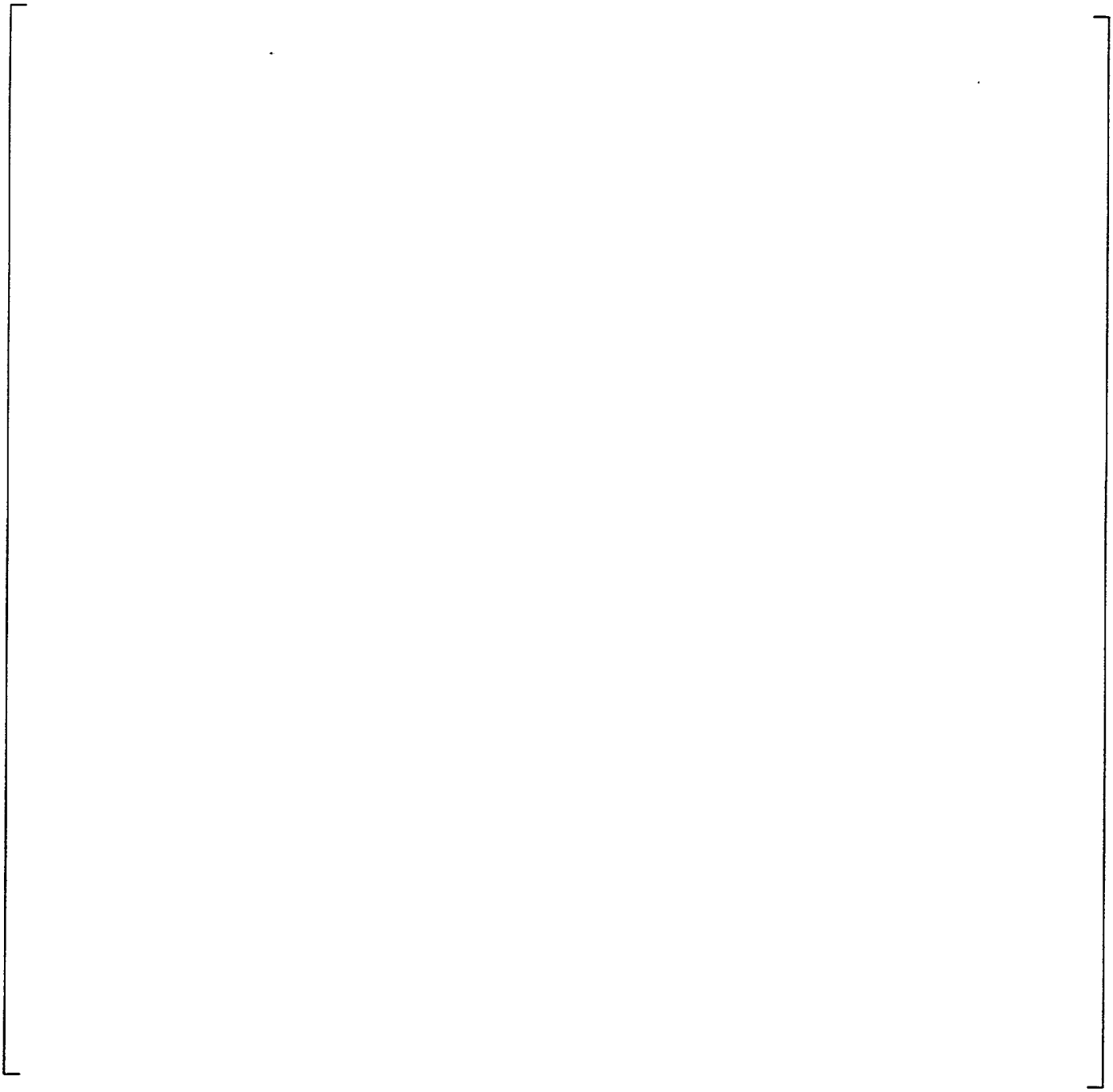

# 7.0 TSP DISPLACEMENT ANALYSIS RESULTS

## 7.1 Displacement Results

As discussed earlier, calculations have been performed for SLB initiating from hot standby, and for SLB initiating from full power. It is the relative plate / tube displacement that is of interest, with the tube and plate positions at the start of the SLB transient defined as the reference position. At hot standby, the TSP positions relative to cracks inside the TSP are essentially the same as at cold shutdown. Every known SG inspection (at cold conditions) shows ODSCC cracks within the non-dented TSP with a trend towards being centered within the TSP. Therefore, the cold condition TSP location relative to the tubes is essentially the same as for the full power condition under which the cracks formed, which is also the position during hot standby. These inspections indicate that there is little relative movement between the tubes and plates throughout the operating cycle. Thus, this analysis calculates relative tube / TSP motions based on the tube / plate positions at the initiation of the SLB transient.

A summary of the maximum / minimum displacements for each of the plates for both transient conditions is provided in Table 7-1. Although the hot leg of the tube bundle is the main area of interest, results are provided for both the hot and cold legs. The results show that, for the hot leg, only Plates N, P, and Q exceed the displacement limit of 0.150 inch for the SLB from hot standby, and only plate Q exceeds the displacement limit for SLB from full power.[1] Note that Plate R has an increased thickness relative to the other plates in the tube bundle. Thus, although Plate R sees the highest pressure loading, the increased thickness causes the maximum displacements to be lower than the plates just below it.

Based on the results in Table 7-1, it is apparent that the SLB from hot standby is the limiting condition. Time history plots for the hot leg plate locations having the maximum displacement are shown in Figures 7-1 to 7-3. A displaced geometry plot for the overall tube bundle is shown in Figure 7-4. Note that the maximum displacement does not occur for all of the plates at the same time in the transient. The plot in Figure 7-4 is at time equal 0.2544 second, which corresponds to the time

---

[1] The 0.15 inch displacement limit is exceeded in the negative (downward) direction for Plate A, the flow distribution baffle. However, this plate is excluded from consideration for this analysis. Results are presented for information only.

of maximum displacement for Plates N and Q, although the general displacement pattern is correct for all of the hot leg plates.

## 7.2 Stayrod / Spacer Stresses

Since the dynamic analysis is based on elastic response, calculations are performed to assure that the stayrods and spacers, significant support members for the plates, remain elastic throughout the transient. The ASME Code minimum yield stress for the stayrods and spacers is 34.0 ksi, and 26.9 ksi, respectively. A summary of the resulting stayrod stresses is provided in Table 7-2. Results for the spacers show a maximum compressive stress of [ ]$^{a,c}$ It is apparent that the stayrod and spacer stresses are well below the material yield strength.

## 7.3 Tube Support Plate Stresses

Also relevant in assessing the appropriateness of the elastic solution, are the stresses in the tube support plates. Thus, stresses are calculated for the tube support plates at the time corresponding to the maximum plate displacements. For the plates, the main area of interest is the hot leg side of the bundle, and the cold leg plates in the upper bundle region. Local yielding of the plates in the preheater region will not have a significant effect on the response of the hot leg plates. The stresses are calculated by extracting displacements from the dynamic analysis for each degree of freedom at the time(s) of maximum displacement, and then applying those displacements to the finite element model. The finite element code then back-calculates the displacements and stresses for the overall model. Displacement boundary conditions are extracted at the times of maximum relative displacement of Plates N through R, and corresponding stress calculations performed.

Additional boundary conditions corresponding to lines of symmetry and channel head constraints are also applied to the model. Plate stresses are all less than [ ]$^{a,c}$. As with the stayrods and spacers, the plate stresses are all below the material yield strength of 21.2 ksi.

## 7.4 Vertical Bar / Wedge Weld Stresses

Calculations have also been performed to determine the stresses in the welds between the vertical bars and the partition plate and wrapper, and between the wedges and the wrapper. The loads at the various support points are extracted

from the static WECAN runs in the form of reaction forces at the times of maximum plate deflection.

The wedges are welded to the wrapper using [

]a,c

Results of the calculations show all of the stresses to be low [ ]a,c. The allowable stress for the SLB transient (a Level D event in the ASME Code) for the welds is based on 2.4 $S_m$ x 0.35 (for fillet welds with visual examination) for carbon steel. $S_m$ at 550°F is 15.5 ksi. The resulting allowable stress intensity is 13.02 ksi, and the weld stresses are acceptable.

## 7.5 Thermal Expansion Effects

Calculations have been performed to investigate the effects of differential thermal expansion on the relative plate / tube displacements. Static calculations were performed that consider both temperature and pressure loads. The temperatures and pressures corresponding to full power and hot standby conditions are summarized in Table 7-3 for all but the active tubes. The full power temperature distribution for the active tubes on the hot leg is summarized in Table 7-4. Based on this distribution, an average temperature for each tube span is calculated, and then the span average temperatures are used to calculate a corresponding thermal growth for the tube. At hot standby, the steam generator is at a uniform temperature of 567°F.

The plate displacements under combined temperature and pressure conditions are calculated using the finite element model for the overall tube bundle. Thermal expansion of the active tubes is calculated using conventional techniques

A summary of relative tube / TSP displacements in going from full power to hot standby due to temperature and pressure is provided in Table 7-5.

The algorithm used for calculating the differential motions is as follows;

$$\Delta D = \text{Plate } \Delta - (\text{Tubesheet } \Delta + \text{Tube } \Delta), \text{ where D is the displacement.}$$

Combining the differential displacements from the temperature / pressure cases with the differential displacements from the dynamic analysis results in the differential displacements summarized in Tables 7-6. It should be pointed out that the maximum differential displacements for the two sets of loads, thermal and SLB, do not occur at the same location on the plate. Thus, the combined maximum displacements are less than the sum of the maximums for each of individual load cases. The results in Table 7-6 show that the 0.150 inch displacement limit is satisfied for Plates C, F, J, L, M, and R.

## 7.6 Full Non-Linear Solution

Due to the large number of degrees of freedom for this analysis (~500), and the large number of non-linear interfaces (~100), it was not feasible to perform a full non-linear analysis for each of the transient cases considered. Therefore, a quasi non-linear solution (hereafter referred to as the linear solution) was used to obtain the majority of the transient results. Since the load time history is applied to the majority of the plates in phase (at the same time), and since the stiffness characteristics of the plates is similar, the plates will generally respond at the same time. Reviewing the pressure time history loads in Section 5, it is observed that the load on the plates in the upper part of the bundle are in the up direction, while the load for the plates in the lower part of the bundle are in the down direction. Accordingly, the spacers between the plates in the upper and lower parts of the bundle will be in compression for the majority of the transient, and the non-linear interfaces between the plates and spacers will not open. For the plate(s) where the load splits, up versus down, the non-linear spacer interface will open. Thus, for the linear solution, only the spacers where the gaps will open due to the load split are defined to be non-linear. The other gaps are defined to be linear.

As a check of this approximation, full non-linear solutions were obtained. A comparison of the linear and non-linear solutions is summarized in Table 7-7. The results show that the non-linear solution gives slightly higher displacement results, but that overall, the linear solution provides a good approximation of the non-linear bundle response.

## Table 7-1

## Summary of Maximum / Minimum Displacement Results

a,c

[

]

**Table 7-2**
**Summary of Stayrod Stresses**
**SLB From Hot Standby**

a,c

[ ]

**Table 7-3**
**Summary of Applied Temperatures and Pressures**

a,c

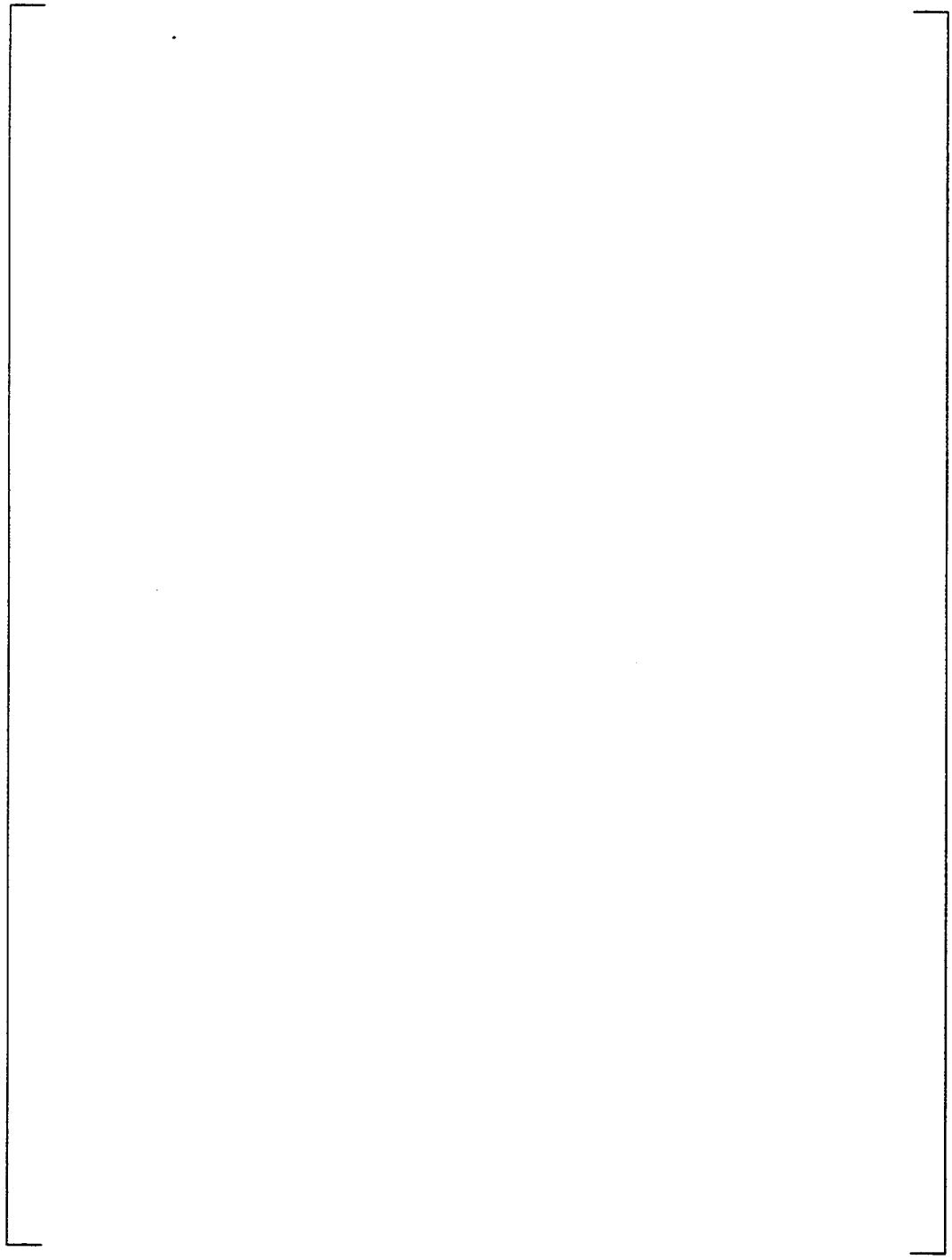

**Table 7-4**
**Typical Tube Temperatures**
**Full Power Conditions**

a,c

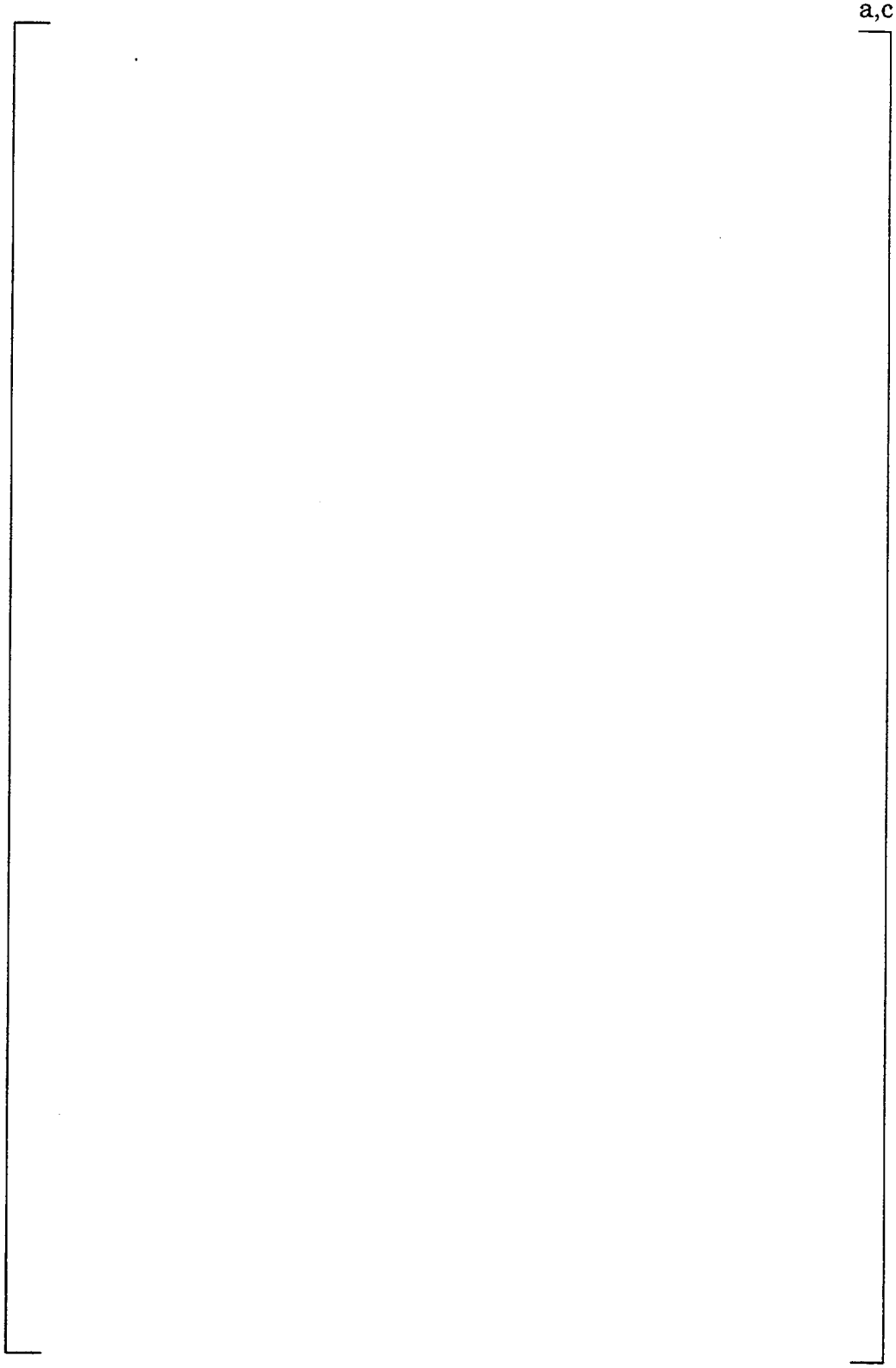

**Table 7-5**
**Summary of Displacement Results**
**Relative Tube / TSP Displacement**
**Temperature / Pressure Condition (Without SLB)**

**Full Power to Hot Standby (Without SLB)**

a,c

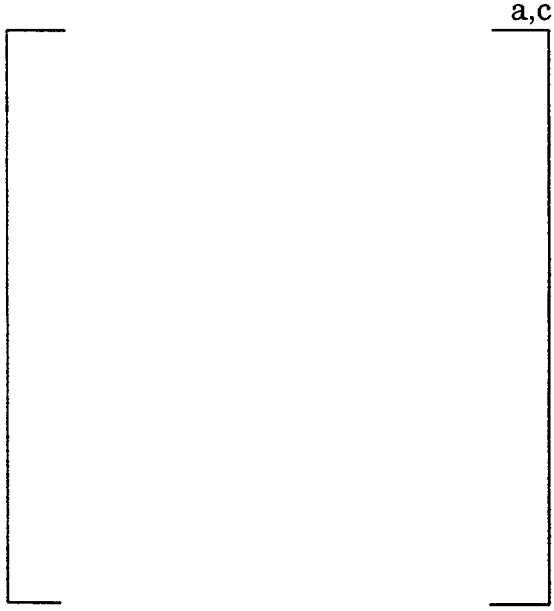

Displacements have units of inches

**Table 7-6**
**Summary of Displacement Results**
**Relative Tube / TSP Displacement**
**Temperature / Pressure Condition With SLB**

**Full Power to Hot Standby +SLB**

a,c

[ ]

Displacements have units of inches

**Table 7-7**
**Summary of Maximum / Minimum Displacement Results**
**Linear Versus Non-Linear Spacer Interaction**

a,c

[

]

Displacements have units of inches

**Figure 7.1 Displacement Time History**
**SLB From Hot Standby**
**Plates A, C, F**

a,c

**Figure 7.2 Displacement Time History**
**SLB From Hot Standby**
**Plates J, L, M**

a,c

**Figure 7.3 Displacement Time History**
**SLB From Hot Standby**
**Plates N, P, Q, R**

a,c

**Figure 7.4 Displaced Geometry Plot**
**SLB From Hot Standby**

a,c

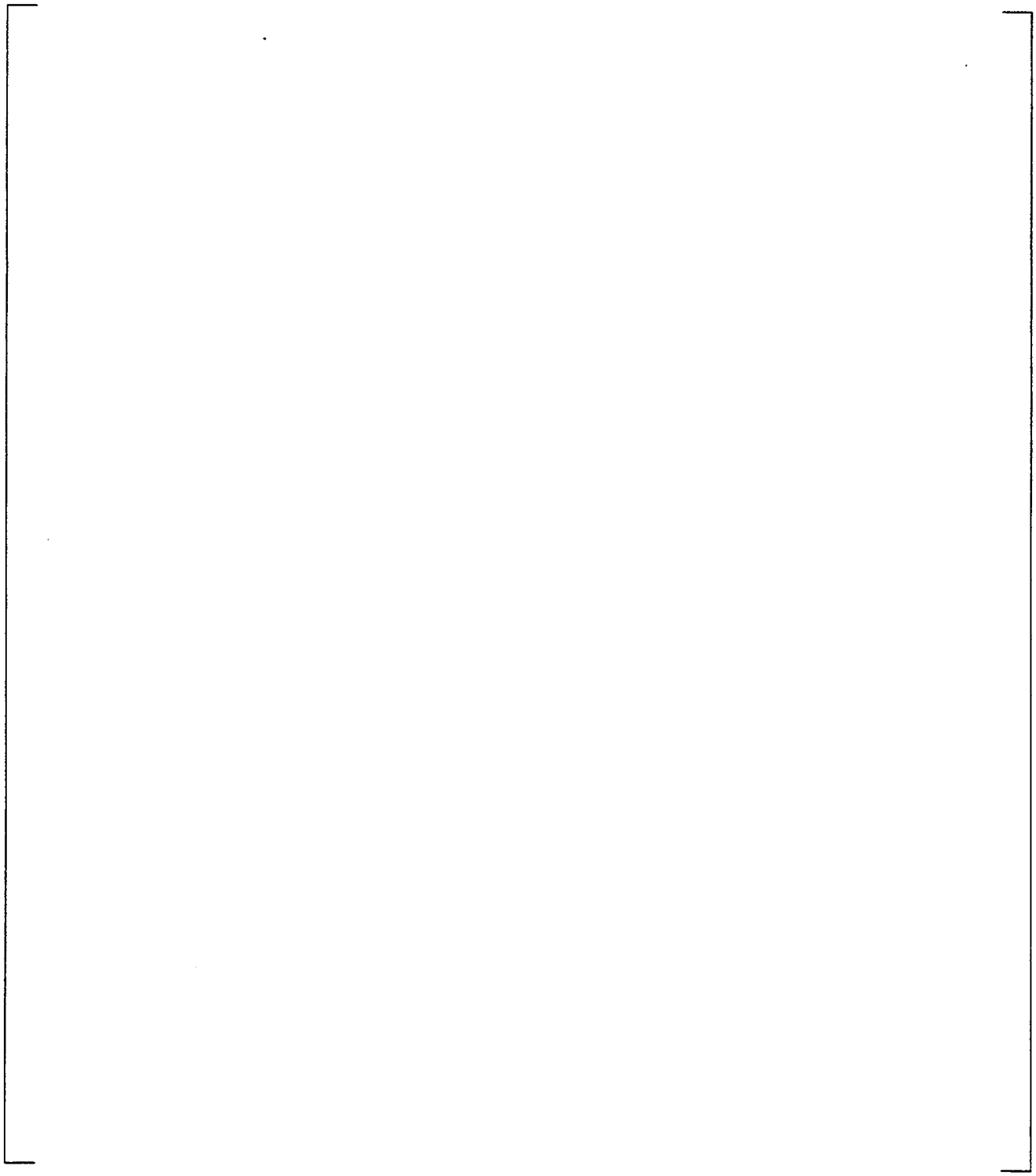

# 8. 0 TEST DATA SUPPORT FOR LEAKAGE FROM CONSTRAINED CRACKS

## 8.1 Introduction

To support implementation of high voltage ARC for limited TSP displacement under postulated SLB conditions, a test program was completed to determine the bounding leak rate and its sensitivity to TSP displacement for throughwall indications restricted from burst (IRB) (Reference 1). The test program was performed under EPRI sponsorship.

An IRB is defined as a tube crack at the intersection of the tube with the support plate, of a size that could burst under SLB conditions if it were a freespan crack. The crack is restricted from burst by the TSP, and it is further demonstrated that the leakage flow from an IRB is limited by the presence of the TSP to less than the freespan leakage for a like crack. During a postulated SLB event, the depressurization of the SG causes the TSPs to deflect from their nominal position as discussed in Section 7, thus potentially partially exposing the cracks at the TSP intersections. The analysis results discussed in section 7 show that the maximum TSP displacement for the Model E2 SG is about 0.25" for plate Q (see Figure 6.1). For plates C, F, J, L and M, the maximum hot leg TSP displacement is shown to be less than 0.15". The limited displacement of the TSPs permits an increase in the acceptable bobbin voltage for indications remaining in service.

It was the objective of this test program to establish a data base for leakage from cracks in prototypic steam generator tubing under prototypic pressure and temperature conditions to verify that the leakage from cracks left in service under a high voltage ARC will not result in unacceptable leakage during SLB accident conditions. SLB conditions are defined as 615°F primary coolant temperature and a pressure differential of 2560 psid. (For South Texas Unit 2, a SLB differential of 2405 psi may be applied based on operation of the PORVs to limit primary pressure.) The bulk of the tests were performed in a high-energy steam test facility that is capable of flow rates of about 8 gpm at these conditions. A complete description of the high-energy leak tests facility and test operations is contained in Reference 1. The high temperature leak tests were augmented by tests performed in a room temperature, high-pressure leak test facility. Room temperature tests are much easier to perform; thus it was the objective of the room temperature tests to demonstrate the adequacy of the EPRI method for adjusting RT data to high temperature conditions.

A specific objective of the test program was to determine a bounding leak rate for an IRB that exceeds the limit of an indication that could remain in service. GL 95-05 specifies that no indication that extends beyond the span of the TSP may remain in service. The TSP thickness is 0.750 inch, thus the maximum indication is limited effectively to less than 0.750 inch for the packed crevice condition causing initiation and growth of the ODSCC indication. The critical throughwall crack length in 3/4"

diameter tubing at lower tolerance limit (LTL) material properties is 0.750 inch (Reference 2). Cracks at, or less than, this throughwall length would not be expected to burst at the SLB pressure differential. Thus, the practical limit of cracks to be tested was set at approximately 0.750 inch, although shorter cracks and one longer crack were also included in the test program to observe the structural and leakage trends of the cracks.

Fifteen specimens were tested as summarized on Table 8.1. The specimens were prepared from prototypic steam generator tubing material, mill annealed Alloy 600. Specimens were prepared by three processes: 1) accelerated corrosion, 2) accelerated corrosion followed by fatigue to increase the length of the crack, and 3) laser cutting. Eight of the specimens were 7/8" diameter specimens, and the remainder were 3/4" specimens. Cracks with different throughwall lengths in a range from 0.24" to 0.809" were tested. The tests simulated a cracked tube at a TSP, but, conservatively, with the maximum diametral clearance of 0.025" between the tube and the TSP. The tests were fixtured to provide a 0.025" gap at the side of the tube with the crack to minimize the restriction provided by the TSP.

The longest throughwall crack length tested, 0.809 inch was greater than any crack that could be formed at a TSP intersection, which is 0.750 inches thick. Also, throughwall cracks of significant length would have bobbin voltages well in excess of the 3-volt limit proposed for the high voltage ARC.

Testing was performed with (a) the cracks completely contained within the span of the TSP with one end of the crack aligned with the edge of the TSP, and (b) with the crack tip intentionally positioned (offset) outside the TSP by a distance. The nominal offset of the crack tip from the tube was 0.1" for the 3/4" diameter specimens and 0.15" for the 7/8" specimens. The actual range of offsets tested extended up to 0.210" for the total crack and 0.173 inch for the throughwall cracks based on in-process examination of the test specimens.

Following tests by pressurizing the ID of the tube and measuring the leak rate through the crack (Flow Pressurization Tests), the crack in the tube was opened by installing a bladder at the location of the crack, and pressurizing the bladder to the predicted freespan burst pressure (based on the length of the crack and the known material properties of the tube). Bladder pressurization was performed with the tube constrained within the TSP, but with the crack tip offset from the TSP. Following this, the bladder was removed, and additional leak tests were performed in both the non-offset and offset conditions. These tests are referred to as Bladder Pressurized flow tests.

Freespan leak tests were performed on some of the specimens to provide a comparison of IRB and freespan leak rates. Some of the specimens were tested at approximately

room temperature conditions as well as prototypic elevated temperature conditions to provide a basis of evaluating analytical techniques for adjusting low temperature data to high temperature conditions. The method of adjusting the conditions of various tests to the standard SLB condition is described in Reference 3.

The burst pressure to bobbin voltage correlation results in very conservative burst pressures and burst probabilities when uncertainties are considered. A wide range of burst pressures occurs at a given voltage since different crack morphologies can result in comparable voltages. When a direct structural parameter such as throughwall crack length is correlated with burst pressure, correlation uncertainties are much smaller than for a voltage correlation. Recall that the EPRI burst correlation (Reference 2) for throughwall axial cracks leads to a throughwall crack length of 0.75 inch at $\Delta P_{SLB}$=2560 psi for lower tolerance limit (LTL) material properties. Thus, the probability of burst at SLB conditions is negligibly small due to the requirement for a throughwall crack length equal to the thickness of the TSP. As noted later in Section 8.2, pulled tubes with throughwall cracks near 0.5 inch long have had voltages between 13 and 20 volts, thus, a 0.75 inch throughwall crack could be expected to exceed 20 volts. This demonstrates the conservatism in the burst /voltage correlation for which 9 volts corresponds to a $10^{-2}$ burst probability.

The intent of the IRB test program was to develop a leak rate for an indication inside the TSP that could burst in freespan at 2560 psi. Since the ODSCC cracks formed in a TSP crevice do not exceed the 0.75 inch TSP thickness at any significant depth (none have been detected in approximately 20 ARC inspections), specimens could not be prepared that would burst at SLB conditions, since LTL materials were unavailable. Consequently, it was necessary to pressurize the cracked specimens with a bladder to the freespan burst pressure to simulate an attempted "burst" (IRB) inside the TSP. None of the indications, including a 0.81-inch throughwall indication, "burst" when tested at pressures near, or above, 2560 psid. The shorter throughwall indications (<0.6-inch) had to be pressurized to well above the SLB pressures; thus, the length and applied pressures are not as representative as the longer cracks of a SLB IRB. The following tests of Table 8-1 are most representative of IRB conditions: 1-1, 1-2, 1-6, 1-7, 11-1 and 11-2.

Since only cracks near 0.75-inch throughwall could burst at SLB conditions, a shorter crack length in a tube with a 0.75-inch crack would not significantly open, and its leak rate would not approach that of the "burst" crack. The potential for two cracks approaching 0.75-inch throughwall length to exist at a TSP is negligible since the associated bobbin voltage would be well above 20 volts. Thus, multiple cracks in a tube would not increase the bounding leak rate obtained from the tests at crack lengths exceeding 0.6 inch. When multiple shorter cracks are tested and the tube must be pressurized to more than 4000 psi to simulate an IRB, both cracks can open up and contribute to the leakage. However, this is a consequence of the artificially high pressurization and is not prototypic of an indication at a TSP intersection that

could burst at SLB conditions. This applies to Test 12-1, which should not be applied to define the bounding IRB leak rate.

8.2 Bobbin Voltage for Crack Lengths Tested

The limiting leak rate and crack/TSP offset data were derived from tests of very long cracks with throughwall lengths approximately equal to the span of the TSP (0.750"). The leakage behavior of shorter cracks is essentially like that of freespan cracks regardless of offset, since the tests indicated negligible interaction of short cracks with the TSP. If longer cracks would be repaired on the basis of their bobbin voltages (i.e., such as the proposed 3V ARC limit), the voltages for the test specimens should be consistent with projected EOC conditions which have operationally been bounded by about 11 volts.

Although EC data were not routinely acquired for the test specimens utilized in these tests, a few of the initial specimens were tested with a bobbin probe to determine the voltage range for the relatively large cracks being tested in this program. The laboratory specimens in this test program were generally cracked in doped steam and were not oxidized prior to bobbin voltage measurements. Prior work has shown that this results in bobbin voltages lower than found in pulled tubes due to the increased conductivity across the crack faces. In addition, other specimens that were not utilized for the leak and burst tests of this program were also examined with a bobbin probe and then were characterized for the size of the crack for other purposes. Finally, a number of tubes have been pulled from operating SGs for which bobbin voltage data are available. Consequently, a small database exists for characterizing the bobbin voltage vs. the crack size (length of throughwall crack).

Among the specimens tested for which bobbin voltages are available (Table 8.2), the shortest throughwall length crack exhibited a bobbin voltage of 17.1 volts; however, the specimen included two separate cracks. A tested specimen with a 0.515 throughwall crack exhibited a bobbin voltage of 8 volts. The lowest voltage for any laboratory specimen for which there is bobbin data is 7.9 volts for a 0.15" throughwall crack. The longest throughwall crack actually tested, for which there is a bobbin voltage, was 0.29 inch (0.600 in. total length), with a bobbin voltage of 11.4 volts.

Among the pulled tubes, summarized in Table 8.2, for which there are bobbin voltage and destructive examination data, the lowest bobbin voltage for a 3/4" diameter tube is 6.08 volts for a throughwall crack of 0.26" based on destructive examination. Similarly, for 7/8" diameter pulled tubes, the lowest voltage is 6.73 volts for a throughwall crack of 0.282". The longest throughwall crack, 0.47 inch (0.67-inch total length) exhibits a bobbin voltage of 15.7 volts. The longest total crack, 0.81 inch (0.42 inch throughwall length) had a bobbin voltage of 13.55 inch. All of these throughwall lengths are much shorter than the 0.74 inch throughwall length of the specimen in Test 1-6 which strongly influences the IRB leak rate. Although the no bobbin test was

performed on the specimen for Test 1-6, it could be expected to have a bobbin voltage exceeding 20 volts.

Therefore, it is concluded that these tests are very conservative with respect to establishing the limiting leak rate of a crack offset from the TSP, since the lowest voltage of any of the available data is more than a factor of 2 greater than the proposed 3V ARC criterion, and the associated throughwall crack length is a factor of 1.5 - 3 less than the throughwall crack length on which the limiting leak rate is based from these tests. It is judged that the IRB leak rate in this report corresponds to indications exceeding about 20 volts.

8.3 Bounding Leak Rate

The bounding leak rate for the limiting indication for which a high voltage ARC could be considered to apply was determined in these tests to be 5.5 gpm for a 2560 psid pressure differential, based principally on Test 1-6. The applicable pressure differential for South Texas Unit 2 is 2405, based on the PORV setpoint plus uncertainties. For a 2405 psid pressure differential, the bounding leak rate is 5.0 gpm based on these tests.

Table 8.3 summarizes the leak rates, based on both flow pressurization and leak testing after bladder pressurization at the SLB conditions of 2560 psid, and an alternate pressure of 2405 for the PORV setpoint plus uncertainties for South Texas Unit 2 for the specimens tested. The pre-tests crack lengths are also shown. The SLB (2560 psid) leak rate after bladder pressurization from test 1-6 was 5.0 gpm. With the exception of three specimens with special circumstances noted below, all other tests had SLB leak rates less than the bounding leak rate of 5.5 gpm for both flow pressurization tests and post-bladder pressurization leak tests.

For the alternate accident pressure differential (2405 psid) based on the PORV setpoint for South Texas Unit 2, the bounding leak rate is 5.0 gpm, based principally on Test 11-2 and Test 1-6.

The bounding leak rate was determined based on the evaluation of the measured leak rate data for the average pressure during the tests. Therefore, the leak rate is conservative since the plastic crack opening is determined by the peak pressure differential at the start of the test, and this was up to 100 psi greater than the average pressure differential for which the bounding leak rate is evaluated. If the measured leak rates are evaluated against the peak pressure differentials, the 2560 psid leak rate is 5.0 gpm.

The bounding leak rate includes the effects of TSP offset, thus no additional consideration of offset is required. For Test 1-6, the defining test, the offset was

established at 0.10" from the crack tip, which included a throughwall length of 0.070". Little crack tearing occurred for this specimen because the crack flanks of a crack of this length rapidly interact with the TSP, which prevents wide crack opening and tearing.

Test 1-6 utilized a specimen with a total crack length of 0.760 inch and a throughwall crack length of 0.740 inch. This test conservatively establishes the bounding leak rate because the throughwall portion (0.740", at beginning of test) of the crack is essentially the full span of the TSP (0.750"). This throughwall length exceeds any found in operating SGs including European plants which operated with no repair limits.

The bounding leak rate from Tests 1-6 is supported by the following additional tests:

- Test 11-2, a test of a 0.729 inch total length (0.630 inch throughwall) crack yielded a SLB leak rate of 5.13 gpm for offset flow pressurization a 5.3 gpm SLB leak rate after bladder pressurization of the specimen. This specimen was a 7/8" diameter specimen.

- Test 11-1, a test of a 0.710-inch total length (0.600 inch throughwall) crack yielded a SLB leak rate of 5.0 gpm for offset flow pressurization and after bladder pressurization. This specimen was a 7/8-inch diameter specimen.

- Test 12-1, a test of a specimen with two cracks, 90° separated, of total length 0.607 inch and 0.465 inch. The throughwall lengths of these cracks were 0.518 inch and 0.360 inch respectively. The SLB leak rate of this specimen was 3.2 gpm for offset flow pressurization and 5.7 gpm after bladder pressurization. Multiple cracks with 90° separation lead to maximum leak rates inside a TSP, since crack openings to interact with the TSP hole diameter are approximately independent of each other. This specimen was a 7/8" diameter specimen.

Three tests are excluded from consideration for defining the bounding leak rate for an IRB that would be conservatively considered for implementation of a high voltage ARC.

- Test 11-7 was a test of a crack that was significantly longer than the span of the TSP, and would therefore not be considered in the population of IRBs that would be considered for implementation of the ARC. This specimen included a crack of 0.813-inch total length and 0.809 inch throughwall length. This length exceeds the TSP thickness of 0.75 inch which provides the crevice environment for crack initiation and growth. However, this test validates the bounding leak rate discussed above by demonstrating that cracks that extend beyond the TSP under normal conditions do not lead to a significant increase in the SLB leak rate. This

conclusion is true even if the crack is pressurized to its freespan burst pressure.

- Test 2-8 was a test of a specimen with a laser cut flaw, to evaluate if these easily prepared specimens are good simulations of corrosion cracks for leak testing. Laser cut flaws, and machined flaws in general, are characterized by smooth-walled, uniform opening slits, that do not simulate the tortuosity of corrosion/ fatigue cracks. This leads to much higher leak rates for the machined flaws compared to similarly sized corrosion/fatigue cracks. Further, the ends of the machined slits have a radius instead of the sharp crack tips of corrosion or fatigue cracks, which causes the slit ends to behave like plastic hinges instead of tearing like corrosion/fatigue cracks. The resulting crack opening under pressurization is much greater than for the corrosion cracks. Consequently, machined flaws were rejected as suitable simulants of corrosion cracks for these leak tests, and the measured leak rate for this tests is non-representative of the IRBs addressed by the proposed ARC.

- Test 12-1 resulted in a leak rate of 5.7 gpm after bladder pressurization to the predicted freespan burst pressure for both the zero-offset and the offset tests. This specimen included two cracks, separated by 90°, 0.607 inch (0.515 inch TW) and 0.465 (0.360 inch TW) long, respectively. For flow pressurization to 2680 psid, the offset SLB leak rate from this specimen was 3.2 gpm. After bladder pressurization to 3310 psi, the offset SLB leak rate was 4.2 gpm. Up to this point, post-tests inspection showed that the secondary crack had not opened, and the primary crack had opened to about 0.005 inch width. After bladder pressurization to the predicted freespan burst pressure (4850 psi), the primary crack opened to 0.022 inch width and the secondary crack also opened to about 0.005 inch. Thus, for the flow pressurization tests exceeding the SLB pressure differential, this specimen with two moderately long cracks had a leak rate less than 60% of the bounding leak rate. After bladder pressurization about 90% greater than SLB pressure differential, this specimen had a leak rate less than 4% greater than the bounding leak rate. As discussed in Section 8.1, the influence of a typically shorter second crack is an artifact of the high bladder pressurization applied to simulate an IRB. At SLB pressure differentials, shorter cracks would not open sufficiently to significantly increase the leak rate above that of the larger crack that could burst at SLB conditions.

## 8.4 Applicable Range of Offset

The data from the IRB leak tests conservatively bound a minimum TSP offset of 0.15 inch. Offset is defined as the length of the total crack outside of the span of the TSP. The maximum offsets tested were 0.210 inch (Test 1-2), 0.208 inch (Test 11-2) and 0.185 inch (Test 11-1) for flow pressurization, and 0.185 inch (Test 11-1) and 0.180 inch (Test 11-2) for leak tests after bladder pressurization. Two of these tests, Tests 11-1 and 11-2, are principal supporting tests for the bounding leak rate; thus the

maximum offsets are represented in the bounding leak rate.

The offset tests were initially set up based on total crack length outside the TSP, nominally 0.10 inch for 3/4" diameter tubes and 0.15 inch for 7/8" diameter tubes. Later offset tests were conservatively set up based on the throughwall length outside the TSP, thus much longer total crack lengths outside the TSP were actually tested. The offset setup based on total crack length outside the TSP simulates the actual condition of TSP deflection during a postulated SLB.

During pressurization, both the total crack length and the throughwall crack length increased; thus, the offset lengths actually tested were frequently greater than the setup offsets. The maximum offsets noted above were the post-test measurements, based on in-process measurement techniques; thus, the measured and bounding leak rates include the effects of the offsets.

Fractographic examination of a number of the specimens was performed after all leak testing had been completed. The results of this examination showed that the in-process measurement techniques were conservative. The crack tips were often tight and could not be observed by the visual methods employed during the IRB tests, even with the aid of a toolmaker's microscope. Similarly, the method of determining throughwall length, using a back-lighting technique, is limited to a crack opening about 0.001 inch that is also approximately normal to the plane of vision. Therefore, the crack length measurements that define the applicable crack offset, either total crack or throughwall crack, are conservative, and the enveloping offset, based on the IRB testing, is 0.21 inch (Test 1-2).

An IRB leak test was also performed on a pulled tube from Plant AA-1 (Reference 4). This test was set up like the test specimens tested in the IRB leak test program (Reference 1). The pulled tube tested, R28C24, had a total crack length of 0.688", with a throughwall portion of 0.260". The crack was offset from the simulated TSP 0.20" based on post-test destructive examination. The leak rate results from the tests performed in the offset condition were the same as the result from tests with the crack completely contained within the span of the TSP.

For the maximum acceptable crack length of 0.750 inch, a limiting offset was defined based on the observations during the IRB test. The maximum contact length between the crack flanks and the TSP in the IRB tests was estimated at 0.3 inch. The crack opening behavior was observed to be symmetric about the axial and longitudinal crack centerline. Therefore, the length of the crack not in contact with the TSP was half the difference between the total length and the length in contact with the TSP, or 0.23-inch. This defines the maximum offset for the limiting crack. An offset less than this distance will not increase the available flow area of the crack, and therefore, the leak rate would not increase up to this offset.

## 8.5 Bounding Leak Rate Sensitivity to TSP Offset

The bounding leak rate conservatively includes the effects of offset, and is insensitive to offset at the limiting crack length.

The offset leak rates were essentially the same as the zero-offset leak rates for the range of crack lengths tested. Figure 8-1 provides a comparison of the leak rates correlated to crack length for the offset tests and for the zero offset tests. Figure 8-1 shows that the slope of the correlation for offset tests is slightly greater than for the zero-offset tests, indicating that there may be a small effect of the offset on the leak rate. However, the leak rate at the limiting crack length, 0.750 inch, is the same for both offset and zero offset tests. Further, the bounding leak rate is based on the offset test results. Therefore, offset is a negligible factor on the bounding leak rate for the range of offsets tested.

## 8.6 Leak Rate Sensitivity to Tube Size

The leak data from the tests of 3/4" diameter specimens and 7/8" diameter specimens are equally applicable for both tube sizes.

The leak rates were correlated to the crack properties, length and limiting throughwall area, and were found to have strong correlations in both crack length and area. Figure 8-2 shows a correlation of the leak rates for all of the tests, including 3/4" and 7/8" diameter tubing and both offset and zero-offset tests for flow and bladder pressurization. No difference in the data scatter was observed, based on the tube diameter, for the leak rate as a function of crack length, the principal correlation parameter.

## 8.7 Effect of A Second Crack on the Bounding Leak Rate

The bounding leak rate does not need to be adjusted for potential multiple throughwall indications.

Leakage from a tube with two cracks is dominated by the principal crack . Similarly, the structural behavior of a specimen with two cracks is dominated by the principal crack.

The leak rate from a crack is an exponential function of the throughwall length of the crack, neglecting any TSP interaction. Thus, if a tube has a longer crack together with a shorter crack, the leak rate is dominated by the longer crack, and the shorter crack contributes only slightly to the leak rate. The combined leak rate from the principal and secondary cracks is much less than the leak rate from a single crack whose length

is the sum of the lengths of the principal and secondary cracks. This observation is supported by pulled tubes from plants AA and AB with indications in the 10-11 volt range, and model boiler tests data both of which show that the secondary crack is much shorter than the principal crack. An exception to this rule is manifested in a tube pulled from Plant S with a 22.9-volt indication that had a principal crack of 0.50 inch and a secondary crack of 0.41 inch. No leak tests were performed on this tube; however, calculations for this tube showed that the principal crack would have a leak rate three times that of the secondary crack.

Test 12-1 of the IRB tests included two cracks comparable in length to the tube pulled from Plant S, in planes about 90° apart. In-process measurements showed that the secondary crack did not open until the specimen was pressurized with a bladder to greater than 70% of the predicted freespan burst pressure for this specimen. Thus, this specimen confirms that the leak rate is dominated by the principal crack in a specimen with two cracks.

The probability of multiple throughwall cracks occurring at the location of the maximum TSP offset is extremely low. The top TSP is the highest loaded (largest displacement) TSP during a postulated SLB accident, while the incidence of ODSCC is dominantly at the lower TSP. The largest TSP offset occurs only at a localized area on the highest loaded TSP. Therefore, it is extremely unlikely that the incidence of multiple cracks will coincide with the location of maximum TSP offset.

Pulled tube data confirm that the location of throughwall cracks is not near the edge of the TSP. Among the sixteen available pulled tubes from Plant AA and AB with bobbin voltages 1-16 volts, 1 tube included an indication located ~0.1 inch inboard from the edge of the TSP, 12 tubes included an indication located ~ 0.2 inch inboard from the edge of the TSP, and the remainder included an indication near the center of the TSP. Therefore, it is concluded that indications do not occur at the edge of the TSP with significant frequency, further reducing the likelihood of multiple indications increasing the SLB leak rate due to TSP offset.

## 8.8 Leak Rate Uncertainties

The bounding SLB (2560 psid) leak rate, 5.5 gpm, is a conservatively high value. Evaluation of the uncertainties of the IRB tests identified four sources of potential uncertainty. These, and their range of uncertainties, are:

1) Fluctuation of leak rate during the tests (±3.1%)
2) Use of the test maximum $\Delta p$ vs. the use of the test average $\Delta p$ for the reported leak rates (-10%)
3) Leak rate adjustment procedure for SLB conditions (negligible)
4) Test loop calibrations (+0.1%)

The combined uncertainty for these four sources of uncertainty varies from -7% to -10%, based on the upper and lower limits of the individual uncertainties. The negative values indicate that the test-based bounding leak rate is conservatively high, that is, the uncertainties would reduce the stated leak rate

8.9 Summary

- The bounding SLB (2560 psid) leak rate for the limiting crack lengths is conservatively demonstrated by these tests to be 5.5 gpm.

- Based on the IRB tests, the bounding leak rate for a 2405 psid pressure differential, based on the PORV setpoint plus uncertainties for South Texas Unit 2 is 5.0 gpm.

- The IRB tests demonstrate that the bounding leak rate applies for TSP offsets up to 0.21 inch, which conservatively bounds the observed maximum displacement of 0.15 inch for the high voltage ARC.

- The bounding leak rate data include the effects of offsets, hence, the bounding leak rate does not need to be adjusted for offset.

- The bobbin voltages of the limiting crack lengths that define the bounding leak rate are expected to be at least 8 volts and, potentially, up to 25 volts, for throughwall cracks much shorter than those tested in the IRB tests. The recommended voltage for limited TSP displacement (high voltage) ARC is 3 volts.

- The limiting offset for the limiting length crack is estimated at 0.23 inch. This is the offset at which the bounding leak rate would be expected to increase with greater offset.

- Cracks longer than the limiting crack length continue the leak rate trends demonstrated for cracks up to the limiting crack length and do not result in a step increase in leakage.

- The measured leak rates do not depend on tube size; thus the combined data for both 3/4" diameter and 7/8" diameter tubes can be applied equally for both tube sizes.

- The bounding leak rate does not need to be adjusted for the potential of multiple indications.

- The bounding leak rate is conservative due to the conservatively large tube/TSP

gap used in these tests. The gap used was 0.025 inch, which is the 95% confidence bound on the expected steam generator tube/TSP gap.

- The bounding leak rate is conservatively high by 7% to 10%, based on evaluation of the tests and analysis uncertainties.

## 8.10 References

1. EPRI TR-107625."Steam Generator Indications Restricted from Burst (IRB) Leak Rate Tests", (Draft) April 1998.
2. W-NSD, SG-95-03-010; "Burst Pressure Correlation for Steam Generator Tubes With Throughwall Axial Cracks"; March 1995.
3. EPRI NP-7480-L, Revision 2, "Steam Generator Tubing Outside Diameter Stress Corrosion Cracking at Tube Support Plates - Database for Alternate Repair Limits"; August 1996.
4. W-NSD SG-98-01-007, "Plant AA-1 Steam Generator Steam Tube Examinations", April 1998

## Table 8.1
## Test Matrix for Indications Restricted from Burst (IRB) - As Tested

| Test No. | Tube Dia. | Specimen Type, No. | Throughwall Crack Length (in.) | | | Free Span Leak Test (1) | Crack to TSP Offset[1] | | | | | | Bladder Press. Applied (psid) | Bladder Press. $\Delta p$[2] Offset (inch) |
|---|---|---|---|---|---|---|---|---|---|---|---|---|---|---|
| | | | | | | | Flow Press. | | | Bladder Press. | | | | |
| | | | .25-.45 | .45-.60 | .60-.75 | | 0.0 in. | 0.10 in. | 0.15 in. | 0.0 in. | 0.10 in. | 0.15 in. | | |
| 1-1 | 7/8 | Corr./Fatg. 8161G | | | 0.62" | H | H | | H | H | | H, C | 4250 | 0.15 |
| 1-2 | 7/8 | Corr./Fatg. 8161E | | | 0.62" | H | H | | H | H | | H, C | 4080 | 0.15 |
| 1-6 | 3/4 | Corrosion 2008E | | | 0.74" | H | H | H | | H | H, C | | 3035 | 0.10 |
| 1-7 | 3/4 | Corr./Fatg. 2051A | | | 0.60" | | H | H | | H | H | | 2970 | 0.10 |
| 2-1 | 7/8 | Corr./Fatg. 8161A | | 0.515" | | H | H | | H | H | | H, C | 4500 | 0.15 |
| 2-4[3] | 7/8 | Corrosion 4C218 | 0.29" | | | H | H | | H, C | C | | C, H | 4125, 5550 | 0.15 |
| 2-7 | 3/4 | Corr./Fatg. 2051E | | 0.577" | | C | C | H | | H | H, C | | 2800, 3950 | 0.10 |
| 2-8 | 3/4 | Laser Cut IRB-LC-2 | | 0.55" | | H | H | H, C | | | | | | None |
| 2-10[3] | 3/4 | Corrosion 2051B | 0.425" | | | H | H | H, C | | H | H, C | | 3850, 4960 | 0.10 |

Table continued next page.

## Table 8.1 (continued)
## Test Matrix for Indications Restricted from Burst (IRB) - As Tested

| Test No. | Tube Dia. | Specimen Type, No. | Throughwall Crack Length | | | Free Span Leak Test | Crack to TSP Offset[1] | | | | | | Bladder Press. Applied | Bladder Press. $\Delta p$[2] Offset |
|---|---|---|---|---|---|---|---|---|---|---|---|---|---|---|
| | | | | | | | Flow Press. | | | Bladder Press. | | | | |
| | | | .25-.45 | .45-.60 | .60-.75 | (1) | 0.0 in. | 0.10 in. | 0.15 in. | 0.0 in. | 0.10 in. | 0.15 in. | (psid) | (inch) |
| 4-1 | 7/8 | Corrosion 4B214 | 0.24" | | | | | | | C | | C | 5800, 6900, 7725, 8900, 10120 | 0.15 |
| 11-1 | 7/8 | Corr./Fatg. 5B403 | | | 0.71 | | H | | H | H | | H | 3670 | 0.15 |
| 11-2 | 7/8 | Corr./Fatg. 8161B | | | 0.63 | | H | | H | H | | H | 2940, 4075 | 0.15 |
| 11-7 | 3/4 | Corr./Fatg. 2008A | | | 0.809 | | H | H | | H | H | | 2900 | 0.10 |
| 12-1 | 7/8 | Corr./Fatg. 8161C | | 0.515[4] 0.360 | | | H | | H | H | | H | 3310, 4850 | 0.15 |
| 12-7 | 3/4 | Corr./Fatg. 2008D | | 0.580[5] | | | H | H | | H | H | | 2800, 6200 | 0.10 |

Table continued next page.

**Table 8.1 (continued)**
**Test Matrix for Indications Restricted from Burst (IRB) - As Tested**

Notes:
1. H is hot test at operating temperatures, C is a room temperature test
2. Test sequences include pressurizing with a bladder typically to the free span burst pressure. Test 4-1 includes incremental increases in bladder pressure beyond that equivalent to a free span burst. Tests 2-4,2-10, 11-1, 11-2, 12-1 and 12-7 include bladder pressurizations below and at the free span burst pressure. Bladder press. is performed to open the crack beyond that obtained within the pressure capability of the facility.
3. Leak tests in small leak test facility prior to bladder pressurization and large facility after pressurization. All other tests in large leak test facility.
4. Specimen has two throughwall cracks 90° apart.
5. Two essentially co-planar cracks (0.012" circumferential offset) separated by a ligament at 0.365" from the end of the longer segment.

**Table 8.2 Voltage Characteristics of Large Cracks**

| Specimen/ Tube | Tube Diameter | IRB Test No./ Plant | Bobbin Volts | Total Crack Length | Throughwall Crack Length | Remarks |
|---|---|---|---|---|---|---|
| **Laboratory Specimens** | | | | | | |
| 4C218 | 7/8" | 2-4 | 11.4 | 0.600" (1) | 0.290" (1) | Two cracks in Specimen |
| 4B214 | 7/8" | 4-1 | 17.1 | 0.670" (1) | 0.24" (1) | Two cracks in Specimen |
| 4B276 | 7/8" | 2-1 | 8.0 | 0.62" (2) | 0.515" (2) | |
| 4C220 | 7/8" | not tested | 7.9 | 0.59" (1) | 0.15" (1) | |
| 4B272 | 7/8" | not tested | 8.0 | 0.72" (2) | 0.38" (2) | |
| **Pulled Tubes** | | | | | | |
| R34C53 | 7/8" | Plant A-2 | 6.73 (3) | 0.612"(4) | 0.282" (4) | Ref 1 |
| R2C85 | 7/8" | Plant A-1 | 13.55 (3) | 0.81" (4) | 0.42" (4) | Ref 1 |
| R16C31 | ¾" | Plant E-4 | 15.70 | 0.67" (4) | 0.47" (4) | Ref 1 |
| R26C34 | ¾' | Plant E-4 | 8.55 | 0.67" (4) | 0.24" (4) | Ref 1 |
| R28C41 | ¾" | Plant S | 11.8 | 0.80" (4) | 0.45" (4) | Ref 1 |
| R33C20 | ¾" | Plant S | 9.8 | 0.47" (4) | 0.33" (4) | Ref 1 |
| R42C43 | ¾" | Plant S | 22.9 | 0.75" (4) | 0.50" (4) | Ref 1; Two cracks in specimen |
| R41C65 | ¾" | Plant AA-1 | 8.93 (3) | 0.698" (4) | 0.268" (4) | Ref 2 |
| R28C24 | 3/4" | Plant AA-1 | 6.08 (3) | 0.688"(4) | 0.260"(4) | Ref 2 |

Notes:
1. Based on dye penetrant measurement prior to any testing
2. Based on UT measurements
3. Field voltage measurement
4. Destructive examination

References:
1. EPRI NP-7480-L, Addendum 1, 1996 Database Update
2. W-NSD; SG-98-01-007, Plant AA-1 Steam Generator Steam Tube Examination

## Table 8.3

## Summary of SLB Leak Rates (2560 psid and 2405 psid) [1] and Crack Length Data

| Test | Specimen | Initial Crack Lengths | | Offset Tests | | | | Zero Offset Tests | | |
|---|---|---|---|---|---|---|---|---|---|---|
| | | Total | TW | TW Length | Offset TW Length | 2560 psi Leak Rate (gpm) | 2405 psi Leak Rate (gpm) | TW Length | 2560 psi Leak Rate (gpm) | 2405 psi Leak Rate (gpm) |
| **Flow Pressurization Tests** | | | | | | | | | | |
| 2-4 | 7/8,4C218 | 0.600 | 0.290 | 0.330 | 0.000 | 0.37 | 0.22 | N.M. | 0.37[8] | 0.22[8] |
| 2-10 | 3/4,2051B | 0.551 | 0.425 | 0.425 | 0.000 | 1.70 | 1.0 | N.M. | 1.70[8] | 1.0[8] |
| 2-1 | 7/8,8161A | 0.640 | 0.515 | 0.504 | 0.134 | 1.65 | 1.28 | 0.230 | 0.93 | 0.73 |
| 2-7 | 3/4,2051E | 0.660 | 0.577 | 0.636 | 0.088 | 4.10 | 4.05 | 0.515 | N.R.[2] | N.R.[2] |
| 2-8 | 3/4,IRB-LC2 | 0.553 | 0.550 | 0.558 | 0.104 | 6.10 | 6.10 | 0.525 | N.R.[2] | N.R.[2] |
| 1-1 | 7/8,8161G | 0.626 | 0.620 | 0.595 | 0.147 | 3.70 | 3.0 | 0.494 | 2.30 | 2.20 |
| 1-2 | 7/8,8161E | 0.645 | 0.620 | 0.666 | 0.145 | 3.20 | 3.20[8] | 0.574 | N.R.[2] | N.R.[2] |
| 1-7 | 3/4,2051A | 0.600 | 0.600 | 0.602 | 0.091 | 4.10 | 4.10 | 0.530 | 3.20 | 3.16 |
| 1-6 | 3/4,2008E | 0.760 | 0.740 | 0.724 | 0.070 | 5.50 | 4.90 | 0.619 | 3.40 | 3.20 |
| 4-1 | 7/8,4B214 | 0.670 | 0.240 | - | - | N.M.[3] | N.M.[3] | - | N.M.[3] | N.M.[3] |
| 11-1[6] | 7/8,5B403 | 0.710 | 0.600<br>0.110 | 0.620<br>0.129 | 0.150 | 5.00 | 4.35 | 0.620<br>0.129 | 4.00 | 3.47 |
| 11-2 | 7/8,8161B | 0.729 | 0.630 | 0.720 | 0.173 | 5.13 | 5.0 | 0.657 | N.R. | N.R. |
| 11-7 | 3/4,2008A | 0.813 | 0.809 | 0.811 | 0.102 | 6.20 | 5.74 | 0.809 | 6.20 | 5.74[8] |
| 12-1[4] | 7/8,8161C | 0.607<br>0.465 | 0.518<br>0.360 | 0.585<br>N.M. | 0.105 | 3.20 | 3.0 | N.M.<br>N.M. | 3.20 | 3.0[8] |
| 12-7[5] | 3/4,2008D | 0.590 | 0.375<br>0.256 | 0.375<br>0.259 | 0.100 | 3.90 | 3.5 | 0.375<br>0.259 | 3.90 | 3.5[8] |

Q:apc/thx98/S8-ANA

## Table 8.3 (continued)

## Summary of SLB Leak Rates (2560 psid and 2405 psid) [1] and Crack Length Data

| Test | Specimen | Initial Crack Lengths | | Offset Tests | | | | Zero Offset Tests | | |
|---|---|---|---|---|---|---|---|---|---|---|
| | | Total | TW | TW Length | Offset TW Length | 2560 psi Leak Rate (gpm) | 2405 psi Leak Rate (gpm) | TW Length | 2560 psi Leak Rate (gpm) | 2405 psi Leak Rate (gpm) |
| **Bladder Pressurization Tests** | | | | | | | | | | |
| 2-4 | 7/8,4C218 | 0.600 | 0.290 | 0.382 | 0.076 | 1.9 | 1.9 | 0.382 | 1.3 | 1.2 |
| 2-10 | 3/4,2051B | 0.551 | 0.425 | 0.492 | 0.081 | 1.6 | 1.3 | 0.492 | 1.6 | 1.3 |
| 2-1 | 7/8,8161A | 0.640 | 0.515 | 0.504 | 0.132 | 3.1 | 3.0 | 0.509 | 3.2 | 3.1 |
| 2-7 | 3/4,2051E | 0.660 | 0.577 | 0.637 | 0.087 | 3.7 | 3.4 | 0.637 | 4.2 | 3.7 |
| 2-8 | 3/4,IRB-L62 | 0.553 | 0.550 | - | - | N.M.[3] | N.M.[3] | - | N.M.[3] | N.M.[3] |
| 1-1 | 7/8,8161G | 0.626 | 0.620 | 0.595 | 0.147 | 2.4 | 2.2 | 0.595 | 3.5 | 3.2 |
| 1-2 | 7/8,8161E | 0.645 | 0.620 | 0.668 | 0.085 | 2.8 | 2.6 | 0.666 | 2.7 | 2.5 |
| 1-7 | 3/4,2051A | 0.600 | 0.600 | 0.613 | 0.100 | 3.3 | 3.0 | 0.613 | 3.2 | 2.9 |
| 1-6 | 3/4,2008E | 0.760 | 0.740 | 0.726 | 0.070 | 5.0 | 4.5 | 0.726 | 4.8 | 4.3 |
| 4-1 | 7/8,4B214 | 0.670 | 0.240 | 0.606 | 0.099 | 4.2 | | 0.606 | 2.5 | |
| 11-1[6] | 7/8,5B403 | 0.710 | 0.600<br>0.110 | 0.754 | 0.154 | 5.0 | 4.5 | 0.754 | 5.0 | 4.5 |
| 11-2 | 7/8,8161B | 0.729 | 0.729 | 0.707 | 0.150 | 5.3 | 5.0 | 0.707 | 4.9 | 4.3 |
| 11-7 | 3/4,2008A | 0.813 | 0.809 | 0.811 | 0.100 | 6.2 | 5.8 | 0.811 | 5.7 | 5.2 |
| 12-1[4] | 7/8,8161C | 0.607<br>0.465 | 0.518<br>0.360 | 0.630<br>0.411 | 0.151 | 5.7 | 5.6 | 0.629<br>0.411 | 5.7 | 5.6 |
| 12-7[5] | 3/4,2008D | 0.590 | 0.375<br>0.256 | 0.726 | 0.100 | 3.3 | 3.0 | 0.726 | 3.2 | 2.9 |

Q:apc/thx98/S8-ANA

**Table 8-3 (continued)**

**Summary of SLB Leak Rates (2560 psid and 2405 psid) [1] and Crack Length Data**

Notes:

(1) Approximate leak rates at 2560 psid and 2405 psid based on linear extrapolation of log leak rate vs ΔP plots.

(2) N.R. - Estimate not reliable due to low pressure tested in zero offset condition or absence of crack to TSP interaction at lower pressures

(3) N.M. - Not Measured. Test not performed.

(4) Specimen has two throughwall cracks 90° apart.

(5) Specimen has two parallel throughwall cracks separated by a circumferential ligament 0.012" at the crack tips

(6) Specimen has two coplanar axial cracks separated by a ligament.

(7) Pressure applicable to Plant AC based on PORV setpoint (2335 psig) plus 3% uncertainty

(8) Data trend is continuous for increasing Δp for zero-offset, freespan and offset tests.

(3)

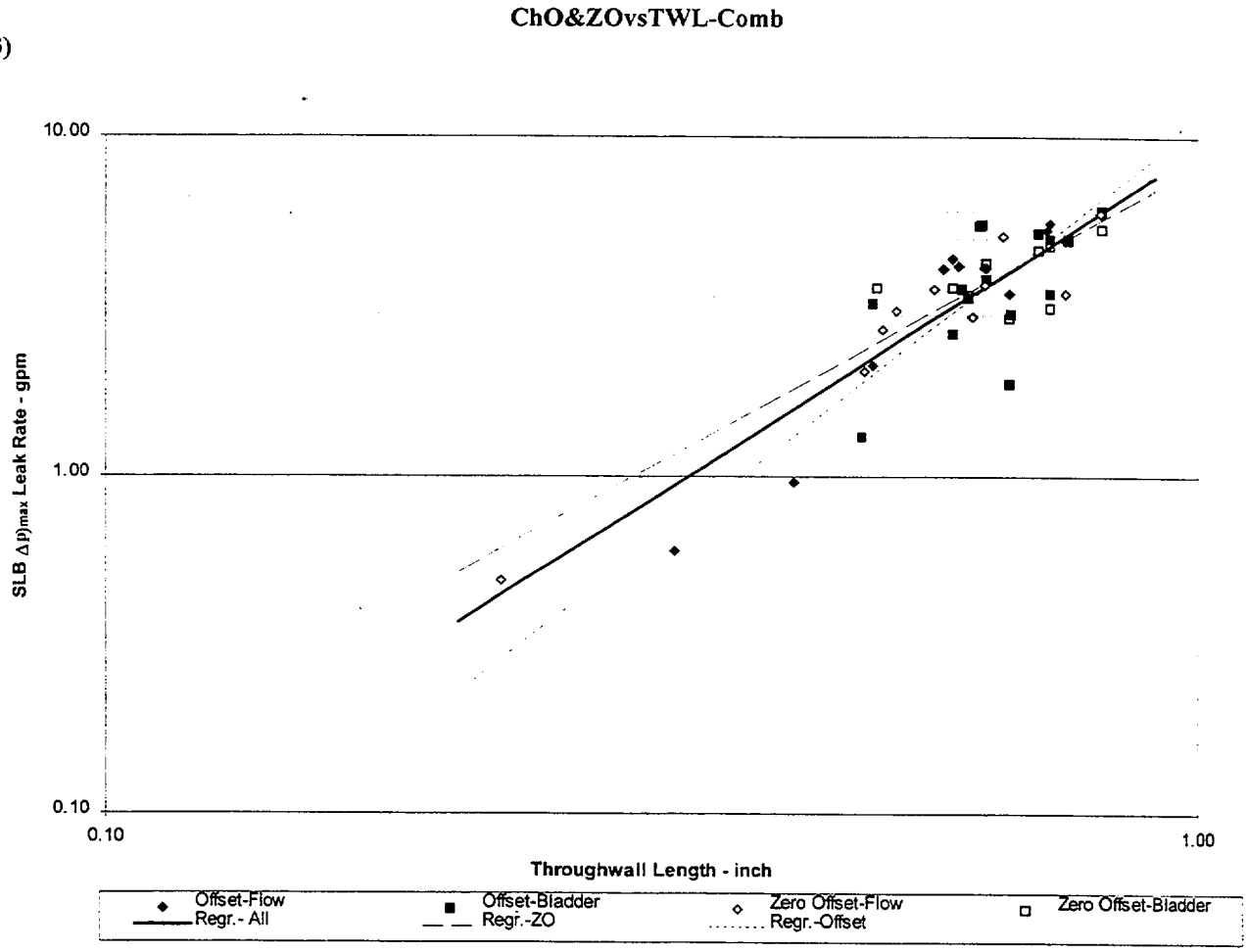


**Figure 8.1**
**Comparison of Offset Leak Rates and Zero-Offset Leak Rates for IRBs**

(2)

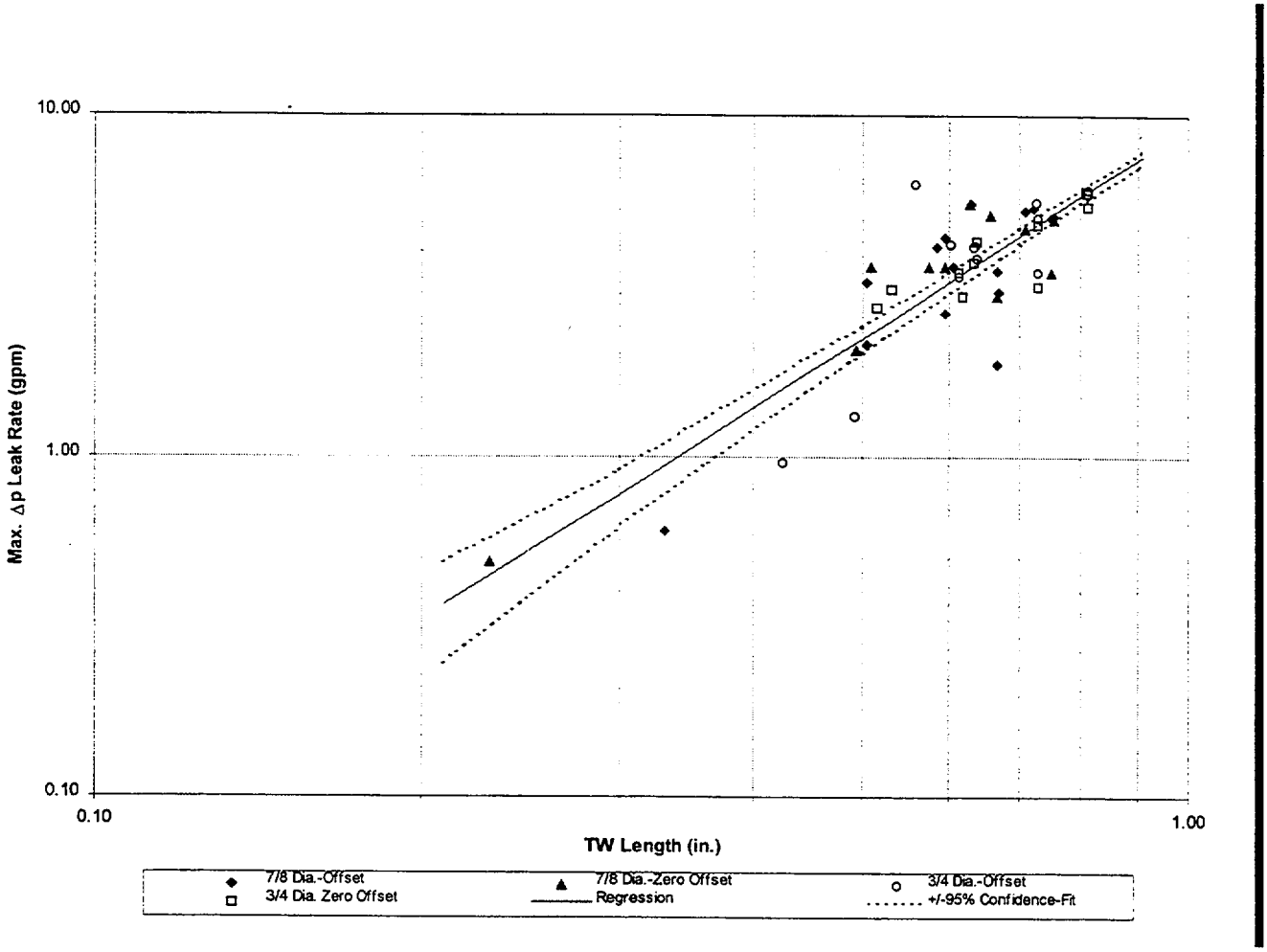


**Figure 8.2**
**Applicability of Measured Leak Rate for ¾" and 7/8" Diameter Tubing; Correlation of IRB Leak Rate with Throughwall Crack Length for Zero-Offset and Offset Tests; (Flow Pressurization and Bladder Pressurization Included)**

# 9.0 ANALYSIS METHODS FOR TUBE BURST AND LEAKAGE WITH LIMITED TSP DISPLACEMENTS

The purpose of this section is to address the likelihood of tube burst and the total potential leak rate from tube indications that are at least partially restrained from bursting by the presence of the TSP. The information contained herein is essentially that presented in Reference 1 for another plant, but, modified to reflect some information developed to respond the NRC staff requests for additional information (RAIs) regarding that report. Since the TSPs do not undergo any displacement relative to indications developed within the upper and lower planes of the TSPs during normal operation, tube burst at pressures less than three times the normal operating differential pressure is obviated by the presence of the TSP, see Appendix A of References 2 and 3 for example. Therefore, the Regulatory Guide (RG) 1.121, Reference 4, requirement for the resistance to burst relative to three times the normal operating differential pressure, $3 \cdot \Delta P$, is inherently met. Hence, the considerations documented in this section are limited to determining the margin against tube burst and the method to account for the leak rate from such indications during a postulated Steam Line Break (SLB). The evaluation of the burst pressure of degraded tubes and the associated probability of burst is contained in Sections 9.1 through 9.5. The treatment of the leak rate from tube indications located wholly or partially within the TSP is discussed in Sections 9.6 and 9.7. Finally, there is also a discussion of the probability of burst by axial separation, i.e., Guillotine break, in Section 9.8.

## 9.1 General Description of Burst Pressure Analysis Methods

The essentials of the analyses consist of consideration of correlations of the burst pressure of throughwall cracks relative to crack length and the burst pressure of ODSCC TSP indications relative to the NDE ECT amplitude, i.e., the bobbin voltage. The concern for the potential of tube rupture during a SLB is based on the consideration that the pressure gradient in the SG will cause the TSPs to deform out of plane and expose TSP intersection tube ODSCC indications such that they behave as free-span indications without the constraint of the TSP. The evaluation of the likelihood of tube rupture, i.e., the probability of burst (PoB), is based on the calculated deformations of the plates to determine the magnitude of potential exposure, the correlation of the burst pressure of tubes with free-span ODSCC indications to bobbin voltage, and the correlation of the burst pressure of tubes with free-span axial cracks to crack length.

Most of the ODSCC TSP tube indications in a SG occur at row and column locations where the TSP undergoes relatively minor displacement, say [ ]$^{a,c}$, during a SLB initiating from normal operating conditions. Since the thickness of the TSP is 3/4", it is unrealistic to treat each indication as though it would be fully exposed

during a SLB. In this case the expected burst pressure can be calculated by considering a throughwall crack which is exposed by an amount equal to the deformation of the plate. The PoB for such a crack can be calculated using the correlation of the burst pressure to the crack length, adjusted as necessary to account for the constraint from the TSP. For larger deformations the PoB is calculated as the larger of the values obtained by using both correlations developed for predicting the burst pressures, i.e., as a function of bobbin or crack length. The rationale for this is that while the PoB may increase significantly for longer throughwall cracks, the actual PoB would be limited by that for a free-span ODSCC indication which can be predicted from the bobbin amplitude. The following Sections of this report present information on the free-span burst pressures for tubes with axial throughwall cracks, Section 9.2, the effect of the radial constraint afforded by the TSP on the burst pressure, Section 9.3, the probability of burst of tubes with free-span throughwall axial cracks, Section 9.4, and the effect of the TSP on the probability of burst of indications located within the TSP hole during normal operation, but which may become partially exposed during a postulated SLB event, Section 9.5.

## 9.2 Burst Pressure Versus Throughwall Crack Length Correlation

Since an essential part of the methodology involves the correlation of the burst pressure to the potentially exposed crack length, it is appropriate to first consider the relationship of the burst pressure to crack length for a free-span indication. This relationship forms the basis for estimating the probability of burst as a function of the exposed crack length, i.e., in subsequent sections the relationship of burst to exposed crack length is developed relative to the free-span correlation.

Recent analysis of burst test data for a variety of tube sizes, Reference 5 indicates a strong correlation between the burst pressure, $P_b$, and the throughwall crack length, $a$, using an exponential relationship, i.e.,

$$P_b = \frac{(S_Y + S_U)t}{R_m}\left[0.0613 + 0.536\, e^{-0.278\lambda}\right], \qquad (9.1)$$

where $t$ and $R_m$ are the thickness and the mean radius of the tube, and $S_Y$ and $S_U$ are the yield and ultimate tensile strength of the tube material. The term in brackets is usually referred to as the normalized or non-dimensionalized burst pressure, $P_N$, i.e.,

$$P_N = \frac{P_B\, r_m}{2\, S_f\, t}\ . \qquad (9.2)$$

Thus, $P_N$ is the ratio of the maximum Tresca stress intensity (taking the average compressive stress in the tube to be $P_B/2$), to twice the flow stress, $S_f$, of the material, taken as $\frac{1}{2}(S_Y+S_U)$ for Alloy 600. The exponent term, $\lambda$, is referred to as the normalized crack length, where

$$\lambda = \frac{a}{\sqrt{R_m t}} . \qquad (9.3)$$

The coefficients of equation 9.1 were found by performing a non-linear regression of $P_N$ on $\lambda$, i.e.,

$$P_N = g_1 + g_2 e^{g_3 \lambda} . \qquad (9.4)$$

The index of determination of the regression was found to be 99.1% with a standard error of the normalized predicted burst pressure of 0.0176. The $p$ values for each of the coefficients was significantly less than 0.1%. The distribution of the residuals was found to be approximately normal. A plot of the resulting relation corresponding to the form of equation 9-1 is provided on Figure 9-1, for a nominal flow stress of 71.6 ksi, the average of the Westinghouse database for tubes at 650°F. Also shown on Figure 9-1 is the regression curve adjusted for lower 95%/95% tolerance limit material properties at 650°F. It is noted that equation 9-1 yields estimates of the critical crack length for burst during SLB of 0.75" for the actual SLB differential pressure and 0.51" for a margin of 1.4 times the SLB differential pressure for material considered to have lower tolerance limit (LTL) yield plus ultimate tensile strength at 650°F.

## 9.3 Burst Pressure vs. Length for Cracks Extending Outside TSPs

The results of burst testing of tubes with throughwall axial cracks has demonstrated a correlation between the burst pressure, or burst strength, and the crack length. The form of the correlation was discussed in Section 9.2. Using the results from the correlation analysis, the probability of burst for tubes with free-span throughwall axial cracks can be calculated. This will be discussed in Section 9.4. Moreover, the calculation can be modified to estimate the probability of burst, i.e., over pressure, if tube/TSP indications that extend partially outside of the TSP, say, due to movement of the TSP during a postulated accident. The calculation of the probability of burst for such indications is discussed in Section 9.5.

For tubes in which a portion of the length of the crack, i.e., indication, is restrained in the radial and circumferential directions, i.e., as would exist within a hole in a TSP, the burst pressure correlates with the exposed crack length. This is because the local condition for burst is the achievement of a critical opening of the crack at the crack tip. For throughwall cracks in thin walled tubing the critical crack tip opening displacement (CTOD) is on the order of the thickness of the tube, i.e., about 40 mils.

In essence, the clearance between the OD of the tube and the ID of a TSP hole is not sufficient to permit the achievement of the critical CTOD for the end of the crack within the TSP at the pressures which would lead to the burst of cracks of significant length.[1] Hence, within the TSP, the crack would not be expected to extend beyond that associated with less-than-critical blunting of the crack tip. If the clearance between the inside of the TSP hole and the tube approaches zero, there can be no CTOD at that end of the crack and the strength of the tube is slightly increased. If the clearance between the tube and the inside of the TSP is significant, the crack flanks may open and the crack would be expected to behave as though it were slightly longer than the exposed length. Finally, if the clearance is between the two extremes, the burst pressure may be slightly elevated or depressed depending on the value of the clearance. In order to address the effect of the TSP on the burst pressure, a series of burst tests were performed to quantify the effect of the clearance between the tube and the TSP hole. A description of the burst test specimens is provided in Section 9.3.1. Because an essential feature of the testing program was the presence of the TSP collar and the diametral clearance between the tube and the hole in the TSP, an evaluation was performed to identify the range of clearances that might be expected in the South Texas 2 SGs. This is documented in the Section 9.3.2. The results from the testing are discussed in Section 9.3.3. Section 9.3.4 repeats a discussion of the potential effect of the proximity of the tube U-bend on burst behavior which was the subject of a prior NRC staff query.

### 9.3.1 Description of Burst Tests

To evaluate the strengthening effect of the constraint afforded by the TSP, a series of low energy (hydraulic as opposed to pneumatic) burst tests was performed to provide a direct comparison between the free-span burst strength and the TSP constrained burst strength. In prior discussions on the subject, the question of whether or not high-energy tests were performed was raised by the staff. For example, pneumatic testing results in the internal pressure being relatively constant for a short time following the initial tearing of the crack ends. This is contrasted to hydraulic testing where the pressure decreases drastically once a leak is achieved. Since the key objective of the testing was to identify the pressure at which unstable crack extension initiates, the use of a high energy facility is not necessary. The rationale for this is that it is explicitly assumed that crack extension will continue after initiation because of the essentially constant source of pressurized water in the SG, hence, it is not necessary to ascertain by test whether or not crack extension will continue after the initial burst pressure is reached. Considerations of free-span burst as described in Section 9.2 have not involved assumptions regarding the nature of the tube opening following the initiation of rupture. The results from a constrained burst test would be expected of be considerably different from results from free-span tests. In the latter case the flanks of the crack are not free to deform significantly (contact

[1] Specimens with 3/4" long cracks, entirely confined with the TSP exhibit burst pressures well above 8500 psi.

with the TSP hole would be expected at about one-half of the burst pressure), and the crack behaves like a shorter crack, with an attendant much lower probability of burst, and hence lower probability of unstable extension.

For the testing, the tubes were lined with a plastic tube, also referred to as a bladder, prior to the test. The OD of the bladder was reinforced with a small, 2 mils thick, low strength, brass foil shim to prevent extrusion of the bladder prior to achieving the burst pressure of the tube. A 3/4" thick collar was slipped over the tube at the elevation of the cracks prior to pressurization to simulate the presence of the TSP. Once the crack tips start to extend and the flanks open significantly, the pressure in the pressurizing medium is released and no further energy is supplied. The results reported on Figure 9-2 of Reference 5 were not from tests performed in a high-energy test facility. However, examination of the specimens revealed that the failed surfaces at the ends of the cracks formed an angle of approximately 45° with the exterior and interior surfaces of the tube. This is similar to the failed surfaces resulting from test cases where the tearing has continued as a result of being in a high-energy test situation, References 6, 7, and 8. Thus, initiation results are independent, as they should be, of considering the burst to occur in a high or low-energy loading configuration.

### 9.3.2 Tube Support Plate Hole Diameter Distribution

Prior to conducting the tests, the TSP hole size to be used to simulate conservative field conditions had to be determined. Specific data relating to the as-built dimensions of the TSP holes in the Model E SGs is not currently available. Hence, information was developed to indirectly support the selection of the collar inside diameter for the test program. The Model E TSP drawings indicate a tolerance for the tube hole size of [ ]$^{a,c,e}$, with a reference dimension of [ ]$^{a,c,e}$. It may be concluded that the drill size used for the E TSPs was either a standard [ ]$^{a,c,e}$ diameter. Random sampling data from TSP holes drilled for another model SG indicated that the average hole diameter is [ ]$^{a,c,e}$ larger than the drill size, and that the standard deviation of the hole diameter is [ ]$^{a,c,e}$ mils. A sample of hole diameters in the tubesheet of a Model 51F SG were found to have a standard deviation of [ ]$^{a,c,e}$ mils. Based on the average and standard deviation of the sample data, holes drilled with a [ ]$^{a,c,e}$ diameter drill would be expected to have a 95% confidence upper bound of [ ]$^{a,c,e}$, or clearances ranging from [ ]$^{a,c,e}$ mils. If the drill size was [ ]$^{a,c,e}$, the corresponding clearance range would be from [ ]$^{a,c,e}$ mils. The tests were conducted with diametral clearances ranging from 13 to 23 mils.

### 9.3.3 Evaluation of the Burst Test Data

The results from the tests are summarized in Tables 9-1 and 9-2, and illustrated on Figure 9-2. Figure 9-2 also illustrates the results from previous testing of 0.75" long

slotted tubes tested with the slot entirely contained within the TSP simulating collar, Reference 2. For the latter tests the diametral clearance ranged from 27 to 30 mils. Free-span burst tests were performed for a range of throughwall crack lengths, simulated by narrow EDM slits, from 0.15" to 0.70". For TSP confined tests, the crack length was always 0.70", and exposure of the crack beyond the TSP boundary ranged from 0.15" to 0.50". Also, for the TSP constrained burst tests the presence of the TSP was simulated by a round collar which is sized to provide a radial stiffness equal to the average radial stiffness of the TSP. For the series of tests performed the diametral clearance between the tube and the TSP hole ranged from [ ]$^{a,c,e}$ mils, or about [ ]$^{a,c,e}$ mils on the circumference.

The results from the tests employing the smaller gap of 11 to 13 mils, Table 9-1 and Figure 9-2, verify the expectation that the burst pressure for a long crack with a portion of the crack constrained by the TSP would be similar to that of a free-span crack with a total length equal to the exposed length of the constrained crack. Hence, if the diametral clearance between the tube and the hole in the TSP in the SG is small, i.e., on the order of 13 mils or less, the throughwall burst pressure correlation may be used to evaluate the probability of burst of exposed cracks as a function of the length exposed. For the larger clearances it would be expected that the strengthening due to the TSP constraint would be significant, but not as significant as for the small clearance range. In other words, the burst pressure would be expected to be slightly less than that for free-span cracks with a total length equal to the exposed length of the constrained test specimens. The results from the larger gap tests, 19 to 23 mils, listed in Table 9-2 and also illustrated on Figure 9-2, confirm this supposition. Over the range of exposure of interest, the effect of the larger clearance is to diminish the burst pressure as predicted using the free-span crack expression, equation 9.1, by about [ ]$^{a,c,e}$ for 3/4" diameter tubes.

The data used to obtain the adjustment factor are illustrated as solid black circles on Figure 9-2. A total of twelve (12) data points were available for the analysis, however, the adjustment factor was obtained as the average for the six (6) data points located farthest below the predicted burst curve. Since the form of the adjustment was chosen to be a constant, the average factor is the same as would be obtained from a least squares solution. The use of a censored database is considered to be conservative since the range of interest is for exposures of about 0.1 to 0.3", i.e., the actual reduction in strength would be expected to be smaller than that used for more limited TSP displacements. The data illustrate that no adjustment is really necessary for exposures in the range of ~0.1 to ~0.2" and that only a slight adjustment is necessary for exposures of ~0.2 to ~0.3". Thus, the selection of the data used for the determination of the adjustment factor essentially bounds the data in the range of interest. Since the use of an adjustment factor of 411 psi is conservative, no further testing was performed or planned.

### 9.3.4 Influence of Proximity of the Tube U-Bend

The following information was developed in response to a staff RAI with respect to a prior application. The tangent point of the U-bend with the straight leg of tubing occurs at an elevation of about 2.1" above the top of the uppermost TSP. The effects of local residual stresses from the forming operation, i.e., resulting in ovality and non-uniform cold working of the material, would affect the tube over a length of about 0.3" from the tangent point. Surface stresses from the original tube straightening operation would be relieved by any blunting of the crack tip. Overall, the load in the tube is tensile in the axial and hoop directions. The tensile stress in the axial direction tends to reduce the size of the plastic zone at the crack tip, thus increasing its resistance to fracture from the hoop stress.

Due to separation of the tangent point from the uppermost TSP, the manufacturing process for the U-bend has no significant influence on the burst capability of the tube at the TSP. In general, burst tests have shown higher burst pressures for the bent U-bend tube sections than for straight sections due to the cold working and curvature of the tube.

## 9.4 SLB Burst Probability as a Function of Throughwall Crack Length

A generalized form of equation 9.1 can be written as,

$$P_B = \left(\frac{2t}{R_m}\right) P_N S_f . \tag{9. 5}$$

Equation 0 may be used to estimate the probability of burst based on the variance of the estimate of $P_N$ about the regression equation and the variance of $S_f$ from a large database of measured properties of tubing installed in Westinghouse steam generators. An unbiased estimate of the variance, V, of $P_B$ is given by

$$\mathbf{V}(P_B) = \left(\frac{2t}{R_m}\right)^2 \left[P_N^2\, \mathbf{V}(S_f) + S_f^2\, \mathbf{V}(P_N) - \mathbf{V}(S_f)\, \mathbf{V}(P_N)\right]. \tag{9. 6}$$

The standard deviation of the burst pressure, $\sigma_P$, is taken as the square root of $\mathbf{V}(P_B)$. If $P_A$ is an actual burst pressure, it is assumed that the statistic

$$t = \frac{(P_B - P_A)}{\sigma_P}, \tag{9. 7}$$

is distributed as a Student's $t$ distribution with degrees of freedom equal to the degrees of freedom ([ ]$^{g}$) used for the regression of $P_N$ on $\lambda$.

Taking $P_A$ equal to the SLB pressure, a $t$ variate is calculated from equation 9-7. The probability of randomly obtaining a $t$ variate as large at that obtained is then

calculated from the cumulative Student's $t$ distribution. A plot of probability of burst as a function of crack length using this approach is provided as Figure 9-1. This is then taken probability of burst (PoB) during a postulated SLB for a tube with a throughwall crack length of $a$.

In actuality, the distribution of $P_B$ does not follow a Student's $t$ distribution in that the distribution is not symmetric. The third moment of the burst pressure distribution, $M_3$, is related to the means and variances of the normalized burst pressure and the flow stress as,

$$M_3(P_B) \propto P_N^2 S_N^2 V(P_N) V(S_f). \tag{9. 8}$$

Since each of the terms in equation 9.5 is positive, $M_3$ will also be positive. Hence the distribution of the product of the normalized burst pressure and the flow stress will be skewed right, i.e., with a higher tail for larger burst pressures. Therefore, the prediction of burst probabilities based on equation 9.4 would be expected to be conservative. In addition. the degree of conservatism would be expected to increase with decreasing probability of burst, i.e., for shorter crack lengths. Monte Carlo simulations of the burst pressures have resulted in distributions which appear close to the form of a Student's $t$ distribution, but which have a longer tail in the higher burst pressure range, i.e., they are skewed right, confirming the analytical expectation. Hence, the use of equation 9-7 to estimate burst probabilities is expected to be conservative. Comparison of individual 95% upper bound Monte Carlo results with predictions from equation 9-7 indicate a small level of conservatism for high probabilities of burst, e.g., PoB greater than 0.1, and an order of magnitude difference for low probabilities of burst, e.g., on the order of $10^{-6}$, see Figure 9-3.

The above equations apply to calculating the PoB for a single throughwall crack or indication. For multiple indications the PoB of one or more of those indications is found as one minus the probability that none of them burst. The probability of no burst, or survival, for any single indication is one minus the PoB, thus the probability of burst of one or more of $m$ indications is given as,

$$\text{PoB (m indications)} = 1 - \prod_{k=1}^{m} (1 - \text{PoB}_k) < \sum_{k=1}^{m} \text{PoB}_k \,, \tag{9. 9}$$

where $PoB_k$ is the probability of burst of the $k^{th}$ indication. In practice, the indications are segregated into crack length bins with all indications in one bin considered to have the length of the upper bound of the bin. Thus, the PoB for all indications in the same bin is the same. By multiple application of equation 9.9, the PoB of one or more of all of the indications in the $n$ bins is,

$$\text{PoB}\,(n \text{ bins}) < \sum_{i=1}^{n} r_i \cdot \text{PoB}_i\,, \tag{9. 10}$$

where $r_i$ is the number of indications in bin $i$ and $PoB_i$ is now the probability of burst for an indication in the $i^{th}$ bin.

It is admitted that this practice omits direct consideration of the uncertainties of the parameters of the regression equation. However, formation of the normalized burst pressures from the test data includes an uncertainty of the material properties of the test specimens. Thus, the variance of an actual $P_N$ about its predicted $P_N$ includes a contribution from the variation of material properties associated with repeated measurements of tensile specimens from the same tube. This, combined with the observation that equation 9-7 yields conservative results relative to Monte Carlo simulations, see Figure 9-3, is judged to outweigh the effect of omitting the uncertainty in the estimate of the coefficients.

In effect, the calculation of the probability of burst of an indication as a function of the bobbin amplitude of the indication is performed in accordance with the guidelines of Reference 11. Parameter uncertainties are explicitly included in the Monte Carlo simulations "using the correlation between burst pressure and voltage." The details of the methods employed in performing the calculations are provided in Reference 10.

For a single indication extending outside of a TSP intersection, the deterministic calculation includes consideration of the uncertainties in the parameters. The effective variance of a predicted normalized burst pressure about the regression curve is

$$V(P_N) = s^2\left(1 + \{f_0\}^T\left[F^T F\right]^{-1}\{f_0\}\right), \tag{9. 11}$$

where s is the standard error of the regression, $\{f_0\}$ is the coefficient derivative vector and $[F^TF]^{-1}$ is the normalized covariance matrix. The term containing the covariance matrix accounts for the variance of the coefficients of the regression equation.

The above discussion that refers to the omission of consideration of uncertainties in the parameters, is with respect to the effect on the *combined probability of burst as a function of crack length* of all of the indications in the SG, not on the probability of burst of any one indication. For this calculation, it is considered that the use of the

deterministic estimate of the probability of burst is justified because the individual calculated probabilities of burst are an order of magnitude higher than obtained from Monte Carlo simulations, the number of intersections with indications is overestimated by at least an order of magnitude, and the assumption that the maximum TSP displacement occurs at all intersections in the SG hot leg likely overestimates the number of indications exposed to that displacement by two orders of magnitude. Thus, the effect of simulating uncertainties in the parameters would have to be sufficient to result in a change in the probability of burst of about four orders of magnitude to increase it above the values stated. The simple fact is that the probability of burst of an indication which is exposed on the order of 0.1 to 0.3" is extremely small. The development of a Monte Carlo code to simulate the distribution of indications over the TSPs, the distribution of indications at a TSP over the area of the TSP, and the distribution of indication lengths in order to simulate a distribution of exposed lengths, in addition to simulating the parameters of the correlation and the material properties is not justified in light of the very low probabilities obtained from the deterministic estimation.

## 9.5 Modeling for Burst Probability with TSP Displacements

One model was considered for the evaluation of the burst probability given the relative displacements of the TSPs during a postulated SLB. This model is based solely on the TSP displacements and estimates the PoB by assuming every intersection to have a throughwall crack equal to the thickness of the TSP. Thus, every intersection is considered to have a throughwall crack exposed by the magnitude of the displacement at each intersection. The prediction of the PoB of a single indication can be estimated using the methods described in the previous section of this report, however, in this case the predicted burst pressure for nominal material would be reduced by a pressure shift value, $P_S$, of [ ]$^{a,c,e}$, i.e., the value of the $t$ distribution variate would be calculated as,

$$t = \frac{[(P_B - P_S) - P_A]}{\sigma_p}, \qquad (9.12)$$

instead of using equation 9-7. This approach implicitly assumes that the standard error of the burst pressure based on performing many tests would be the same as that obtained from the testing of free-span cracks. Given the large database from the free-span burst tests, this is not an unreasonable assumption.

A more realistic estimate of the PoB could be obtained by considering only the estimated number of indications and the spatial distribution of those indications in a steam generator. Furthermore, assessment of the PoB of a tube at SLB conditions for limited TSP displacement only requires an estimate of the probability of a large indication occurring at the corners of the TSP where the TSP displacements are significant.

Although the flow distribution baffle (FDB, plate 1) has a few TSP intersections with significant displacements, no bobbin indications have been found at the FDB. The FDB in the Model E S/Gs has large tube to FDB gaps (nominally [ ]$^{a,c,e}$ diametral clearance toward the center of the plate and [ ]$^{a,c,e}$ with radialized holes for the outer region). Thus, there is a significantly lower likelihood of packed crevices with associated tube corrosion at the FDB intersections. Since no indications at the FDB have been found at South Texas 2, the FDB is not included in the tube burst assessment.

In Section 9.3, it was shown that the burst pressure of a throughwall indication extending outside the TSP has a burst pressure almost equal to the burst pressure for a free span crack at the length extending outside the TSP. Thus, the length of crack remaining within the TSP does not significantly affect the burst pressure. Similarly, the burst probability for TSP displacements with postulated throughwall cracks can be calculated as that associated with a crack length equal to the TSP displacement. This assumes that the throughwall part of a crack is located at the edge of the plate rather than, as more commonly found in pulled tubes, near the center of the TSP. Alternately, it can be postulated that there is a throughwall crack equal to the TSP thickness and the burst probability for this indication is the same as the crack length exposed by the TSP displacement.

The most conservative possible assumption to define a goal for limited TSP displacement is to assume that all intersections at all hot leg TSPs (excluding the FDB, which is covered by the 1V ARC) have throughwall crack lengths at least equal to the TSP displacements. This assumption is applied to develop the allowable limits on TSP displacement so that the proposed ARC are generic and envelop any possible tube degradation.

Even under the above bounding assumption on postulated tube degradation, it is desirable that the associated tube burst probability be small compared to acceptable levels for application of steam generator degradation specific management (SGDSM). Then, if multiple ARCs are applied as part of SGDSM, the hot leg indications at TSPs will have a negligible contribution to the tube burst probability. The most conservative guideline for an acceptable SGDSM burst probability is the value of $10^{-2}$ given in the NRC generic letter, Reference 11. If this value is exceeded, the generic letter requires that the higher burst probability be reported to the NRC and that an assessment be performed of the significance of the result. If the burst probability for limited TSP displacement under postulated SLB conditions is then $<10^{-3}$, the TSP indications would contribute <10% to the NRC reporting level. This $10^{-3}$ value is the starting point for developing a limited TSP displacement burst probability requirement based on sensitivity analyses given in the following sections. By applying the tube burst probability as a function of throughwall crack length, as

developed in Section 9.3, and the bounding assumption of throughwall cracks at all hot leg TSP intersections, tube burst probabilities can be developed as a function of TSP displacements. The tube burst probabilities are developed in Section 12 for the postulated 43,659 indications for the 9 hot leg TSPs with 4,851 tube intersections at each plate. For simplicity, and because the individual burst probabilities are so small, the burst probabilities are calculated as the number of TSP intersections times the single tube burst probability for a throughwall crack equal to the displacement.

## 9.6 SLB Leak Rates Based on Assumed Free Span Indications

A discussion of the methods employed to evaluate the leak rate from tubes during a postulated SLB are given in Reference 9. A linear model relating the common logarithm of the leak rate from a tube at SLB conditions to the common logarithm of the bobbin amplitude of an ODSCC indication is used, Reference 9. The relationship was developed and verified to be valid in accord with the requirements of the NRC generic letter, Reference 11. The use of the model to develop EOC total S/G leak rates by appropriately simulating the parametric uncertainties is also described in Reference 9, and are also in accord with the requirements of the NRC generic letter. The data and the results of the analyses are discussed in a later section relative to the potential leak rate from indications at TSP elevations.

## 9.7 SLB Leak Rate Analyses for Over Pressurized Tubes

This section describes the results of a Westinghouse analysis for SLB leak rates from an over pressurized tube which expands within the TSP until the crack flanks contact the ID of the TSP drilled hole. The term over pressure refers to the fact that burst would be expected if the indication were located in the free span portion of the tube. The indications is also referred to as an indication restrained from burst. The test program and data to support the analyses are described in detail in Section 8 of this report.

Several models for predicting leakage under postulated accident conditions were developed. The methodology that was used for calculating the primary-to-secondary leakage under postulated accident conditions, i.e., how the SG tube leakage from the hot leg side was calculated, and how it was combined with the SG tube leakage from the cold leg side and FDB baffles.

The objective of demonstrating limited TSP displacements under postulated SLB conditions is to allow the voltage limits of the alternate plugging criteria to increase without increasing the probability of a free-span burst of a tube. However, the probability of occurrence of indications with higher PoBs if they were free-span indications is increased. Thus, even though constrained, the probability of occurrence of indications which could experience increased crack flank deflections, referred

to as over pressurization, is increased. Therefore, it is appropriate to modify the prediction methodology to account for the leak rate from potentially over pressurized tubes. The standard ARC leak rate prediction methodology, described in detail in Reference 9, was only slightly modified to deal with additional leakage from IRBs.

The SG tube leakage from the hot leg side is calculated using a modification of the free span leakage methodology of the Westinghouse methods report, Reference 9, which is in concert with the guidelines provided in Reference 11. This method involves Monte Carlo simulation of the distribution of indications, uncertainties in the measurement of the indications, the growth of the indications, etc. A modification to the methodology used for the calculations has been effected which increases the leak rate for hot leg indications which are simulated as being restrained from bursting (designated as IRBs). If the simulation of the burst pressure results in a value which is less than the differential pressure during a postulated SLB, indicating a probability of burst (PoB) of one instead of zero, the probability of leak (POL) of the indication is set to unity and the leak rate from that indication is assumed to be 5.5 gpm [2]. All indications simulated to be IRBs are assigned the bounding leak rate regardless of the bobbin amplitude of the indication. If the indication is predicted to not burst, the probability of leak is found from the logistic correlation of the POL to the common logarithm of the bobbin amplitude. A random uniform deviate is than generated to determine if the indication leaks, i.e., the POL is either zero or one. If the indication leaks, the leak rate is calculated from the correlation of the common logarithm of the leak rate to the common logarithm of the bobbin amplitude.

The simulation is conservative in that the estimated leak rate obtained from the correlation is used even if it exceeds the bounding leak rate for an IRB. Thus, the total leak rate obtained from one simulation of the SG, with n indications in service, is given by,

$$Q_{SG\ Total} = \sum_{i}^{n} \left[ \mathrm{PoB} \cdot 5.5 + (1 - \mathrm{PoB}) \cdot \mathrm{POL} \cdot 10^{\beta_3 + \beta_4 \log(V_i) + Z_i \beta_5} \right] \qquad (9.13)$$

where $\beta_3$, $\beta_4$, and $\beta_5$ are the simulated population intercept, slope, and standard error of the leak rate correlation, and $Z_i$ is a random normal deviate. The probability of burst is either zero or one and is calculated for each indication. The probability of leak for each indication is either zero or one as described in Reference 10. The estimated EOC total leak rate for a SG is calculated as a 95% confidence bound on 95% of the possible population of leak rates based on the results of many, i.e., greater than 100,000, Monte Carlo simulations of the total leak rate.

---

2 This is an upper bound value determined from leak testing of indications that were deformed by internal pressurization to simulate an attempted burst within the TSP. The value corresponds to a differential pressure of 2560 psi. A value of 5.0 GPM may be used for a differential pressure of 2405 psi.

The total leak rate from all of the indications in the SG is calculated and retained. The 95% confidence bound on the total leak rate would then be found using the ordered array of total leak rates from all of the simulations of the SG as described in Reference 9.

## 9.8 Potential Structural Limit for Indications at TSP Intersections

For free-span indications, the structural limit that determines tube repair limits is based on satisfying RG 1.121 margins for burst of a tube. With the limited displacements of the lower TSPs demonstrated by the analysis in Section 7, the constraint of the TSP reduces the tube burst probability to negligible levels and tube repair limits are not required to prevent tube burst. For the small TSP displacements and the expected tube degradation, the need for tube repair is dictated by the need to satisfy allowable SLB leakage limits. However, at some level of cellular or IGA corrosion, it becomes possible for the axial loads resulting from the pressure differential across the tube to result in axial tensile severing of the tube. This tensile load requirement establishes the applicable structural limit for tube expansion based on limited TSP displacement. Section 6.3 of Reference 2 provides a detailed discussion, based on the information contained in Reference 1, of the evaluation of resistance to axial tensile tearing based on the percent degraded area of the tube section. Section 6.3 of Reference 3 provides an update of the Reference 2 information based on the evaluation of additional test data. A description of the tensile tests is provided in Section 9.8.1 of this report.

It is noted that the bobbin coil voltage is being used to assess the potential for a SG tube to fail circumferentially, although the bobbin coil is relatively insensitive to SG tube circumferentially oriented cracking, an inherent assumption in the methodology is that there is a significant axial component in the SG tube flaw such that is can be detected with the bobbin coil. The degradation morphology that has been found in pulled tubes for ODSCC at TSP intersections is dominantly axial SCC with varying extent of cellular patches including the absence of cellular corrosion. Cellular corrosion is a combination of axial and oblique angle cracks that form small cells of undegraded tubing within the crack pattern. The patterns of cellular corrosion have been characterized by radial grinds from the tube surface through the tube wall. The axial cracks are consistently deeper than the oblique cracks. That is, as the radial grinds progress through the wall, the crack pattern changes from cellular to multiple axial micro-cracks with the oblique cracks typically less than 50% to 60% of the tube wall when the axial crack are near throughwall. The oblique cracks in the cellular pattern are typically < 90° (i.e., not circumferential) and the bobbin coil voltage responds to both the axial and oblique cracks.

It can be noted that the bobbin voltage responds primarily to the deepest and longest axial cracks. In correlating bobbin voltage with the axial tensile capability of the tube, it is assumed that the cellular pattern will increase in circumferential extent in

some close proportion to the length and depth of the dominant axial cracks. Since this is not generally the case, it can be expected that the spread in the correlation (range of tensile force capability at a given voltage) will be significant and greater than that found for the axial burst pressure correlation with voltage. Cellular corrosion can generally be seen with modest magnification on the OD of the specimen following the axial burst test since the pressure tends to expand the tube diameter and increase the visibility of the tube degradation. The absence of cellular corrosion to eliminate the tensile test can be identified in this manner although the final criterion for inclusion in the tensile force correlation would be based on metallographic specimens.

The conclusion from the Reference 3 evaluation of the data is that the probability of rupture during a postulated SLB event of a single indication with an amplitude of 10 V is $< 3 \cdot 10^{-6}$, and that the overall structural limit for axial separation during a postulated SLB event is on the order of 100 V. Moreover, all indications with an amplitude of $\leq 3$ V would be expected to have significant margin to burst relative to the RG $3 \cdot \Delta P$ limit during normal operation.

9.8.1 Performance of the Tensile Tests

The axial tensile tests are performed following the axial burst testing of the specimens. The burst tested specimens are typically about 10 inch long sections of steam generator tubing with the TSP crevice regions centered in the sections (the location of the axial burst opening) and with Swagelok fittings attached to each end of the sections. Simply pulling a burst tested specimen using its attached Swagelok fittings would not work, as the local stresses associated with the Swagelok ferrule would be the source of the tensile fracture. In order to bypass the stresses concentrated at the ferrules, the Swagelok fittings are welded onto the tube above the ferrules using a buttering type weld with a non-uniform weld front that would diffuse local stresses at the weld front. A tensile test gripper mandrel (metal plug) small enough to pass through the compressed Swagelok ferrule regions of the tube is also utilized.

The burst tested specimens are then tensile tested following guidelines in Section 6.9.1 and Figure 11 of ASTM E8. The snug-fitting metal plugs are inserted far enough into the ends of the specimens to permit the testing machine jaws to grip the specimen properly. The plugs do not extend into the gage length portion of the specimens, which is 4 inches long with the burst opening centered in the gage lengths. The specimens are then pulled at a crosshead speed of 0.05 inch per minute and the load to failure recorded on the load-time recorder chart. Only the loads to failure from the tensile tests are considered meaningful for detemining the residual cross sectional area.

## 9.9 Conclusions

A conservative estimate of the probability of burst of one or more indications in a S/G during a postulated SLB event indicates a likelihood of burst less than that required in the NRC's draft Generic Letter on Alternate Plugging Criteria for tube ODSCC indications at the elevations of the TSPs. Consideration of the aggregate of the largest individual indications in the South Texas 2 SGs results in an expected probability of burst of one or more tubes of several orders of magnitude less than the requirement of the draft Generic Letter respectively.

The methodology of accounting for the leak rate from tube indications restrained from burst, i.e., over pressurized tubes, is in concert with, the results from the IRB leak rate tests. Since the bounding leak rate from the tests is used in the simulations regardless of indication size, the methodology is conservative relative to the actual leak rate expectations should a SLB event occur.

The probability of an axial separation of a tube, i.e., becoming circumferentially severed, during a postulated SLB event is very small, e.g., several orders of magnitude less than required for implementation of an ARC.

## 9.10 References


1. WCAP-14273 (Proprietary), "Technical Support for Alternate Plugging Criteria with Tube Expansion at Tube Support Plate Intersections for Braidwood 1 and Byron 1 Model D4 Steam Generators," Westinghouse Electric Corporation (February 1995).
2. EPRI NP-7480-L (EPRI licensed material), Addendum 1, "Steam Generator Tubing Outside Diameter Stress Corrosion Cracking at Tube Support Plates Database for Alternate Repair Limits, 1996 Database Update," Electric Power Research Institute (November 1996).
3. EPRI NP-7480-L (EPRI licensed material), Addendum 2, "Steam Generator Tubing Outside Diameter Stress Corrosion Cracking at Tube Support Plates Database for Alternate Repair Limits, 1998 Database Update," Electric Power Research Institute (April 1998).
4. Regulatory Guide 1.121 (Draft), "Bases for Plugging Degraded PWR Steam Generator Tubes," United States Nuclear Regulatory Commission (August 1976).
5. SG-95-03-10, "Burst Pressure Correlation for Steam Generator Tubes with Throughwall Axial Cracks," Westinghouse Electric Corporation for the Electric Power Research Institute (February 1995).
6. Nadai, A., *Theory of Flow and Fracture of Solids*, Second Edition, McGraw-Hill Book Company, New York (1950).
7. Davis, E. A., "The Effect of Size and Stored Energy on the Fracture of Tubular Specimens," Journal of Applied Mechanics, Vol. 15, American Society of Mechanical Engineers (September 1948).
8. Hernalsteen, P., "The Influence of Testing Conditions on Burst-Pressure Assessment for Inconel Tubing," International Journal of Pressure Vessels and Piping, Vol. 52 (1992).
9. EPRI NP-7480-L (EPRI licensed material), Volume 2, Revision 2, "Steam Generator Tubing Outside Diameter Stress Corrosion Cracking at Tube Support Plates - Database for Alternate Repair Limits, Volume 2: 3/4 Inch Diameter Tubing," Electric Power Research Institute (August 1996).
10. WCAP-14277, Revision 1, "SLB Leak Rate and Tube Burst Probability Analysis Methods for ODSCC at TSP Intersections," Westinghouse Electric Corporation (January 1995).
11. Generic Letter (GL) 95-05, "Voltage-Based Repair Criteria for Westinghouse Steam Generator Tubes Affected by Outside Diameter Stress Corrosion Cracking," United States Nuclear Regulatory Commission (August 3, 1995).

**Table 9-1: Burst Pressure as a Function of Crack Length and Crack Extension Outside of the TSP**
**Series 1**

| Specimen Identification | Slit (Crack) Length (inch) | TSP Hole Clearance (inch) | Slit Extension Out of TSP (inch) | Burst Pressure (ksi) |
|---|---|---|---|---|
| TSP3-1-015-1 | 0.149 | N/A | Free Span | 9.130 |
| TSP3-1-015-2 | 0.149 | N/A | Free Span | 8.710 |
| TSP3-1-015-3 | 0.149 | N/A | Free Span | 8.350 |
| TSP3-1-030-1 | 0.298 | N/A | Free Span | 6.800 |
| TSP3-1-030-2 | 0.301 | N/A | Free Span | 6.300 |
| TSP3-1-030-3 | 0.299 | N/A | Free Span | 6.220 |
| TSP3-1-050-1 | 0.502 | N/A | Free Span | 4.200 |
| TSP3-1-050-2 | 0.501 | N/A | Free Span | 4.500 |
| TSP3-1-050-3 | 0.500 | N/A | Free Span | 4.320 |
| TSP3-1-070-1 | 0.700 | N/A | Free Span | 3.250 |
| TSP3-1-070-2 | 0.700 | N/A | Free Span | 3.160 |
| TSP3-1-070-3 | 0.699 | N/A | Free Span | 3.210 |
| TSP3-2-070-1 | 0.700 | 0.013 | 0.150 | 8.980 |
| TSP3-2-070-2 | 0.700 | 0.013 | 0.150 | 9.160 |
| TSP3-2-070-3 | 0.699 | 0.013 | 0.150 | 8.870 |
| TSP3-3-070-1 | 0.699 | 0.012 | 0.300 | 6.600 |
| TSP3-3-070-2 | 0.698 | 0.013 | 0.300 | 6.250 |
| TSP3-3-070-3 | 0.700 | 0.013 | 0.300 | 6.290 |
| TSP3-4-070-1 | 0.702 | 0.011 | 0.500 | 4.500 |
| TSP3-4-070-2 | 0.700 | 0.011 | 0.500 | 4.600 |
| TSP3-4-070-3 | 0.699 | 0.012 | 0.500 | 4.200 |
| Tube Material: HT 1797 for 3/4" tubes. | | | | |

**Table 9-2: Burst Pressure as a Function of Crack Length and Crack Extension Outside of the TSP Series 2**

| Specimen Identification | Slit (Crack) Length (inch) | TSP Hole Clearance (inch) | Slit Extension Out of TSP (inch) | Burst Pressure (ksi) |
|---|---|---|---|---|
| TSP3-6-070-1 | 0.699 | 0.021 | 0.150 | 8.100 |
| TSP3-6-070-2 | 0.700 | 0.021 | 0.150 | 8.580 |
| TSP3-6-070-3 | 0.699 | 0.021 | 0.300 | 6.090 |
| TSP3-7-070-1 | 0.700 | 0.019 | 0.300 | 6.070 |
| TSP3-7-070-2 | 0.700 | 0.021 | 0.500 | 3.800 |
| TSP3-7-070-3 | 0.699 | 0.022 | 0.500 | 3.820 |
| TSP7-2-070-1 | 0.701 | 0.022 | 0.150 | 8.970 |
| TSP7-2-070-2 | 0.702 | 0.023 | 0.150 | 9.310 |
| TSP7-3-070-1 | 0.700 | 0.023 | 0.300 | 6.780 |
| TSP7-3-070-2 | 0.700 | 0.023 | 0.300 | 7.100 |
| TSP7-4-070-1 | 0.700 | 0.021 | 0.500 | 4.880 |
| TSP7-4-070-2 | 0.701 | 0.023 | 0.500 | 5.000 |
| Tube Material: HT 1797 for 3/4" tubes and HT 1282 for 7/8" tubes. | | | | |

**Burst Pressure vs. Crack Length**
3/4" x 0.043", Alloy 600 MA SG Tubes, $\sigma_f$ = 71.6 ksi

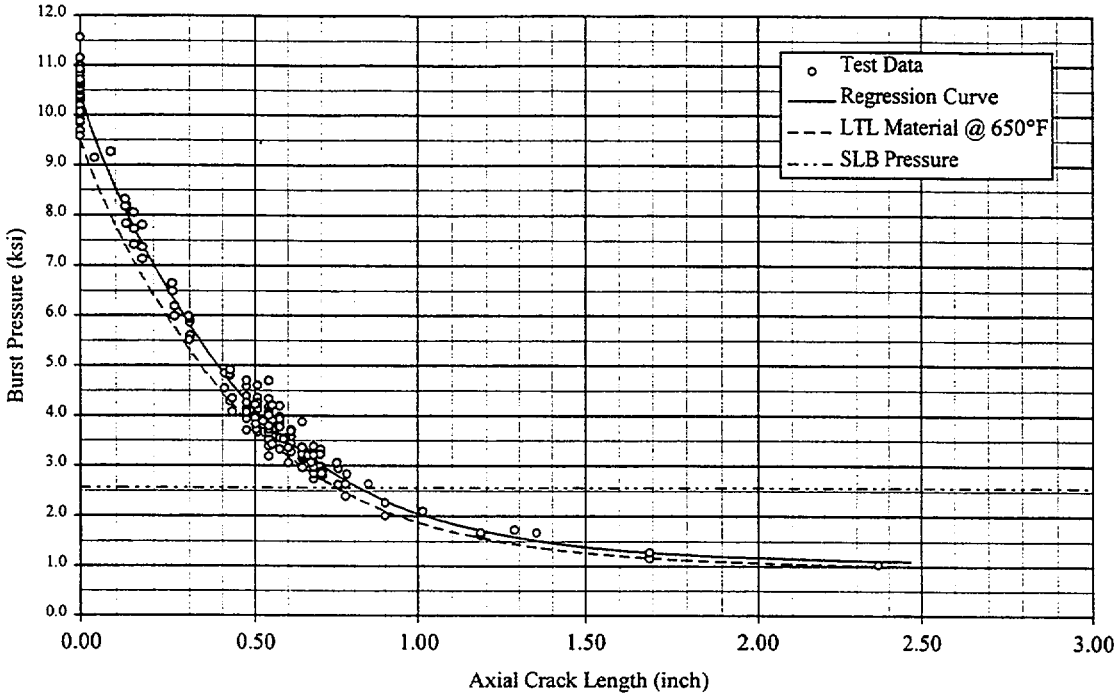


**Figure 9-1**

**Burst Pressure vs Exposed Crack Length for Probability of Burst**
**3/4" x 0.043", Alloy 600 MA SG Tubes, Average Material @ 650°F**

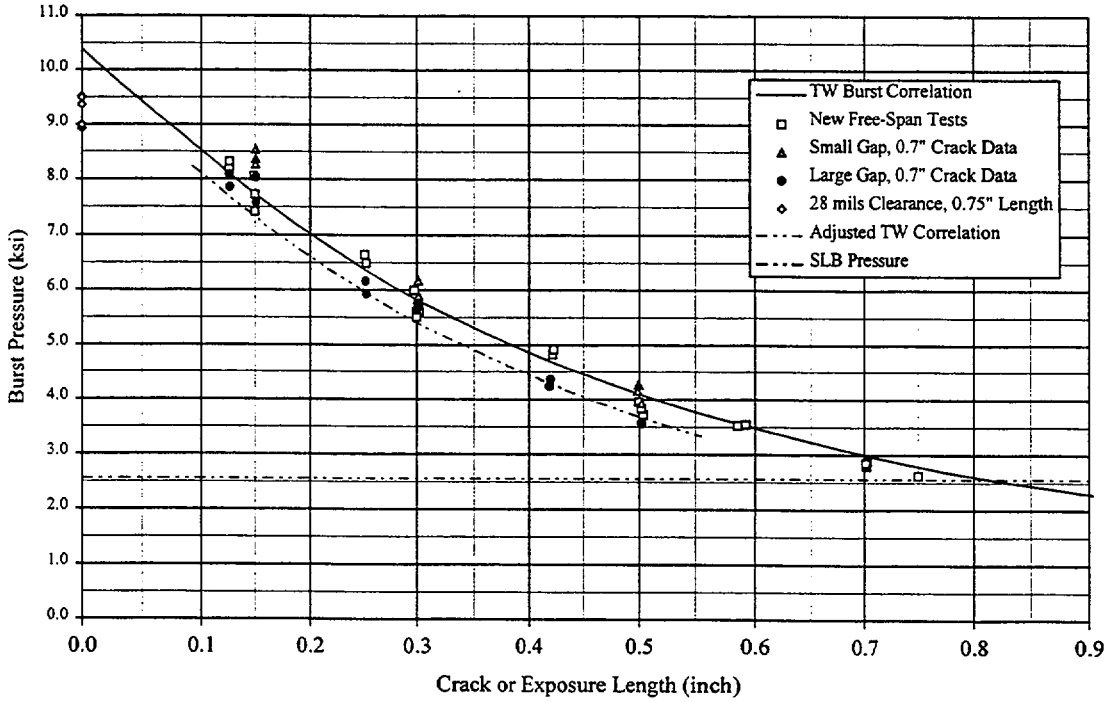


**Figure 9-2**

**Effect of TSP Clearance on the Probability of Burst**
**3/4" x 0.043", Alloy 600 MA Steam Generator Tubes**

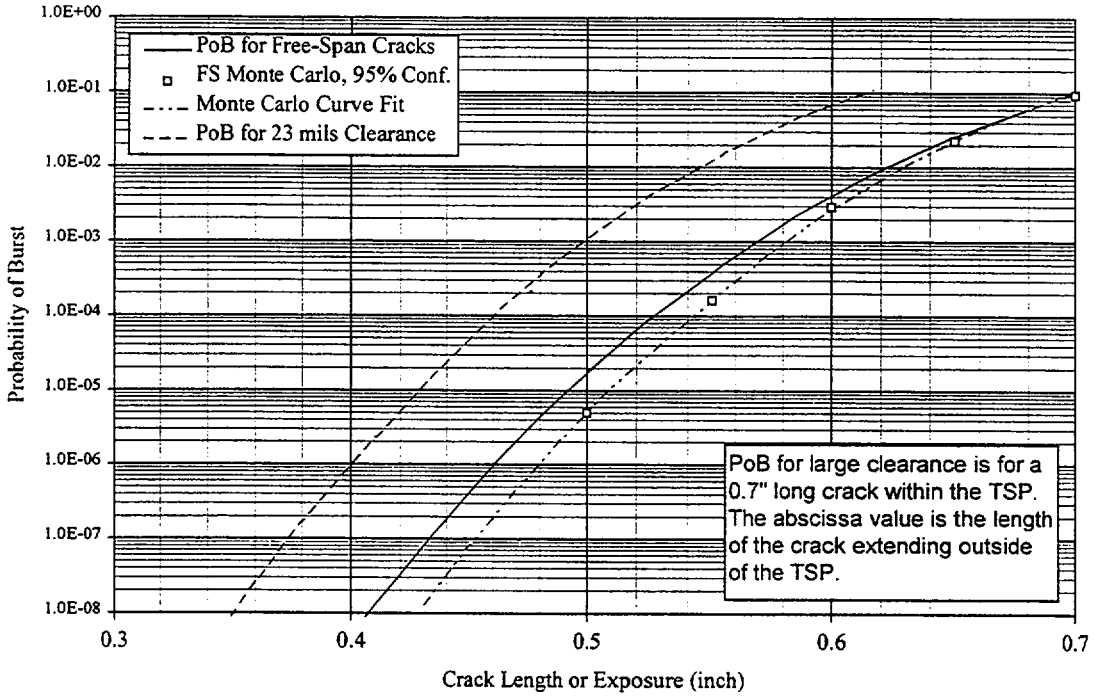


**Figure 9-3**

**Effect of TSP Clearance on the Probability of Burst**
**3/4" x 0.043", Alloy 600 MA Steam Generator Tubes**

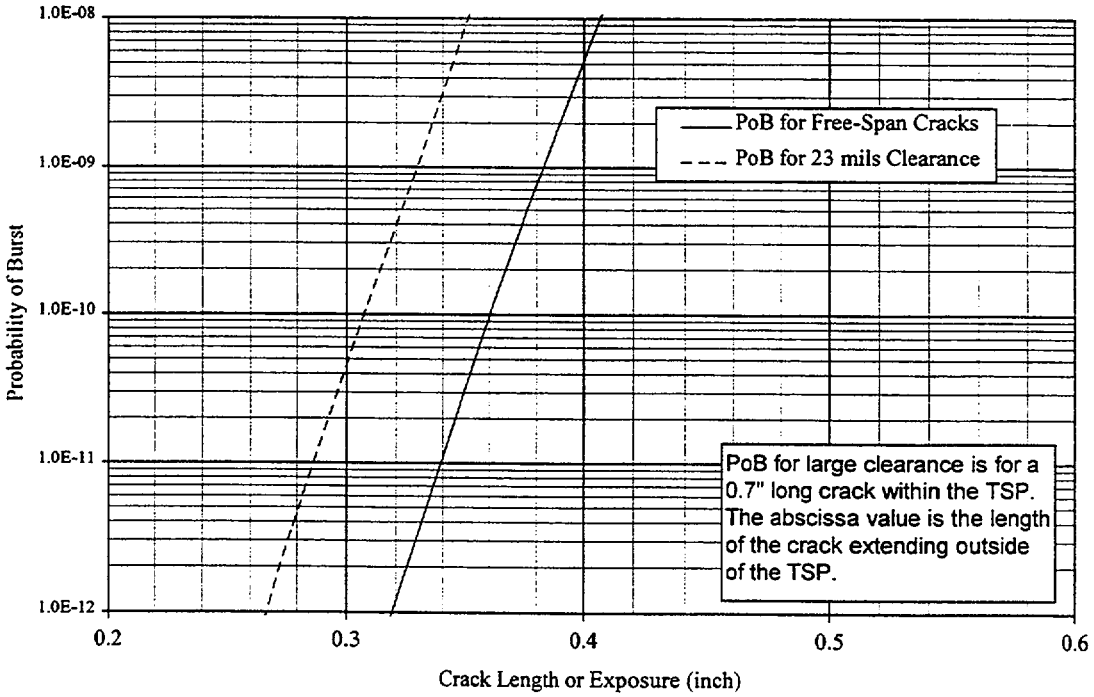


**Figure 9-4**

# 10.0 STEAM GENERATOR INTERNALS - INSPECTION PLAN

## 10.1 Introduction

The STPNOC 3-volt Alternate Repair Criteria (ARC) technical specification amendment request for Unit 2 relies on ODSCC indications remaining within the bounds of the tube support plates (TSPs) during a SLB event. Analyses have been performed to determine the loads placed on each TSP and the resulting displacements during such events. The analysis takes credit for specific steam generator internal components to provide a load path that limits TSP displacement.

To ensure that the load path components are not degraded to the level that they can no longer perform their intended function, STPNOC has developed a steam generator internals inspection program that will be implemented prior to, or during, the outage in which the 3-V ARC will be implemented. This program contains specific inspection logic, scope, inspection method, and acceptance criteria.

The inspection logic included 1) identifying the most significant load carrying components, 2) reviewing the industry experience, 3) establishing the most plausible degradation mechanism associated with these components, and 4) evaluating existing steam generator access openings and available inspection techniques to view these critical components.

## 10.2 Steam Generator Internals Industry Experience

Information Notice (IN) 96-09 and IN 96-09, Supplement 1 have been issued by the NRC to alert operating PWRs of various damage seen in the steam generator internals at foreign PWR facilities. Subsequently, the NRC issued GL 97-06 which requires licensees to document inspection plans, including scope frequency, methods and equipment for inspecting the SGs for the damage mechanisms discussed in IN 96-09 and GL 97-06.

The damage mechanisms reported, included, 1) wastage of the uppermost support plate caused by the misapplication of a chemical cleaning process, 2) broken tube support plate ligaments near both a radial seismic restraint and anti-rotation key at the upper most, and sometimes at the next lower tube support plate, and 3) wastage of tube support plate ligaments not associated with chemical cleaning. In addition to the tube support plate damage, wrapper drop and cracking of the wrapper above the original upper support have been observed at a foreign PWR facility. An evaluation of the probable causes of these foreign experiences is contained in EPRI Document GC-109558, Steam Generator Internals Degradation: Modes of Degradation Detected in EDF Units, which has been distributed to the NRC by NEI. With the issuance of IN 96-09 and GL 97-06, operating PWRs have participated in an Industry Program which evaluates and ranks steam generator models relative to the need for inspecting the steam generator internals for evidence of the various damage mechanisms by either visual and/or eddy current techniques. No evidence of wrapper drop or cracking has been reported. Tubes found without adequate support lateral support are being plugged.

The carbon steel support plates in STPNOC Unit 1 have been 100% inspected. No evidence of any support plate degradation or ligament cracking was found. The support plates for Unit 2 are stainless steel and are bounded by the inspection results from Unit 1.

Additional steam generator internal inspections have been performed in preheater steam generators, similar to, but not identical to the South Texas Model E2 design. These inspections were performed at two sites in support of a 3.0 volt IPC amendment. The inspection included extensive visual inspection of the top tube support in one steam generator at each site. Emphasis was placed on determining if degradation similar to that seen in the EDF units was present. No degradation was seen. Visual inspection was performed on eight (8) of the ten (10) tie rod nuts in one of the four steam generators at each site. The nuts were found to be tight against the top support plate and no degradation seen.

Eddy current inspection was performed on all four (4) steam generators, at each site, in the area of the anti-rotational devices at the top tube support plate for identification of cracked TSP ligaments. In addition, eddy current inspection of the patch plate area in all four (4) steam generators, at each site, was performed. No degradation was noted.

Approximately five (5) wedges and eighty-nine (89) vertical bars were visual inspected at each site. No degradation was noted.

Verification that the wrapper had not shifted was performed for each steam generator at each site by assuring there was not obstructions when inserting the sludge lance equipment through the wrapper openings. No shift in the wrapper location was noted.

## 10.3 Model E2 Steam Generator Internal Support Structure

The general layout of the STPNOC Unit 2 steam generators is shown in Figure 10.1. Most of the feedwater enters the S/G through the preheater inlet nozzle into the preheater region. A detailed layout of the preheater region is shown in Figure 10.2. A partition plate between plates B and K (see Figure 10.2) separates the preheater and the hot leg sides of the S/G. The S/G tubes pass through the various Type 405 stainless steel plates which are drilled and provide lateral support to the tubes. The nomenclature for each of the plates is shown in Figure 10.3. Support plates C, F, J, L, M, N, P, Q and R contain circulation holes through which water/steam passes through the tube bundle. On the cold leg side of the preheater region, plates B, D, E, G, H, and K are referred to as baffle plates, contain no circulation holes, and act to direct the flow across the tubes. Plate A referred to as the flow distribution baffle, at an elevation of [ ]$^{a,c}$ inches above the top of the tubesheet, contains no individual circulation holes, and distributes the flow across the tubesheet and upward through a cutout in the plate on the hot leg. The flow distribution baffle, preheater baffle plates and tube support plates are supported vertically using stayrods/spacers and vertical bars welded to the wrapper and/or partition plate. In-plane supports are provided by wedges located around the

circumference of each plate. The wedges are welded to the wrapper. Their tapered design provides additional resistance to upward movement, in addition to in-plane support.

### 10.3.1 Stayrod and Spacer Pipe Geometry

All of the hot leg plates are supported by a total of three tie-rods/spacers in each of the plate quadrant. Each plate has three additional tie-rod assemblies located on the XZ axis. Each tie-rod consists of a [ ]$^{a,c}$ inch diameter rod threaded on each end with [ ]$^{a,c}$ threads. They are threaded into the tube-sheet for a length of [ ]$^{a,c}$ inches. The center stay rod-(the one on the vertical axis of the steam generator) is threaded into the top of the partition plate. The stay-rods extend continuously through the tube bundle assembly to the top tube support plate where a nut is attached. The nut is welded to the top surface of the top tube support plate, Plate R, while the nut on the additional preheater stayrods is welded to the top surface of Plate H. Around the outside of the tie-rods are spacers that are located between each of the support plates. The spacer pipes are [ ]$^{a,c}$ pipe, which translates to an outer diameter of [ ]$^{a,c}$ inches and an inner diameter of [ ]$^{a,c}$ inches. The length is equal to the span between the two plates separated by the pipe. This serves to keep the plates separated and to provide interior supports to the plates. The spacers are tacked welded to the under-side of each TSP, but are not attached to the plate below. Consequently, the spacer pipes act only as compressive members. For the central tie-rod, located on the XZ axis, the lower end is threaded into a special coupling welded to the top of the partition plate at Plate L. The general tie-rod/spacer assembly configuration is shown in Figure 10.4.

### 10.3.2 Vertical Support Bars - TSP Wedges

A schematic of the vertical support bars is shown in Figure 10.5. These vertical bars are located above and below each plate and are welded to the wrapper, partition plate, and impingement plate. These bars have a minimum cross section of [ ]$^{a,c}$. The bars overlap the perimeter of the plate by a minimum of [ ]$^{a,c}$ inch. Typically they extend full length between plates.

Wedges are used between the tube support plates and the wrapper to help attain an integrated alignment of the tubes with the support plates and to provide in-plane support. Wedges are installed side by side on the periphery of the plates as illustrated in Figure 10.6. The wedges are welded to the wrapper or center partition plate, but are not welded to the support plates.

### 10.3.3 Wrapper Support Geometry

The wrapper support configuration consists of wrapper support blocks that are welded to the inside of the stub barrel wall, the upper and lower wrapper position blocks that rest against either side of the wrapper support blocks and are welded to the wrapper, and the wrapper itself, which provides support for the tube support plates. The eight wrapper

support blocks and wrapper position blocks provide restraint to the wrapper in the vertical direction during seismic and blowdown events. The geometry of the wrapper support blocks and the wrapper position blocks are shown in Figure 10.7, while Figure 10.8 depicts the anti-rotation support. The wrapper support blocks are welded to the inside of the stub barrel wall with full penetration welds. The upper and lower position blocks which rest against both sides of the wrapper support blocks are welded to the wrapper with full penetration welds. The wrapper support blocks lugs are made of SA-516 Grade 70 carbon steel and the wrapper position blocks are made from PDS-10105 AP carbon steel.

## 10.4 Degradation Assessment

Even though the STPNOC Unit 2 steam generator plates are fabricated from Type 405 stainless steel, the structure load path is composed of carbon steel components. Two mechanisms are plausible to cause active degradation of the welds in the carbon-steel load path components. These are corrosion fatigue and stress corrosion cracking (SCC). Since active stresses and variations in stress are low in these components, corrosion fatigue is unlikely. This includes either initiation or propagation. Environmental effects have been observed in corrosion fatigue tests of carbon and low alloy steels in high temperature water. However, high cycle stresses and / or oxygen levels are needed for these effects to be substantial. These conditions do not exist based on the South Texas operating conditions.

The temperature, environment and chemistry are essentially the same for all TSP support bars, hot leg and cold leg. Environment changes from the top to bottom of the steam generator are primarily increases in void fraction as a function of elevation in the steam generator while temperature is nearly constant at the secondary water saturation temperature. Thus, all TSP support bars (above and below the TSP or hot and cold leg) are equally susceptible to the same induced degradation. Similarly, manufacturing differences between bars are negligible.

Therefore, for the purpose of inspection, any carbon steel component identified in the TSP load path, represents an adequate sample for integrity verification. Any weld on any bar, wedge, or stayrod is a random weld and an acceptable sample for developing an inspection plan for determining the likelihood of a crack weld. This permits the inspection sampling-plan to be based on the inspection of any TSP load support weld, either hot or cold leg, while applying the results of the inspection to the most critical hot leg welds.

## 10.5 STPNOC Steam Generator Internals Inspection Plan

The objective of this inspection plan is to provide adequate confidence that the required structural load path to support a 3 volt Alternate Repair Criteria for STPNOC Unit 2, is not degraded. As was discussed previously, no load path component degradation has been observed in Westinghouse fabricated steam generators without denting. STPNOC has performed a variety of secondary side inspections of Unit 1 and Unit 2 steam

generators during past refueling outages. No load path degradation was observed during any of these inspections. These inspections included 100% eddy current inspection of the Unit 1 carbon steel tube support for ligament cracking and visual inspection of Unit 1 and Unit 2 plates, wedges, stayrods/spacers, vertical backing bars and wrappers. The results of these inspections are summarized in Tables 10.1 and 10.2. These inspections focused on the preheater and flow distribution regions due to available openings for access into the secondary side.

To further assure the integrity of the load path components in the STPNOC Unit 2 steam generators, additional inspections through available access openings will be performed at a preceding outage or during the refueling outage at which the 3-volt ARC is implemented. Inspection of the plates, stayrods, wedges and vertical backing bars will be performed. The tube support plates transmit the load to the surrounding support structures. The integrity of this load path can be verified, although degradation of the base materials and welds due to SCC, corrosion, erosion or fatigue is not considered likely. Visual inspection will emphasize the lower TSP regions where most ODSCC indications have occurred. The structural integrity of the uppermost plate relative to critical load carrying features will be determined. The extent of these inspections will be based on existing accessibility, risk of "sticking" visual probes, radiation exposure and outage schedule.

Existing shell openings in the STPNOC Unit 2 steam generators are located in the preheater area and below the first tube support plate. A total of twenty (20) secondary side openings exist in each steam generator, with eleven (11) located below the first tube support plate (Plate C) and seven (7) in the preheater area. The two (2) remaining openings, i.e., secondary side manways, are located in the upper steam drum. The only access to the bundle is through the primary separator swirl vanes. The geometry of the Model E2 steam generator along with tooling limitations constrain the extent of hot leg in-bundle or periphery inspections that can be performed. Table 10.3 identifies the location of the available inspection openings.

The plan is to perform 20 % eddy current inspection of all tube support plates for ligament degradation, along with visual inspection of the wrapper blocks, vertical backing-bars and wedges associated with the flow distribution plates in all four steam generators. In addition, the top support plate wedges, vertical backing-bars and preheater stayrod/spacers/nuts will be inspected in one steam generator. These inspections along with results from previous inspections are adequate to verify the structural integrity of the Unit 2 load path components. Table 10.4 and 10.5 lists the additional inspections to be performed.

## Table 10.1 STPNOC Unit 1 SG Internals – Inspection Results

| Load Path Component | Inspection Date - Extent - Method | Results |
|---|---|---|
| Tube Support Plates | 1RE07 - All Steam Generator - All Elevations<br><br>Bobbin coil examination based on EPRI Report "Investigation of Applicability of Eddy Current to the Detection of Potentially Degraded Support Structures" dated May 1996, SG-96-05-003. | No Degradation Found. Fabrication trimmed plates were noted and reconciled with fabrication records. |
| Wrapper | 1RE01 - 1RE03 - 1RE05 - 1RE06<br><br>Visual inspection of wrapper alignment based on sludge lance accessibility.<br><br>Visual inspection of baffle plate H - near feedwater nozzle. | No Deformation or Drop Noted. |
| Preheater Baffle Support Bars | 1RE05 - S/G C<br><br>Visual inspection of preheater baffle plate H inside the preheater through preheater access port. | No weld cracking or baffle support deformation. |

## Table 10.2 STPNOC Unit 1 SG Internals - Inspection Results

| Load Path Component | Inspection Date - Method - Extent | Results |
|---|---|---|
| Plates | 2RE03 - SG 2A | |
| | Visual inspection of ligaments for plates "B" and "C" | No ligament cracking or erosion observed |
| | Visual inspection of cold leg periphery tube crevices and plate ligaments at each plate elevation in the preheater area | No ligament cracking or erosion observed |
| Wrapper | 2RE03, 2RE04 and 2RE05 | |
| | Visual verification of alignment of wrapper and shell openings for all S/G's | No misalignment |
| | 2RE03 - S/G 2B | |
| | Visual inspection of cold leg wrapper seam weld near plate "K" | No cracking or distortion noted |
| Wedges - Stayrods - Vertical Backing Bars | 2RE03 - S/G 2B | |
| | Visual inspection of preheater plate backing bars, support clips and associated welds for plates "K", "B", "C", and "D" | All wedges, support bars, clips and stayrods inspected showed no distortion or cracking. All features were consistent with design configuration |
| | Visual inspection of five (5) wedges for plate "K", four (4) wedges for plate "B", and two (2) for plate "A", including all top wedge to wrapper welds, and one (1) side wedge to wrapper weld for each plate | |
| | Visual inspection of two (2) stayrods each on plates "B" and "K". | |

**Table 10.3**
**STPNOC Unit 2 Steam Generator Inspection Openings**

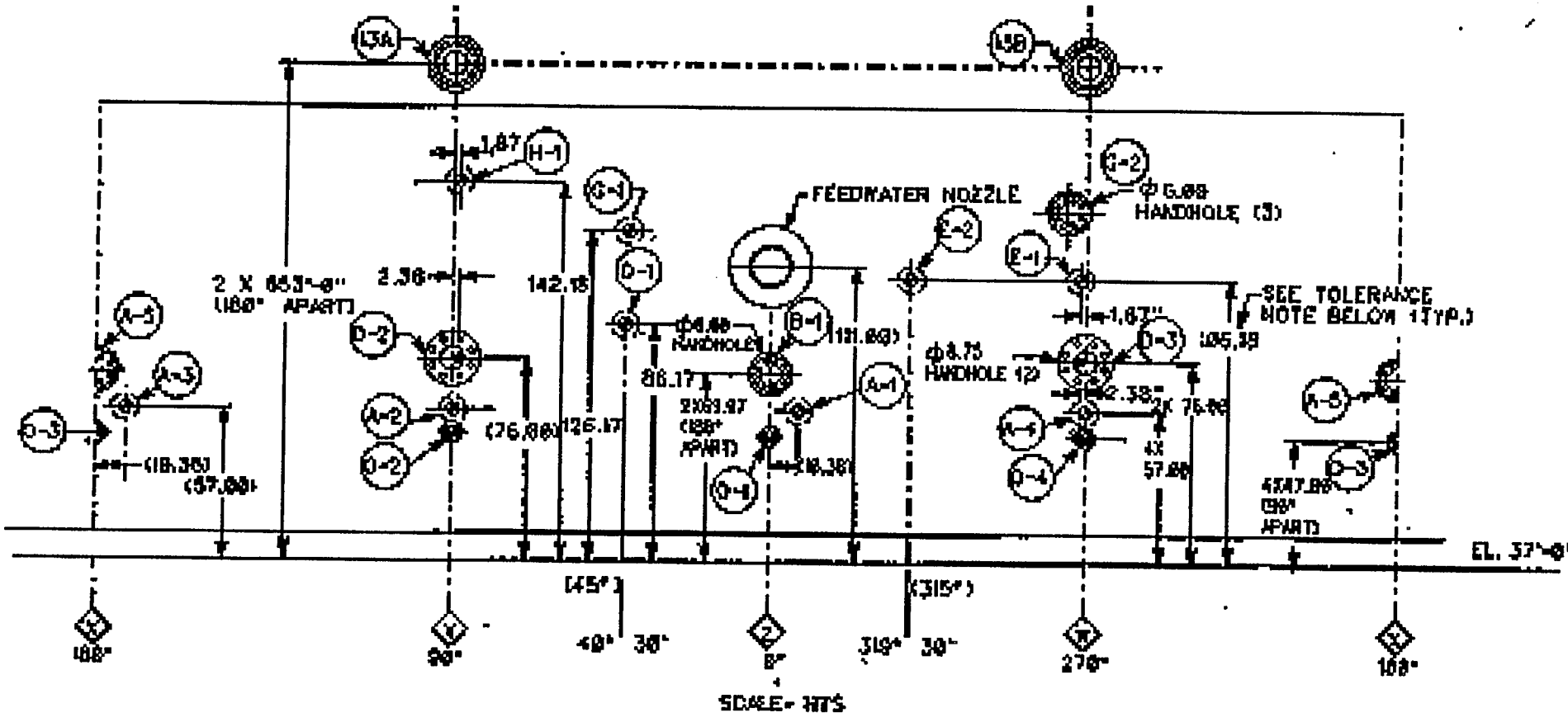


TOLERANCE NOTE:

UNLESS OTHERWISE SPECIFIED, ALL DIMENSIONS LOCATING THE INSPECTION PORTS FOR MACHINING MUST BE WITHIN ±.06.

(table continued next page)

**Table 10.3 (continued)**
**STPNOC Unit 2 Steam Generator Inspection Openings**

a,c

[redacted]

**Table 10. 4**
**INSPECTIONS TO BE PERFORMED IN ALL STEAM GENERATORS**

| LOAD PATH COMPONENT | INSPECTION METHOD | PLANNED INSPECTION | ACCEPTANCE CRITERIA | INSPECTION ACCESS |
|---|---|---|---|---|
| **Vertical Support Bars (Welds)** | Visual | Lowered FDB | Bars - alignment, no distortion, correct location, welds | Through sludge ports - to be performed as part of post sludge lancing video |
| **TSPs** | Eddy Current | All TSP intersections | No Cracking | Low frequency bobbin - auto analysis - plus point characterization |
| **Wrapper Support Blocks** | Visual | 90 Degree Locations | Alignment between shell - wrapper | Through sludge lance ports |

**Table 10.4 (continued)**
**VISUAL INSPECTION TO BE PERFORMED IN ONE STEAM GENERATOR**

| LOAD PATH COMPONENT | INSPECTION METHOD | PLANNED INSPECTION | ACCEPTANCE CRITERIA | INSPECTION ACCESS |
|---|---|---|---|---|
| **Vertical Support Bars (Welds)** | Visual | Hot leg bars below plate C and above FDB<br><br>Tube support plates "R" and "Q". Number of bars inspected will be determined by accessibility | Bars - alignment, no distortion, correct location:<br><br>Welds - no longitudinal cracking | A-5 Opening - below the first TSP (Plate C)<br><br>Through separator package or lower deck hatch |
| **TSPs** | Visual | Anti-rotation devices at "R" plate. | No cracking | Through separator package or lower deck hatch |
| **Wedges** | Visual | Wedges at TSPs "R" and "Q" | Wedge present - weld present | Through separator package or lower deck hatch. |
| **Wrapper Support Blocks** | Visual | Wrapper support block welds between wrapper and shell | Weld present - no longitudinal cracking | Tubesheet inspection ports or down annulus from lower deck. |
| **Stayrods** | Visual | Tube support plates "R" and "Q"<br>Number of stayrods to be inspected will be based on accessibility. | Nut tight against top TSP, weld present, spacers not degraded | Through separator package or lower deck hatch |

**Figure 10.1 Model E2 Steam Generator Layout** a,c

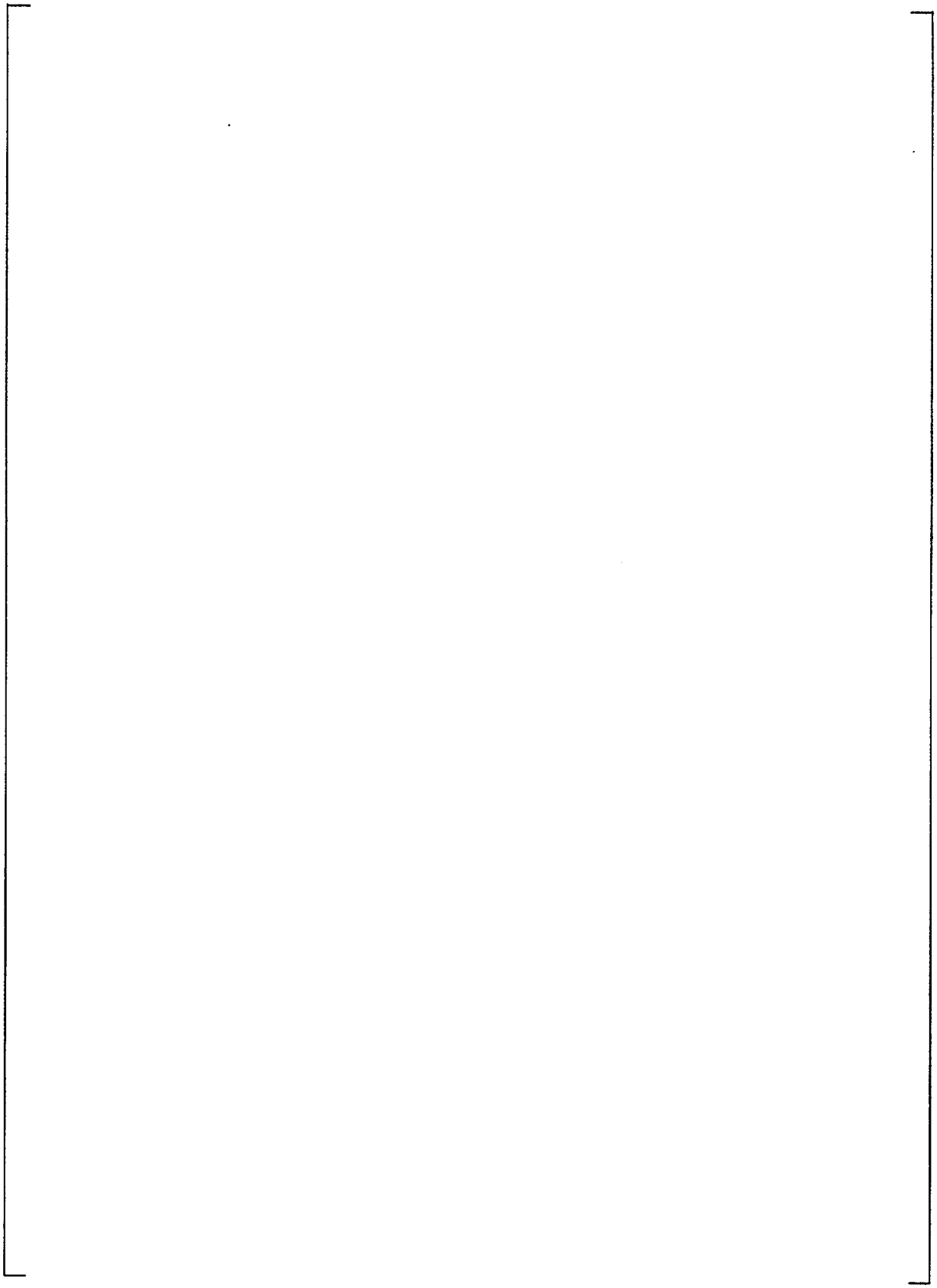

**Figure 10.2 Model E2 Steam Generator Preheater Region**

a,c

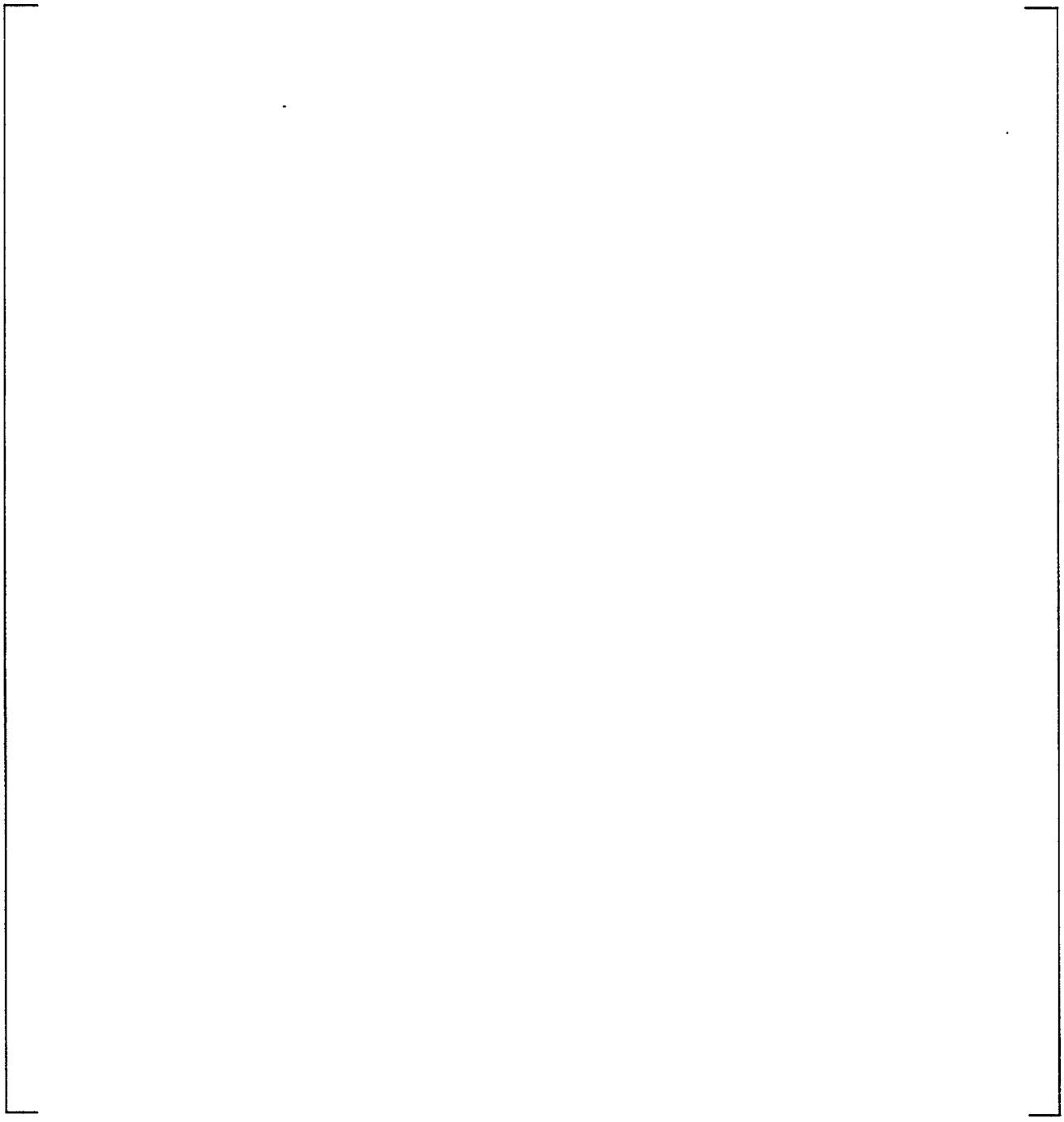

**Figure 10.3 Model E2 Tube Bundle Plate Nomenclature**

a,c

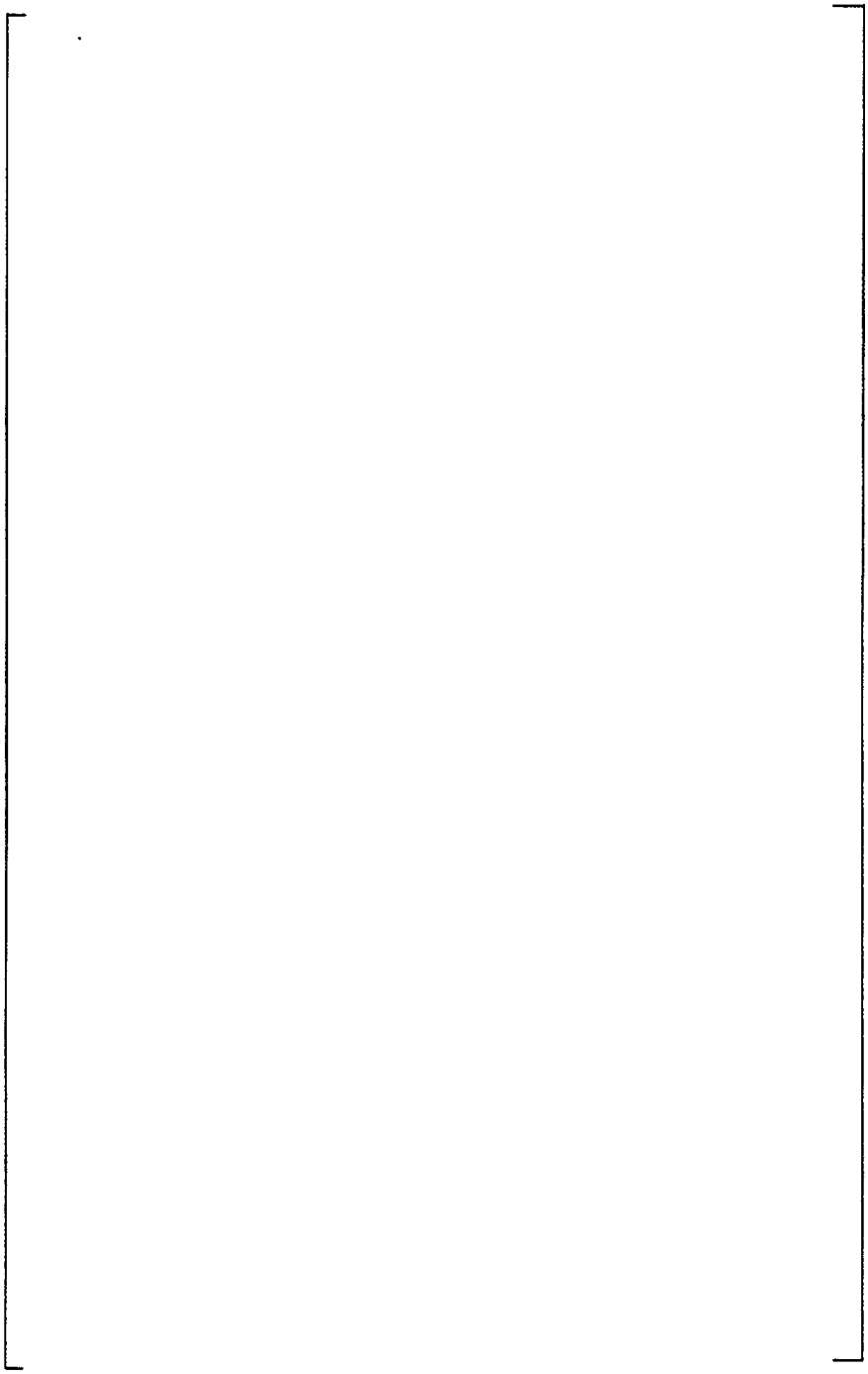

**Figure 10.4 Schematic of Model E2 Stayrod and Spacer Assemblies**

a,c

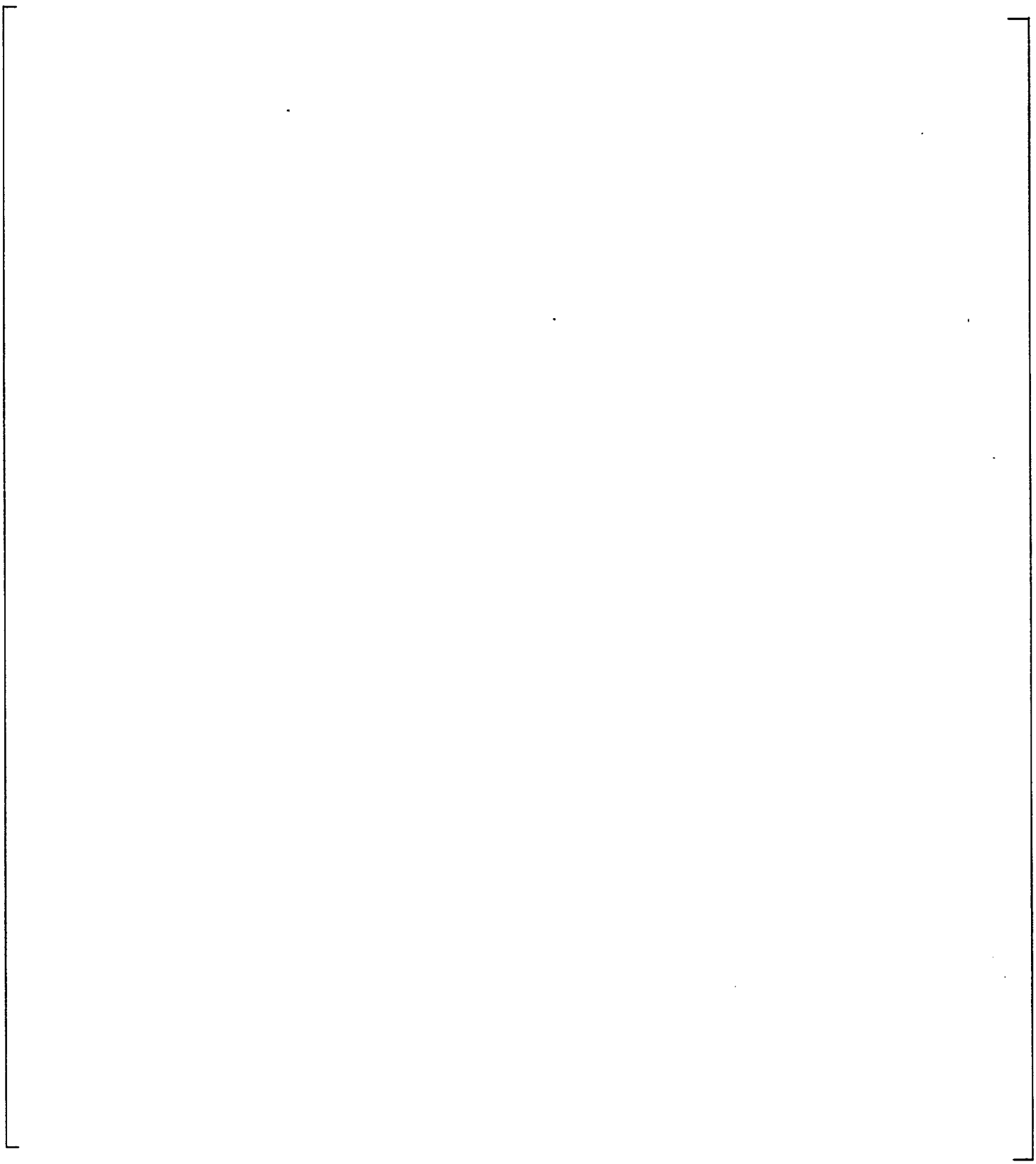

**Figure 10.5 Model E2 Plate Vertical Bar Support**

a,c

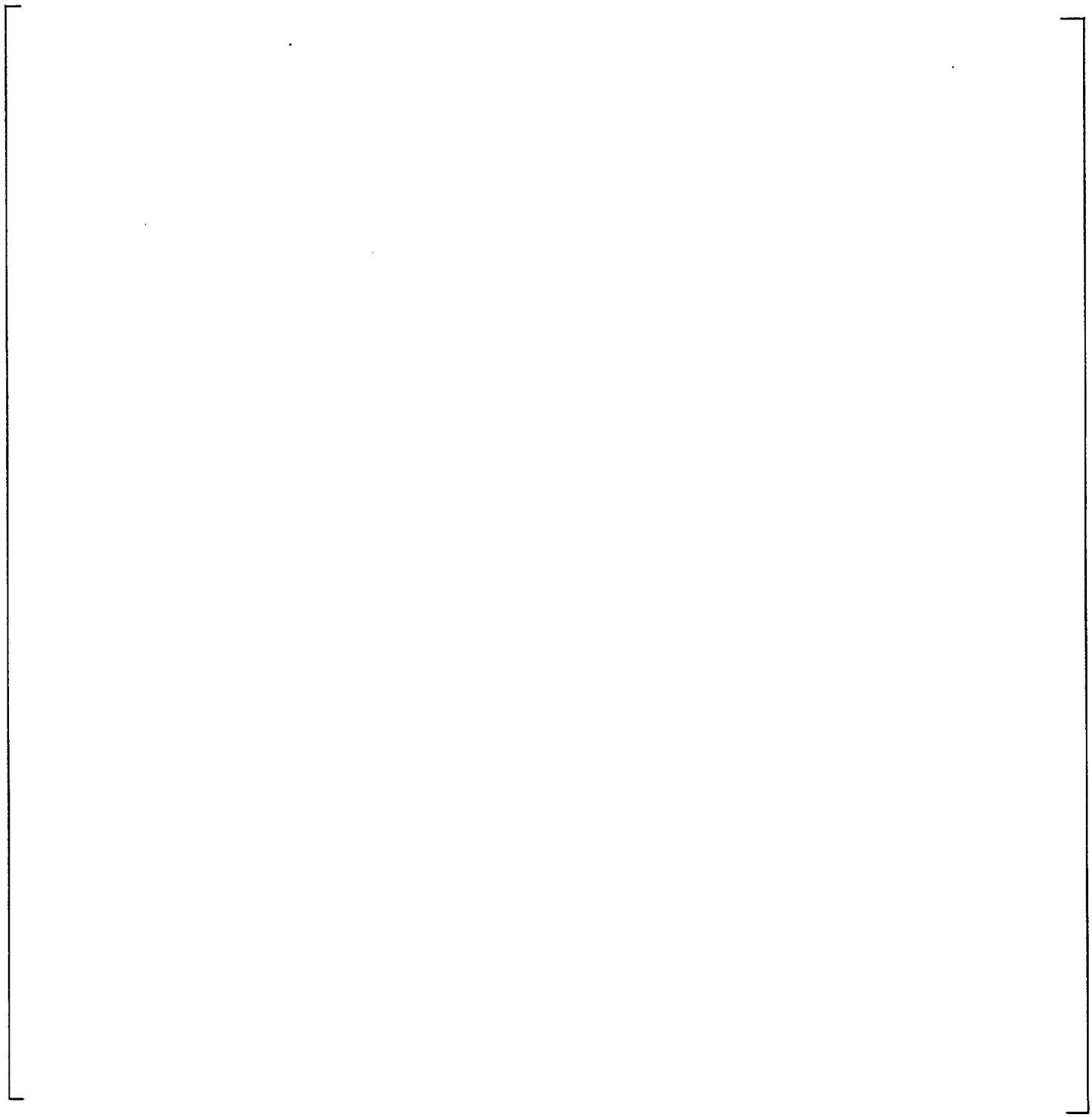

**Figure 10.6 Schematic of Model E2 Plate Wedge Geometry** a,c

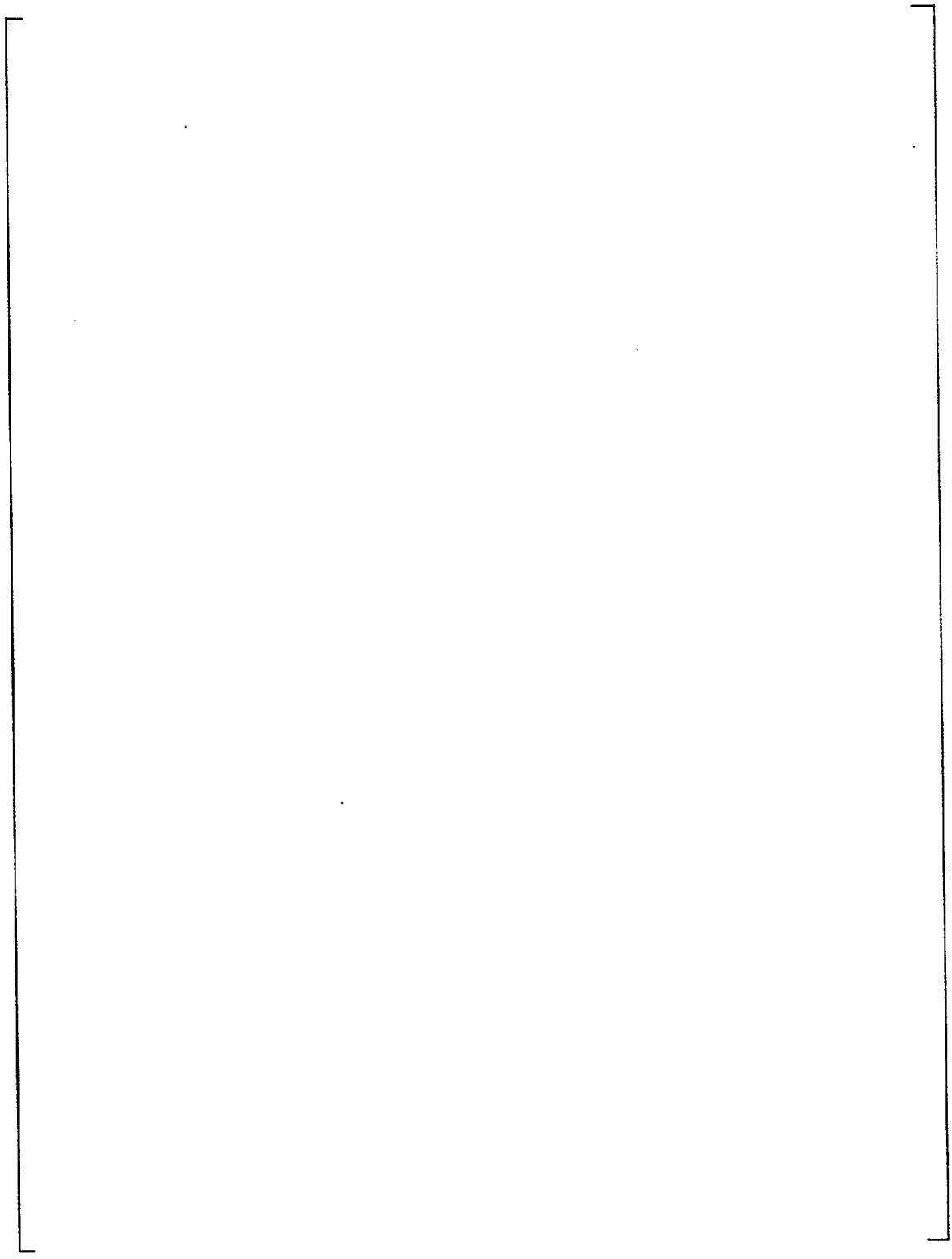

**Figure 10.7 Model E2 Wrapper Vertical Support**

a,c

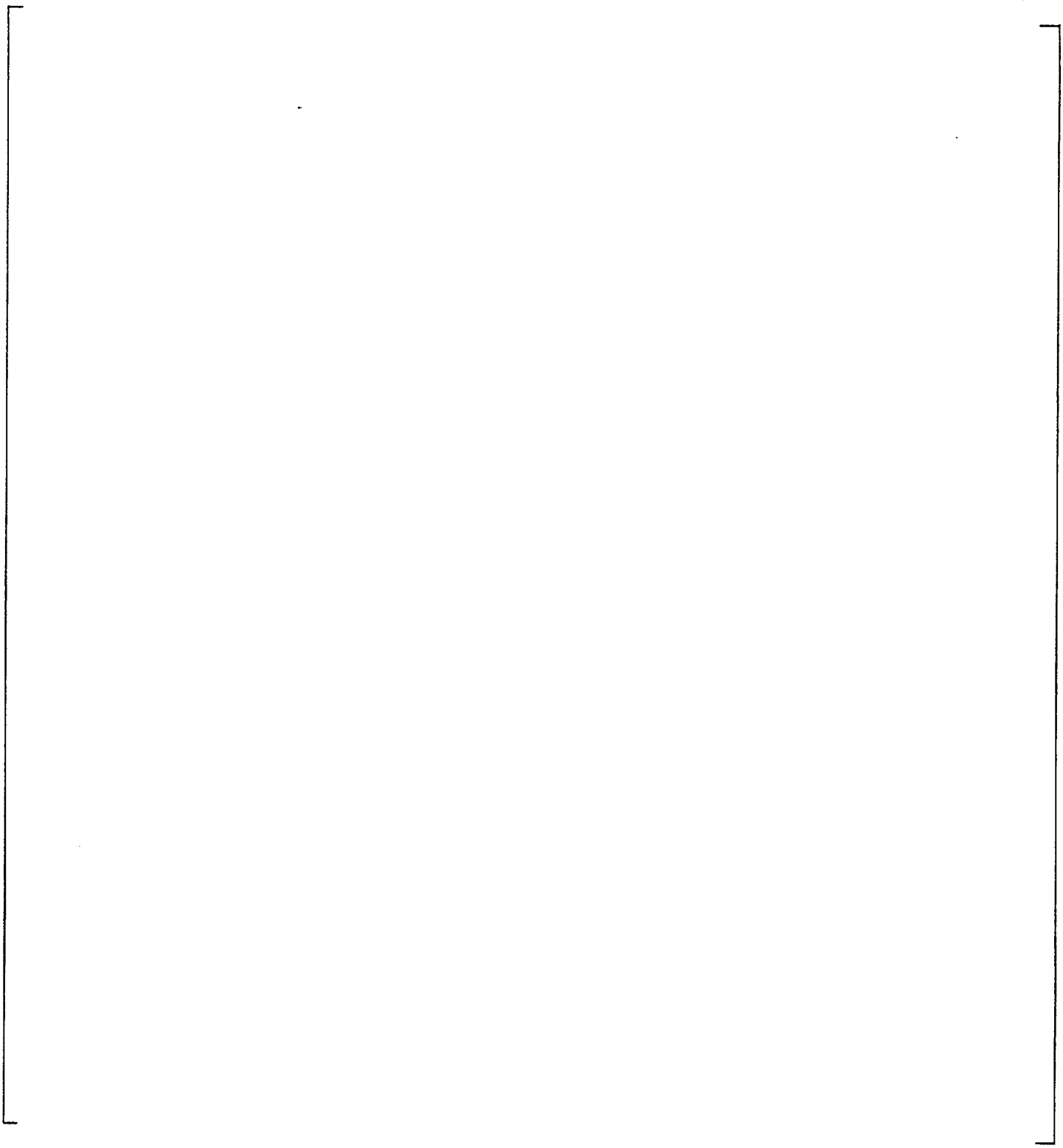

**Figure 10.8 Model E2 Anti-Rotation Support Configuration**

a,c

# 11.0 HIGH VOLTAGE ALTERNATE REPAIR CRITERIA AT TUBE SUPPORT PLATES FOR SOUTH TEXAS UNIT 2

This section integrates the results of the prior sections of this report to develop the alternate repair criteria at hot leg TSP intersections with displacements less than 0.15", specifically plates C through M. The general approach, design requirements, performance summary and recommended alternate repair criteria are provided in this section for the South Texas-2 SGs. Tube repair limits for the FDB and all cold leg TSP intersections are based on NRC Generic Letter 95-05 (Reference 1) and the South Texas Unit 2 1-volt ARC submittal (Reference 2).

## 11.1 General Approach to Tube Repair Criteria

The approach applied to developing the tube repair criteria is based on a) developing the minimum requirements and, b) demonstrating by analysis that the SG response to the limiting loading conditions is within the minimum requirements. The general approach can be described as follows:

- Ensure that TSP displacements are less than or equal to 0.15 inches to reduce the tube burst probability to negligible levels
  - The tube burst probability at 0.15 inch TSP displacement should be negligible compared to the NRC GL 95-05 reporting guideline of $10^{-2}$ even with the bounding assumption that all hot leg TSP intersections have exposed throughwall indications equal to the limiting TSP displacement which results from a postulated SLB event
  - An incremental cumulative tube burst probability requirement of $10^{-5}$ is a negligible change to the total tube burst probability.
  - A TSP displacement of [ ]$^{a,c}$ inch (Table 11-1) is acceptable to obtain a tube burst probability of $10^{-5}$, conservatively assuming that all TSP intersections are equally displaced by this distance during a postulated SLB event.

- Conservatively apply a factor of 1.5 margin on the RELAP5 TSP hydraulic loads
  - A factor of 1.5 applied to the RELAP5 loads envelopes collective uncertainties in RELAP5 analyses (Section 5)

- Ensure that the TSP displacements are less than, or equal to, the limiting displacement for utilizing the existing leak rate test results for indications restricted from burst (IRBs) as discussed in Section 8
  - A TSP displacement of 0.21 inch is acceptable for application of IRB leak test results
  - For South Texas-2, this displacement guideline is more limiting than the acceptable displacement to meet incremental burst probability objectives, and is the requirement that limits application of the high voltage ARC to tube support plates A through M.

- Demonstrate, by structural TSP displacement analyses, that the TSP displacements due to a postulated SLB event are less than the [ ]$^{a,c}$ inch acceptance limit for burst

and the more limiting 0.21 inch acceptance limit for application of the IRB leak rate data

- It is shown in Section 7 that the goal of ≤ 0.15 inch TSP displacement is satisfied by TSPs A through M during a postulated SLB event initiated from hot standby conditions (i.e., the limiting transient) without any physical modifications to the steam generators.
- For a postulated SLB event initiated from full power, only a local area of tube support plate Q exceeds the 0.15 inch displacement objective. The maximum predicted displacement of plate Q is [ ]$^{a,c}$ inch.
- For the limiting transient (SLB at hot standby conditions), the 0.15 inch displacement goal is satisfied by all TSPs except for a few tube locations on TSPs N, P and Q.

Sections 11.3 to 11.5 develop the tube repair limits, the inspection requirements and the SLB analysis requirements. A summary of the tube repair criteria is given in Section 11.6.

## 11.2 Allowable TSP Displacements

### 11.2.1 Allowable TSP Displacements for Acceptable Tube Burst Probability

In Section 9.3, it is shown that the burst pressure of a throughwall indication extending outside the TSP is approximately equal to the burst pressure for a free span crack equal to the length of the crack extending outside the TSP. Thus, the length of crack remaining within the TSP does not affect the burst pressure. Similarly, the burst probability for limited TSP displacements with postulated throughwall cracks can be calculated as that associated with a crack length equal to the TSP displacement. This assumes that the throughwall part of a crack is located at the edge of the TSP rather than, as more commonly found from pulled tubes, near the center of the TSP. Alternately, it can be postulated that there is a throughwall crack equal to the TSP thickness and the SLB burst probability for this indication is the same as the crack length exposed by the TSP displacement during the postulated SLB event.

The most conservative possible approach to define requirements for TSP displacement is to assume that all intersections at all hot leg TSPs have throughwall crack lengths at least equal to the TSP displacements, and that these cracks are located at the edge of the TSP. This assumption is applied to develop the allowable limits on TSP displacements so that the design is generic and envelopes any possible tube degradation, thus eliminating the need for tube burst probability calculations for indications at hot leg TSP intersections. Even under the above bounding assumption on postulated tube degradation, it is desirable that the associated tube burst probability be very small compared to acceptable levels for application of steam generator degradation-specific management (SGDSM). Then, if multiple ARCs are applied as part of SGDSM, the hot leg indications at TSPs will have a negligible contribution to the tube burst probability. The most conservative guideline for an acceptable SGDSM burst probability is the value of $10^{-2}$ given in the NRC GL 95-05. If

this value is exceeded, the generic letter requires that the higher burst probability be reported to the NRC and that the significance of the result assessed. If the burst probability for the limited displacement case is assumed to be $<10^{-3}$, the TSP indications would contribute <10% to the reporting level established by GL 95-05. This $10^{-3}$ value is the starting point for developing a burst probability requirement for the limited displacement case based on sensitivity analyses given below.

By applying the tube burst probability as a function of throughwall crack length, as developed in Section 9.3, and the bounding assumption of throughwall cracks at all hot leg TSP intersections, tube burst probabilities can be developed as a function of TSP displacements. The tube burst probabilities are developed in Table 11-1 for the postulated [ ]$^{a,c}$ indications for the 9 hot leg TSPs with [ ]$^{a,c}$ tube intersections at each plate. Burst probabilities are given in Table 11-1 for the conservative assumption of uniform TSP displacements at all tube intersections. For simplicity, the burst probabilities are calculated as the number of TSP intersections times the single tube burst probability for a throughwall crack equal to the displacement. Also, note that the calculation includes all of the hot leg TSP intersections, including the plates for which the maximum displacement exceeds the chosen goal of 0.15 inch.

Since multiple combinations of non-uniform TSP displacements are difficult to include in a generic assessment, an assumption of uniform TSP displacement during a postulated SLB event is applied to develop a limiting displacement requirement. Although the analysis of Section 7 shows that uniform TSP displacements are not realistic due to the varying locations of TSP supports, this assumption leads to a minimum allowable TSP displacement. For burst probabilities of $10^{-3}$, $10^{-4}$ and $10^{-5}$, the acceptable SLB TSP displacements are [ ]$^{a,c}$ inch, respectively.

11.2.2 Allowable TSP Displacement for SLB Leakage Considerations

Although an indication inside the TSP cannot burst, the flanks of a crack that could burst at SLB conditions can open up within the confines of the TSP, a condition for which a bounding leak rate was previously undetermined due to the assumption that the TSP would displace during a postulated SLB event. This condition has been labeled as an indication restricted from burst, or an IRB. Conceptually, the IRB leak rate can vary with TSP displacement that exposes part of the throughwall crack. A leak test program was performed to determine a leak rate that would conservatively envelop the leak rate from an IRB. This test program and results are described in Section 8.

For South Texas-2, the applicable SLB pressure differential is 2405 psi, based on the PORVs for pressure relief. At this pressure differential, the bounding IRB leak rate is 5.0 gpm (Section 8). The IRB leak rate, as compared to the much larger leak rate from a freespan burst, is dependent upon the ID of the TSP hole limiting the crack opening at or near the center of the crack. This crack opening constraint leads to a limit on TSP displacement. It is shown in Section 8 that a maximum TSP displacement of 0.21 inch is acceptable for utilizing the bounding IRB leak rate of 5.0 gpm. For conservatism, the

design goal for maximum TSP displacement is set at 0.15 inch to provide a conservative margin on the IRB leak rate application. Thus, the goal displacement, 0.15 inch, is conservative relative to both the acceptable displacement 0.21 inch, for applicability of the IRB leak rate, and the acceptable displacement, [ ]$^{a,c}$ inch, for the limiting tube burst probability of $10^{-5}$.

## 11.3 Overall TSP Limited Displacement ARC Functional Requirements and Summary of Performance

The general approach described above has led to the overall functional requirements given in Table 11-2. The bases for each requirement are also given in the tables. The tube burst probability analyses supporting the [ ]$^{a,c}$ inch TSP displacement requirement are given in Section 11.2.1. The TSP displacement limit for application of the IRB leak rate test results is 0.21 inch (Section 11.2.2). While limiting TSP displacements to [ ]$^{a,c}$ inch is adequate to achieve a negligible tube burst probability of $10^{-5}$ and a 0.21 limit is acceptable for application of the IRB leak rate results, the design goal is to obtain a maximum TSP displacement of 0.15 inch.

The design goal maximum displacement of 0.15 inch permits application of in situ leak testing. The small 0.15 inch TSP displacement in a SLB event is not expected to significantly affect leakage compared to the in situ measurements even for the very unusual, high voltage indications for which the throughwall part of the crack might extend to the edge of the TSP. Of 16 throughwall indications on pulled tubes with 1 to 16 volt indications for which sufficient data are available to obtain the location of the edge of the throughwall length relative to the edge of the TSP, only 1 throughwall length was within 0.15 inch of the edge of the TSP and 12 were > 0.2 inch from the edge of the TSP. Thus, in situ measurements can be expected to be representative of leak rates with TSP displacements < 0.15 inch. The in situ leak tests can be applied to improve the accuracy of the leak rate calculations for condition monitoring assessments if a few large indications are found in an inspection. The measured leak rates can be substituted for the calculated leak rate of the indications tested.

It is seen from Table 11-4 that all design requirements are satisfied with significant margin at all of the tube support plates. The more conservative design goal of 0.15 inch displacement is also satisfied at tube support plates C through M without physical modifications to the steam generators for the limiting loading, SLB initiated from hot standby conditions. As shown in Table 11-4, all TSPs except plate Q satisfy the 0.15 inch displacement goal for a SLB at full power conditions. The design requirement of [ ]$^{a,c}$ inch TSP displacement to limit burst probability is satisfied at all TSPs without physical modifications. Overall, it is concluded that acceptable TSP displacements under limiting postulated SLB loading are achieved for plates C through M to effectively reduce tube burst probabilities to negligible levels and to apply the bounding IRB leak rate even when conservative (factor of 1.5 on RELAP5 loads) loads are applied.

## 11.4 Tube Repair Limits for South Texas Unit 2

Tube repair limits are required for ODSCC indications at the hot leg TSPs, at the FDB and at the cold leg TSPs. At the time of this report, few indications in Model E SGs have been reported at the FDB intersections or at cold leg TSP intersections. Therefore, for the cold leg TSPs and for the FDB, it is adequate and conservative to apply the GL 95-05 ARC for ODSCC at TSPs, which are based on the assumption of free span indications at SLB conditions. The GL 95-05 criteria are the recommended repair criteria for ODSCC indications at the FDB and cold leg TSP intersections. The repair limit for these indications is 1.0 volt. For the cold leg TSP indications, the appropriate structural limit would be $1.43\Delta P_{SLB}$ since the R.G. 1.121 margin of $3\Delta P_{NO}$ is satisfied at normal operating conditions due to the constraint provided by the TSPs. Due to the large tube to FDB clearances, constraint against burst cannot be confidently assured and the $3\Delta P_{NO}$ structural margin requirement is appropriate for indications at the FDB intersections. GL 95-05 requires the upper voltage repair limit to be updated on an outage-by-outage basis to the latest database, correlations and growth information. Separate upper voltage repair limits will be provided for the cold leg TSP and FDB intersections as described in the South Texas-2 1-volt ARC submittal of Reference 11.2. Bobbin indications >1.0 volt and below the upper voltage repair limit that are not confirmed by RPC inspection may be left in service.

For free span indications, tube repair limits are based on the R.G. 1.121 guidelines for structural margins against tube burst as discussed above for indications at cold leg TSPs and at FDBs. Since the small maximum displacement of the TSPs during a postulated SLB event reduces the tube burst probability to negligible levels ($< 10^{-5}$), independent of the degree of ODSCC at the hot leg TSP intersections (all hot leg TSP intersections are assumed to have throughwall indications), tube repair limits for axial tube burst are not required. Tube repair is primarily required only as necessary to maintain SLB leakage within acceptable limits. The structural limit for the hot leg TSP intersections and the full ARC repair limit for limited displacement of the TSPs is addressed below. Allowable SLB leakage limits are given in the South Texas-2 Technical Specifications and are not developed in this report. As developed in Section 9.8, a structural limit for axial tensile tearing of cellular and IGA indications applies at very high voltages with limited TSP displacements. This structural limit appears to be in excess of [ ]$^{a,c}$ volts. Even if a factor of two reduction is applied is applied for growth and NDE allowances (factor of about 1.5 to 1.75 is typical), the full ARC repair limit would be about [ ]$^{a,c}$ volts. For conservatism in defining the ARC repair limit for limited TSP displacement, a tube repair limit of > 3.0 volts is conservatively applied for hot leg TSP indications at the South Texas-2 SGs. (Because TSPs N, P and Q exceed the conservative displacement limit of 0.15 inch imposed by design, these plates require additional physical modifications, such as tube expansions, to be included in the recommended 3V ARC.) Bobbin indications > 3.0 volts are repaired independent of RPC (or equivalent probe) confirmation.

The technical data of this report support a high degree of conservatism in the 3.0 volt repair limit for ODSCC at hot leg TSP intersections.

## 11.5 Inspection Requirements

The GL 95-05 requirements applied for the 1-volt ARC eddy current inspections also apply for implementation of the limited displacement ARC. However, the inspection threshold for RPC confirmation of bobbin indications should be adjusted for the increased repair limits. RPC inspection of bobbin indications greater than the 3.0 volt repair limit with a sample inspection of a minimum of 100 intersections below the 3.0 volt repair limit will be applied at hot leg TSP intersections. The GL 95-05 1.0 volt RPC threshold is applied for the 1.0 volt repair limit at hot leg intersections at plates N through R, at the FDB and at cold leg TSP intersections.

## 11.6 SLB Analysis Requirements

Per GL 95-05, SLB leak rate and tube burst probability analyses for condition monitoring are required prior to returning to power and the results are to be included in a report to the NRC within 90 days of restart. SLB leak rates and burst probabilities obtained for the actual voltage distribution measured at the inspection (condition monitoring) are required prior to restart and the projected next EOC values (operational assessment) are required in the 90 day report. If allowable limits on leak rates and burst probability are exceeded for either the condition monitoring or operational assessment, the results are to be reported to the NRC and an assessment of the significance of the results is to be performed. For the limited displacement ARC, SLB leak rates must be calculated for the hot leg TSP indications at plates C through M, and both leak rates and tube burst probability are to be calculated for FDB and cold leg TSP indications and hot leg indications at plates N through R. The required SLB analyses are discussed below.

The SLB leak rates for hot leg TSP indications at plates C through M are to be calculated as free span leakage using the GL 95-05 leak rate methods, if the sampled indication is not found to be a potentially overpressurized indication. For indications that are found to be potentially overpressurized indications, the bounding leak rate for indications restricted from burst (IRB) is applied. Free span leak rate methods must be applied for the FDB and cold leg TSP indications and hot leg indications at plates N through R. The free span leak rates are based on the EPRI methodology for correlating probability of leakage and SLB leak rates with bobbin voltage. Acceptable methods are described in WCAP-14277, Revision 1 (Reference 11.3).

As noted above, in addition to the free span leak rates, the leak rate analyses for hot leg TSP indications at plates C through M are to include the potential leakage from overpressurized indications within the TSP. There is a finite probability that a crack might open up significantly more than the crack opening that occurred in the SLB leak rate measurements. The probability that a crack will open up to the limits of the tube to TSP gap is equivalent to the probability of free span burst. The analysis methods for the overpressurized condition are given in Section 9.5. The overpressurized condition leak rates are obtained from the probability of free span burst and a bounding leak rate (IRB bounding leak rate) for the overpressurized condition.

The SLB leak rate analysis can be symbolically represented as:

$$LRSLB = [(1\text{-}POB)*POL*LR_c + POB*LR_b]\text{Hot Leg TSPs} + [POL*LR_c]\text{FDB+Cold Leg TSPs}$$

where:

LRSLB= Total SLB leak rate
POL = Probability of leakage based on POL versus voltage correlation
$LR_c$ = Leak rate based on leak rate versus voltage correlation
POB = Probability of burst at SLB conditions for hot leg TSP indications based on free span burst pressure versus voltage correlation (zero or one)
$LR_b$ = Bounding leak rate for overpressurized indications as developed in Section 9.6

The free span tube burst probability must be calculated for the FDB and cold leg TSP indications per the requirements of the GL 95-05. Analysis methods are described in Reference 11.3. Per NRC GL 95-05, the burst probability limit for the FDB and cold leg TSP indications for reporting results to the NRC is $>10^{-2}$.

## 11.7 Summary of South Texas-2 ARC at TSPs

This section provides a summary of the alternate tube repair criteria (ARC), as developed above, to be applied at South Texas-2 tube support plates, including plates C through M with limited SLB displacement. This summary includes the tube repair limits, general inspection requirements, SLB leak rate and tube burst probability analysis requirements. SLB analysis methodology is summarized in Section 11.6 and described in detail in Section 9. No physical modifications are required to support these ARC.

South Texas-2 Tube Repair Limits

- For hot leg TSP indications at plates C through M, bobbin flaw indications >3.0 volts shall be repaired independent of RPC confirmation.

- For indications at hot leg plates N through R, at the FDB and at cold leg TSP intersections, bobbin flaw indications >1.0 volt and confirmed by RPC inspection shall be repaired. Bobbin flaw indications greater than the upper voltage repair limits for South Texas-2 indications at FDBs and hot leg TSP intersections, respectively, shall be repaired independent of RPC confirmation. The upper voltage repair limits for hot leg plates N through R, for the FDB and for cold leg TSP intersections shall be updated at each inspection based on the latest database, correlations and plant specific growth rate information. Growth rates as required by GL 95-05, 2.a.2 shall be used to develop the upper voltage repair limits.

- All indications found to extend outside of the TSP and all circumferential crack indications shall be repaired and the NRC shall be notified of these indications prior to returning the SGs to service.

- All flaw indications found in the RPC sampling plan for mechanically induced dents (corrosion denting is not present with stainless steel TSPs at South Texas-2) at TSP intersections and bobbin mixed residuals potentially masking flaw indications shall be repaired.

- For the South Texas-2 Model E SGs, no intersections near TSP wedge supports are excluded from application of ARC repair limits due to potential deformation of these tube locations under combined LOCA + SSE loads.

General Inspection Requirements

- The bobbin coil inspection shall include 100% of all hot leg FDB and TSP intersections and cold leg TSP intersections down to the lowest cold leg TSP with ODSCC indications. The lowest cold leg TSP with ODSCC indications shall be determined from an inspection of at least 20% of the cold leg TSP intersections.

- All bobbin flaw indications exceeding 3.0 volts for hot leg TSP intersections at plates C through M, and 1.0 volt for hot leg intersections at plates N through R, for all FDB intersections and for all cold leg TSP intersections shall be RPC (or equivalent probe) inspected. In addition, a minimum of 100 hot leg TSP intersections at plates C through M with bobbin voltages less than or equal to 3.0 volts shall be RPC inspected. The RPC data shall be evaluated to confirm responses typical of ODSCC within the confines of the TSP.

- A RPC inspection shall be performed for intersections with mechanically induced dent signals >5.0 volts and with bobbin mixed residual signals that could potentially mask flaw responses near or above the voltage repair limits.

SLB Leak Rate and Tube Burst Probability Analyses

- SLB leak rates and tube burst probabilities shall be evaluated for the actual voltage distribution found by inspection and for the projected next EOC distribution.

- Based on the voltage distribution obtained at the inspection, the SLB leak rate shall be compared to the South Texas-2 allowable limits as given in the Technical Specifications. The SLB tube burst probability for FDB and cold leg TSP intersections and the hot leg intersections at plates N through R shall be compared to the reporting value of $10^{-2}$ and the NRC shall be notified prior to returning the SGs to service if the allowable limits are exceeded. If the allowable limits are exceeded for the projected EOC distribution, the NRC shall be notified and an assessment of the significance of

the results shall be performed. A report shall be prepared that includes inspection results and the SLB analyses within 90 days following return to power.

## 11.8 References

1. NRC GL 95-05; "Voltage Based Repair Criteria for Westinghouse Steam Generator Tubes Affected by Outside Diameter Stress Corrosion Cracking"; August 1995
2. SG-98-01-004; South Texas Project Unit2 Technical Justification for License Amendment to Implement NRC Generic Letter GL 95-05 Voltage Based Repair Criteria for Steam Generator Tube ODSCC; January 1998
3 WCAP 14277; SLB Leak Rate and Tube Burst Probability Analysis Methods for ODSCC at TSP Intersections (Revision 1); December 1996

**Table 11-1**
**Allowable Model E SLB TSP Displacements for Acceptable SLB Tube Burst Probability(1)**

| No. Hot Leg TSP Intersections | Assumed SLB TSP Displacement | Burst Probability Per Indication | Total SLB Tube Burst Probability |
|---|---|---|---|
| **Uniform TSP Displacements at All TSPs and Tube Locations** | | | |
| [ ]a,c | [ ]a,c | $2.3 \times 10^{-8}$ | $1.0 \times 10^{-3}$ |
| [ ]a,c | [ ]a,c | $2.3 \times 10^{-9}$ | $1.0 \times 10^{-4}$ |
| [ ]a,c | [ ]a,c | $2.3 \times 10^{-10}$ | $1.0 \times 10^{-5}$ |
| [ ]a,c | [ ]a,c (2) | $1.3 \times 10^{-13}$ | $5.8 \times 10^{-9}$ |
| [ ]a,c | 0.15" (3) | $3.8 \times 10^{-19}$ | $1.7 \times 10^{-14}$ |

Notes:
1. Burst probability estimates very conservatively postulate that all hot leg TSP intersections have a throughwall crack length equal to, or greater than, the SLB TSP displacement. The tip of the crack is assumed to be at the edge of the TSP.
2. Maximum TSP displacement at any plate (occurs on Plate Q, cold leg)
3. Maximum limiting TSP displacement by design

**Table 11-2**
**Summary Requirements for TSP Limited Displacement ARC Application**

| Requirement | Rationale |
|---|---|
| **TSP Displacements and Tube Expansion Process Design Loads Shall be Based on a Factor of 1.5 Margin on RELAP5 Hydraulic Loads** | Provides a conservative margin against load uncertainties based on RELAP5 analyses. |
| **The Maximum TSP Displacement Under A Postulated SLB Event Shall Be:**<br>**a) Less Than [ ]$^{a,c}$ inch to Limit Tube Burst Probability, and**<br>**b) Less Than 0.21 inch for Application of IRB Leak Test Bounding Leak Rate Results** | 1. Results in a tube burst probability $<10^{-5}$, even under the extremely conservative assumption of throughwall cracks at all hot leg TSP intersections, including all TSPs<br>2. Justifies use of the bounding IRB leak rate test results that include offsets up to 0.21 inches |
| **As a Design Goal for Implementing the High Voltage ARC, the Maximum TSP Displacement Under a Postulated SLB Event Shall Be Less Than 0.15 inch** | 1. Provides a Conservative Margin for application of IRB bounding leak rate test results<br>2. Provides a tube burst probability of $<10^{-10}$, even under the extremely conservative assumption of throughwall cracks at all hot leg TSP intersections, including all TSPs |

## Table 11-3
## Comparison of Tube Expansion Design Requirements and Demonstrated Performance

a,c

[

]

**Table 11-4**
**Summary of Conservatism In The Application of the Limited TSP Displacement ARC**

| Issue | Conservatism Identified |
|---|---|
| Hydraulic Loads for TSP Displacements | For displacement and stress analyses, RELAP5 hydraulic loads on TSPs were increased by factor of 1.5 to envelop RELAP5 uncertainties. |
| TSP Displacements | TSP displacements are limited by design to 0.15" compared to the acceptable [ ]$^{a,c}$ required to limit tube burst probability to $10^{-5}$, and compared to the 0.21" required for application of the IRB bounding leak rate |
| Burst Probability Estimate | 1. All hot leg TSPs are assumed to have a throughwall indication equal to, or greater than, the maximum TSP displacement, with the tip of the indication located at the edge of the TSP.<br>2. The displacement of each TSP is assumed to be the maximum displacement for that TSP for all tube intersections. |
| SLB Leakage | 1. SLB leakage is based on a bounding IRB leak rate for indications predicted to burst under free span conditions and free span leakage for indications not predicted to burst under free span conditions.<br>2. All leak rates very conservatively assume open crevice conditions with maximum tube to TSP hole clearance |
| Tube Repair Limit | Although axial tensile rupture data support a much higher repair limit, the tube repair limit is very conservatively set at 3 volts. |